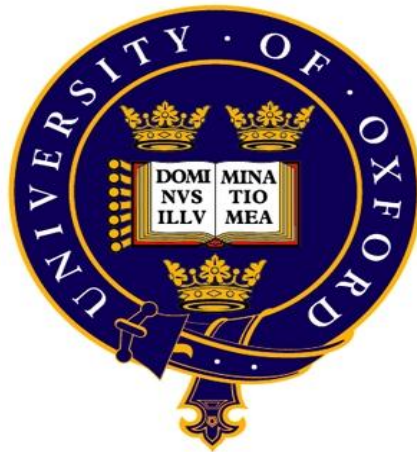


The Molecular Genetics of Insulin Secretion and Signalling

A thesis submitted to the University of Oxford



in candidature for the degree of Doctor of Philosophy

by

Laura Jade McCulloch

Green-Templeton College

University of Oxford

and

Oxford Centre for Diabetes, Endocrinology and Metabolism

Nuffield Department of Clinical Medicine

University of Oxford

Trinity 2011

Memorandum

The work presented in this thesis is the original work of the author. Experiments were undertaken at the Oxford Centre for Diabetes, Endocrinology and Metabolism, University of Oxford, under the supervision of Dr Anna Gloyn and Professor Patrik Rorsman. Funding was provided by Diabetes UK.

The work on transcript profiling in human islets and beta-cells (**chapter 3**) was performed as part of two international collaborative meta-analyses (Dupuis, et al., 2010; Voight, et al., 2010). Statistical geneticists, led by Voight, Scott, Steinthorsdottir, Morris and Dina in the DIAGRAM+ consortia (Voight, et al., 2010) and Dupuis, Langenberg, Prokopenko, Saxena and Soranzo in the MAGIC consortia (Dupuis, et al., 2010), performed all statistical analysis. My role within the consortia focused on transcript profiling and signal refinement. Further clarification of author contributions is provided in **published manuscripts**. Follow up of the novel fpg association signal, *SLC2A2*, (**chapter 4**) was performed in collaboration with Martijn van de Bunt, a DPhil student at Oxford University, whilst mutational screening of *G6PC2* (**chapter 5**) was performed in collaboration with Dr Emma Edghill, Peninsula Medical School, University of Exeter.

Work on transcript profiling of T2D and fpg associated genes in human beta-cells (**chapter 3**), screening of *G6PC2* in monogenic beta-cell dysfunction cohorts (**chapter 5**) and the follow up of the novel fpg association signal, *SLC2A2* (**chapter 4**), have been published previously in Nature Genetics, Diabetic Medicine and Molecular Genetics and Metabolism respectively (Dupuis, et al., 2010; Edghill, et al., 2009; McCulloch, et al., 2011; Voight, et al., 2010) (**published manuscripts**).

I hereby state that no part of this thesis has been submitted for any other degree at this or another university. This thesis is approximately 45,000 words.

The Molecular Genetics of Insulin Secretion and Signalling

Laura McCulloch

Green-Templeton College

In candidature for the degree of Doctor of Philosophy

Trinity Term 2011

Abstract

Type 2 diabetes (T2D) and fasting plasma glucose (fpg) levels have distinct genetic components which are as yet only modestly understood. Understanding the genetics of this complex disorder and its related traits is likely to be of significant benefit to the field. Not only will it shed light on critical genes, pathways and mechanisms of regulation, but it may also contribute to the development of pharmaceutical anti-hyperglycaemic agents via the identification of key therapeutic targets. Therefore the aim of this thesis was to utilise a broad, multidisciplinary approach to study the genetics of insulin secretion and signalling.

Traditionally genes which harbour rare variants causing monogenic beta-cell dysfunction have also been found to harbour common variants associated with T2D and fpg. As genome-wide association studies (GWAS) identify an increasing number of common variants and genes, they also increase the number of genes which act as monogenic candidates. I screened *G6PC2*, a novel fpg associated gene, in patients with monogenic forms of beta-cell dysfunction and demonstrated that rare variants in this gene are unlikely to be a common cause of monogenic beta-cell dysfunction.

Although GWAS have been of considerable benefit to our understanding of complex disease genetics, they are not without their own limitations, primarily concerning signal refinement. To try to overcome this barrier for T2D and fpg signals I established a pipeline for fluorescence activated cell sorting of human islets to obtain pure beta-cells. In these cells, I performed transcript profiling of genes falling within T2D and fpg associated loci, demonstrating how this approach, alongside physiological analysis, can be of benefit for GWAS researchers and provide a starting point for fine mapping. Access to human beta-cells also enabled me to follow up one novel fpg association signal, *SLC2A2*. Through analysis within this metabolically relevant tissue I was able to establish that the mechanism for increased fpg levels is unlikely to be mediated via a beta-cell pathway.

Although GWAS have highlighted a number of key genes associated with beta-cell dysfunction; they have been far less successful at identifying genes associated with insulin resistance, another key component of T2D pathogenesis. Additional approaches, including the study of rodent models, may be required to study this aspect of T2D. *PTEN* is known to negatively regulate the insulin signalling pathway and adipose tissue specific *Pten*^{-/-} animals were shown to be markedly insulin sensitive. To assess the role of *PTEN* in human insulin sensitivity I performed mRNA expression profiling of *PTEN* in human adipose tissue biopsies from subjects with T2D and matched controls, demonstrating that *PTEN* is significantly reduced in the subcutaneous adipose tissue of the former. This response is likely to be a compensatory mechanism to counteract muscular insulin resistance although further investigation needs to be performed to determine the mechanism of compensatory downregulation.

These data provide insights into a number of aspects of T2D genetics, and demonstrate how a multidisciplinary approach is of benefit to T2D genetic research.

Acknowledgements

Although the work presented in this thesis is entirely my own, I most certainly could not have achieved all I have without the help and support of many colleagues, friends and family. I would like to take this opportunity to thank my supervisors Dr Anna Gloyn and Professor Patrik Rorsman for their support and guidance over the past three years as well as the opportunities for personal and professional development they have provided me with. I am also extremely grateful to have had the opportunity to work with such an amazing group of individuals on a daily basis. I would like to take this opportunity to thank all members of the Gloyn/McCarthy lab team who not only made me feel so welcome in the beginning but who have since supported me throughout this entire process. Special thanks to Chris Groves, Nicholas Tribble, Amy Barrett, Mandy Bennett and Bahram Jafar Mohammadi for being constant sounding boards and providing sanity and pearls of wisdom in times of stress. I also cannot forget to thank Dr Anne Clark for 'keeping an eye on me' and always having my best interests at heart. She is a lady I feel lucky to have met and she really is a true inspiration. I am also extremely grateful to Professor Philippe Halban and Dr Karim Bouzakri at Geneva University for hosting my travelling fellowship. The time spent in their country and in their laboratories is something I will always remember. Similar thanks also go to Professors Blüher and Kovacs at Leipzig University for their unreserved kindness and hospitality whilst I was a guest at their institute.

Although I have received exceptional support academically I cannot forget to thank those who have personally been there for me for the past four years. Friends I have made in Oxford are people I know I will stay in touch with for the rest of my life and for that I feel very lucky. For the fun times I will always remember and for those I wish I could forget I thank Mary Travers, Sarah Cooper, Matthew Rees, Neelam Hassanali, Katie Gaynor, Robert Massam and David Cooper. I am also indebted to my Chesterfield friends who have never let me forget my Northern roots and made it their mission to keep me grounded. Vicki Tonner, Stefanie Malia, Jenna Vaughan, Sarah Taylor and Hannah Slack, friends for life and I thank you all. Above all else, one person deserves a huge 'Thank you' and that is to my 'twin' and best friend Nicola Beer. On my first day in Oxford I did not expect to meet a person so like minded and so similar in all ways. She has been my major support system for the past three years, made me laugh until I cry and without her my experiences would not have been the same. Here's to always being twins!!!

Last, but by no means least, I would like to thank my family. To my sister Hannah and grandparents Margaret and Dennis Potter, who have provided constant entertainment and support. Final thanks go to my mum and dad, Jackie and Bill, for never pushing me but allowing to make my own decisions and believing in me whatever. As a final gift I surrender my 'office' and you may now have your dining room and social life back.

This thesis is dedicated to Mr John Jefferson an inspiring teacher who told me I could, and I did!!

Table of Contents

List of Tables	1
List of Figures	2
List of Abbreviations	4
Chapter 1. Introduction	7
1.1 Insulin	8
1.1.1 The discovery of insulin	8
1.1.2 Insulin processing	9
1.1.3 Insulin secretion	11
1.1.4 Insulin signalling	12
1.1.5 Disorders of insulin secretion and signalling	15
1.1.5.1 Disorders of insulin signalling	16
1.1.5.2 Disorders of insulin secretion	20
1.2 Non-insulin dependent diabetes mellitus	22
1.2.1 Type 2 diabetes	22
1.2.2 Monogenic disorders of beta-cell function	25
1.2.3 Investigating the genetics of non-insulin dependent diabetes	32
1.3 Approaches to study the genetics of diabetes mellitus and related metabolic traits	34
1.3.1 Candidate gene approach	34
1.3.2 Genome-wide studies	37
1.3.3 Insights into glucose homeostasis from mouse models	43
1.3.4 Thesis aims	47
Chapter 2. General Methods	49
2.1 Subjects studies	52
2.1.1 Patient cohorts – monogenic disorders of beta-cell function	52
2.1.2 Human tissue samples – MOLPAGE surgical collection	52

2.2	Genomic DNA amplification	56
2.2.1	Primer design	56
2.2.2	Polymerase chain reaction (PCR) components and cycling conditions	56
2.2.3	PCR product size validation using agarose gel electrophoresis	57
2.3	DNA sequencing	58
2.4	RNA extraction	59
2.4.1	Human islet processing and storage for RNA extraction	59
2.4.2	RNA extraction from human islets using the phenol-chloroform methodology	59
2.4.3	Human tissue biopsy processing and storage for RNA extraction	60
2.4.4	RNA extraction from human tissue biopsies using the phenol-chloroform extraction methodology	61
2.5	RNA quality determination	62
2.5.1	RNA purity testing using spectrophotometric Nanodrop technology	62
2.5.2	RNA integrity determination	62
2.6	Reverse Transcription	63
2.6.1	Removal of genomic contamination from RNA using DNase I	63
2.6.2	cDNA synthesis	63
2.7	mRNA quantification	65
2.7.1	Taqman methodology and probe selection	65
2.7.2	Choice of analysis	66
2.7.3	Housekeeping gene selection	66
2.7.4	Standard curve generation for use in efficiency calculations	67
2.7.5	Quantitative real time PCR (qRT-PCR)	67
2.7.6	qRT-PCR as a method to determine human islet purity	68
2.8	Protein extraction and quantification	69
2.8.1	Protein extraction from human adipose tissue	69
2.8.2	Protein quantification	69
2.9	Western Blotting	70
2.10	Fluorescence activated cell sorting (FACS)	71

2.10.1	Human islet preparation	71
2.10.2	Preparation of Krebs buffer for FACS	71
2.10.3	Preparation of islets for FACS	72
2.10.4	FACS principles	73
2.10.5	Determination of beta-cell purity	76
Chapter 3. Development of a method for isolating pure human beta-cells and utilisation as a tool for interpreting GWAS signals		77
3.1	Introduction	78
3.1.1	GWAS as a tool to further our understanding of the genetics of T2D and related quantitative traits	78
3.1.2	Limitations of GWAS	83
3.1.3	Understanding molecular mechanisms of GWAS signals	85
3.1.4	Purification of human beta-cells	88
3.1.5	Flow sorted beta-cells as a tool for biological refinement of GWAS signals	89
3.2	Methods	90
3.2.1	FACS of human islets	90
3.2.2	Samples	91
3.2.3	Probe selection	91
3.2.4	mRNA expression – novel T2D and fpg loci in a human tissue panel	91
3.2.5	mRNA expression – novel T2D and fpg loci in human beta-cells	92
3.3	Results	94
3.3.1	mRNA expression profiling of genes within novel T2D loci: Human tissue panel	94
3.3.2	mRNA expression profiling of genes close to novel T2D loci: Human islets	101
3.3.3	mRNA expression profiling of genes close to novel T2D loci: Human beta-cells	102
3.3.4	mRNA expression profiling of novel fpg genes: Human tissue panel	105
3.4	Discussion	108

Chapter 4. GLUT2 (<i>SLC2A2</i>) is not the principal glucose transporter in human pancreatic beta-cells: Implications for understanding genetic association signals at this locus	118
4.1 Introduction	118
4.2 Methods	121
4.2.1 Samples	121
4.2.2 mRNA expression analysis of <i>SLC2A1-4</i> in human tissues	121
4.2.3 mRNA expression analysis of <i>Slc2a1-4</i> in mouse tissues	122
4.2.4 Immunohistochemistry	122
4.3 Results	124
4.3.1 GLUT mRNA expression in metabolically relevant human tissues	124
4.3.2 Glut mRNA expression in metabolically relevant murine tissues	125
4.3.3 Protein expression of GLUT1-3 within islets and FACS beta-cells	127
4.4 Discussion	128
Chapter 5. Mutations within the third gene shown to affect fasting plasma glucose in the general population (<i>G6PC2</i>) are not a common cause of monogenic beta-cell dysfunction	131
5.1 Introduction	132
5.2 Methods	136
5.2.1 Subjects studied	136
5.2.2 Patient DNA	137
5.2.3 Amplification of <i>G6PC2</i> in patients with monogenic beta-cell dysfunction	137
5.2.4 Sequencing of amplified DNA to identify novel <i>G6PC2</i> mutations	138
5.3 Results	140
5.4 Discussion	145
Chapter 6. An investigation of the role of phosphatase and tensin homologue deleted on chromosome ten (<i>PTEN</i>) in patients with Type 2 diabetes	149
6.1 Introduction	150

6.2	Methods	155
6.2.1	Subjects studied	155
6.2.2	RNA extraction and processing of tissue biopsies	157
6.2.3	Quantitative realtime PCR – Adipose tissue samples	158
6.2.4	Quantitative realtime PCR – Muscle samples	159
6.2.5	Protein extraction and quantification – Adipose tissue samples	159
6.2.6	Western Blotting – Total PTEN protein expression	160
6.2.7	Statistical Analysis	161
6.3	Results	162
6.3.1	PTEN expression in human adipose tissue – MoISURG samples	162
6.3.2	PTEN expression in human muscle – MoISURG samples	164
6.3.3	mRNA expression – Related insulin signalling genes	166
6.3.4	Replication of mRNA expression analysis – Leipzig biobank	168
6.3.5	Oxford and Leipzig combined analysis	170
6.3.6	Protein expression in adipose tissue biopsies	171
6.3.7	Effects of glucose challenge on PTEN mRNA expression	172
6.4	Discussion	179
Chapter 7	Discussion	186
References		197
Published Manuscripts		221

- Dupuis J, Langenberg C, Prokopenko I, Saxena R, Soranzo N, Jackson AU, Wheeler E, Glazer NL, Bouatia-Naji N, Gloyn AL and others. 2010. New genetic loci implicated in fasting glucose homeostasis and their impact on type 2 diabetes risk. *Nat Genet* 42(2):105-16.
- Edghill EL, McCulloch L, Fulton P, Beer N, Hattersley AT, Gloyn AL. 2009. Mutations in the third gene shown to alter fasting glucose levels in the population (G6PC2) are not a common cause of monogenic forms of pancreatic B-cell dysfunction. *Diabet Med* 26(1):113-4.
- McCulloch LJ, van de Bunt M, Braun M, Frayn KN, Clark A, Gloyn AL. 2011. GLUT2 (SLC2A2) is not the principal glucose transporter in human pancreatic beta cells: Implications for understanding genetic association signals at this locus. *Mol Genet Metab*.
- Voight BF, Scott LJ, Steinthorsdottir V, Morris AP, Dina C, Welch RP, Zeggini E, Huth C, Aulchenko YS, Thorleifsson G and others. 2010. Twelve type 2 diabetes susceptibility loci identified through large-scale association analysis. *Nat Genet* 42(7):579-89.

List of Tables

Table		Page
Table 2.1	Characteristics of MoISURG subjects selected for PTEN expression analysis	54
Table 2.2	PCR reagents used for standard in house amplification reactions	57
Table 2.3	Reaction components for cDNA synthesis	64
Table 2.4	ABI Taqman probe identification numbers for islet purity analysis	68
Table 3.1	DIAGRAM+ associations exceeding levels of genome-wide significance	80
Table 3.2	MAGIC associations exceeding levels of genome-wide significance	82
Table 3.3	Additional genes located within DIAGRAM+ associated loci	84
Table 3.4	ABI Taqman probe identification numbers used for transcript profiling of genes within DIAGRAM+ and MAGIC associated loci	93
Table 4.1	ABI Taqman probe identification numbers for GLUT1-4 assays designed for detection of human and rodent mRNA	122
Table 5.1	Clinical characteristics of patients with monogenic disorders of beta-cell function	137
Table 5.2	<i>G6PC2</i> primer sequences	138
Table 5.3	<i>G6PC2</i> variants identified in patients with monogenic disorders of beta-cell function	144
Table 6.1	Summary characteristics of subjects in whom PTEN expression was determined.	156
Table 6.2	ABI Taqman identification numbers for probes used to determine the expression of key insulin signalling genes	159
Table 6.3	mRNA expression levels of key insulin signalling genes in MoISURG subjects	167
Table 6.4	mRNA expression levels of key insulin signalling genes in Leipzig subjects	169
Table 6.5	mRNA expression levels of key insulin signalling genes in abdominal and gluteal adipose tissue pre-glucose versus post-glucose challenge	174
Table 6.6	mRNA expression levels of key insulin signalling genes pre-glucose versus post-glucose challenge in lean and obese individuals	175
Table 6.7	mRNA expression profiling of key insulin signalling genes pre-glucose versus post-glucose challenge, in lean and obese subjects	175
Table 6.8	mRNA expression profiling of key insulin signalling genes in lean subjects versus obese subjects	177

List of Figures

Figure		Page
Figure 1.1	Structure of human insulin	10
Figure 1.2	Insulin secretion from the pancreatic beta-cells	12
Figure 1.3	Insulin signalling in skeletal muscle and adipose tissue	14
Figure 1.4	Insulin signalling downstream of AKT/PKB	15
Figure 2.1	RNA integrity analysis using the Agilent Bioanalyser	63
Figure 2.2	Gating parameters for flow sorting of human beta-cells	75
Figure 3.1	Transcript profiling of <i>HNF1A</i> , <i>HMGA2</i> and <i>BCL11A</i> in a human tissue panel. DIAGRAM+ consortia	94
Figure 3.2	Transcript profiling of genes at the 5q14 locus. DIAGRAM+ consortia	96
Figure 3.3	Transcript profiling of genes at the 7q23 locus. DIAGRAM+ consortia	97
Figure 3.4	Transcript profiling of genes at the 8q22.1 locus. DIAGRAM+ consortia	98
Figure 3.5	Transcript profiling of genes at the 9q21 locus. DIAGRAM+ consortia	99
Figure 3.6	Transcript profiling of genes at the 11q13 locus. DIAGRAM+ consortia	100
Figure 3.7	Transcript profiling of genes at the 15q25 locus. DIAGRAM+ consortia	101
Figure 3.8	Transcript profiling of genes at the 15q6 locus. DIAGRAM+ consortia	102
Figure 3.9	Transcript profiling within human islets. DIAGRAM+ consortia	103
Figure 3.10	Immunocytochemistry determination of beta-cell purity	104
Figure 3.11	mRNA expression profiling of DIAGRAM+ genes within human beta-cells	105
Figure 3.12	Transcript profiling of novel fasting plasma glucose genes in a human tissue panel. MAGIC consortia	107
Figure 3.13	Transcript profiling of fasting plasma glucose genes in human islets. MAGIC consortia	108
Figure 4.1	mRNA expression profiling of GLUT1-4 in metabolically relevant human tissues	124
Figure 4.2	mRNA expression profiling of Glut1-4 in metabolically relevant murine tissues	125
Figure 4.3	Immunohistochemistry analysis of GLUT1-3 in human and rodent islets	126
Figure 4.4	Immunohistochemistry analysis of GLUT1-3 in human beta-cells	127

Figure 5.1	Demonstration of a novel H177HY variant in <i>G6PC2</i> in a proband with hyperinsulinaemic hypoglycaemia (HH)	141
Figure 5.2	Determination of evolutionary conservation of the <i>G6PC2</i> residue 256 in multiple species	143
Figure 6.1	Insulin signalling in skeletal muscle and adipose tissue	151
Figure 6.2	<i>PTEN</i> mRNA expression in adipose of MoISURG subjects	162
Figure 6.3	Correlation between <i>PTEN</i> mRNA expression and subject BMI and subject age	163
Figure 6.4	<i>PTEN</i> mRNA expression in muscle biopsies from MoISURG subjects	165
Figure 6.5	mRNA expression profiling of key insulin signalling genes in adipose tissue of MoISURG subjects	167
Figure 6.6	<i>PTEN</i> mRNA expression in adipose tissue of subjects from the Leipzig biobank	169
Figure 6.7	mRNA expression profiling of key insulin signalling genes in adipose tissue of patients from the Leipzig biobank	170
Figure 6.8	<i>PTEN</i> protein expression in adipose tissue of MoISURG subjects	172
Figure 6.9	mRNA expression profiling of key insulin signalling genes in the adipose tissue of subjects pre-glucose versus post-glucose challenge	173
Figure 6.10	<i>PTEN</i> mRNA expression in adipose tissue of subjects pre-glucose versus post-glucose challenge, BMI stratified	175
Figure 6.11	<i>PTEN</i> and <i>IRS1</i> mRNA expression analysis in adipose tissue of lean versus obese subjects	178

List of Abbreviations

λs	Sibling relative risk
7AAD	7 aminoactinomycin D
ADP	Adenosine diphosphate
ATP	Adenosine triphosphate
BMI	Body mass index
bp	Base pairs
BSA	Bovine serum albumin
cDNA	Complementary deoxyribonucleic acid
Chr	Chromosome
DAPI	4'6-diamidino-2-phenylindole
ddNTPs	Dideoxyribonucleotide
DIAGRAM+	Diabetes genetics replication and meta-analysis consortium
DNA	Deoxyribonucleic acid
dNTPs	Deoxyribonucleotide
EFSD	European foundation for the study of diabetes
eQTL	Expression quantitative trait loci
ER	Endoplasmic Reticulum
FACS	Fluorescence-activated cell sorting
FITC	Fluorescein isothiocyanate
fpg	Fasting plasma glucose
FPLD	Familial partial lipodystrophy
G6PC2	Glucose-6-phosphatase, catalytic, subunit, 2
GCK	Glucokinase
GLUT	Glucose transporter
GOI/HKG	Gene of interest / Housekeeping gene
GSIS	Glucose-stimulated insulin secretion
GWAS	Genome-wide association studies
HbA1c	Haemoglobin A1c/Glycated haemoglobin
HH	Hyperinsulinaemic hypoglycaemia
HI/HH	Hyperinsulinism and hyperammonemia
HKG	Housekeeping gene
HLA	Human leukocyte antigen
HNF1A	Hepatocyte nuclear factor 1 homeobox A

HOMA-B	Homeostatic model assessment of beta-cell function
HOMA-IR	Homeostatic model assessment of insulin resistance
IFG	Impaired fasting glucose
IGT	Impaired glucose tolerance
IHC	Immunohistochemistry
K_{ATP}	ATP sensitive potassium channel
LCM	Laser capture microdissection
LD	Linkage disequilibrium
LOD	Logarithm [base10] of odds
MAF	Minor allele frequency
MAGIC	Meta-analysis of glucose and insulin related traits consortium
MES	2-(N-morpholino)ethanesulfonic acid
miRNA	Micro ribonucleic acid
MODY	Maturity onset diabetes of the young
mRNA	Messenger ribonucleic acid
NEFA	Non-esterified fatty acids
NG	Newport green
OGTT	Oral glucose tolerance test
OHA	Oral hyperglycaemic agents
OR	Odds ratio
OXCIT	Oxford centre for islet transplantation
PBS	Phosphate buffered saline
PCOS	Polycystic ovary syndrome
PCR	Polymerase chain reaction
PFA	Paraformaldehyde
PH domain	Pleckstrin homology
PIP₂	Phosphatidylinositol 4,5-bisphosphate
PIP₃	Phosphatidylinositol (3,4,5)-triphosphate
PNDM	Permanent neonatal diabetes mellitus
PTEN	Phosphatase and tensin homologue deleted on chromosome ten
PVDF	Polyvinylidene fluoride
qRT-PCR	Quantitative real time polymerase chain reaction
Rhod	Rhodamine
RIN	RNA integrity number

RNA	Ribonucleic acid
RRP	Readily releasable pool
RT	Reverse transcriptase
SD	Standard deviation
SDS	Sodium dodecyl sulfate
SEM	Standard error of the mean
SH	Src-homology-2
siRNA	Small interfering ribonucleic acid
SLC2A2	Solute carrier family 2 (facilitated glucose transporter), member 2
SNP	Single nucleotide polymorphism
T1D	Type 1 diabetes
T2D	Type 2 diabetes
TBE	Tris/Borate/EDTA
TBS	Tris buffered saline
TNDM	Transient neonatal diabetes mellitus
UTR	Untranslated regions
WHO	World health organisation
WT	Wildtype

Chapter 1

Introduction

1.1 Insulin

Insulin is a hormone which is crucial for all forms of eukaryotic life. Since its discovery in the early twentieth century it has been found to have a multitude of physiological effects including vasodilation as a direct consequence of insulin-stimulated nitric oxide release, as well as aiding in brain functions including mood, confidence and in particular verbal memory (Benedict, et al., 2004; Zeng and Quon, 1996). Its most well-studied function, however, is in the regulation of carbohydrate and fat metabolism [reviewed in (Saltiel and Kahn, 2001)]. Its central role in regulation of these processes ensures that when deficient or deregulated, severe metabolic disturbances occur including increased glucose levels and lipid accumulation. Insulin is synthesised and processed within the pancreatic beta-cells, one cellular component of the pancreatic endocrine tissue, commonly referred to as the islets of Langerhans (Steiner, et al., 1985).

1.1.1 The discovery of insulin

Islets of Langerhans are so termed following their identification by a German medical student, Paul Langerhans, in 1869. He carefully described these irregular shaped clumps of cells of 0.1-0.24mm diameter and defined their location throughout the pancreas, however by his own admissions at the time, was unable to postulate any viable explanation as to the role of these novel pancreatic structures (Jolles, 2002). Twenty years later Minkowski and colleagues established the connection between the pancreas and diabetes following their discovery that a pancreatectomised dog demonstrated elevated blood sugar levels, glycosuria and excessive weight loss despite nutritional supplementation (Luft, 1989). However, it wasn't until 1901 that the specific link between the islets of Langerhans and diabetes was finally established.

The pioneering work of Banting and Best in 1920 saw the final breakthrough in identification of the functional role (and secretory product) of islets when they were able to keep a pancreatectomised dog alive using crude canine islet extract. At this time, individuals suffering with diabetic ketoacidosis were treated in hospitals where they were inevitably expected to die as a result of their condition. In 1922 Banting and Best felt ready to implement their islet extract therapy on humans in Toronto General Hospital with Leonard Thompson being the first patient recorded to have received isletin (insulin) therapy (Banting, et al., 1922). Through enlisting the help of the biotechnology company, Eli Lilly, vast quantities of insulin were able to be generated for clinical use. The decades following the discovery saw a huge amount of work performed to generate synthetic insulin which was finally achieved in the 1960s by Helmut Zahn at Aachen University (Zahn, 2002).

The primary structure of bovine insulin was identified in 1951 by Fredrik Sanger. It was the first protein whose primary structure was totally elucidated for which Sanger received the Nobel Prize in 1958 (Sanger and Tuppy, 1951a; Sanger and Tuppy, 1951b). The primary structure of the insulin gene from over 30 species including homo sapiens has now been established using similar techniques (Bell, et al., 1980). Interestingly, its structure is extremely well conserved across all species demonstrating the crucial role of this protein from an evolutionary perspective (Steiner, 1976).

1.1.2 Insulin processing

In humans, insulin is transcribed from the proinsulin gene (*INS*) located on the short arm of chromosome 11 (p15.5) (Owerbach, et al., 1980). Full-length proinsulin consists of an A chain and a B chain linked by a connecting peptide (C-peptide) and four basic residues (Arginine or Lysine) in the order of NH₂-Bchain-Arg-Arg-C-peptide-Lys-Arg-Achain-COOH (Chance, et al., 1968; Nolan, et al., 1971; Steiner and Oyer, 1967). The initial translational product of the *INS*

gene however is preproinsulin, which includes an additional 24 amino acid signal peptide linked to the N terminal of proinsulin (Bell, et al., 1979; Chan, et al., 1976). Cleavage of the N-terminal signal peptide occurs in the endoplasmic reticulum (ER), and is believed to be linked closely to translation, therefore proinsulin is generated rapidly and preproinsulin is not present at high levels in the cell (Steiner, et al., 1984).

Proinsulin is transported from the ER to the Golgi where it is packaged into secretory vesicles with converting proteolytic enzymes including prohormone convertases and carboxypeptidase E (Steiner, et al., 1984; Vollenweider, et al., 1995). During maturation of the secretory vesicle, granule contents are crystallised with zinc ions whilst the C peptide is simultaneously cleaved from the peptide. The remaining A chain (21 amino acids) and B chain (30 amino acids) are linked by two disulphide bridges to generate the full length 51 amino acid insulin protein (Figure 1.1) (Humbel, et al., 1972; Sanger and Tuppy, 1951a; Sanger and Tuppy, 1951b). Insulin and C-peptide are therefore secreted in a 1:1 ratio (Steiner, et al., 1971).

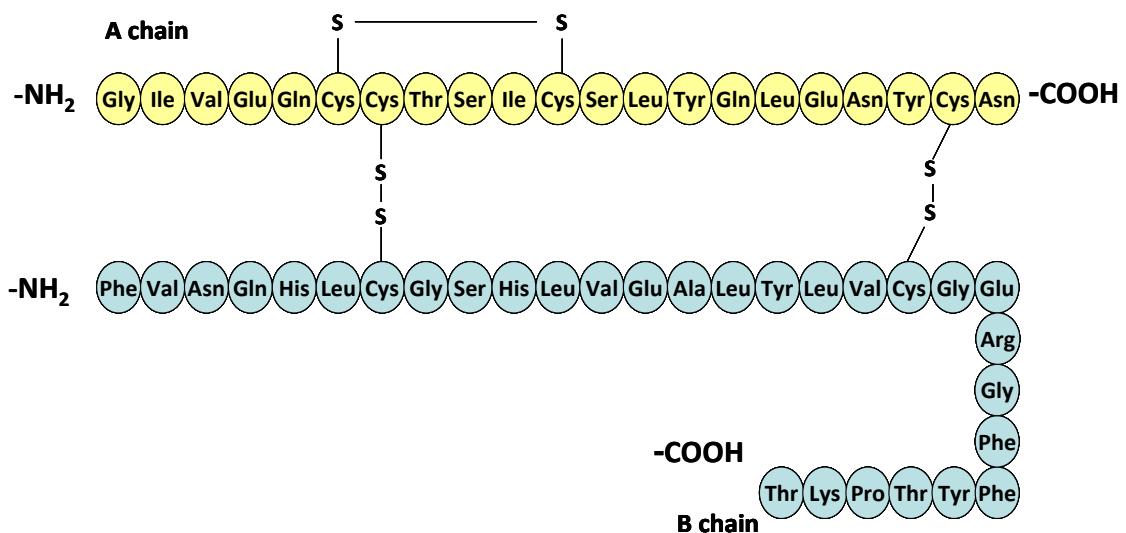


Figure 1.1 Structure of human insulin peptide composed of a 21 amino acid A chain and a 30 amino acid B chain. Following cleavage of the intermediate C-peptide, the A and B chain are held together by two disulfide bridges between Cys7(A)-Cys7(B) and Cys20(A)-Cys19(B), whilst the A chain also contains an internal disulfide bridge Cys6-Cys11. S-S represents disulfide bridge formations.

1.1.3 Insulin secretion from pancreatic beta-cells

Insulin secretion from the pancreatic beta-cells occurs in a glucose-dependent manner with a sigmoidal relationship observed between the two (Ashcroft, et al., 1972). In healthy individuals the postprandial increase in blood glucose concentration is sensed by the pancreatic beta-cells. Glucose enters the beta-cell via facilitated diffusion using passive glucose transporters. Intracellularly, glucose enters into glycolysis and is phosphorylated on carbon 6 by glucokinase (GCK) to generate glucose-6-phosphate (G6P) (Matschinsky, 2002). This is the rate limiting step of glycolysis and as such GCK is termed the pancreatic glucose sensor. G6P is further metabolised to generate ATP with the subsequent increase in the ATP:ADP ratio resulting in closure of the ATP sensitive potassium channel (K_{ATP}) (Tucker, et al., 1997).

In response to an increase in intracellular K^+ the beta-cell membrane undergoes slow membrane depolarisation from the resting membrane potential of -70mV to a less negative membrane potential. Electrical activity switches between depolarised and repolarised phases such that oscillations in membrane potentials are observed. Each membrane depolarisation triggers the opening of voltage gated L-type calcium channels with subsequent calcium influx into the cells. The increase in intracellular calcium levels triggers the exocytosis of the previously synthesised insulin secretory vesicles (Barbosa, et al., 1998; Hedekov, 1980; Hellman, et al., 1971; Henquin, 1978a; Henquin, 1978b; Prentki and Matschinsky, 1987). In 1993 it was demonstrated that the oscillations in membrane depolarisation correspond with the pulsatile release of insulin from the beta-cells (Bergsten, et al., 1994). A schematic representation of the insulin secretion pathway is provided in Figure 1.2

Insulin secretion from the pancreatic beta-cells *in vivo* is not continuous in response to a glucose challenge. Instead insulin release typically occurs in a bi-phasic manner with a rapid

increase in insulin secretion within the first 5-10 minutes, commonly referred to as the “first phase” followed by a secondary prolonged secretion phase (Grotsky, et al., 1968). It has been speculated that the bi-phasic secretion is due to the occurrence of distinct pools of secretory granules. A small quantity of vesicles (<5%) are believed to exist in a readily releasable pool (RRP) whilst the majority (>95%) exist within a reserve pool as has been observed with a variety of other excitable cells (Parsons, et al., 1995).

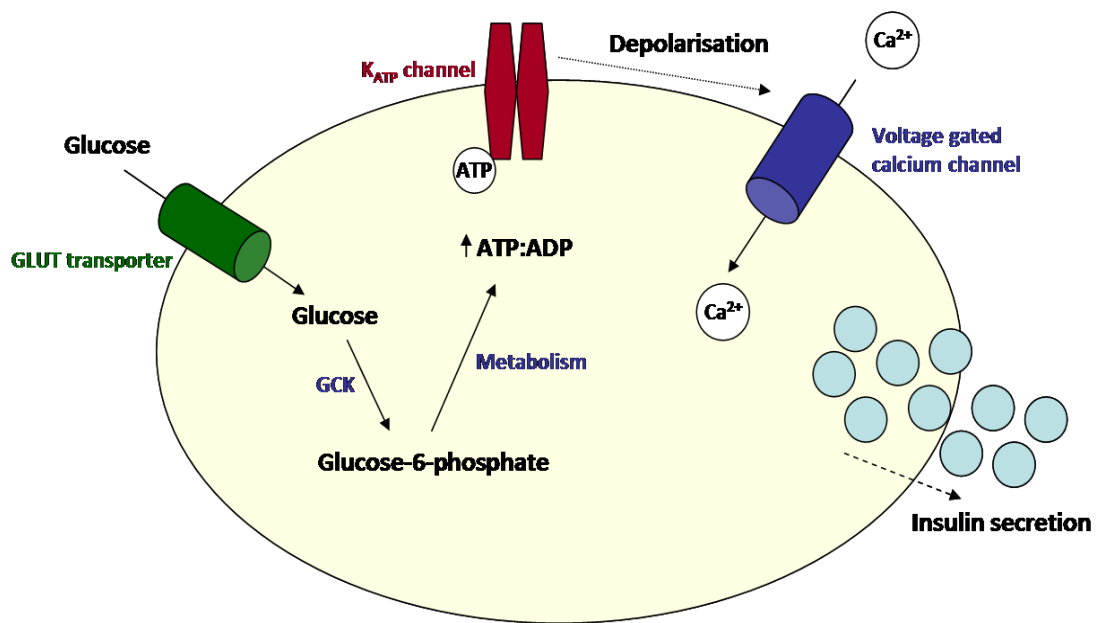


Figure 1.2 Insulin secretion from the pancreatic beta-cells. Glucose enters the pancreatic beta-cells via glucose transporters (GLUT). Once inside the cell, glucose is metabolised by glucokinase (GCK), the first enzyme in glycolysis. The product of this reaction, glucose-6-phosphate, is metabolised further leading to an increase in the cellular ATP:ADP ratio. An increase in ATP levels leads to closure of the ATP sensitive potassium (K_{ATP}) channel, resulting in membrane depolarisation and subsequent opening of voltage gated L-type calcium channels. The rise in intracellular calcium (Ca^{2+}) is the trigger for exocytosis of insulin secretory granules.

1.1.4 Insulin Signalling

Insulin is secreted from the pancreatic beta-cells directly into the bloodstream where it is transported to peripheral target tissues expressing the insulin receptor (gene name *INSR*). The physiological effects of insulin are wide ranging as are the tissues through which these effects are mediated, however many of these tissues and mechanisms work synergistically to control glucose homeostasis. For example, insulin binding to *INSR* on the surface of hepatocytes is of pivotal importance as it stimulates the disposal of glucose as glycogen, in

turn rendering glucose-generating gluconeogenic pathways non-functional (Saltiel and Kahn, 2001). In myocytes, insulin stimulates the translocation of GLUT4 to the plasma membrane increasing glucose uptake and glycogen synthesis, whilst in adipocytes insulin additionally stimulates the synthesis and esterification of fatty acids. As a result, blood glucose concentrations are reduced and maintained at physiological levels [reviewed in (Saltiel and Kahn, 2001)].

The metabolic consequences of insulin are mediated via a complex signalling cascade, itself regulated by numerous serine/threonine/tyrosine protein kinases and protein and lipid phosphatases. Insulin binding to its cell surface tyrosine kinase receptor (INSR) results in auto-phosphorylation of the intracellular β -subunit kinase domain, in turn recruiting and phosphorylating (p-Tyr) a number of intracellular effector molecules including the insulin receptor substrates 1 and 2 (IRS1/2) (Kasuga, et al., 1982; Sun, et al., 1991; Sun, et al., 1995). The p-Tyr residues of IRS1/2 subsequently interact directly with Src-homology-2 (SH2) domain containing intracellular molecules including phosphatidylinositol-3 kinase (PI3K) (Taniguchi, et al., 2006a). PI3K is a heterodimer composed of a regulatory (p85) and a catalytic (p110) subunit. Binding of IRS1/2 to regulatory subunit SH2 domains results in activation of the catalytic subunit and production of the phospholipid secondary messenger phosphatidylinositol(3,4,5)-triphosphate (PIP₃) from its precursors, phosphatidylinositol(4,5)-bisphosphate (PIP₂) and ATP (Hawkins, et al., 1992; Myers, et al., 1992). PIP₃ activates the relocalisation of a multitude of proteins with pleckstrin homology (PH) domains to the plasma membrane, including 3-phosphoinositide-dependent protein kinase 1 (PDK1) (Alessi, et al., 1997b) and protein kinase B (PKB/AKT), resulting in activation of a serine/threonine phosphorylation cascade. PDK1 is constitutively active within the cell but it is believed that the binding of AKT to PIP₃ alters the AKT conformation such that PDK1 is able to phosphorylate (Thr308) and activate the protein (Alessi, et al., 1997a). Other molecules also

phosphorylated and activated by PDK1 include PKC ζ at Thr410 (Le Good, et al., 1998). For complete activation AKT/PKB must also be phosphorylated at Ser473 by mTORC2 (Alessi, et al., 1996; Sarbassov, et al., 2005).

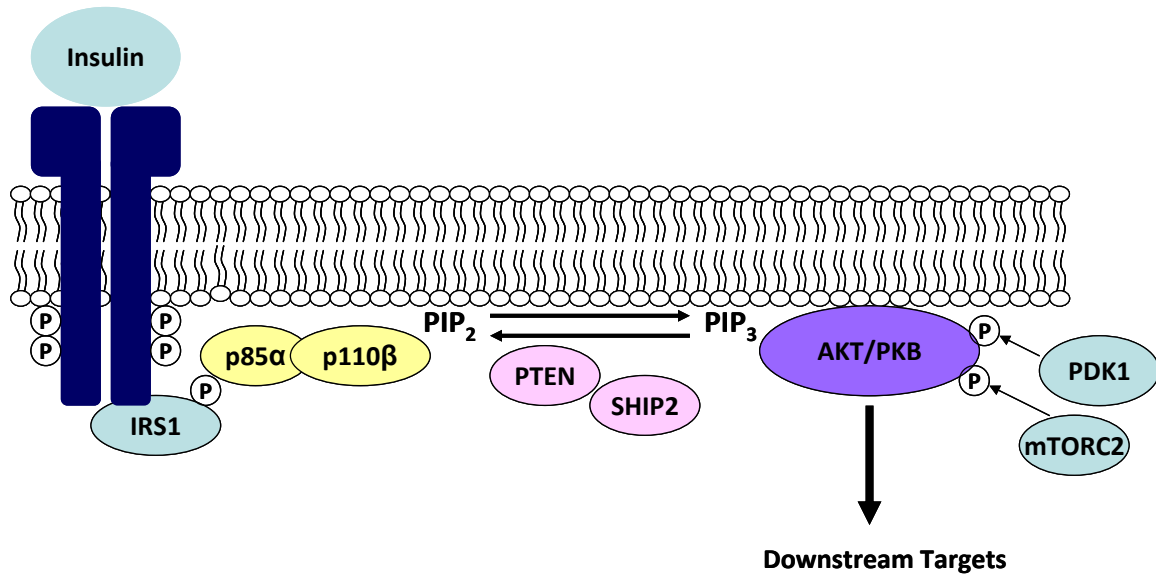


Figure 1.3 Insulin signalling within skeletal muscle and adipose tissue. Insulin binding to its tyrosine kinase receptor triggers a serine/threonine/tyrosine signalling cascade. Activation of the catalytic subunit of p110 β stimulated the conversion of PIP₂ to PIP₃, a key secondary messenger which is able to recruit AKT/PKB to the plasma membrane to undergo PDK1 and mTORC2 phosphorylation. AKT is then able to phosphorylate a number of key downstream targets. P represents phosphorylation.

Phosphorylation and activation of AKT is a critical node in the insulin signalling pathway as it functions as a primary regulator of a number of downstream metabolic signalling targets including glycogen synthase kinase-3 (GSK-3), forkhead box O1 (FOXO1), tuberous sclerosis complex 2 (TSC2) and AKT substrate 160kDa (AS160). Phosphorylation of GSK-3 at Ser9 inactivates the protein thus preventing inhibition of glycogen synthase (GS) and promoting the conversion of glucose to glycogen (Cross, et al., 1995). Activated AKT also phosphorylates and inhibits AS160, leaving Rab-GTPase's free to mediate cytoskeletal organisation and participate in GLUT4 translocation to the plasma membrane (Sano, et al., 2003). Phosphorylation of TSC2 results in inactivation of this protein reducing mTORC1 pathway inhibition and resulting in increased protein synthesis (Harris and Lawrence, 2003). Finally

AKT is also known to phosphorylate FOXO1 causing it to associate with 14-3-3, stopping translocation of this transcription factor to the nucleus and preventing transcription of a number of gluconeogenic genes (Tran, et al., 2003).

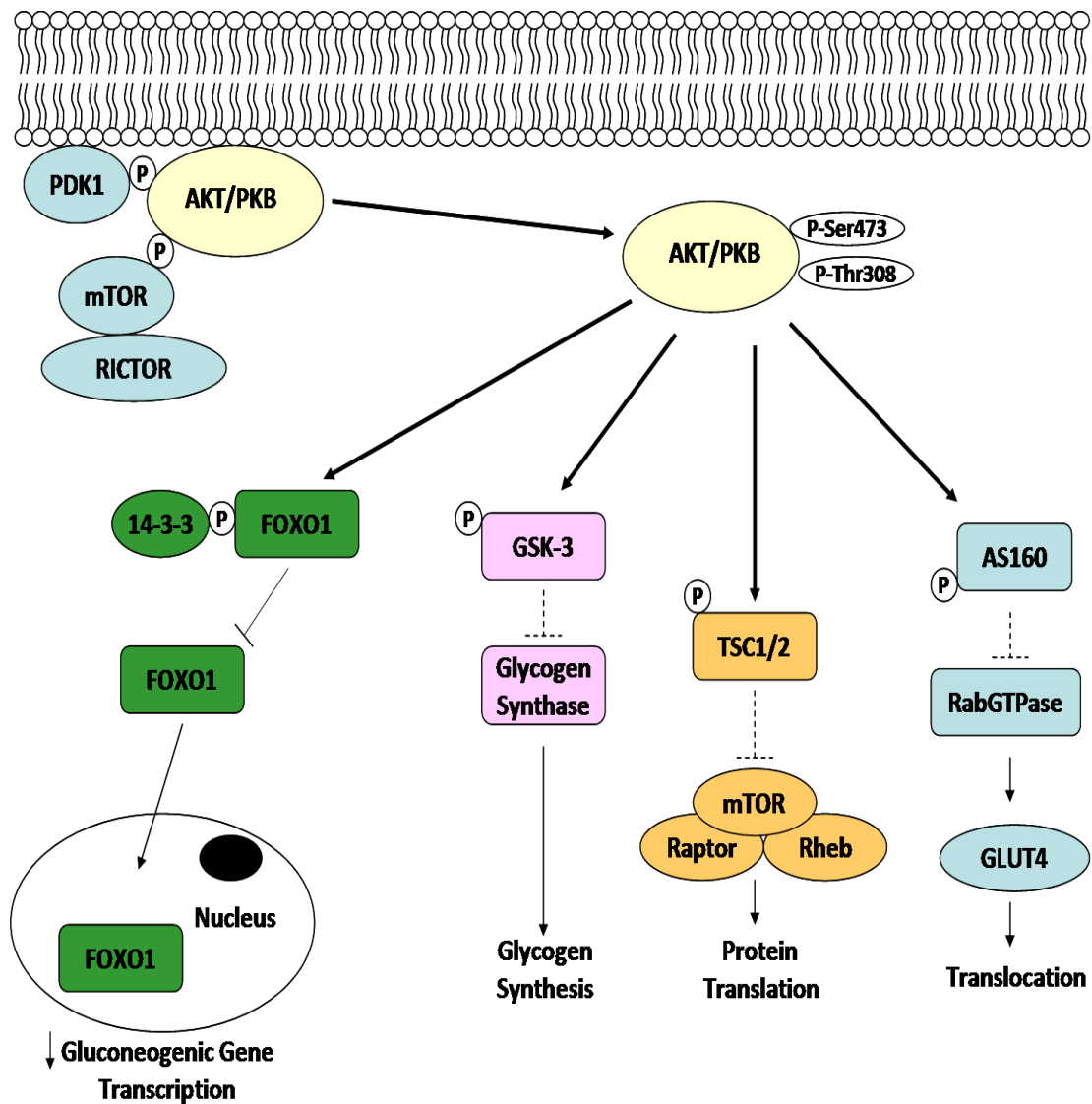


Figure 1.4 Insulin signalling within key target tissues downstream of AKT/PKB. The node/pathway which the signal may take is tissue-dependent but the key signalling mechanisms are outlined above.

1.1.5 Disorders of insulin secretion and signalling

Insulin secretion and signalling are tightly regulated as the above signalling cascades demonstrate. The temporal regulation of insulin secretion with concomitant stimulation of glucose disposal ensures that glucose levels are maintained within the physiologically desirable range of 4-6mmol/L. As this hormone is of utmost importance for glycaemic control

it goes without saying that deregulation of either the secretion or signalling pathway may manifest in metabolic disorders with severe homeostatic consequences. To date, a number of metabolic disorders with a strong insulin signalling and/or insulin secretory defect have been well characterised.

1.1.5.1 Disorders of insulin signalling

Insulin receptoropathies

Severe insulin resistance is characterised clinically as the presence of acanthosis nigricans and ovarian hyperandrogenism alongside hyperinsulinaemia and aberrant glucose homeostasis (Semple, et al., 2011). To date, mutations within the insulin receptor gene (*INSR*) have been shown to be the most common cause of severe monogenic insulin resistance syndromes (Longo, et al., 2002; Suliman, et al., 2009). The mode of inheritance, coupled with the location of the *INSR* mutation, is often predictive of disease severity with autosomal recessive disorders (Donahue and Rabson-Mendenhall syndromes) located towards the severe end of the spectrum, whilst autosomal dominant Type A insulin resistance (Type A IR) is located towards the milder end (Semple, et al., 2011).

Donohue syndrome was initially discovered in 1954 by Donohue and Uchida following the identification of a severe growth retardation phenotype in two sisters born to consanguineous parents, originally termed Leprachaunism (Donohue and Uchida, 1954). The subjects were found to exhibit truncated growth from seven months of gestation, elfin features, flaring nostrils, enlarged pancreas and premature death (<1 year) (Donohue and Uchida, 1954). An increase in the number of probands diagnosed with the disorder since the initial study has seen the phenotype extended to incorporate additional symptoms including acanthosis nigricans, hyperinsulinaemia and reduced subcutaneous adipose tissue (Elsas, et

al., 1985). The life-expectancy for subjects with Donohue syndrome is <1 year (Elsas, et al., 1985; Psiachou, et al., 1993).

Rabson-Mendenhall syndrome was discovered in 1956 following identification of an unusual phenotype in three siblings born to consanguineous parents (Rabson and Mendenhall, 1956). Subjects showed signs of early dental development, skin abnormalities and severe hirsutism. In addition each subject also showed signs of early mental development and upon autopsy enlargement of the endocrine pineal gland was found (Rabson and Mendenhall, 1956). Each of the siblings developed insulin resistant diabetes which led to diabetic ketoacidosis and premature death (Rabson and Mendenhall, 1956). As with Donohue syndrome, mutations within the *INSR* gene were also found within these probands, although the majority of mutations causing this syndrome are believed to affect intracellular components of the insulin receptor, allowing some residual insulin binding to the receptor (Longo, et al., 1994; Longo, et al., 1999; Longo, et al., 2002).

In contrast, inheritance of an *INSR* mutation in an autosomal dominant manner results in a markedly less severe insulin resistance phenotype, often termed Type A insulin resistance (Type A IR). This disorder is often diagnosed in peripubertal, lean women in whom hyperandrogenism, oligomenorrhoea and acanthosis nigricans are also present (Musso, et al., 2004). To date around 10-20% of all Type A IR patients have been found to possess heterozygous mutations within the intracellular domain of *INSR* (Semple, et al., 2010).

Severe Insulin Resistance due to Insulin Signalling Gene Mutations

The observation that only 10-20% of Type A IR patients possess an *INSR* mutation dictates that mutations within additional insulin signalling genes, downstream of the insulin receptor, are likely to harbour monogenic insulin resistance mutations (Semple, et al., 2010). Despite

this hypothesis, and increased understanding of the insulin signalling cascade, only a small number of mutations have been identified in key downstream signalling genes. These include identification of a heterozygous *AKT2* mutation in a family with acanthosis nigricans, hyperandrogenism and dyslipidemia (George, et al., 2004) and a heterozygous mutation within *TBC1D4* (encoding AS160, a key downstream target of AKT) in a severely hyperinsulinaemic family (Dash, et al., 2009). Interestingly, there is one report within the literature of a severe digenic form of insulin resistance due to inheritance of heterozygous mutations in two insulin signalling genes (Savage, et al., 2002). Affected family members all possessed a heterozygous frameshift mutation in peroxisome proliferator-activated receptor gamma (*PPARG*) and a heterozygous mutation in protein phosphatase 1, regulator (inhibitor) subunit 3 (*PPP1R3A*) (Savage, et al., 2002; Savage, et al., 2008). *PPARG* functions as a regulator of adipocytes differentiation (Chawla and Lazar, 1994; Tontonoz, et al., 1998) whilst *PPP1R3A* is a regulator of glycogen accumulation in muscle (Savage, et al., 2008). Family members who were heterozygous for only the *PPARG* or the *PPP1R3* mutation all demonstrated normal insulin sensitivity, whilst the five individuals who were compound heterozygotes demonstrated severe hyperinsulinaemia (Savage, et al., 2002). This was the first and only time a digenic cause of severe insulin resistance has been documented.

Familial Partial Lipodystrophy (FPLD)

The term FPLD is used to describe a heterogeneous group of lipodystrophies which are all inherited in an autosomal dominant manner and characterised by a general lack of subcutaneous adipose tissue (Garg, 2004). As lipids are unable to accumulate in adipose tissue, they amass ectopically and within skeletal muscle, leading to insulin resistance and subsequent beta-cell dysfunction (Savage, 2009). Molecular and genetic aspects of the two most common forms of FPLD, FPLD2 and FPLD3 have demonstrated that they are caused by heterozygous mutations in *LMNA* and *PPARG* respectively. FPLD-LMNA predominantly

affects the gluteal and peripheral adipose depots demonstrating modest to severe insulin resistance (Jackson, et al., 1997). FPLD3-PPARG however shows a lack of gluteal and peripheral adipose tissue whilst central adipose tissue is preserved and generally enlarged (Semple, et al., 2006). Individuals tend to present with severe insulin resistance as a result of lack of PPAR γ transcriptional activity and it has been suggested that even the remaining adipose tissue in the central areas does not function normally (Savage, et al., 2003; Tan, et al., 2008).

Polycystic Ovary Syndrome (PCOS)

Unlike the previous insulin resistance syndromes, PCOS is a relatively common (5-10%) neuroendocrine disorder observed in pre-menopausal women (Asuncion, et al., 2000; Azziz, et al., 2004). Although the disorder is relatively heterogeneous, classical hallmarks include hyperandrogenism, anovulation and polycystic ovaries, with two of the three symptoms resulting in a clinical diagnosis (Azziz, 2006). In 1980, Burghen *et al.* identified a positive correlation between hyperandrogenism and hyperinsulinaemia in PCOS patients, absent in weight matched control subjects (Burghen, et al., 1980). Most women with PCOS have since been shown to have impaired glucose tolerance, reduced insulin sensitivity and to be at increased risk of developing T2D (Baptiste, et al., 2010; Dunaif and Thomas, 2001). A routine part of the clinical diagnosis procedure now involves assessment of clinical manifestations of the insulin resistance syndrome including waist circumference (>88cm), triglyceride (>1.68mmol/L) and fpg (>6.05mmol/L) (Sheehan, 2004). Although the molecular mechanisms are not fully understood, research to date suggests that insulin resistance in individuals with PCOS occurs post insulin binding (Diamanti-Kandarakis and Papavassiliou, 2006; Dunaif, et al., 1995) whilst increased insulin levels directly stimulate androgen release from the ovaries (Nelson-Degrave, et al., 2005).

1.1.5.2 Disorders of insulin secretion

Insulinomas

Insulinomas are tumours derived from the insulin-secreting pancreatic beta-cells. As a result of cellular overgrowth, beta-cells lose their normal stimulation-secretion coupling response to glucose, secreting insulin in an excessive and unregulated manner. Subjects with an insulinoma therefore present with hypoglycaemia, elevated fasting insulin and C-peptide levels, lethargy and in severe cases may also suffer from seizures or even coma (Abbasakoor, et al., 2011). The optimal treatment is surgical removal of the tumour however in unique cases, when this option is unavailable, subjects may respond to diazoxide treatment, a potassium channel activator which thus prevents beta-cell membrane depolarisation and insulin secretion (Gill, et al., 1997). In the majority of patients (80-90%), insulinomas are benign and solitary and excision is sufficient to return a patients glycaemia to normal (Service, et al., 1991) however there are occasions when insulinomas are malignant and form part of the autosomal dominant cancer predisposition syndrome, multiple endocrine neoplasia Type1 syndrome (White and Doherty, 2008).

Type 1 Diabetes

Type 1 diabetes (T1D) also occurs as a result of defective insulin secretion, but more specifically as a result of auto-immune destruction of the pancreatic beta-cells in genetically susceptible individuals (Knip, et al., 2005). Patients present clinically with classic signs of T1D including polyuria, polydipsia, polyphagia, fatigue and weight loss, generally after the age of 6 months. One of the earliest signs of auto-immune beta-cell destruction is the presence of diabetes-associated auto-antibodies, four of which are routinely tested in at risk or clinically presenting subjects (islet auto-antibodies, insulin auto-antibodies [IAAs], tyrosine phosphatase-related IA-2 molecule [ICA2] and glutamic acid decarboxylase [GAD] auto-antibodies).

Familial clustering studies have demonstrated the sibling relative risk (λ_s) for T1D is 15, indicating a strong genetic component to this disease (Risch, 1987; Todd, et al., 2007). Sibling relative risk, a measure of familial aggregation, is defined as the risk of suffering from a disorder given that one's sibling is also affected, in comparison to the general population. To date the major susceptibility locus, identified through linkage analysis, has been shown to map to the HLA class II loci, HLA-DRB1 and HLA-DQB1, on the short arm of chromosome 6 (p21) (Noble, et al., 1996). Despite the evident genetic component to the disorder and data supporting familial aggregation, studies in monozygotic twins demonstrate only 13-33% concordance for T1D, indicating environmental factors are also of importance (Barnett, et al., 1981; Kaprio, et al., 1992). To further support this notion approximately 20% of the general population carry the T1D HLA-high risk genotype however the lifetime prevalence for T1D is only 1%. The observation that only 5% of all risk allele carriers develop overt diabetes within their lifetime points to additional susceptibility factors which have yet to be elucidated (Knip, et al., 2005).

1.2 Non-insulin dependent diabetes mellitus

The disorder most commonly associated with defective insulin regulation is non-insulin dependent diabetes mellitus. The term is broadly used to define a heterogeneous group of disorders in which insulin regulation of glucose homeostasis is lost, and can be further subdivided into two major categories. 1) Type 2 diabetes mellitus, a common, complex disorder which occurs as the result of peripheral insulin resistance and beta-cell dysfunction and 2) Monogenic forms of beta-cell dysfunction, a heterogeneous group of rare disorders which occur as a result of mutations within key beta-cell genes.

1.2.1 Type 2 diabetes (T2D)

Diagnosis and Treatment of T2D

The symptoms of T2D are much the same as T1D including increased thirst, urination and tiredness. However, in comparison, the symptoms are far less pronounced and as such the disorder may go undiagnosed for a number of years. Clinical diagnosis is usually made using a combination of the subjects fasting glucose value and their response to an oral glucose tolerance test (OGTT), as measured by their glucose levels 2 hours post glucose load (75g). The World Health Organisation (WHO) suggests that T2D be diagnosed when an individuals readings are ≥ 7 mmol/L and ≥ 11.1 mmol/l respectively (WHO, 2006). They also suggest that those individuals with fasting values ≥ 6.1 - < 7.0 mmol/L and those with 2 hour values of ≥ 7.8 – < 11.1 mmol/L be diagnosed with impaired fasting glucose (IFG) and impaired glucose tolerance (IGT) respectively (WHO, 2006). These individuals represent a pre-diabetic population who are at a significantly increased risk of developing T2D in the future and are therefore often targeted with lifestyle intervention strategies.

Treatment of T2D initially focuses on improvement of insulin sensitivity through weight loss and lifestyle changes. However, in the majority of cases, treatment with an oral

hyperglycaemic agent (OHA), or a combination of these drugs, is also required to reduce glucose levels. Treatment with metformin, an insulin sensitizer, or a thiazolidinedione, a PPAR γ agonist, may be administered initially. Metformin binds AMPK and decreases glucose output from hepatocytes and has the added benefit of limited weight gain (Kim, et al., 2008; Zhou, et al., 2001). Thiazolidinediones work by altering adipose tissue metabolism although weight gain is a side-effect observed in some patients (Fonseca, 2003; O'Moore-Sullivan and Prins, 2002; Spiegelman, 1998). One final class of OHA used to treat patients with T2D are sulfonylureas which bind to the SUR1 subunit of K_{ATP}, stimulating insulin secretion.

Treatment and medication are closely monitored on a case by case basis by physicians. Although only recently accepted as an appropriate marker for the diagnosis of diabetes by the WHO, glycated haemoglobin (HbA1c) levels are the benchmark for monitoring a patient's glycaemic control (WHO, 2006). This assessment mirrors the subject's plasma glucose levels over the past 2-3 months with HbA1c levels $\leq 6.5\%$ indicating good glycaemic control . If a patient fails to control their HbA1c levels accordingly then a change in treatment strategy should be considered.

Insulin Resistance in T2D

In patients with T2D, loss of glucose homeostasis occurs as a result of an inadequate beta-cell response to increased insulin resistance in peripheral tissues (Stumvoll, et al., 2005). Insulin resistance is believed to be caused by both a reduction in glucose disposal within myocytes as well as an increase in glucose production from the liver (Dinneen, et al., 1992). Although its onset is complex there is strong evidence to suggest that it is, at least in part, related to the effects of physical inactivity and weight gain (Zimmet, et al., 2001). Both of these factors reflect individual lifestyle choices and both, in turn, result in increased fat accumulation within adipocytes as well as ectopically. Accumulation of triglycerides directly within adipose

tissue increases the size of the cell and reduces the ability of insulin to inhibit lipolysis (Boden, 1997; Boden and Shulman, 2002). As a result, levels of circulating non-esterified fatty acids (NEFA) increase, reducing insulin sensitivity in myocytes and increasing gluconeogenesis within hepatocytes (Boden, 1997; Boden and Shulman, 2002; Shulman, 2000). The deposition of fat directly within hepatocytes and myocytes is also directly correlated with insulin resistance (Bajaj, et al., 2003; Machann, et al., 2004). Increased adipose tissue mass results not only in the release of NEFA, but also leads to an increase in the release of inflammatory cytokines (adipokines) such as tumour necrosis factor α (TNF α) (Hotamisligil, et al., 1995). TNF α acts in a paracrine manner to enhance lipolysis, thus further increasing NEFA (Boden, 1997; Patton, et al., 1986), although in addition it has also been found to exhibit its own negative effects on insulin sensitivity in skeletal muscle (Plomgaard, et al., 2005). Interestingly, levels of an insulin sensitising adipokine, adiponectin, are also reduced when NEFA levels are elevated (Goldstein and Scalia, 2004).

Beta-cell dysfunction in T2D

Pancreatic beta-cells are capable of responding to changes in insulin sensitivity by increasing their insulin output, therefore it is widely accepted that an increase in insulin resistance is initially compensated by the beta-cells (Stumvoll, et al., 2003). Progression to T2D occurs when the beta-cells can no longer meet the increased demand for insulin. Many have speculated that beta-cell dysfunction in T2D occurs simply as a result of beta-cell exhaustion due to prolonged hyperglycaemia, however other studies have since shown that defective beta-cell function has a definitive genetic basis (Prokopenko, et al., 2009a; Saxena, et al., 2007; Scott, et al., 2007; Sladek, et al., 2007; Steinthorsdottir, et al., 2007; Zeggini, et al., 2007).

Genetics of T2D

T2D is a complex, multifactorial, polygenic disorder. Within European populations the estimated sibling relative risk (λ_s) of T2D is 3 (Kobberling and Tillil, 1982). Despite the well documented heritable component, only a handful of genes had been reproducibly associated with the disorder prior to 2007, *TCF7L2* identified through classical linkage analysis and positional candidacy and *PPARG* and *KCNJ11* via the candidate gene screening approach (Altshuler, et al., 2000; Gloyn, et al., 2003; Grant, et al., 2006; Kobberling and Tillil, 1982). Following the implementation of genome-wide association studies (GWAS), and multi-centre data sharing, the number of loci significantly associated with the disorder now lies at >30, providing proof of principle that this technique is an important tool for elucidating the genetic basis of complex, common disorders (Prokopenko, et al., 2009a; Saxena, et al., 2007; Scott, et al., 2007; Sladek, et al., 2007; Steinthorsdottir, et al., 2007; WTCCC, 2007; Zeggini, et al., 2008; Zeggini, et al., 2007).

1.2.2 Monogenic disorders of beta-cell dysfunction

Rare monogenic forms of beta-cell dysfunction are caused by mutations within genes integral to beta-cell function. The disorders are themselves heterogeneous but can be subdivided into three major categories, neonatal diabetes mellitus (NDM) (both transient and permanent), maturity-onset diabetes of the young (MODY) and hyperinsulinaemic hypoglycaemia (HH). Although monogenic forms of beta-cell dysfunction account for only 1-2% of non-insulin dependent forms of diabetes (Ledermann, 1995), understanding the molecular mechanisms behind their presentation can not only tell us more about the biology of the beta-cell but enable improvement in patient care and treatment (Gloyn and Ellard, 2006).

Neonatal diabetes mellitus (NDM)

Neonatal diabetes is classically referred to as the onset of insulin-requiring diabetes within the first six months of life, which can be either permanent or transient (Shield, et al., 1997). Patients are distinguished from T1D subjects via their age at diagnosis (<6 months) as well as absence of any T1D associated auto-antibodies (Edghill, et al., 2006b; lafusco, et al., 2002).

Transient neonatal diabetes (TNDM) accounts for around 50% of all NDM cases (Flanagan, et al., 2007), and is so termed due to its remittance in early childhood (within an average of 3 months) (Mackay and Temple, 2010). However in as many as 50% of cases, diabetes is found to relapse later in life (Metz, et al., 2002; Temple, et al., 2000). Classical symptoms of TNDM include insulin-dependent hyperglycaemia and intra-uterine growth retardation (Diatloff-Zito, et al., 2007). A breakthrough in defining the genetic aetiology of TNDM came from the observation that the majority of cases are caused by abnormalities of an imprinted region on chromosome 6q24 imprinted region (Temple, et al., 1996). It is of interest that the abnormalities are due to overexpression of genes in the region rather than a loss of function (Mackay and Temple, 2010). More recently, it has also been demonstrated that TNDM can be caused by mutations within the genes encoding the beta-cell ATP dependent potassium channel (K_{ATP}), *ABCC8/KCNJ11* (Flanagan, et al., 2007; Gloyn, et al., 2005) and less frequently by mutations within *HNF1B* (Edghill, et al., 2006a)

As with TNDM, permanent neonatal diabetes mellitus (PNDM) cases present with insulin requiring diabetes within the first six months of life (Aguilar-Bryan and Bryan, 2008; Edghill, et al., 2006b), although in these cases, the disorder persists past the age of 12 months. Classical symptoms also include intrauterine growth retardation, reduced subcutaneous adipose tissue and low or undetectable C-peptide levels (Fosel, 1995). PNDM is a rare

disorder affecting approximately 1/260,000 live births (Slingerland, et al., 2009). The most common cause of PNDM are heterozygous activating mutations within *KCNJ11* or *ABCC8* (Babenko, et al., 2006; Flanagan, et al., 2006; Flanagan, et al., 2007; Gloyn, et al., 2004; Massa, et al., 2005; Sagen, et al., 2004; Vaxillaire, et al., 2004), which collectively account for approximately half of all PNDM cases. These mutations may be inherited in an autosomal dominant manner however the majority of mutations within these genes have been shown to arise de novo (Edghill, et al., 2007; Gloyn, et al., 2004; Slingerland and Hattersley, 2005). Mutations located within *KCNJ11* reduce the sensitivity of Kir6.2 to ATP, preventing channel closure and membrane depolarisation (Gloyn, et al., 2004) whilst mutations located within *ABCC8* alter sensitivity to Mg-ADP leading to an increase in channel opening and hyperpolarisation (Babenko, 2008).

Sulphonylureas have been recognised as an effective anti-hyperglycaemic agent for some time due to their ability to bind to pancreatic K_{ATP} channels, reducing potassium efflux and limiting membrane hyperpolarisation (Eliasson Science 1996). The identification of PNDM mutations within *KCNJ11*, coupled with elucidation of their molecular mechanism, led to the hypothesis that closing of K_{ATP} channels via an ATP independent mechanism may be a useful strategy for reducing hyperglycaemia in these subjects (Gloyn, et al., 2004; Pearson, et al., 2006; Sagen, et al., 2004). A number of patients were therefore transferred from their classical therapy of insulin to high-dose sulphonylureas, with many demonstrating a significant improvement in glycaemic control (Pearson, et al., 2006). The same approach has since been utilised for patients with *ABCC8* PNDM mutations with similar positive benefits observed (Rafiq, et al., 2008).

Rare mutations within other key beta-cell genes have also been shown to cause PNDM. These include homozygous, or compound heterozygous, mutations within glucokinase (*GCK*)

which are sufficiently inactivating that stimulation of glucose-stimulated insulin secretion (GSIS) cannot be reached (Njolstad, et al., 2003; Njolstad, et al., 2001), as well as both autosomal dominant and recessive mutations within the insulin gene (*INS*) itself (Edghill, et al., 2008; Garin, et al., 2010; Stoy, et al., 2007). A number of other rare causes of syndromic PNDM also exist. For example, mutations within insulin promoter factor 1 (*IPF1*) cause PNDM in association with pancreatic agenesis (Stoffers, et al., 1997b), *HNF1B* mutations cause PNDM in association with polycystic kidneys and pancreatic atrophy (Edghill, et al., 2006a; Yorifuji, et al., 2004) whilst Walcott-Rallison syndrome encompasses PNDM and spondyloepiphyseal dysplasia and is caused by mutations within the eukaryotic initiation factor 2- α kinase 3 (*EIF2AK3*) gene (Senee, et al., 2004).

Maturity-onset diabetes of the young (MODY)

MODY is used to describe an autosomal dominantly inherited form of diabetes which is non-insulin dependent and typically presents in early life (<25 years) (Tattersall, 1974). MODY is inherently a disorder of beta-cell function and to date a number of monogenic mutations have been identified in key beta-cell genes. The genetic aetiology dictates disease severity, associated complications, clinical features and treatment regimes (Ellard, et al., 2008).

The two most common causes of MODY in the UK arise from mutations in the genes encoding glucokinase (*GCK*) and the hepatocyte nuclear factor 1 homeobox A (*HNF1A*), collectively accounting for approximately 70% of all MODY cases (Ellard, et al., 2008; Frayling, et al., 1997; Froguel, et al., 1993; Hattersley, et al., 1992; Yamagata, et al., 1996). Subjects with *HNF1A*-MODY mutations experience a progressive decline in beta-cell function with age leading to diabetes in early adulthood (Frayling, et al., 1997). In early life, mutation carriers are able to maintain sufficient insulin secretion to control fasting glucose levels within the physiological range however, in response to an oral glucose challenge, they demonstrate a markedly

blunted insulin response (Byrne, et al., 1996; Stride, et al., 2002). As they age and their beta-cell function declines, so does their regulation of insulin secretion at all glucose concentrations (Byrne, et al., 1996). HNF1A-MODY has historically been misdiagnosed as T1D due to the presence of hyperglycaemia in young, lean adults and therefore patients were placed on insulin therapy from diagnosis. The observation that *HNF1A* lies upstream of the K_{ATP} channel led to the discovery that HNF1A-MODY patients are sensitive to sulphonylurea therapy (Pearson, et al., 2003). Although treatment with this oral hyperglycaemic agent is still required for life, the benefits of taking one tablet a day, apposed to 2-4 injections, is of considerable benefit to the patient (Shepherd and Hattersley, 2004; Shepherd, et al., 2003).

In contrast, GCK-MODY patients experience only mild, stable hyperglycaemia defined by fpg levels between 5.5-8mmol/L and a small increment (<3mmol/L) in 2 hour glucose levels as determined using an OGTT (Stride, et al., 2002). This defect in glucose-sensing causes a shift to the right on the dose-response curve of GSIS but their maximal insulin secretion is not altered (Byrne, et al., 1994). Patients show minimal reduction in beta-cell function with age (Frayling, et al., 2001) and are treated principally by dietary restrictions alone as oral hyperglycaemic agents and insulin have little, if any, effect on HbA1c levels (Gill-Carey, et al., 2007; Stride, et al., 2002). Individuals with GCK-MODY are often asymptomatic and therefore tend to evade clinical diagnosis unless identified during routine testing procedures, such as compulsory medical examinations or during pregnancy. Identification of the precise genetic aetiology in these subjects is however of clinical importance and can alter patient management strategies. A mother with a heterozygous *GCK* activating mutation has a 50% chance of passing the mutation to her offspring. If the foetus inherits the mutation, they also inherit a shift in their GSIS threshold, therefore they secrete insulin normally and growth persists as normal (Hattersley, et al., 1998; Velho, et al., 2000). If the foetus does not inherit the mutation then their GSIS threshold is lower than their mothers. They therefore respond

to maternal hyperglycaemia by increasing insulin secretion, consequently resulting in macrosomia (Spyer, et al., 2001). If the foetus is showing increased growth *in utero*, indicative of a *GCK* mutation, then insulin therapy will be required for the duration of the pregnancy to manage maternal hyperglycaemia and foetal growth (Spyer, et al., 2001). This is the one instance where therapeutic intervention is required for management of glycaemia in GCK-MODY patients.

Although the majority of MODY cases are accounted for by *HNF1A* and *GCK* mutations, around 30% are caused by mutations within other key beta-cell genes. These include mutations within *HNF4A*, a transcription factor within the same pathway as *HNF1A*, which therefore results in a similar phenotype (Ellard, et al., 2008). Rarer forms of MODY occur as a result of heterozygous mutations within *IPF1* (Stoffers, et al., 1997a), *NEUROD1* (Malecki, et al., 1999) and *INS* (Molven, et al., 2008). Rare mutations also exist within *CEL* and *HNF1B*, although these cause syndromic diabetes associated with pancreatic exocrine dysfunction and renal cysts respectively (Edghill, et al., 2006a; Horikawa, et al., 1997; Raeder, et al., 2006).

Hyperinsulinaemic Hypoglycaemia (HH)

HH is defined as the inappropriate oversecretion of insulin despite hypoglycaemia. It affects 1/37,000 – 1/50,000 (Glaser, et al., 2000) live births every year and its early diagnosis in neonates is critical to avoid brain damage due to prolonged hypoglycaemia (Menni, et al., 2001). It is a clinically heterogeneous disorder with the most severe cases requiring total pancreatectomy. Typical symptoms include poor feeding, irritability, macrosomia, seizures and mild facial dysmorphism in certain cases (Hussain, 2008).

HH may occur transiently or persistently (congenital). Transient cases usually occur as a compensatory mechanism to intra-uterine growth retardation whilst the persistent forms are

present from birth and continue into early childhood (Hussain, 2008). The genetic aetiology behind the persistent forms can be further subdivided into two major categories, channelopathies, caused by mutations within the K_{ATP} channel genes, or metabolopathies, caused by mutations within genes which alter the intracellular accumulation of metabolites (Hussain, 2008)

Mutations within K_{ATP} channel genes, *ABCC8* and *KCNJ11*, are the most common cause of HH (De Leon and Stanley, 2007; Thomas, et al., 1996; Thomas, et al., 1995b). These mutations alter the sensitivity of the channel to ATP and ADP, reducing channel activity (Nestorowicz, et al., 1997). Recessive *ABCC8/KCNJ11* mutations tend to cause medically unresponsive HH (Kapoor, et al., 2011) whilst dominant *ABCC8/KCNJ11* mutations generally lead to milder HH (Huopio, et al., 2000; Pinney, et al., 2008), although instances have been reported of autosomal dominant *ABCC8* mutations causing severe medically unresponsive HH (Flanagan, et al., 2011). Histological analysis should be performed on these individuals to determine the correct management strategy. If HH results from a focal lesion of hyperplastic islet cells, the likely cause is due to the loss of an imprinted maternal allele at 11p15 alongside a mutation of either *ABCC8* or *KCNJ11* on the paternal allele (Glaser, et al., 1999; Verkarre, et al., 1998). Surgery can be targeted to remove these specific lesions from the pancreas to treat the disorder. If HH is diffuse then the K_{ATP} channel defect affects beta-cells throughout the entire pancreas and may require total pancreatectomy to control hyperinsulinism.

Mutations have also been identified in key pancreatic enzymes including glucokinase (*GCK*) (Glaser, et al., 1998) and glutamate dehydrogenase 1 (*GLUD1*) (Stanley, et al., 1998). Heterozygous activating *GCK* mutations are a rare cause of HH, which function by lowering the threshold for GSIS (Christesen, et al., 2008). Increased affinity for glucose increases glycolysis and subsequent insulin secretion, however these patients benefit from their

mutations existing upstream of the K_{ATP} channel. They therefore tend to respond well to pharmacological agents such as diazoxide which bind to and open K_{ATP} channels, reducing insulin secretion (James, et al., 2009). *GLUD1* encodes the intra-mitochondrial enzyme glutamate dehydrogenase whose primary function involves the oxidative deamination of glutamate to α -ketoglutarate and ammonia (Fahien, et al., 1988). Activating *GLUD1* mutations have been identified as a cause of the unusual hyperinsulinism and hyperammonemia (HI/HA) syndrome in which children present with recurrent hypoglycaemia and elevated serum ammonia levels (Stanley, et al., 1998). Testing of ammonia levels within hypoglycaemic subjects may be utilised as a biomarker, with increased ammonia levels highly suggestive of a *GLUD1* mutation. Genetic and functional analysis has revealed that the majority of *GLUD1* mutations fall within the allosteric GTP binding domain (Stanley, et al., 2000). These mutations are sufficient to reduce the sensitivity of *GLUD1* to GTP inhibition leading to activation of the enzyme, elevated glutamate oxidation and insulin secretion accompanied by impairment of ammonia detoxification by the liver (Stanley, et al., 1998). More recently, autosomal dominant mutations within the monocarboxylate transporter (*SLC16A1*) have been shown to be a rare cause of exercise induced hyperinsulinism (Otonkoski, et al., 2007) whilst mutations within 3-hydroxyacyl-CoA dehydrogenase (*HADH*) (Clayton, et al., 2001) and *HNF4A* (Pearson, et al., 2007) have also been identified in HH probands, although the molecular mechanisms behind these later genes are as yet ill defined.

1.2.3 Investigating the genetics of non-insulin dependent diabetes

Diabetes is creating ever increasing pressures on health systems around the world. T2D is now a disorder reaching epidemic status with the world health organisation predicting 336 million will be affected by 2030 (WHO, 2011). This will itself increase the socio-economic burden via an increased demand for therapeutic OHA whilst associated micro and

macrovascular complications, including diabetic retinopathy, nephropathy, neuropathy and cardiovascular disease (Fowler, 2008), will also pose their own burden.

It is therefore of paramount importance to understand the pathophysiology behind these disorders. The observation that each of the subtypes of non-insulin dependent diabetes has a clear genetic component is of importance as it provides a practical approach to pathophysiology elucidation. Identification of genes associated with the disorders will hopefully provide further insight into the biology of pancreatic beta-cells and insulin responsive tissues. In addition, the identification of novel genes, pathways and mechanisms of regulation may also lend itself to assisting in the generation of novel therapeutic agents.

1.3 Approaches to studying the genetic component of diabetes and related metabolic traits

1.3.1 Candidate gene approach

In the era preceding the implementation of GWAS, candidate studies were a commonly used approach. It is a hypothesis-driven approach, undertaken as a direct result of the gene's location within a region of disease linkage or because the biological function of the gene fits with the disorder in question. With regards to diabetes, the major successes have come from the study of disorders with a Mendelian, early onset mode of inheritance, such as those observed in monogenic disorders of beta-cell dysfunction, where in many cases the disease and variant are found to co-segregate completely between family members.

One of the earliest linkage scans performed in hyperinsulinaemic hypoglycaemic (HH) families identified a region of linkage on chromosome 11p15.1 (Thomas, et al., 1995a). The gene encoding SUR1 (*ABCC8*), the sulfonylurea receptor, was located within this region of linkage and due to its crucial role as a component of the beta-cell K_{ATP} channel was considered a likely candidate gene. Sequencing of the gene in affected hypoglycaemic family members identified novel causal mutations (Thomas, et al., 1995b). The beta-cell K_{ATP} channel is an octameric complex composed of four SUR1 subunits and four inwardly rectifying potassium channel subunits, Kir6.2, encoded by the *KCNJ11* gene (Shyng and Nichols, 1997). Identification of HH causal mutations within the SUR1 subunit naturally led to investigation of the Kir6.2 subunit as a candidate for HH mutations (Thomas, et al., 1996). Mutations within genes encoding the K_{ATP} channel genes now account for the majority of inherited cases of HH and are routinely screened for mutations in affected individuals.

The identification of novel inactivating mutations within these genes cemented their importance in maintenance of glucose homeostasis (Thomas, et al., 1996; Thomas, et al.,

1995b). The observation that inactivating K_{ATP} gene mutations cause monogenic hypoglycaemia led a number of other research groups to hypothesise that activating mutations may be a novel cause of monogenic hyperglycaemia. This hypothesis was supported by data from a transgenic mouse model which demonstrated that rodents with reduced K_{ATP} channel sensitivity present with hyperglycaemia and hypoinsulinaemia (Koster, et al., 2000). The observation that *KCNJ11* and *ABCC8* do harbour rare activating PNDM mutations, provided proof of principle that candidate gene screening is of benefit for monogenic disorders of beta-cell function (Babenko, et al., 2006; Gloyn, et al., 2004). The observation of both activating and inactivating mutations within the same gene also highlighted the importance of common genes and common pathways for this spectrum of monogenic beta-cell dysfunction disorders (Babenko, et al., 2006; Gloyn, et al., 2004; Thomas, et al., 1995a; Thomas, et al., 1995b). Success has also been achieved using the above approach for other key beta-cell genes including *GCK*, originally identified via linkage analysis, which has since been shown to harbour both inactivating and activating mutations responsible for multiple forms of monogenic beta-cell dysfunction (Froguel, et al., 1992; Glaser, et al., 2000; Hattersley, et al., 1992; Njolstad, et al., 2001).

Determining the genetic aetiology in patients with monogenic forms of beta-cell dysfunction is of utmost importance as it can transform their treatment strategy and clinical management. For example, the identification of heterozygous *GCK* mutations in MODY patients led to the observation that insulin therapy has little, if any, benefit for their glycaemic control (Gill-Carey, et al., 2007). Since this date the advice has been to remove all *GCK*-MODY patients from insulin therapy instead managing their hyperglycaemia through diet alone (Gill-Carey, et al., 2007). Similarly the observation that activating *KCNJ11* mutations are a common cause of PNDM saw infants transferred from insulin therapy to high dose sulphonylurea with a

concomitant improvement in glycaemic control (Gloyn, et al., 2004; Pearson, et al., 2006; Sagen, et al., 2004).

The improvement to a patient's wellbeing and quality of life, achieved by simply transferring from insulin therapy to OHA or diet management, should not be underestimated. Patients with HNF1A-MODY were shown to be responsive to sulphonylureas and subsequently transferred from long-standing insulin therapy. Interviews conducted with patients found that their lifestyle and self image improved dramatically with the removal of daily insulin injections providing proof of principle that determining the genetic aetiology in these patients is of benefit clinically (Shepherd and Hattersley, 2004).

One very real difficulty faced when identifying novel causes of monogenic pancreatic beta-cell dysfunction is that the vast majority of families, in which a genetic aetiology is unknown, are limited in size and therefore statistical power. This problem has already presented itself to researchers interested in elucidating the genetic component of MODY in 23 small affected families (Frayling, et al., 2003). Their approach of combining genome-wide data from all families demonstrated a number of chromosomal candidate regions but did not identify one clear MODY gene demonstrating that the remaining cases are likely to be heterogeneous (Frayling, et al., 2003).

Identification of candidate genes in the future is likely to occur via two main routes. Firstly, our understanding is likely to rely heavily upon our increased understanding of beta-cell biology, achieved via additional genetic approaches including genome-wide association studies (GWAS). This non-hypothesis-driven approach to variant detection, although primarily utilised to identify variants associated with common traits, such as T2D, is likely to identify key beta-cell genes which may act as candidates for monogenic screening.

Historically the identification of rare variants of large effect size within key beta-cell genes has highlighted them as candidates for harbouring common variants of smaller effect size. Using this approach, substantial overlap has been observed between monogenic and related complex disorders (Agostini, et al., 2006; Altshuler, et al., 2000; Dupuis, et al., 2010; Froguel, et al., 1993; Gloyn, et al., 2004; Gloyn, et al., 2003; Weedon, et al., 2005a; Yamagata, et al., 1996). It is thought that in the future, working backwards from common variants may produce its own successes in rare variant identification. The difficulty however, is likely to lie in identifying which if any of these genes are biologically plausible and worthy of mutational screening. Secondly, as the field of next generation sequencing moves forwards, exome sequencing may be a useful approach to pathogenic variant identification. However, as the number of novel coding variants identified in this genome screen is likely to be extensive, the difficulties will lie in providing evidence of pathogenicity for any identified variant. Never the less, this methodology has already been implemented by some researchers in the field of monogenic diabetes, with Bonnefond et al identifying a novel mutation in a patient with PNDM, which had been missed by traditional Sanger sequencing (Bonnefond, et al., 2010a).

1.3.2 Genome-wide studies

Genome-wide linkage studies

As with candidate gene screening, linkage studies were traditionally used for disease gene identification and were particularly successful in identifying causal genes for monogenic disorders. For example glucokinase was identified as the first MODY gene following linkage studies in multiple large French pedigrees and in two UK pedigrees (Froguel, et al., 1992; Hattersley, et al., 1992). Similarly the first causal gene for HH was also identified following linkage to chromosome 11p14-15.1 in five consanguineous Saudi Arabian families (Thomas, et al., 1995a; Thomas, et al., 1995b).

The method utilises the presence of highly polymorphic markers (microsatellites) which are dispersed throughout the genome. Genotyping of these markers in large, multi-generation pedigrees highlights regions of the genome which co-segregate with the disease in affected individuals more commonly than would be expected by chance (Dawn Teare and Barrett, 2005). Statistical tests can be applied to the data to generate a LOD score (logarithm [base10] of odds) which assesses the likelihood of obtaining the data if the loci are linked, compared to the likelihood of obtaining the results purely by chance. A LOD score of >3 is arbitrarily considered evidence for linkage (Dawn Teare and Barrett, 2005; Morton, 1955).

Monogenic disorders of beta-cell function are often clinically well defined and are frequently caused by rare, highly penetrant mutations. They often present in early life which make the accumulation of large-scale pedigrees easier, thus increasing power to detect linkage. This is in stark contrast to complex disorders which tend to present later in life, have lower heritability, relatively imprecise definitions of phenotype and are both polygenic and multifactorial (Hirschhorn and Daly, 2005). All of these factors decrease the power of linkage studies to identify causal regions. However the accumulation of large-scale data sets, including affected sib pairs and multi-generation T2D families, accompanied by the availability of whole genome polymorphic markers and improved genotyping technology meant these studies could be undertaken for complex T2D.

Although numerous groups performed linkage analysis studies in independent cohorts, no single locus was linked to T2D. Conversely multiple peaks of linkage ($\text{LOD}>3$) were identified at a multitude of chromosomal locations including 1q25.3, 2q37.3, 3p24.1, 3q28, 10q26.13, 12q24.31, and 18p11.22 (Duggirala, et al., 1999; Ehm, et al., 2000; Hanis, et al., 1996; Hanson, et al., 1998; Mahtani, et al., 1996; Parker, et al., 2001; Vionnet, et al., 2000). Linkage to chromosome 1q was initially identified in a scan in Pima Indians who are known to have an

extremely high incidence of T2D (Hanson, et al., 1998). Additional evidence for linkage at this locus came from a number of other studies performed in American (Elbein, et al., 1999), French (Vionnet, et al., 2000) and UK (Wiltshire, et al., 2001) Caucasian subjects. Coupled with the evidence that the equivalent region of the rat chromosome is the major susceptibility locus for T2D, made this an extremely interesting region for functional follow-up (Galli, et al., 1999). Understanding linkage at this region became the basis of an international collaborative project 'Type 2 diabetes 1q consortia'. The region was found to encompass a large number of biologically plausible genes and fine mapping has since been performed to elucidate the variant driving the linkage. Common variant fine mapping failed to identify any variants contributing to the signal (Prokopenko, et al., 2009b), whilst resequencing of candidate genes within the region including liver pyruvate kinase (*PKLR*) failed to identify any coding variants which could account for the linkage (Wang, et al., 2009). Work is still currently ongoing to refine the susceptibility genes at this locus, however this acts as a useful example of how genome-wide linkage studies, in some cases, can be utilised to identify complex disease susceptibility loci.

Genome-wide association studies

Completion of the human genome sequence with subsequent identification of its haplotype structure, open access to single nucleotide polymorphism (SNP) databases and improved quality and reduced cost genotyping methods have allowed association studies to be carried out on a genome-wide scale (Gibbs, 2003; Lander, et al., 2001; Sachidanandam, et al., 2001; Venter, et al., 2001). Genome wide association studies (GWAS) are powerful tools for researchers interested in studying the genetic component of common diseases or quantifiable traits for whom the traditional approaches of linkage analysis and candidate gene screening have proved unsuccessful.

An association study requires a population for whom phenotypic information is available and on whom genotyping of a specific variant can be carried out. If there is a genotype/phenotype correlation there is said to be association between the variant and the trait (Hirschhorn and Daly, 2005). Genome-wide association studies investigate a subset of selected SNPs across the whole genome to identify associations between common variants and a particular trait or disease. Due to the high levels of linkage disequilibrium (LD) which occur across regions of the genome a minimal number of tagging SNPs from each LD block can be selected for genotyping. The high LD ($r^2 > 0.8$) of these tagging SNPs with other SNPs in the LD block are seen to be informative for the genotype of the non-typed SNPs. This significantly reduces the number of SNPs to genotype and it is thought that genotyping 500,000 to 1,000,000 SNPs in European populations is sufficient to capture 67-89% of common genetic variation (Frazer, et al., 2007).

The selection and genotyping of these carefully chosen, informative tagging SNPs across the entire genome provides researchers with an unbiased approach to genetic variation detection in thousands of individuals, a prerequisite for the common disease, common variant hypothesis (Hirschhorn and Daly, 2005). Understanding of the genetic component of T2D and related traits including fasting plasma glucose, has considerably improved since the implementation of genome-wide association studies in 2007.

Review of T2D GWAS to date

The first wave of GWAS, undertaken in 2007, was largely performed in modest cohorts of T2D patients and control chromosomes by independent research groups. Despite lack of power, these studies identified six novel loci reproducibly associated with T2D including *CDKAL1*, *HHEX* and *SLC30A8*, providing proof of principle that the method was of benefit for complex disease investigation (Saxena, et al., 2007; Scott, et al., 2007; Sladek, et al., 2007;

Steinthorsdottir, et al., 2007; WTCCC, 2007; Zeggini, et al., 2007). Although invaluable in pinpointing key T2D-associated regions of the genome, the novel loci were found to account for only a modest percentage of the heritability of T2D.

Explanations for this may be attributed to the fact that GWAS are unlikely to capture rarer variants of larger effect size or the potential overestimation of heritability; however it could also relate to the numbers of cases and controls included within the initial studies, with low sample sizes providing limited power to detect common variants of more modest effect sizes. To this end, since 2008 there has been a general consensus that combining genetic and phenotypic data from multiple centres via meta-analysis is likely to be of benefit.

This belief was held by Zeggini *et al.* who in 2008 performed a meta-analysis study of three previously published case-control studies which were part of the initial wave of T2D GWAS (Zeggini, et al., 2008). The meta-analysis combined data from the Wellcome Trust Case Control Consortium (WTCCC), Diabetes Genetics Initiative (DGI) and the Finland-United States Investigation of NIDDM Genetics (FUSION) and was referred to as the DIAGRAM (Diabetes Genetics Replication and Meta-analysis) consortium (Saxena, et al., 2007; Scott, et al., 2007; WTCCC, 2007). Through combination a significantly larger sample size (4,549 cases and 5,579 controls) was achieved providing Zeggini *et al.* with additional power to detect novel loci. As a result the consortium identified 6 novel variants (*JAZF1*, *CDC123-CAMK1D*, *TSPAN8-LGR5*, *THADA*, *ADAMTS9*, *NOTCH2*) significantly associated with T2D (Zeggini, et al., 2008).

Review of FPG GWAS to date

Chronic hyperglycaemia in the fasting state is one criterion which can be used to identify individuals with T2D (Genuth, et al., 2003). Within healthy individuals fasting glucose levels are tightly regulated within a small physiological range (4-6mmol/L) and are controlled

through complex feedback mechanisms (Mason, et al., 2007; Xiang, et al., 2006). Despite this tight regulation even healthy individuals with fpg levels at the highest end of the physiological spectrum (5.6-6mmol/L) are at increased risk of mortality and a linear correlation between FPG and coronary heart disease has been shown to extend under the threshold for diabetes (Bjornholt, et al., 1999; Coutinho, et al., 1999; Khaw, et al., 2001). Approximately one third of the inter-individual variation in FPG is believed to be heritable (Watanabe, et al., 1999). The causal genes identified to date only account for a small percentage of this heritability however it has been demonstrated that they exert their effects predominantly through beta-cell dysfunction and aberrant glucose-sensing. It was therefore postulated that the assessment of FPG as a quantitative trait in healthy individuals using a GWAS approach may not only illustrate variants affecting physiological glucose levels and shed further light on its regulation, but may also highlight important genes and pathways implicated in pathological variance in glucose levels (T2D).

In 2008 the MAGIC consortium (meta-analysis of glucose and insulin related traits consortium) was established as a collaborative effort to combine data from multiple GWAS with the aims of identifying novel variants associated with fasting glucose and related metabolic traits in the healthy, non-diabetic population (Prokopenko, et al., 2009a). Data regarding fasting glucose levels initially came from four individual consortia, the European Network for Genetic and Genomic Epidemiology [ENGAGE], Genetics of Energy Metabolism [GEM], DFS [DGI, FUSION and SARDINIA] and Framingham Heart Study [FHS]. A meta-analysis of all individual GWA studies identified the three strongest association signals as mapping close to *G6PC2*, *GCK* and *MTNR1B*, the latter of which was a previously unknown FPG locus (Prokopenko, et al., 2009a). Replication analysis has since shown the G allele at SNP rs10830963, mapping within an intron of *MTNR1B*, has an effect size of 0.07mmol/L and is also associated with

increased risk of T2D, demonstrating that the search for variants affecting quantitative traits can aid in the identification of novel disease loci (Dupuis, et al., 2010).

The future of GWAS for T2D and related traits

Identification of additional variants associated with T2D or fpg therefore seems to lie in the amalgamation of larger data sets of cases and controls via meta-analysis, providing additional power to detect common variants of more modest effect size. Although this increased power is likely to be of significant benefit, diabetes scientists will still be faced with the difficulty of refining these association signals, identifying the true causal variant and translating these variants into molecular mechanisms.

One approach to aiding signal refinement may come from the incorporation of complementary biological methods into the GWAS. These may take the form of expression quantitative trait loci (eQTL) studies, whereby novel SNPs are tested for association with transcript levels to determine which if any of the genes in the associated loci are likely to be driving the observed phenotype. Alternatively, the statisticians may benefit from information gleaned from transcript expression profiling within metabolically relevant tissues. This is likely to be of particular use when an associated loci contains multiple genes or when the signal maps to a gene of unknown biological function. For the study of T2D and related quantitative traits, expression profiling would need to take place within metabolically relevant human tissues where possible, including adipose tissue, liver, muscle, pancreas, islets and if available insulin-secreting beta-cells.

1.3.3 Insights into glucose homeostasis from mouse models

Our understanding of diabetes and its related traits have been enhanced through lessons learnt from the study of mouse models. In a laboratory in Maine in 1950, researchers

observed sporadic obesity in a subset of their mouse stock (Ingalls, et al., 1950). Affected animals demonstrated severe obesity by the age of 4-6 weeks and cross-breeding demonstrated this to be a recessive trait (Ingalls, et al., 1950). Although researchers knew little of the gene involved or the mechanisms responsible they referred to this novel gene as obese, *ob*.

This was the first example of a single gene mutation causing an obesity phenotype, however it was not until 1994 that positional cloning of the *ob* gene was performed (Zhang, et al., 1994). The study of *ob* mice demonstrated that the *ob* gene encoded an adipose tissue-specific mRNA, the translated product of which is secreted from this tissue (Zhang, et al., 1994). The protein encoded by this gene has since been named leptin. In the years following its discovery, the mechanistic action of leptin was shown to act through binding and signalling via hypothalamic receptors to suppress appetite, whilst leptin therapy in *ob/ob* mice was found to be beneficial in correcting their metabolic disturbances (Campfield, et al., 1995; Halaas, et al., 1995; Maffei, et al., 1995; Vaisse, et al., 1996). However, at this point, there was no evidence that mutations in the human leptin gene could cause obesity in humans.

In 1997, Montague *et al.* studied two cousins with severe early-onset obesity from a highly consanguineous family of Pakistani origin, in whom karyotype analysis was shown to be normal. DNA sequencing of the leptin gene however, identified the presence of a frameshift mutation resulting in generation of a premature stop codon in both affected individuals, with concomitant lack of leptin secretion (Montague, et al., 1997). The mutation was present in all four parents in the heterozygous state and homozygous in both probands confirming that this was a recessive trait. This was the first observation that mutations within the leptin gene caused the same phenotype in man as observed in rodents and confirmed the importance of leptin in maintenance of human energy balance.

Since this discovery a number of other patients have been identified carrying the same leptin mutation alongside a large Turkish family who possess a distinct leptin mutation (Farooqi, et al., 2002; Gibson, et al., 2004; Strobel, et al., 1998). Regardless of their specific mutation, all patients present with strikingly similar phenotypes. They demonstrate normal weight at birth followed by rapid weight gain within the first months of life, with adipose deposition within the subcutaneous adipose tissue predominantly on the trunk and limbs (Farooqi, et al., 2002). Affected individuals also present with excessive hyperphagia, food seeking behaviour and are often aggressive if food is unavailable. As a consequence of severe obesity, hyperinsulinaemia is also common (Farooqi, et al., 2002). Leptin therapy has since been utilised in these leptin deficient probands with dramatic effects on weight loss. Daily injections in affected individuals dramatically reduced hyperphagia and hunger scores (Farooqi, et al., 1999; Farooqi, et al., 2002). Leptin identification, mutational analysis and subsequent therapeutic use therefore provides a succinct example of how studying mouse models of a disorder is able to lead to advancements in our understanding, and subsequently aid in the treatment, of humans with related disorders.

Due to the complex, polygenic nature, of T2D many researchers have tried to establish inbred mouse models recapitulating many of the hallmarks of the disorder. The hope is that genetic analysis in these models may be used as a complementary tool to further our understanding of the human disorder. Although many of the models generated to date provide weak correlation with, and translation to, human forms of the disease, there are notable exceptions where our understanding of T2D has been aided through information gleaned from these animals.

One such model is the Goto-Kakizaki (GK) rat which was originally developed in Japan in 1976 via the cross-breeding on Wistar rats with mild glucose intolerance (Goto, et al., 1976). This spontaneous non-insulin dependent diabetic animal, demonstrating impaired insulin secretion, fasting hyperglycaemia and insulin resistance, is used routinely as a model for T2D (Goto, et al., 1976). The major T2D susceptibility locus in the GK rat has been mapped to a 52Mb locus on chromosome 1 (Galli, et al., 1999), which interestingly corresponds to the syntenic region of the human genome highlighted as a T2D susceptibility loci through linkage analysis (Hanson, et al., 1998). This locus within the GK rat was refined to identify a 16Mb segment which conferred susceptibility to impaired insulin secretion without defective insulin signalling (Lin, et al., 2001) whilst further analysis demonstrated a 1.4Mb region associated with aberrant beta-cell exocytosis (Granhall, et al., 2006; Rosengren, et al., 2010). Researchers interested in understanding the genetic component of polygenic beta-cell dysfunction believed that identification of the causal variant at this locus in rodents may also provide a useful locus for investigation in humans.

The 1.4Mb locus on rodent chromosome 1 was found to encompass five genes of which *Adra2a*, encoding the alpha2a-adrenergic receptor [$\alpha(2A)AR$], was considered the most biologically plausible (Rosengren, et al., 2010). Alpha(2A)AR suppresses insulin secretion via an adrenaline mediated mechanism. Whilst *Adra2a* knockout models have been shown to exhibit hyperinsulinaemia (Fagerholm, et al., 2004), this was the first study which highlighted a role for the receptor in the pathogenesis of diabetes. The authors postulated that naturally occurring variants within *Adra2a* may result in increased alpha(2a)AR expression thus contributing to reduced beta-cell exocytosis. Expression analysis showed that *Adra2a* mRNA levels were increased by 59% in the pancreatic islets of their GK rat strain, with a 90% increase in receptor expression (Rosengren, et al., 2010). siRNA-mediated knockdown of the receptor rescued insulin secretion in these animals (Rosengren, et al., 2010).

Translating their findings into human studies, the authors genotyped common SNPs within *ADRA2A* in a cohort of patients for whom information on insulin secretion and fasting glycaemic traits was readily available (Rosengren, et al., 2010). They observed significant association of a SNP within the 3'UTR of *ADRA2A* with increased *ADRA2A* islet mRNA and protein expression, reduced insulin levels, reduced insulin secretion and increased risk of T2D (Rosengren, et al., 2010). Their findings have since been replicated by an independent study in over 50,000 individuals, confirming association between common *ADRA2A* variants and elevated fasting plasma glucose and increased T2D susceptibility (Dupuis, et al., 2010).

This work provides a useful example of how the study of rodent models of a disorder can be of benefit to our understanding of complex, polygenic disorders. In the future, the utilisation of mouse models and information gleaned from these studies is likely to be of considerable importance, especially for those disorders in which the traditional genetic approaches (i.e. GWAS) have been of little benefit. As it currently stands, our understanding of the genetics of insulin resistance, a major component of T2D, is limited even after the implementation of GWAS. Mouse models generated to study specific components of the insulin signalling pathway may help to further our understanding of the specific regulation of this important pathway.

1.3.4 Thesis Aims

The above examples demonstrate the success of using a multidisciplinary approach to investigate the genetic component of diabetes and related complications. The aims of my thesis were therefore to use a combination of techniques and approaches to further our understanding of the genetics of diabetes and related traits.

More specifically, I aimed to use data generated from recent GWAS for T2D and related quantitative traits to select biologically plausible candidate genes for mutational screening within cohorts of patients with monogenic forms of beta-cell dysfunction. I performed transcript profiling within human islets and beta-cells as a tool to aid in the refinement of novel T2D and fpg association signals, additionally highlighting the difficulties faced in following up these signals by studying one chosen variant in a physiologically relevant system. Finally I followed up data generated from mouse models to assess the effects of phosphatase and tensin homologue deleted on chromosome ten (PTEN) in the regulation of human insulin signalling in patients with T2D.

Chapter 2

General Methods

Contents

2.1 Subjects Studied

- 2.1.1 Patient cohorts – Monogenic disorders of beta-cell function
- 2.1.2 MOLPAGE surgical collection (MoISURG) tissue biobank

2.2 Genomic DNA amplification

- 2.2.1 Primer design
- 2.2.2 PCR reaction components and cycling conditions
- 2.2.3 PCR product validation using agarose gel electrophoresis

2.3 DNA sequencing

2.4 RNA extraction

- 2.4.1 Human islet processing and storage for RNA extraction
- 2.4.2 RNA extraction from human islets
- 2.4.3 Human tissue biopsy processing & storage for RNA extraction
- 2.4.4 RNA extraction from human tissue biopsies

2.5 RNA quality determination

- 2.5.1 RNA purity testing using spectrophotometric NanoDrop™ technology
- 2.5.2 RNA Integrity Determination using Agilent Bioanalyser Technology

2.6 Reverse Transcription

- 2.6.1 Removal of Genomic Contamination from RNA using DNase I
- 2.6.2 cDNA synthesis

2.7 mRNA quantification

- 2.7.1 Taqman methodology and probe selection
- 2.7.2 Choice of analysis
- 2.7.3 Housekeeping gene selection
- 2.7.4 Standard curve generation (qRT-PCR)
- 2.7.5 Quantitative real-time PCR
- 2.7.6 qRT-PCR as a method to determine purity of human islets

2.8 Protein extraction & quantification

- 2.8.1 Protein extraction from human adipose tissue
- 2.8.2 Protein Quantification

2.9 Western Blotting

2.10 Fluorescence-activated cell sorting (FACS)

- 2.10.1 Human islet preparation

- 2.10.2 Preparation of modified Krebs buffer
- 2.10.3 FACS of human islets
- 2.10.4 FACS principles
- 2.10.5 Determination of beta-cell purity - immunocytochemistry

2.1 Subjects studied

2.1.1 Patient cohorts – Monogenic disorders of beta-cell dysfunction

Patients with monogenic disorders of beta-cell function were identified through existing collaborations with consultant molecular geneticists and clinicians at Peninsula Medical School, Exeter (Dr Sian Ellard) and Great Ormond Street Children's Hospital, London (Dr Khalid Hussain). Classification into monogenic subtypes was provided by clinicians based upon the patient's clinical phenotype and providing they met specific inclusion criteria detailed further in **Chapters 5**. DNA from maturity-onset diabetes of the young (MODY), permanent neonatal diabetes mellitus (PNDM) and hyperinsulinaemic hypoglycaemia (HH) cases were stored and screened at Peninsula Medical School, Exeter. Further details on these individuals are provided in **Chapter 5**. DNA from patients with glucokinase-like MODY were stored and screened at the Oxford Centre for Diabetes, Endocrinology and Metabolism.

Glucokinase (GCK) like-MODY

Forty two patients were identified who presented with a GCK-like MODY phenotype but in whom mutation screening of the *GCK* gene was found to be negative. The mean age of diagnosis of these individuals was 17 years [range 1-29] with all individuals presenting with FPG \geq 5.5mmol/l (mean 6.6mmol/l [range 5.5-7.8mmol/L]) and with detectable C peptide levels. The average BMI of the cohort was 23.6 kg/m² (range 14.4-40 kg/m²). In the majority of cases (27/42) the disorder was managed through diet alone however five individuals required treatment with oral hyperglycaemic agents (OHA) whilst the remaining eight were treated by insulin therapy.

2.1.2 Human tissue samples – MOLPAGE surgical collection (MoISURG)

MOLPAGE (molecular phenotyping to accelerate genomic epidemiology) was a 4 year European Union funded initiative co-ordinated from Oxford University by Professors John Bell

and Mark McCarthy. The primary aim of the project was to identify biomarkers which may highlight individuals on a trajectory to develop diabetes and vascular disease using a range of genomic, proteomic and metabonomic techniques. One component of the project undertaken at the Oxford Radcliffe Hospitals (MoISURG) focused primarily on the collection of solid tissue samples and blood from research participants undergoing elective surgery. Alongside a detailed extensive database of phenotypic data collating details on patient's medical history, diabetic status, anthropometric measurements, full blood chemistry, C-reactive protein and lipid profiles, tissue biopsy aliquots could be utilised for method development and biomarker discovery with additional replica aliquots stored for other research programmes within the consortium.

The nature of the collection programme ensured that at the end of the study a significant proportion of the patients recruited (20/110) were classed as having type 2 diabetes (T2D). Collection of tissue from these individuals in such quantities is rare for research purposes and a request for access to the resource was granted to study the expression of *PTEN* in the adipose tissue and muscle of these individuals. T2D patients were only selected if subcutaneous, visceral adipose tissue and muscle were available, reducing the numbers to 17. Extensive collection of additional phenotypic data ensured that the database could then be trawled to identify age, gender and BMI matched control subjects from the remaining 90 normoglycaemic participants. Individuals were classed as 'normoglycaemic' if they were self-reporting non-diabetic and with fpg and/or HbA1c ≤ 7 mmol/L and 6.5% respectively. HbA1c was considered a more sound method for evaluating diabetic status as it represents a measure of glucose exposure over a period of three months. Physiological stress of surgery was considered a variable which may have affected patients fasting plasma glucose values. A summary of the 34 individuals (17 pairs) used for *PTEN* expression analysis is provided in Table 2.1.

MoISURG ID	Diabetic Status	Age at Collection (years)	Gender	BMI (kg/m²)	Family history of diabetes	Fasting Glucose (mmol/L)	HbA1C (%)	Treatment Regime
OXO298	Diabetic	62	Male	24.2	No	14.2	14	Gliclazide, Metformin
OXO271	Non-Diabetic	62	Male	24.1	No	5.4	NA	-
OXO412	Diabetic	64	Female	24.1	No	7.4	6.8	None
OX1759	Non-Diabetic	65	Female	22.3	No	5.2	4.9	-
OXO713	Diabetic	61	Female	30.4	No	10.1	7.3	Metformin
OXO409	Non-Diabetic	61	Female	30.8	No	6.6	NA	-
OXO714	Diabetic	72	Male	38.3	No	13.8	10.9	Metformin
OXO716	Non-Diabetic	71	Male	29.9	No	5.0	5.4	-
OXO720	Diabetic	74	Female	24.1	Yes (paternal)	4.6	6.8	Gliclazide
OXO719	Non-Diabetic	72	Female	22.2	No	7.0	5.9	-
OXO722	Diabetic	69	Male	32.3	Yes (paternal)	11.9	8.1	Novorapid, Lantus, Metformin
OXO399	Non-Diabetic	71	Male	32.2	No	7.8	6.0	-
OXO723	Diabetic	25	Female	19.3	Yes (maternal)	6.2	6.1	Novorapid, Lantus, Metformin
OX1764	Non-Diabetic	33	Female	19.1	No	5.3	5.1	-
OXO921	Diabetic	72	Female	19.4	Yes (maternal)	13.5	9.8	Mixtard
OX1752	Non-Diabetic	76	Female	21.3	No	5.6	5.4	-
OXO923	Diabetic	71	Female	23.8	No	5.2	7.0	Rosiglitazone, Metformin
OX1780	Non-Diabetic	68	Female	23.7	Yes	4.8	5.4	-
OXO927	Diabetic	45	Male	30.8	Yes (paternal)	20.7	7.4	Metformin
OXO936	Non-Diabetic	48	Male	30.3	Yes (maternal)	6.6	5.7	-

MoISURG ID	Diabetic Status	Age at Collection (years)	Gender	BMI (kg/m²)	Family history of diabetes	Fasting Glucose (mmol/L)	HbA1C (%)	Treatment Regime
OX0930	Diabetic	56	Male	30.7	No	7.9	7.5	Insulin
OX0730	Non-Diabetic	58	Male	31.1	No	8.2	5.5	-
OX0935	Diabetic	63	Male	30.3	Yes	7.6	7.8	Insulin
OX0727	Non-Diabetic	61	Male	31.4	No	5.6	4.8	-
OX0940	Diabetic	67	Female	24.8	No	8.9	6.0	Gliclazide
OX0396	Non-Diabetic	70	Female	27.5	No	7.9	NA	-
OX0944	Diabetic	67	Male	36.6	Yes	6.4	6.3	Metformin
OX0947	Non-Diabetic	62	Male	33.7	No	6.6	5.3	-
OX0945	Diabetic	40	Male	22.1	No	6.0	8.9	Gliclazide
OX0933	Non-Diabetic	42	Male	21.3	No	7.3	5.6	-
OX1751	Diabetic	45	Female	38.1	No	16.6	10.8	Metformin, Pioglitazone
OX0929	Non-Diabetic	44	Female	38	Yes (paternal)	4.5	5.5	-
OX1762	Diabetic	74	Male	32.5	No	11.1	6.6	Metformin, Glibenclamide
OX1765	Non-Diabetic	73	Male	32.5	No	6.0	5.7	-

Table 2.1 Seventeen patients with diabetes were individually matched on the basis of age, gender and BMI to 17 normoglycaemic controls. Physiological data including fasting plasmas glucose, HbA1C and medication were available for most subjects. Patients were considered normoglycaemic if FPG \leq 7mmol/L and/or HbA1C \leq 6.5%, with HbA1C considered the more reliable measure. No normoglycaemic individuals were receiving anti-diabetic therapies. NA= not available

2.2 Genomic DNA amplification

2.2.1 Primer design

DNA sequences of novel candidate genes were identified using UCSC genome browser (<http://genome.ucsc.edu/>) (Kent, et al., 2002). Primers for DNA amplification were designed using Primer 3 software (frodo.wi.mit.edu) (Rozen and Skaletsky, 2000) ensuring coverage of all coding regions, intron/exon boundaries, 5' and 3' untranslated regions (UTRs) and a minimal region of the promoter (<1000bp). Primer pairs were selected on the basis of their length (18-27 bp), size of amplicon generated (300-700bp), melting temperature (57°C-63°C), guanine/cytosine (GC) content (40-60%) and were automatically excluded from consideration if they were found to span a single nucleotide polymorphism (SNP). Universal M13 tags (F-tgtaaacgacggccagt, R-caggaaacagctatgacc) were added for sequencing ease where possible. Specific primer pairs designed for amplification of *G6PC2* are provided in **Chapter 5**.

2.2.2 Polymerase chain reaction (PCR) components & cycling conditions

Polymerase Chain Reaction (PCR) was used to exponentially amplify fragments of genomic DNA providing sufficient quantity to perform dye-terminator DNA sequencing. Standardised in-house PCR conditions were used for amplification of all gene segments where possible utilising the hot-start properties of AmpliTaq Gold. 40ng of patient DNA was amplified in 25µl reaction volumes comprising 10X PCR Buffer II, 25mM Magnesium Chloride (Applied Biosystems, Warrington, UK), 8mM deoxynucleoside triphosphates (dNTPs) (Promega, Southampton, UK), 5pM forward and reverse primers (Operon, Ebersberg, Germany), 0.1U AmpliTaq Gold (Applied Biosystems, Warrington, UK) and sterile water (see Table 2.2 for specific volumes). Samples were denatured at 95°C for 12 minutes followed by 35 cycles of 94°C: 1 minute, specific primer annealing temperature: 1 minute, 72°: 1 minute and a final 10 minute elongation step at 72°C. Samples were stored at -20°C until required. Where

deviation from the standard cycling conditions was required for successful amplification, further details are provided in the specific chapter methodology.

PCR component	Volume
10X PCR Buffer II	2.5 μ l
25mM Magnesium Chloride	1.5 μ l
8 mM dNTPs	1 μ l
5pM Forward Primer	1 μ l
5pM Reverse Primer	1 μ l
Amplitaq Gold	0.1 μ l
Distilled water	15.9 μ l
DNA (20ng/ μ l)	2 μ l

Table 2.2 PCR reagents and volumes to be used in standard 25 μ l reaction volumes.

2.2.3 PCR product size validation using agarose gel electrophoresis

2% agarose gels were generated by dissolving 3g agarose (Sigma Aldrich, Gillingham, UK) in 150ml 1X Tris/Borate/EDTA (TBE) (NBS Biologicals, Huntingdon, UK). 4 μ l of the intercalating agent Ethidium Bromide (Sigma Aldrich, Gillingham, UK) was added to the gel prior to solidification. PCR products were mixed in equal quantities (v/v) with sample loading buffer Orange G (4g sucrose in 10ml dH₂O and 20mg Orange G [Sigma Aldrich, Gillingham, UK]) and 10 μ l loaded into wells of the pre-poured gel. Samples were run at 120V for 40 minutes alongside a 100bp ladder (New England BioLabs, Hitchin, UK) to ensure amplicons were the correct size. Gels were visualised using Ultra Violet (UV) technology on a Gel Doc illuminator system (BioRad, Hemel Hempstead, UK).

2.3 DNA Sequencing

DNA sequencing was performed bi-directionally for all samples using dye-termination methodology (Smith, et al., 1986). 1µl of PCR product was added to 0.5µl Exonuclease I (New England Biolabs, Hitchin, UK) and 0.5µl Shrimp Alkaline Phosphatase (Promega, Southampton, UK). Reactions were heated to 37°C for 30 minutes allowing enzymes to remove residual PCR contaminants, before a final 15 minute heat shock of 80°C to denature the enzymes. Samples were sequenced using Big Dye Terminator Sequencing Mix v1.1 (0.25µl) containing fluorescently labelled dideoxy nucleoside triphosphates (ddNTPs). Big Dye Dilution Buffer (1.875µl) (Applied Biosystems, Warrington, UK), 5µM M13 sequencing primers (2µl) [F-tgtaaacgacggccagt, R-caggaacagctatgacc] (Operon, Ebersberg, Germany) and sterile water (3.875µl) were also added.

All samples were amplified using 25 cycles of: 96°C: 10 seconds, 50°C: 5 seconds and 60°C: 4 minutes. Sequencing products were centrifuged at 1000xg for 2 minutes and 5µl deionised water added to each well. Samples were transferred to wells of a 96well Performa DTR V3 short clean up plate (VH Bio, Gateshead, UK) before centrifugation at 850xg for 5 minutes. Eluants were collected in a clean 96 well non-skirted PCR plate (ThermoScientific, Cramlington, UK) and dried down at 70°C for 90 minutes. Samples were run on an ABI3730xl capillary sequencer (Applied Biosystems, Warrington, UK) at the Department of Zoology, Oxford University. Fluorescence emitted by ddNTPs was detected, converted to a digital output ab1 file and sample read outs analysed against genomic reference sequences using Mutation Surveyor v3.4 (Soft genetics, Cambridge, UK). Further details are provided in

Chapter 5.

2.4 RNA Extraction

2.4.1 Human islet processing and storage for RNA extraction

Human islets were available through collaboration with Professor Paul Johnson and the Oxford Centre for Islet Transplantation (OXCI). Islets cells in suspension were transferred to a 15ml centrifuge tube before centrifugation at 300rpm for 3 minutes (4°C) to pellet. Suspension media was removed and 1X phosphate buffered saline (PBS) (Sigma Aldrich, Gillingham, UK) added to sufficiently cover the pellet. Islets were centrifuged at 300rpm for an additional 3 minutes before an additional two washes in 1X PBS were performed. Following the final wash, islets were fully re-suspended in 5 volumes of *RNAlater*[®] (Applied Biosystems, Warrington, UK) to prevent RNA degradation. Samples were kept at 4°C for 24 hours before transferring to -80°C for long term storage.

2.4.2 RNA extraction from human islets using the phenol-chloroform methodology

RNA extraction was performed using the guanidinium-thiocyanate-phenol-chloroform extraction method originally described in 1987 (Chomczynski and Sacchi, 1987) based on its sensitivity and ability to purify small RNAs (<200 nucleotides). *RNAlater*[®] preserved islets were thawed on ice before centrifugation at 600rpm for 3 minutes (4°C) to pellet the cells. If *RNAlater*[®] appeared viscous an equal volume of 1X PBS was added to dilute the solution allowing pellet formation. After removal of *RNAlater*[®], 1 ml TRIZOL (Applied Biosystems, Warrington, UK) was added to the cells. To ensure rapid inhibition of RNase activity, cells were lysed immediately by gently passing the solution ten times through a 20 gauge needle (Becton Dickinson, Oxford, UK). Following 10 minute incubation at room temperature, lysates were transferred to clean 1.5ml RNase-free centrifuge tubes (Applied Biosystems, Warrington, UK) with 200µl chloroform (FisherScientific, Loughborough, UK). Tubes were shaken vigorously for 15 seconds to begin organic and aqueous phase separation and incubated at room temperature for 5 minutes before centrifugation at 12,000xg for 10

minutes (4°C). After this time, phase separation was evident with a pink organic phenol phase at the base of the tube, DNA present in the white interphase and RNA present in the aqueous phase at the top of the tube. The aqueous phase was transferred to a clean 1.5ml RNase-free tube and 500µl isopropanol (FisherScientific, Loughborough, UK) added to precipitate out RNA. After inversion of the tube and 5 minute room temperature incubation, the solution was stored overnight at -20°C. The following day RNA/isopropanol fractions were centrifuged at 12,000xg for 50 minutes (4°C) to pellet the RNA. If a pellet was not visible after this time the samples were spun for an additional 30 minutes at the same force and temperature. Isopropanol was carefully removed ensuring the pellet was not dislodged and 1ml 75% ethanol (Sigma Aldrich, Gillingham, UK) added to wash the pellet. After centrifugation at 12,000xg for 30 minutes the same procedure was repeated with 1ml fresh ethanol. The final ethanol wash was removed and the RNA pellet allowed to air dry for 10 minutes before resuspension in 20µl RNase-free water (Ambion, Warrington, UK).

2.4.3 Human tissue biopsy processing and storage for RNA extraction

Human tissues used for the duration of the project were either obtained from patients undergoing elective surgery or through voluntary adipose tissue biopsies in study subjects. In all cases written consent was obtained from the patients. Samples obtained through surgery were provided by collaborating surgeons and handed directly to a research nurse within theatre. Samples were immediately washed in saline solution and dissected into smaller aliquots using a scalpel. Samples were placed directly into aluminium foil before snap freezing in a dewar of liquid nitrogen. Samples were then placed into labelled Cryovials (AlphaLabs, Hampshire, UK) before transferring to long term storage in liquid nitrogen tanks at OCDEM. Samples obtained through voluntary adipose tissue biopsies were collected by research nurses within the clinical research unit, OCDEM. Gluteal and abdominal biopsies were taken from the same individual following anaesthetising of the biopsy site with 50mg

lignocaine. Biopsies were washed using saline solution before sectioning into 200mg aliquots and snap freezing using liquid nitrogen.

2.4.4 RNA extraction from human tissue biopsies using phenol-chloroform extraction methodology

Samples were removed from liquid nitrogen and rapidly dissected on dry ice before transferring to 2ml eppendorf tubes with a ball bearing and 1ml TRIZOL per 100mg tissue. Tissues were homogenised for 5 minutes on the highest frequency of a Retsch free standing homogeniser (Retsch UK, Leeds, UK) to ensure total tissue ablation. Lysate was transferred to a clean 1.5ml RNase-free tube and centrifuged at 12,000xg for 20 minutes (4°C) to remove any insoluble fragments and lipids. Supernatant was removed through the lipid layer into a clean 1.5ml RNase-free tube with 200µl chloroform. From this stage onwards the RNA extraction protocol for human tissue biopsies followed the guanidinium-thiocyanate-phenol-chloroform protocol as outlined above for human islets (2.4.2).

2.5 RNA Quality Determination

Assessment of RNA quality was performed using a combination of spectrophotometric determination of RNA purity and Agilent BioAnalyser analysis of RNA integrity.

2.5.1 RNA purity testing using spectrophotometric NanoDrop™ technology

A ThermoScientific NanoDrop™ spectrophotometer was used to assess RNA purity. After setting the equipment to measure RNA using the RNA-40 programme, 1µl of nuclease free water was added to the pedestal to blank the spectrophotometer. 1µl of each sample was added sequentially to the arm of the pedestal to determine the concentration of the sample and assess purity through 260/280 and 260 /230 ratios. RNA was classified as pure if 260/280 ratio's were greater than 2 and if 260/230 values fell between 2 – 2.2.

2.5.2 RNA integrity determination using Agilent Bioanalyser technology

RNA integrity was determined using a total eukaryotic RNA 6000 nano kit (Agilent, Wokingham, UK). The chip priming station and BioAnalyser were set up according to manufacturer's instructions. Prior to analysis gel solutions were prepared through filtration in a spin column at 1500xg for 10 minutes and 65µl aliquots generated in labelled RNase free tubes. Aliquots were stable at 4°C for up to four weeks after the filtration date. To perform the analysis 1µl of RNA 6000 Nano dye concentrate was added to a 65µl aliquot of gel matrix. After centrifugation at 13,000xg for 10 minutes, 9µl was added to well 12 (G) of the RNA chip. The chip priming station was locked for 30 seconds to allow the gel to disperse throughout the chip before 9ul of gel-dye mix was added to positions 4 and 8 of the chip. 5µl of marker was added to all other wells of the chip along with 1µl of sample in wells 1 – 11 and 1µl of RNA 6000 ladder into well 16. The chip was vortexed at 2400rpm for 1 minute before placing on the BioAnalyser. Samples were drawn sequentially through micro-channels of the chip where they were injected into the separation column. RNA's were separated on the basis of

size and detected after passing through a laser and emitting fluorescence. RNA integrity was calculated using a computer derived algorithm presented as RIN scores with RIN scores >5.5 deemed acceptable.

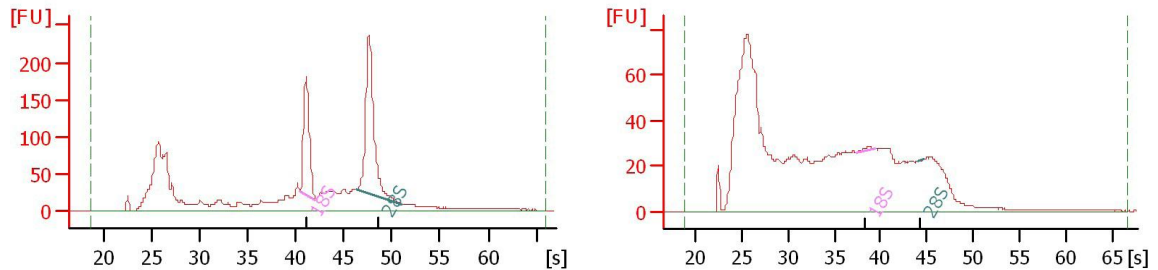


Figure 2.1 RNA integrity testing as performed by the Agilent Bioanalyser. The first trace is produced from good quality RNA generating a RIN score of 8.1 with strong identifiable peaks illustrating ribosomal 18S and 28S peaks. The trace on the right is from a sample which has experienced considerable degradation generating a RIN score of only 2.3. Identifiable peaks are no longer present and RNA would not be considered unusable.

2.6 Reverse Transcription

2.6.1 Removal of genomic contamination from RNA using DNase I

To ensure RNA samples contained no residual genomic DNA contamination all samples were subjected to DNase I (Ambion, Warrington, UK) treatment prior to cDNA synthesis. 1µl 10X DNase I buffer and DNase I were added to each sample before incubation at 37°C for 30 minutes to activate the enzyme. 2µl DNase inactivation buffer was added to each sample to halt enzyme action and reactions incubated for 2 minutes at room temperature. Samples were centrifuged at top speed in a desktop centrifuge to pellet the inactivation reagent and DNA free RNA supernatants transferred to clean tubes.

2.6.2 cDNA synthesis

Single stranded cDNA was generated from RNA using the high capacity cDNA reverse transcription kit (Applied Biosystems, Warrington, UK) containing MultiScribe™ reverse transcriptase, a recombinant Moloney murine leukaemia virus reverse transcriptase. cDNA

synthesis reactions were performed in both the presence (RT positive) and absence (RT negative) of the MultiScribe™ reverse transcriptase enzyme in a 20µl reaction volume comprising 10X Buffer, 10X reverse transcription random primers, 100mM dNTP mix and 50U reverse transcriptase (RT positive only) (Table 2.3). The additional 10µl volume comprised RNA at a total starting amount of up to 2µg. Samples were placed in a thermocycler and subjected to the following cycling conditions (optimised for the Multiscribe RT enzyme) 25°C: 10 minutes, 37°C: 120 minutes and 85°C: 5 minutes. Samples were stored at -20° until required.

cDNA synthesis	RT positive	RT Negative
10X RT Buffer	2µl	2µl
10X RT Random Primers	2µl	2µl
100mM dNTP Mix	0.8µl	0.8µl
Reverse Transcriptase 50U/µl	1µl	-
RNase free water	4.2µl	5.2µl
RNA (2µg)	10µl	10µl

Table 2.3 Reaction components for cDNA synthesis reactions RT positive and negative

2.7 mRNA Quantification

2.7.1 Taqman methodology and probe selection

Taqman technology was used for all quantitative real-time PCR (qRT-PCR) reactions due to its high specificity. The Taqman methodology adapted by Applied Biosystems for research purposes utilises oligonucleotide probes which are designed to bind between specific primer pairs. The probes themselves have a fluorophore covalently attached to the 5' end of the oligonucleotide and a quencher at the 3' end, the close proximity of which prevents emission of fluorescence from the fluorophore. 5'-3' exonuclease activity of Taq polymerase hydrolyses the oligonucleotide during PCR releasing the fluorophore from its quenched state (Holland, et al., 1991) therefore this method dictates that fluorescence will be directly proportional to the amount of fluorophore released and therefore the amount of DNA generated. Alternatively SYBR Green I is an additional method which can be used to perform qRT-PCR. SYBR Green is an intercalating agent which will emit fluorescence when bound to double stranded DNA however this agent can also fluoresce when bound to single stranded DNA and other complexes including primer dimers. The potential carcinogenic properties of this agent alongside its reduced specificity made it unsuitable for use in quantitative real-time PCR in these studies.

All gene specific primer/probes were selected from an inventoried list at Applied Biosystems where possible. To prevent non-specific amplification probes were selected on the basis that they crossed exon-exon boundaries (_m1) rather than lying within a single exon (_s1) or within genomic DNA (_g1). Specific probe identification numbers are provided in **Chapters 3, 4 and 6.**

2.7.2 Choice of analysis

Analysis methods were pre-determined before each experiment to ensure sufficient data was available for correct and accurate quantification. Of the two available quantification methods (absolute and relative), the relative comparative C_T method ($\Delta\Delta C_T$) was used in almost all cases. Fluorescence was emitted from each sample exponentially during each round of PCR. The cycle number at which fluorescence crossed a pre-determined threshold value (set in the exponential phase of the PCR reaction) was recorded for each sample as C_T values. Expression levels of target genes were determined firstly through calibration to a control sample (ΔC_T) before secondly normalising to an endogenous reference gene ($\Delta\Delta C_T$). Prior to statistical analysis the exponential C_T values were linearised using $2^{-\Delta\Delta C_T}$. For the $\Delta\Delta C_T$ to be suitable the efficiency of each assay must be similar. To test this and correct for any minor differences within our calculations, standard curves of five serial dilutions of known concentration were run alongside samples for each assay. The efficiency of each assay was calculated from the slope of the standard curve and incorporated into our calculations using $(1 + \text{Efficiency})^{-\Delta\Delta C_T}$, as originally defined by Pfaffl *et al.* (Pfaffl, 2001)

2.7.3 Housekeeping gene selection

Prior to each experiment a considerable amount of work was performed to elucidate the appropriate housekeeping genes (HKG)/endogenous references appropriate to that experiment. When determining gene expression within adipose tissue peptidylprolyl isomerase A (*PPIA*) and ubiquitin C (*UBC*) were chosen as the principle HKGs as these have robustly been shown to be stable and ubiquitously expressed within this depot (Neville, et al., 2010). Analysis of appropriate housekeeping genes for use within human islets has previously been undertaken within our laboratory (data not shown). Within this depot hypoxanthine-guanine phosphoribosyltransferase 1 (*HPRT1*), glyceraldehydes-3-phosphate dehydrogenase (*GAPDH*) and *PPIA* have been shown to be the most stably expressed

reference genes and other well established groups principally working in human islets have also found this to be the case (Yang, et al.). Selection of housekeeping genes for use across a human tissue panel is notoriously more difficult as inter-tissue variation becomes more apparent. Therefore when selecting appropriate housekeepers for this task we chose common, well established housekeepers including β -2-microglobulin (*B2M*), beta-actin (*ACTB*) and DNA topoisomerase 1 (*TOP1*) alongside previously mentioned HKG and performed test analysis prior to each experiment to select the most stable and ubiquitously expressed genes. Further explanations for the housekeeping genes selected are provided in **Chapters 3, 4** and **6**. Unless otherwise stated, at least two endogenous reference genes were used for analysis purposes as obtaining the geometric mean of carefully selected HKG has been shown to be a more accurate method of normalisation (Vandesompele, et al., 2002).

2.7.4 Standard curve generation for use in the efficiency calculation

A pool of concentrate cDNA was generated using 1 μ l of each sample to be used within the experiment. Five standards were generated through serial dilution to encompass the dilution at which the samples would be run. For example, if samples were to be run at a 1:100 dilution, standards were generated at 1:50, 1:100, 1:200, 1:400 and 1:800 using 0.01M Tris HCl. Linear regression was used to calculate a line of best fit and efficiency calculated using the equation **Efficiency = (10^[-1/slope])-1**

2.7.5 Quantitative real-time PCR (qRT-PCR)

Stock cDNA samples were diluted to reaction concentrations (predetermined prior to the experiment but normally 1:100) in Tris HCl (pH 6.8). All samples assayed with one probe were run on the same plate as the standard curve for the same assay to ensure the efficiency calculation was appropriate. 4 μ l of sample cDNA was used in 10 μ l reaction volumes with 5.5 μ l gene expression mastermix (Applied Biosystems, Warrington, UK) and 0.5 μ l gene

specific probe. Standards were used at the same volume and all were amplified in triplicate. Samples were amplified on an ABI7900 HT machine using the following amplification programme: 50°C: 2 minutes, 95°C: 10 minutes, 40 cycles of 95°C: 15 seconds and 60°C: 1 minute.

2.7.6 qRT-PCR as a method to determine human islet purity

qRT-PCR can be used as a tool to determine the purity of an islet preparation by directly comparing the expression of exocrine pancreas markers (Chymotrypsin, Amylase, alpha2A and Pancreatic Lipase) with markers of the endocrine pancreas (Somatostatin, Insulin and Glucagon). Human islet cDNAs were diluted to a starting concentration of 1:100 and 4µl used in 10µl reaction as described in 2.7.5. In total nine assays are required to determine islet purity, 3 markers of the exocrine pancreas, 3 markers of endocrine pancreas and 3 housekeeping genes (*HPRT*, *PPIA* and *GAPDH*), therefore care must be taken to ensure enough starting material is present. Samples were amplified using an ABI7900HT as mentioned previously and samples amplified alongside standard curves to calculate efficiency. $\Delta\Delta C_T$ values were generated for each islet sample and six genes of interest (3 endocrine and 3 exocrine). Geometric means were then calculated individually for the endocrine genes versus the exocrine genes and the corresponding values used to calculate the exocrine:endocrine ratio of the preparation.

Gene	Assay ID
Insulin (<i>INS</i>)	Hs00355773_m1
Glucagon (<i>GCG</i>)	Hs00174967_m1
Somatostatin (<i>SST</i>)	Hs00356144_m1
Chymotrypsin (<i>CTRB</i>)	Hs00200713_m1
Pancreatic Lipase (<i>PNLIP</i>)	Hs00609591_m1
Amylase, alpha-2A (<i>AMY2A</i>)	Hs00420710_g1

Table 2.4 Three exocrine and three endocrine markers of human pancreas with gene expression identification references (Applied Biosystems) which can be used to estimate the purity of a human islet preparation.

2.8 Protein Extraction and Quantification

2.8.1 Protein extraction from human adipose tissue

1ml ice cold lysis buffer (75mM Tris Base pH6.8, 3.8% SDS, 4M Urea, 20% glycerol) and a ball bearing were added to a 2ml eppendorf tube with 10µl Halt Protease and Phosphatase Inhibitor cocktail. Adipose tissue samples were dissected on dry ice before adding to the lysis buffer and homogenising for 5 minutes in a Retsch free standing homogeniser (Retsch UK, Leeds, UK). Samples were stored at 4°C for 2 hours on an orbital shaker ensuring constant agitation before centrifugation at 12,000xg for 15 minutes (4°C). Whole cell lysate was removed through the solid upper lipid layer into a clean tube.

2.8.2 Protein Quantification

Protein quantification was performed using the BioRad DC assay (BioRad Laboratories, Hemel Hempstead, UK), a colorimetric modification of the Lowry assay (Lowry, et al., 1951). Bovine Serum Albumin (BSA) (Serological Corporation, California, US) stock standard solutions of 1.5mg/ml were generated by dissolving BSA in cell lysis buffer and standards of 0.2, 0.5, 0.8, 1, 1.2, 1.5mg/ml generated again through dilution in cell lysis buffer. Proteins to be quantified were run at neat concentration alongside 1/1.5 and 1/2 dilutions for accurate quantification. Samples and standards were run in triplicate and 5µl plated out into Costar 96 well assay plates (Appleton Woods, Birmingham, UK). For the colorimetric reaction 25µl working reagent A (20µl detergent specific reagent S per 1ml of reagent A [alkaline copper tartrate solution]) was added to each well with 200µl reagent B (Folin reagent). Under alkaline conditions copper (Reagent A) reacts with peptide bonds of the protein generating Cu^+ , which subsequently reduces Folin reagent (Reagent B) providing the deep blue colour change proportional to the amount of protein present in the sample. The plate was incubated at room temperature for 15 minutes before reading on spectrophotometer at 650nm.

2.9 Western Blotting

Prior to western blotting all samples were diluted to a starting concentration of 1mg/ml in cell lysis buffer to ensure equal loading of protein in all wells. 15µg cell lysate was added to 5µl 4X NuPAGE LDS sample buffer (Invitrogen, Paisley, UK) and 5% beta-mercaptoethanol (Sigma Aldrich, Gillingham, UK). Mastermix's were heated to 70°C for 10 minutes ensuring reduction and denaturation of proteins. An Invitrogen Novex Mini Cell was set up containing two pre-cast Novex 4-12% Bis-Tris mini gels, 1mm, 10well (Invitrogen, Paisley, UK) and filled with 1X 2-(N-morpholino)ethanesulfonic acid (MES) running buffer, 20µl mastermix was added to wells using gel loading tips. One lane per gel was reserved for pre-stained See Blue II molecular weight marker (Invitrogen, Paisley, UK). The outer tank of the chamber was filled with 1X MES running buffer and the gels run at 200V for 45 minutes.

Proteins were transferred to polyvinylidene fluoride (PVDF) membranes using the iBlot dry blotting system, programme 3, 7 minutes. Gels were incubated overnight in Simply Blue Safe stain (Invitrogen, Paisley, UK) to assess protein transfer efficiency. PVDF membranes were washed twice in deionised water before incubating for 1 hour in blocking solution (10ml Tris buffered saline (TBS) [0.05M Tris Base pH7.5, 0.15M NaCl], 0.1% tween 20 [Sigma Aldrich, Gillingham, UK] and 5% Marvel non-fat milk). All incubations and washes took place on an orbital shaker. Membranes were washed for 3 x 10 minutes in blotting solution (TBStween) before incubation overnight at 4°C in primary antibody solution (10ml TBS, 0.1% tween 20, 5% non-fat milk, primary antibody). Following overnight incubation membranes were washed for 1 hour in blotting solution, changing every 15 minutes, before incubating for an hour in secondary antibody solution (10ml TBS, 0.1% tween 20, 5% non-fat milk, goat anti-rabbit horseradish peroxidase-linked secondary antibody [BioRad, Hemel Hempstead, UK]). Membranes were washed for 1 hour in blotting buffer, changing every 15 minutes, before incubation in 3ml SuperSignal West Pico Chemiluminescence detection substrate

(ThermoScientific, Cramlington, UK). Membranes were exposed to Amersham hyperfilm (GE Healthcare, Chalfont St Giles, UK). Semi-quantitative analysis was performed using Image J quantification (<http://rsbweb.nih.gov/ij/>). Specific antibody concentrations and blotting conditions for anti-PTEN are provided in **Chapter 6**.

2.10 Fluorescence-activated Cell Sorting (FACS)

2.10.1 Human Islet Preparation

Human islets were centrifuged in a non-stick 50ml Falcon centrifuge tube (Becton Dickinson, Oxford, UK) at 600rpm for 2 minutes to pellet the islets. Cell culture suspension media was removed and islets resuspended in 1ml human islet culture media (88ml CMRL 1066 (without glutamine), 10ml foetal calf serum, 1ml glutamine stock (2mM final concentration), 1ml HEPES stock, 500µl gentamycin, 60µl penicillin/streptomycin). Islets were plated onto polystyrene 10cm petri dishes (Becton Dickinson, Oxford, UK) at 3000 islets/petri and an additional 9ml human islet media added to each dish. Islets were stored in an incubator at 37°C overnight to allow recovery.

2.10.2 Preparation of Krebs buffer for FAC Sorting

Prior to the experiment 4X Bicarbonate HEPES Buffer was prepared using 0.1M HEPES (Sigma Aldrich, Gillingham, UK), 0.02M Sodium Chloride [NaCl] (Sigma Aldrich, Gillingham, UK) and 0.02M Sodium Bicarbonate [NaHCO₃] (FisherScientific, Loughborough, UK)}. Mixed Salts were also prepared using 0.6M Sodium Chloride [NaCl] (Sigma Aldrich, Gillingham, UK), 0.02M Potassium Chloride [KCl] (Sigma Aldrich, Gillingham, UK), 0.005M Calcium Chloride Dehydrate [CaCl₂·H₂O] (AppliChem, Lancaster, UK), 0.006M Potassium Dihydrogen Phosphate [KH₂PO₄] (Sigma Aldrich, Gillingham, UK) and 0.006M Magnesium Sulphate [MgSO₄·7H₂O] (Sigma Aldrich, Gillingham, UK). Modified Krebs-Ringer bicarbonate HEPES buffer (pH7.4) was prepared using 80ml dH₂O, 37.5ml 4X Bicarbonate HEPES Buffer and 30ml Mixed Salts with

2.8mM glucose (Sigma Aldrich, Gillingham, UK). 10ml of Krebs buffer was transferred to a separate beaker before 0.7g BSA was added to the remaining 140ml to generate Krebs+BSA (0.5%). 10ml was removed from Krebs+BSA (0.5%) and added to the pre-separated 10ml generating Krebs+BSA (0.25%). Both buffers were incubated at 37°C before FACS.

2.10.3 Preparation of islets for FACS

Following overnight recovery, islets were transferred to a 50ml non-stick falcon tube pre-coated with human islet media. Islets were centrifuged at 600rpm for 1 minute and resuspended in 1ml fresh human islet media before transferring to a pre-coated 15ml non-stick falcon tube. To wash the islets 14ml Tampon Noir (0.15M Sodium Chloride [NaCl], 0.008M Sodium Phosphate Dibasic Dihydrate [$\text{Na}_2\text{HPO}_4 \cdot 2\text{H}_2\text{O}$], 0.003M Potassium Chloride [KCl], 0.0015M Potassium Dihydrogen Phosphate [KH_2PO_4] Sigma Aldrich, Gillingham, UK) was added to the tube and islets spun at 600rpm for 1 minute. An additional 2 washes in Tampon Noir were performed ensuring the pellet was dislodged to thoroughly wash the cells. Following removal of the final Tampon Noir wash, 1ml Accutase (PAA Laboratories, Yeovil, UK) was added to disperse the islets into single cells. The reaction was incubated in a water bath (37°C) for 10 minutes ensuring agitation and dispersal of the pellet every 30 seconds. The reaction was stopped by adding Krebs+BSA (0.5%) and spinning at 800rpm for 5 minutes (repeated twice) before resuspending the pellet in 1ml Krebs+BSA (0.5%). 2 FACS tubes (Becton Dickinson, Oxford, UK) were coated with Krebs+BSA (0.5%) and labelled Newport Green (NG) or Control. 200 μl Krebs+BSA (0.5%) and 10 μl resuspended cells were added to the control tube whilst the remainder of the cells were added to the NG tube with 40 μl anti-ductal antibody (AcNCA19-9) (Novacastra, Newcastle Upon Tyne, UK) (Gmyr, et al., 2004). Both tubes were incubated at 4°C for 1 hour, resuspending the pellet every 10 minutes.

Following incubation, Krebs+BSA (0.5%) was added to the NG cells and the sample spun at 1200rpm for 5 minutes (repeated twice). The pellet was resuspended in 1ml Krebs+BSA (0.5%) and 5µl anti-mouse Alexa 633 antibody (Invitrogen, Paisley, UK). Both the NG and control tube were incubated at 4°C for an additional hour, resuspending the pellet every 10 minutes. Krebs+BSA (0.25%) was added to the NG tube following this incubation and the sample spun at 1200rpm for 5 minutes (repeated twice). 750µl Krebs+BSA (0.25%) was used to resuspend the pellet and an additional 750µl Newport Green solution (1ml Krebs+BSA (0.25%), 15µl pre-warmed pluritonic (Invitrogen, Paisley, UK), 2µl Newport green (Invitrogen, Paisley, UK) added to the resuspended pellet (Lukowiak, et al., 2001). Both the NG and control tube were incubated for 30 minutes at 37°C resuspending every 10 minutes.

1ml Krebs+BSA (0.5%) was added to the NG tube and the sample spun at 1200rpm for 5 minutes before the supernatant was removed and the pellet resuspended in a further 1ml Krebs+BSA (0.5%). 10µl 7-aminoactinomycin D (Invitrogen, Paisley, UK) was added to the NG tube and 2µl to the control tube as a means of detecting dead cells (Ichii, et al., 2005), and both tubes incubated at 4°C for 10 minutes. Krebs+BSA (0.5%) was added to both the NG and control tubes and both spun at 1200rpm for a further 5 minutes. Pellets were resuspended thoroughly in 1ml Krebs+BSA (0.5%) before straining through a 100µm filter to ensure only single cells were added to the FAC sorter. Sorting was performed using a Beckman Coulter 7 – colour MoFlo high speed cell sorter. Cells were sorted on the basis of low ductal marker expression, low 7-aad expression and high NG staining using gating parameters.

2.10.4 FACS principles

FACS can be utilised to sort a heterogeneous mixture of cells into subpopulations on a cell by cell basis. Cells are suspended in a stream of liquid and the light scattering and fluorescent characteristics of each cell detected using lasers as they travel through the stream. The laser

detection and gating systems used to obtain pure beta-cells are complex and shown in Figure 2.2. Initially a blank containing a small percentage of cells stained only with 7-AAD is used to calibrate the machine. Any fluorescence detected from this sample will indicate apoptotic cells and a gating system can be implemented to class any cells falling within this spectrum as waste (Figure 2.2, R2). This gating can then be carried over and utilised in the FACS of cells stained with AcN19-9, NG and 7-AAD.

Cells to be sorted are firstly analysed on the basis of size and complexity. A laser and detector are present within the cell sorter in line with the stream of cells and are used to detect the light scatter pattern for each individual cell. If the cells are small the photons will experience an unobstructed path through the stream with very little signal detected. Alternatively if the cells are large, the photons will diverge via diffraction and a higher intensity signal will be detected. This process is referred to as forward scatter (FSC) and the intensity of this signal generated is proportional to cell size. In addition a detector is also present perpendicular to the laser to detect side scatter (SSC). When photons strike an organelle within a cell the light is reflected at a larger angle than can be detected by the FSC detector and the presence of this side scatter detector is required. The intensity of the SSC signal is therefore proportional to cell complexity. For the sorting of human islets a gating system is used based upon FSC and SSC (Figure 2.2 – R1). Cells which have low FSC and SSC values and fall within gate R1 are automatically rejected from the sorting process as they are too small and low in complexity to be a human beta-cell. Cells are also excluded at this time if fluorescence emitted by 7-AAD falls within the limits originally established in the earlier calibration test (R2). The final exclusion of cells is based upon their staining with AcN19-9, a marker for ductal cells. The fluorophore Alexa 633 conjugated to the AcN19-9 antibody emits at 647nm when excited by a 632nm laser. Staining for ductal cells is plotted logarithmically against staining for Newport Green and cells which are high in the ductal cell marker

excluded from the analysis. Cells have up to this point been enriched in the 7-AAD and AcN19-9 negative populations. The cells are subjected to one final analysis, determining which cells to sort on the basis of Newport Green staining. Cells staining for Newport Green are excited by a laser at 495nm with maximal emission at 520nm. A logarithmic scale of NG staining is plotted against side scatter profile for the cell, providing information on staining as well as cell complexity. The cells which show the highest levels of NG staining and with the highest SSC values are likely to be the true beta-cells and are shown in gate R4, whilst cells which are slightly lower in staining and complexity (R5) are sorted into a separate tube and retained as a less pure fraction of beta-cells.

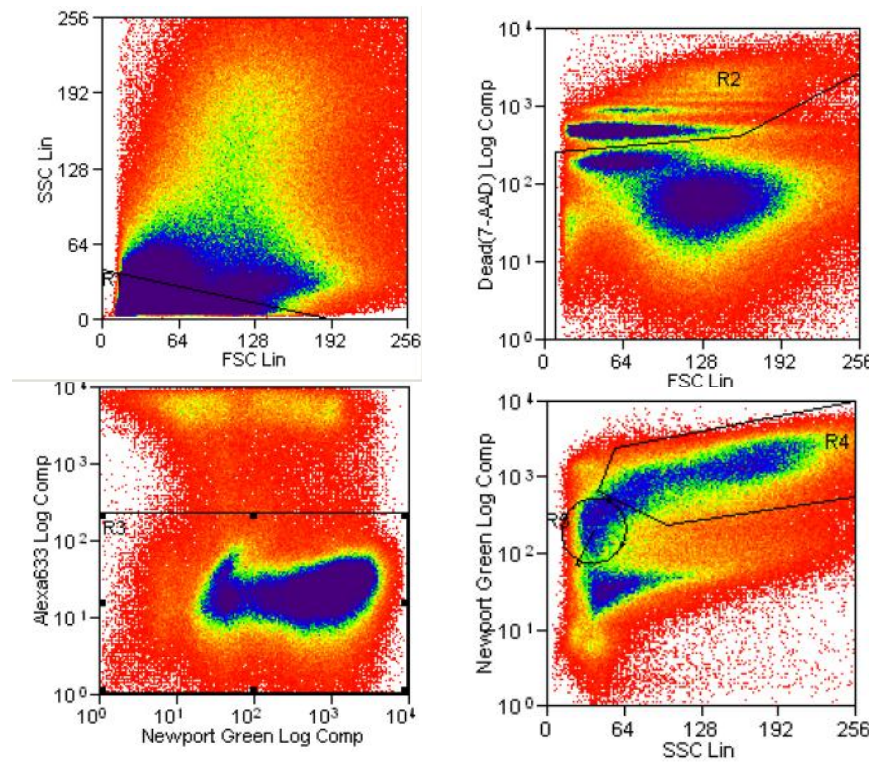


Figure 2.2 Gating systems employed on Beckman Coulter MoFlo to obtain pure beta-cells. Cells are initially rejected if their forward (FSC) and side (SSC) scatter intensities indicating cell size and complexity are low (R1). Apoptotic cells will emit fluorescence of 7-AAD at 647nm when excited by a 488nm laser. Cells with high levels of 7-AAD fluorescence are also emitted from the sorting process (R2). The final exclusion is based upon staining with a ductal cell marker AcN19-9, this fluorophores maximal emission is also at 647nm and if intensity is too high when plotted against NG staining (falling outside of gate R3) the cells are also excluded. If negative for all of the above gating properties cells are finally assessed by levels of NG fluorescence (detected at 520nm) against SSC. The cells with highest NG staining and cell complexity (SS) are pure beta-cells(R4) whereas cells which are less complex but high in NG staining (R5) are deemed less pure beta-cells.

2.10.5 Determination of beta-cell purity - Immunocytochemistry

A fraction of pure and non-pure beta-cells were saved for purity testing. Beta-cells were incubated overnight in human islet media on adherent petri dishes pre-coated in Poly-Lysine (Sigma Aldrich, Gillingham, UK). Human islet media was removed ensuring no disruption of the islets adhered to the polylysine and cells washed in 2ml PBS for 2 minutes. An additional 2 washes in PBS were performed before cells were fixed in 2% Paraformaldehyde (PFA) (Sigma Aldrich, Gillingham, UK) for 20 minutes. PBS washes were performed before cells were permeabilised for 4 minutes using 0.5% Triton (Sigma Aldrich, Gillingham, UK). Cells were washed again in PBS before incubating in PBS+BSA (0.5%) for 1 hour to block all non-specific proteins. PBS was removed and the petri dish blotted dry before cells were encircled using a hydrophobic pen (Sigma Aldrich, Gillingham, UK). Anti-glucagon and anti-insulin primary antibodies (in house) were diluted to optimised strength in PBS and 100µl of each added to the centre of the hydrophobic ring. After 2 hours incubation inside a humid chamber the primary antibodies were removed and cells washed 3 times in PBS. Secondary antibodies were diluted to working concentrations in PBS and again 100µl of each added to the centre of the hydrophobic ring. After 1 hour incubation in the dark, cells were washed 3 times in PBS, before addition of 100µl of the nuclear stain at predetermined concentration. Cells were incubated for 15 minutes in the dark. Cells were briefly washed in 3 quick changes of PBS before blotting of the petri dish. Mounting media was applied to the cells with a glass cover slip placed on top, excess liquid was removed from the petri before the cover slip was fixed in place using nail varnish. Cells were visualised using confocal microscopy with each of the nuclear, glucagon and insulin antibodies fluorescing a different colour and detectable using DAPI, Rhod and FITC.

Chapter 3

Development of a method for isolating pure human beta-cells and utilisation as a tool for interpreting GWAS signals

3.1 Introduction

3.1.1 Genome-wide association studies (GWAS) as a tool to further understand the genetic component of Type 2 diabetes (T2D) and related quantitative traits

Within European populations the estimated sibling relative risk (λ_s) of T2D is 3; clearly demonstrating that alongside environmental factors there is a large heritable component to the disorder which is as yet only modestly understood (Kobberling and Tillil, 1982; Lango, et al., 2008). Chronic hyperglycaemia in the fasting state is one criterion which can be used to identify individuals with T2D (Genuth, et al., 2003; WHO, 2006). In healthy individuals fasting plasma glucose (fpg) levels are tightly regulated within a small physiological range (4-6mmol/L) and are controlled through complex feedback mechanisms (Mason, et al., 2007; Xiang, et al., 2006). Despite this tight regulation even healthy individuals with fpg levels at the highest end of the physiological spectrum (5.6-6mmol/L) are at increased risk of mortality and a linear correlation between fpg and coronary heart disease has been shown to extend under the threshold for diabetes (Bjornholt, et al., 1999; Coutinho, et al., 1999; Khaw, et al., 2001). Approximately one third of the inter-individual variation in fpg is believed to be heritable (Watanabe, et al., 1999). It has therefore been postulated that the assessment of fpg as a quantitative trait in healthy individuals may not only identify variants affecting physiological glucose levels and shed further light on its regulation, but may also highlight important genes and pathways implicated in pathological variance in glucose levels, such as in T2D.

The large heritable component of both T2D and fpg levels dictates that elucidation of their genetic architecture may be aided through utilisation of case-control or cohort-based genome-wide association studies (GWAS) respectively. GWAS bypass the requirement for initial hypothesis generation and provide researchers with an unbiased approach to variant detection across the entire genome through genotyping of common SNPs in thousands of

individuals. Prior to 2010 multiple centres, with access to genomic DNA and phenotypic information from T2D cases and normoglycaemic controls, performed GWAS within their independent data sets (Prokopenko, et al., 2009a; Saxena, et al., 2007; Scott, et al., 2007; Steinthorsdottir, et al., 2007; WTCCC, 2007; Zeggini, et al., 2007). Novel T2D-associated loci identified in this manner collectively accounted for only ~10% of the heritability of the disorder (Bonnetfond, et al., 2010b; Lango, et al., 2008), whilst those loci associated with fpg levels accounted for <10% of the heritability of this continuous trait (Prokopenko, et al., 2009a). Explanations for this may be attributed to the inability of GWAS to capture rarer variants or the potential overestimation of heritability; however it could also be that the GWAS performed prior to this date were poorly powered to detect common variants of more modest effect sizes. To this end, the future of GWAS was postulated to lie in the ability and willingness of multiple centres to share data sets and conduct large-scale meta-analyses to identify additional susceptibility variants.

Diabetes genetics replication and meta-analysis consortium+ (DIAGRAM+):

The largest T2D meta-analysis to date

To build on the successes of their earlier 2008 meta-analysis, the DIAGRAM+ consortium, led by Voight, Scott, Steinthorsdottir, Morris and Dina under the guidance of McCarthy, Boehnke, Altschuler and Stefansson, expanded their case-control cohort to include data from 42,542 cases and 98,912 control subjects. With additional power provided by the increased sample size the geneticists were able to identify 14 loci which upon replication reached levels of genome-wide significance ($p < 5 \times 10^{-8}$) (Table 3.1).

SNP	Chr	Position	Gene	Risk Allele	Frequency	P value	OR (95%CI)
Novel susceptibility loci							
rs243021	2	60,438,323	<i>BCL11A</i>	A	0.46	2.9×10^{-15}	1.08 (1.06-1.10)
rs4457053	5	76,460,705	<i>ZBED3</i>	G	0.26	2.8×10^{-12}	1.08 (1.06-1.11)
rs972283	7	130,117,394	<i>KLF14</i>	G	0.55	2.2×10^{-10}	1.07 (1.05-1.10)
rs896854	8	96,029,687	<i>TP53INP1</i>	T	0.48	9.9×10^{-10}	1.06 (1.04-1.09)
rs13292136	9	81,141,948	<i>CHCHD9</i>	C	0.93	2.8×10^{-8}	1.11 (1.07-1.15)
rs231362	11	2,648,047	<i>KCNQ1</i>	G	0.52	2.8×10^{-13}	1.08 (1.06-1.10)
rs1552224	11	72,110,746	<i>ARAP1</i>	A	0.88	1.4×10^{-22}	1.14 (1.11-1.17)
rs1531343	12	64,461,161	<i>HMGA2</i>	C	0.10	3.6×10^{-9}	1.10 (1.07-1.14)
rs7957197	12	119,945,069	<i>HNF1A</i>	T	0.85	2.4×10^{-8}	1.07 (1.05-1.10)
rs11634397	15	78,219,277	<i>ZFAND6</i>	G	0.60	2.4×10^{-9}	1.06 (1.04-1.08)
rs8042680	15	89,322,341	<i>PRC1</i>	A	0.22	2.4×10^{-10}	1.07 (1.05-1.09)
rs5945326	X	152,553,116	<i>DUSP9</i>	G	0.21	3.0×10^{-10}	1.27 (1.18-1.37)
Previously known loci							
rs7578326	2	226,728,897	<i>IRS1</i>	A	0.64	5.4×10^{-20}	1.11 (1.08-1.13)
rs1387153	11	92,313,476	<i>MTNR1B</i>	T	0.28	7.8×10^{-15}	1.09 (1.06-1.11)

Table 3.1 DIAGRAM+ associations which exceeded the threshold for genome-wide significance ($p < 5 \times 10^{-8}$) as identified by lead statistical geneticists Voight, Scott, Steinthorsdottir, Morris and Dina. Gene names provided are those of the closest neighbouring genes.

Association signals mapping close to *MTNR1B* and *IRS1* had previously been discovered in T2D GWAS studies (Bouatia-Naji, et al., 2009; Lyssenko, et al., 2009; Prokopenko, et al., 2009a; Rung, et al., 2009) whilst signals close to *BCL11A* and *HNF1A* had also been highlighted but failed to reach genome-wide significance (Bonnycastle, et al., 2006; Weedon, et al., 2005b; Winckler, et al., 2005; Zeggini, et al., 2008). *KCNQ1* was shown to be a novel T2D gene in two East Asian GWAS populations (Unoki, et al., 2008; Yasuda, et al., 2008), although it is worth noting that the SNP identified in DIAGRAM+ was independent of these SNPs. A role for *DUSP9* in regulation of insulin action had previously been proposed following generation of a rodent model in which over-expression of this gene was shown to improve insulin sensitisation and reverse the negative effects of TNF α on insulin signalling (Emanuelli, et al., 2008). The remaining eight signals mapped close to genes which were associated with T2D for the first time by the DIAGRAM+ geneticists (Table 3.1).

Meta-analysis of glucose and insulin related traits consortium (MAGIC):

FPG meta-analysis

In 2010 the MAGIC consortium also extended their initial 2008 meta-analysis to identify novel fpg associated loci. Led by Dupuis, Langenberg, Prokopenko, Saxena and Soranzo under the guidance of Barroso, Florez and McCarthy, meta-analysis was performed in up to 46,186 non-diabetic individuals (fpg <7mmol/L) for whom information of not only fasting glucose but also fasting insulin was available. The aims were to identify novel variants affecting glycaemia within the physiological range as well as assessing the effects these novel loci had on related metabolic traits including T2D. Following replication in up to 76,558 non-diabetic individuals, my statistical collaborators led by Dupuis, identified 14 loci associated with fpg levels, nine of which were novel (Table 3.4).

The SNPs mapping close to or within *GCK*, *G6PC2*, *GCKR* and *MTNR1B* had previously been associated with fpg (Prokopenko, et al., 2009a; Saxena, et al., 2007). The association signal mapping to chromosome 7p21 fell between the genes *DGKB* and *TMEM195*. An independent study had recently highlighted an fpg association at this locus although this did not reach genome-wide significance and the authors did not assert which was the likely candidate gene (Sabatti, et al., 2009). Of the remaining 9 novel loci the association signal mapped to introns of *ADCY5*, *MADD*, *FADS1*, *CRY2* and *SLC2A2*. The novel association signal at 1q41 mapped to the promoter of *PROX1* and the association signals at 9q24 and 15q22 mapped upstream of *GLIS3* and downstream of *FAM148B* respectively. The novel association signal at 10q25 mapped within a gene desert with the closest gene (*ADRA2A*) lying 2Kb upstream.

SNP	Chr	Position	Gene	Risk	Frequency	Fasting Plasma Glucose		HOMA-B		T2D
						P value	Effect size (mmol/L)	P value	Effect HOMA-B	OR (95%CI)
Novel FPG susceptibility loci										
rs340874	1	212,225,879	<i>PROX1</i>	C	0.52	6.6×10^{-12}	0.13	5.3×10^{-6}	-0.008	1.07 (1.05-1.09)
rs11708067	3	124,548,468	<i>ADCY5</i>	A	0.78	7.1×10^{-22}	0.027	2.5×10^{-12}	-0.023	1.12 (1.09-1.15)
rs11920090	3	172,200,215	<i>SLC2A2</i>	T	0.87	8.1×10^{-13}	0.02	4.5×10^{-6}	-0.012	1.01 (0.99-1.04)
rs7034200	9	4,279,050	<i>GLIS3</i>	A	0.49	1×10^{-12}	0.018	1.2×10^{-13}	-0.020	1.03 (1.01-1.05)
rs10885122	10	113,032,083	<i>ADRA2A</i>	G	0.87	2.9×10^{-18}	0.022	2×10^{-6}	-0.010	1.04 (1.01-1.07)
rs11605924	11	45,829,667	<i>CRY2</i>	A	0.49	1×10^{-14}	0.015	3.2×10^{-5}	-0.005	1.04 (1.02-1.06)
rs7944584	11	47,292,896	<i>MADD</i>	A	0.75	2×10^{-18}	0.021	3.5×10^{-5}	-0.007	1.01 (0.99-1.03)
rs174550	11	61,328,054	<i>FADS1</i>	T	0.64	1.7×10^{-15}	0.017	5.2×10^{-13}	-0.020	1.04 (1.02-1.06)
rs11071657	15	60,221,254	<i>FAM148B</i>	A	0.63	3.6×10^{-8}	0.008	0.002	-0.013	1.03 (1.01-1.05)
Previously identified FPG loci										
rs780094	2	27,594,741	<i>GCKR</i>	C	0.62	5.6×10^{-38}	0.029	3.2×10^{-4}	0.014	1.06 (1.04-1.08)
rs560887	2	169,471,594	<i>G6PC2</i>	C	0.70	8.7×10^{-218}	0.075	1.5×10^{-66}	-0.042	0.97 (0.95-0.99)
rs2191349	7	15,030,834	<i>DGKB-</i> <i>TMEM195</i>	T	0.52	3.0×10^{-44}	0.030	2.8×10^{-17}	-0.017	1.06 (1.04-1.08)
rs4607517	7	44,202,193	<i>GCK</i>	A	0.16	6.5×10^{-92}	0.062	1.8×10^{-16}	-0.025	1.07 (1.05-1.10)
rs10830963	11	92,348,358	<i>MTNR1B</i>	G	0.30	5.8×10^{-175}	0.067	2.7×10^{-43}	-0.034	1.09 (1.06-1.12)

Table 3.2 Dupuis, Langenberg, Prokopenko, Saxena and Soranzo, as lead statistical geneticists of the MAGIC consortia, assessed fasting glycaemic traits in up to 76,558 individuals, identifying 14 loci which upon replication reached genome wide significance ($p < 5 \times 10^{-8}$) for either FPG and/or HOMA-B. Effect sizes on both fpg and HOMA-B per copy of the risk allele are provided. The gene mapping closest to the association signal is provided for ease of presentation.

3.1.2 Limitations of GWAS

Despite the huge successes attributed to GWAS, as initial work by the DIAGRAM+ and MAGIC geneticists clearly demonstrate, they are not without their limitations. For example, identification of an associated SNP within a gene does not necessarily infer causality of that gene. The haplotype structure of the human genome is such that only a proportion of SNPs are typed in a GWAS, as determining the genotype of these so-called tagging SNPs is seen to be informative of the genotypes of neighbouring SNPs within the same linkage disequilibrium (LD) block (Gabriel, et al., 2002; Johnson, et al., 2001). Therefore, when a SNP is associated with a disorder care should be taken when inferring this to be causal before further work has been performed to identify whether an additional SNP (within the same LD block) is the true variant driving the phenotype. In instances where the LD block is large and spans numerous genes the true causal variant may lay within a neighbouring gene and therefore the signal must be subjected to fine-mapping. Additionally, the lead association signal may map to an area of the genome in which no known genes are present (gene desert), to a gene of which little biological information is available or to a gene-dense region in which many biologically plausible genes reside making associations extremely difficult to explain mechanistically.

These problems were encountered by my statistical collaborators within both the DIAGRAM+ and MAGIC consortia. In the DIAGRAM+ meta-analysis, Voight provided a gene name with each of the novel association signals (Table 3.1) although these were provided as a reference point and are simply the closest gene (or the most biologically plausible) to the index SNP. In seven of the 14 associated loci the signal fell close to only one gene (*BCL11A* and *HMGA2*) or close to genes already implicated in diabetes in previous studies (*MTNR1B*, *IRS1*, *DUSP9*, *KCNQ1* and *HNF1A*). In the remaining seven loci there were multiple genes of which the authors knew little of the biology (Table 3.3).

Lead candidate gene	Chr	Position (bp)	Additional genes at susceptibility loci	Position (bp)
<i>ZBED3</i>	5	76,408,288 – 76,418,786	<i>AGGF1</i>	76,361,988 – 76,396,794
			<i>PDE8B</i>	76,542,462 – 76,758,999
<i>KLF14</i>	7	130,068,018 – 130,069,400	<i>TSGA13</i>	130,004,026 – 130,021,946
			<i>COPG2</i>	129,933,318 – 130,004,108
<i>TP53INP1</i>	8	96,007,377 – 96,030,767	<i>INTS8</i>	95,904,710 – 95,961,897
			<i>CCNE2</i>	95,961,628 – 95,976,660
<i>CHCHD9</i>	9	81,196,002 – 81,196,775	<i>TLE4</i>	81,376,698 – 81,531,478
<i>ARAP1</i>	11	72,073,762 – 72,115,821	<i>STARD10</i>	72,143,532 – 72,181,939
			<i>PDE2A</i>	71,964,833 – 72,063,060
			<i>ATG16L2</i>	72,203,099 – 72,218,328
			<i>FCHSD2</i>	72,225,439 – 72,530,739
<i>ZFAND6</i>	15	78,139,076 – 78,217,767	<i>FAH</i>	78,232,396 – 78,265,737
<i>PRC1</i>	15	89,310,272 – 89,338,808	<i>FURIN</i>	89,212,889 – 89,227,691
			<i>FES</i>	89,228,713 – 89,240,010
			<i>UNC45A</i>	89,274,414 – 89,298,327
			<i>RCCD1</i>	89,299,110 – 89,307,359
			<i>MAN2A2</i>	89,248,424 – 89,266,819
			<i>HDDC3</i>	89,275,159 – 89,276,780
			<i>VPS33B</i>	89,342,907 – 89,366,817

Table 3.3 Within seven of the novel loci the presence of a lead candidate gene was not obvious often due to the high density of genes and presence of a strong LD block at this locus. Potential candidate genes at each of the associated loci are shown above. Chromosomal positions, taken from NCBI build 36, are presented in base pairs (bp).

Dupuis and lead statistical collaborators within the MAGIC working group experienced similar difficulties. The association signal mapping to chromosome 7p21 fell between two biologically plausible candidate genes *DGKB* and *TMEM195* whilst the signal mapping to an intron of *MADD* on chromosome 11 also fell within the vicinity of an additional biological candidate gene *SLC39A13*. Many of the remaining novel fpg signals mapped to genes of which little biological information was available including *FAM148B*.

Therefore although GWAS are clearly useful in identifying loci associated with a particular trait or disorder, additional biological investigation is often required to refine and determine the true causal gene. Therefore although of considerable benefit they regularly generate further challenges regarding elucidation of molecular mechanisms driving associated phenotypes.

3.1.3 Understanding molecular mechanisms of GWAS signals

To aid in understanding, and to provide support for the epidemiological findings, it is becoming increasingly common for geneticists to utilise both biological and statistical methods to complement their GWAS analysis. These techniques can be used alongside each other to refine novel signals and elucidate molecular mechanisms.

The observation that the majority of GWAS signals identified to date lie outside of coding regions dictates that they may play important roles in gene regulation (Gilad, et al., 2008). To this end, determining the association between genetic variants and gene expression, in which gene expression is viewed as a quantitative trait, is of paramount importance. Expression quantitative trait loci (eQTL) mapping is increasingly utilised to determine whether novel genetic variants have any physiological consequences on proximal (*cis* eQTL) or distal (*trans* eQTL) gene expression (Gilad, et al., 2008). Seminal work was performed in this field in 2007 by Stranger *et al.* who performed eQTL analysis in transformed lymphoblastoid cell lines from all HAPMAP individuals (Stranger, et al., 2007). Through testing of over 2.2 million SNPs they identified 831 genes with proximal eQTL and concluded that most proximal eQTL lie close (< 100Kb) to the transcriptional start site of the regulated gene (Stranger, et al., 2007). Association testing of novel SNPs with transcript levels, both in *cis* and *trans*, is now performed routinely by numerous groups, a number of which have discovered novel

regulatory elements which will require functional follow-up (Below, et al., 2011; Small, et al., 2011).

An additional statistical tool which is of increasing importance in GWAS follow-up involves replication of novel susceptibility variants within ethnically diverse populations. The Northern European population is relatively homogeneous with large LD structures dispersed throughout the genome, making refinement of the association signals difficult. Replication within diverse populations including African, Japanese or Mexican-Americans, whose genetic background (and therefore LD structure) differ substantially, will not only confirm whether this signal confers susceptibility in distinct populations, but may also aid in refinement of the 'true' association signal. This method was of benefit to Icelandic researchers undertaking refinement of the *TCF7L2* susceptibility variant (Helgason, et al., 2007). Through studies within their own T2D case-control cohort they identified three associated SNPs within intron 3 and exon 4 of *TCF7L2*. Refinement was not aided through replication within an additional Danish cohort, however analysis within a West-African population demonstrated significant association for only one of the SNPs providing proof of principle that this technique is of significant benefit to signal refinement (Helgason, et al., 2007).

Biological methods are also becoming increasingly popular tools for signal refinement and mechanism elucidation. Detailed physiological characterisation of the novel variants may be undertaken in appropriate situations to define the significance of these variants in vivo. In the field of T2D genetics a number of similar studies have been undertaken to assess the effects of novel T2D risk alleles on insulin secretion, insulin sensitivity and surrogate measures of beta-cell function and insulin resistance in hundreds of individuals using OGTT and euglycaemic clamp data, providing further insight into how these variants are contributing to disease pathogenesis (Ingelsson, et al., 2010; Saxena, et al., 2010). Tissue

expression profiling of novel candidate genes is an additional biological tool which can provide useful information regarding transcript/tissue-specific expression if the appropriate metabolically relevant tissues are tested. For the field of T2D it is therefore pertinent to screen liver, muscle, adipose tissue and brain in the event that the variant may be affecting insulin sensitivity or obesity, alongside pancreas, islets and insulin-secreting beta-cells to assess whether the variant is likely to be acting through beta-cell dysfunction.

Accumulating evidence suggests that rodent and human islets differ considerably more than originally believed therefore dictating that, where possible, expression studies be performed in human tissues (Bosco, et al., 2010; Braun, et al., 2008; Fiaschi-Taesch, et al., 2009). Until recently access to human pancreas and islets and therefore research within these tissues was limited, however the current wealth of research into the viability of human islet transplantation has seen the evolution of several islet isolation units with human islets becoming more accessible for research purposes. Islet isolation from the pancreas by collagenase digestion is however a laborious process yielding islet preparations of varying purity, often with high levels of ductal and acinar cell contamination (Lee, et al., 2004; Street, et al., 2004). In addition even pure hand-picked islet preparations will not elucidate a clear beta-cell signal as confounding noise exists from alpha and delta cells, which are more abundant in human islets compared to rodents. Therefore the ability to isolate pure insulin-secreting human beta-cells for genetic and physiological testing is of significant interest to diabetes researchers interested in further understanding the molecular basis of beta-cell dysfunction and for those interesting in developing and testing novel beta-cell specific compounds.

3.1.4 Purification of human beta-cells

A number of groups have developed methodologies within their own laboratories to purify human beta-cells. In 2008, Marselli *et al.* published on their use of laser capture microdissection (LCM) in which they utilised the auto-fluorescent nature of beta-cells to visualise target cell populations before dissecting directly from the pancreas using lasers (Marselli, et al., 2008). The complex structure of human islets however means there is often the possibility that alpha and delta cells lie at the core of the section which would result in impure preparations (Weir, et al., 2009). The procedure is also time consuming in proportion to the low yield of beta-cells obtained and by the authors own admissions their sectioning based on auto-fluorescence is unlikely to be representative of the entire beta-cell population. Data suggests that levels of beta-cell auto-fluorescence increases proportionally with accumulation of lipofucin bodies, storage organelles of the lysosomal system which accumulate in ageing cells (Cnop, et al., 2010).

Banerjee *et al.* used magnetic sorting and differential antigenic presentation in endocrine and exocrine cells to obtain beta-cells (Banerjee and Otonkoski, 2009). Their two-step process was based on previous rodent studies in which the antigen PSA-NCAM was shown to be expressed solely by pancreatic beta-cells (Bernard-Kargar, et al., 2001). Banerjee *et al.* report the simplicity of this method over others however a pertinent observation is that unlike rodents, PSA-NCAM is present on all human islet endocrine cells (Banerjee and Otonkoski, 2009). Therefore although the authors assert that binding to beta-cells is preferential over other cell types there is potential for high levels of alpha and delta cell contamination using this technique.

To date fluorescence-activated cell sorting (FACS) is the most commonly cited method for purification of human beta-cells (Parnaud, et al., 2008). Parnaud *et al.* developed their

method through combination and adaptation of three previously reported methods (Gmyr, et al., 2004; Ichii, et al., 2005; Lukowiak, et al., 2001). It utilises the differential staining of ductal cells with anti-Ac19-9, apoptotic cells with 7-amino actinomycin D and beta-cells with the lipophilic zinc binding dye Newport Green. Through enrichment and calculated gating systems the group were able to obtain viable beta-cells with approximately 92% purity which they have reproducibly shown could be utilised in secretion, apoptosis and proliferation studies (Bouzakri, et al., 2009). Other researchers have implemented this methodology within their own laboratories performing gene expression profiling in human beta-cells (Boni-Schnetzler, et al., 2009; Kirkpatrick, et al., 2010). I applied for and was successful in obtaining an Albert Renold Travelling Fellowship award from the European Foundation for the Study of Diabetes (EFSD) allowing me to travel to the laboratories of Professor Philippe Halban (Geneva, Switzerland) to learn this technique. During this six week visit I was lucky enough to have access to a number of human islet preparations on which to learn, practice and develop the technique to be able to implement in Oxford.

3.1.5 Flow sorted beta-cells as a tool for biological refinement of GWAS signals

Regular access to human islets and pure beta-cells now provides us with a unique opportunity to perform expression profiling within these tissues. As such I was asked to join the teams led by Voight (DIAGRAM+) and Dupuis (MAGIC) to add further biological weight to their epidemiological findings. To this end the aims of the work presented in this chapter were to perform expression profiling for each of the genes falling within or close to the associated T2D and fpg loci, to firstly determine whether the genes are transcribed and expressed within human islets and beta-cells and secondly, for those loci containing multiple biological candidate genes, to aid in refinement of the signal and provide potential starting points for fine mapping studies.

3.2 Methods

3.2.1 FACS of human islets

Following overnight culture human islets were washed in Mg^{2+} and Ca^{2+} free buffer before Accutase (PAA Laboratories, Yeovil, UK) was added to disperse the islets. After incubation (37°C, 10 minutes) the reaction was halted through addition of modified Krebs-Ringer bicarbonate HEPES buffer. Dispersed cells were initially stained with mouse anti-pan-ductal cell antibody (AcNCA19-9) (Novacastra, Newcastle Upon Tyne, UK) for one hour before resuspension in buffer containing anti-mouse Alexa 633 secondary antibody (Invitrogen, Paisley, UK). Following ductal cell staining, cells were resuspended in buffer containing Newport Green, a lipophilic zinc binding dye used to selectively detect beta-cells. The final dye used to treat the cells, 7-amino actinomycin D, is a nuclear stain used as a marker for apoptosis (Invitrogen, Paisley, UK). Pellets were resuspended thoroughly in Krebs-Ringer bicarbonate HEPES buffer before sorting on a Beckman Coulter 7-colour MoFlo using parameters defined further in **Chapter 2**.

To determine purity, beta-cells were fixed in 2% paraformaldehyde (PFA) (Sigma Aldrich, Gillingham, UK) before being treated with 0.5% Triton (Sigma Aldrich, Gillingham, UK) to permeate the cells. Cells were washed in PBS before incubating in PBS+BSA (0.5%) for 1 hour to block all non-specific proteins. Anti-glucagon and anti-insulin primary antibodies (Vector Laboratories, Peterborough, UK) were diluted to optimised strength (1:500) in PBS and added to the cells. Following 2 hour incubation, primary antibodies were removed and replaced with secondary antibodies. After 1 hour, cells were washed in PBS, before addition of a nuclear stain (Invitrogen, Paisley, UK). Cells were again briefly washed in PBS before mounting medium was applied to the cells with a glass cover slip placed on top. Cells were visualised using confocal microscopy with each of the nuclear, glucagon and insulin

antibodies (attached to different fluorophore; DAPI, Rhod and FITC respectively) emitting at different wavelengths and detectable using separate filters.

3.2.2 Samples

Adult Total Pooled RNA samples (cerebellum[n=10], cortex[n=5], spleen[n=12], pancreas[n=3], lung[n=3], kidney[n=1], liver[n=1], skeletal muscle[n=2], heart[n=3], testes[n=39], adipocytes[n=3] and brain[n=1]) were purchased in the form of a commercially available tissue panel (Clontech, Oxford, UK) for mRNA expression profiling of genes within novel DIAGRAM+ and MAGIC associated loci. Adult human islets and FACS beta-cells were available through existing collaborations at Oxford University, and were obtained with full ethical consent. FACS beta-cell preparations contained >95% insulin-positive cells.

3.2.3 Probe selection

As gene expression profiling was to be splice variant independent, assays were selected on the basis of their coverage of all RefSeq genes. All gene expression assays were purchased from Applied Biosystems (Warrington, UK) and where possible, selected on the basis that the oligonucleotide probe spanned exon junctions (_m1 suffix) to reduce non-specific amplification. Assay identification numbers are provided in Table 3.3.

3.2.4 mRNA expression - Novel T2D and fpg loci in a human tissue panel

Samples were DNase I (Applied Biosystems) treated to remove residual genomic contamination before 1µg of each RNA sample was used in a random primed first strand cDNA synthesis reaction (Applied Biosystems). Full details of these protocols are provided in **Chapter 2**. Reverse transcription was also performed on all samples in the absence of the enzyme, reverse transcriptase, and these samples used as negative controls. cDNA was diluted to 1:100 in 0.01M Tris-HCl and 4µl used in a 10µl qRT-PCR reaction with 5.5µl gene

expression mastermix (Applied Biosystems) and 0.5µl gene specific assay. All samples were run in triplicate. A standard curve was generated by pooling 1µl of each cDNA, serially diluting (1:50, 1:100, 1:200, 1:400, 1:800) and running as above. Expression levels were determined with respect to the geometric mean of 3 endogenous housekeeping genes [HKG] (*B2M*, *HPRT1*, *TOP1* in the DIAGRAM+ analysis and *B2M*, *HPRT1* and *β-actin* in the MAGIC analysis). HKG are notoriously difficult to select for tissue panel testing therefore each of the HKG was screened before the experiment to determine their ubiquitous expression. Four HKG were included in each experiment although *TOP1* failed within the MAGIC and *β-actin* within the DIAGRAM+ analysis. Calibration was performed to the mean of the 1:100 standard for the assay of interest ($\Delta\Delta C_T$). For ease of presentation the maximum gene expression has been equalled to one and all other tissue expressions reported as a fraction of this.

3.2.5 mRNA expression - Novel T2D loci in flow sorted beta-cells

cDNA was generated from 150ng RNA (as RNA was limiting) and treated as above. Resulting cDNA was diluted 1:50 and 4µl used in a 10µl qRT-PCR reaction. Assays which had failed to demonstrate expression in human islets were excluded from this experiment. Analysis was performed as above. The threshold value was set to the same arbitrary value for each assay and HKG to make comparisons uniform. Relative expression was then calculated through normalisation to the housekeeping gene *B2M* and calibration to the expression of *HNF1A* within beta-cells. Genes mapping close to fpg association signals were also assessed in purified beta-cells, however due to the collaborative nature of the project this work was performed by consortia members in Lille, France and are not presented here.

MAGIC Analysis		
Gene ID	Gene Name	Assay ID
<i>ADCY5</i>	Adenylate cyclase 5	Hs00766287_m1
<i>ADRA2A</i>	Adrenergic, alpha-2A	Hs00265081_s1
<i>CRY2</i>	Cryptochrome 2 (photolyase-like)	Hs00323654_m1
<i>DGKB</i>	Diacylglycerol kinase, beta, 90KDa	Hs00391660_m1
<i>FADS1</i>	Fatty acid desaturase 1	Hs01096547_m1
<i>FAM148B</i>	Family with sequence similarity 148, member B	Hs02379187_s1
<i>GLIS3</i>	GLIS family zinc finger 3	Hs00541450_m1
<i>MADD</i>	MAP kinase activating death domain	Hs00366249_m1
<i>PROX1</i>	Prosperohomeobox 1	Hs00160463_m1
<i>SLC2A2</i>	Solute carrier family 2 (facilitated glucose transporter), member 2	Hs01096904_m1
<i>SLC39A13</i>	Solute carrier family 39 (zinc transporter), member 13	Hs00378317_m1
<i>TMEM195</i>	Transmembrane protein 195	Hs00417148_m1
DIAGRAM+ Analysis		
<i>HNF1A</i>	HNF1 homeobox A	Hs00167041_m1
<i>BCL11A</i>	B-cell CLL/lymphoma 11A (zinc finger protein)	Hs00256254_m1
<i>HMGA2</i>	High mobility group AT-hook 2	Hs00171569_m1
<i>ZBED3</i>	Zinc finger, BED-type containing 3	Hs00260688_m1
<i>AGGF1</i>	Angiogenic factor with G patch and FHA domains 1	Hs00203293_m1
<i>PDE8B</i>	Phosphodiesterase 8B	Hs00405493_m1
<i>TSGA13</i>	Testis specific, 13	Hs00364691_m1
<i>KLF14</i>	Kruppel-like factor 14	Hs00370951_s1
<i>COPG2</i>	Coatomer protein complex, subunit gamma 2	Hs00273295_m1
<i>TP53INP1</i>	Tumor protein p53 inducible nuclear protein 1	Hs01003820_m1
<i>INTS8</i>	Integrator complex subunit 8	Hs00215334_m1
<i>CCNE2</i>	Cyclin E2	Hs01051894_m1
<i>ZFAND6</i>	Zinc finger, AN1-type domain 6	Hs00375275_m1
<i>FAH</i>	Fumarylacetoacetate hydrolase	Hs00164611_m1
<i>ARAP1</i>	ArfGAP with RhoGAP domain, ankyrin repeat and PH domain 1	Hs00373707_m1
<i>STAR10</i>	StAR-related lipid transfer (START) domain containing 10	Hs00246405_m1
<i>PDE2A</i>	Phosphodiesterase 2A, cGMP-stimulated	Hs01042255_m1
<i>ATG16L2</i>	ATG16 autophagy related 16-like 2 (S.Cerevisiae)	Hs01057324_m1
<i>FCHSD2</i>	FCH and double SH3 domains 2	Hs00207952_m1
<i>FURIN</i>	Furin (paired basic amino acid cleaving enzyme)	Hs00159829_m1
<i>FES</i>	Feline sarcoma oncogene	Hs01120751_m1
<i>PRC1</i>	Protein regulator of cytokinesis 1	Hs01597831_m1
<i>UNC45A</i>	Unc-45 homolog A (C.elegans)	Hs00218751_m1
<i>RCCD1</i>	RCC1 domain containing 1	Hs00364408_m1
<i>MAN2A2</i>	Mannosidase, alpha, class 2A, member 2	Hs00196172_m1
<i>HDDC3</i>	HD domain containing 3	Hs00826828_g1
<i>VPS33B</i>	Vacuolar protein sorting 33 homolog B (yeast)	Hs00218719_m1
<i>TLE4</i>	Transducin-like enhancer of split 4 (E[spl] homolog, Drosophila)	Hs00419101_m1
<i>CHCHD9</i>	Coiled-coil-helix-coiled-coil-helix domain containing 9	Hs01892561_sH
Housekeeping Genes		
<i>B2M</i>	Beta-2-microglobulin	Hs99999907_m1
<i>HPRT</i>	Hypoxanthine Phosphoribosyltransferase 1	Hs99999909_m1
<i>B-ACTIN</i>	Beta-actin	Hs99999903_m1
<i>TOP1</i>	Topoisomerase 1	Hs01052828_m1

Table 3.4 Gene names and gene ID's of probes used to amplify genes within novel T2D and FPG associated loci as well as those used to amplify glucose transporters and all housekeeping genes. All probes were purchased from Applied Biosystems and selected on the basis that they covered all RefSeq genes and specifically amplified mRNA (_m1) where possible.

3.3 Results

3.3.1 mRNA expression profiling of genes within novel T2D loci: Human tissue panel

Expression profiling of genes within the novel loci was performed in tissues from a commercially available panel. Where possible, profiling was performed in tissues pooled from multiple donors to minimise single sample bias. However, due to donor scarcity of certain tissues, and inability to collect human samples ourselves, profiling was only performed within brain, liver and kidney was only performed in tissue from a single individual.

Expression profiling for the genes mapping close to signals on chromosome 11q21 (*MTNR1B*), 2q36 (*IRS1*), 11p15 (*KCNQ1*) and Xq28 (*DUSP9*) was not deemed necessary as the biological candidacy and/or molecular mechanisms behind these signals were considered sound at the time. I carried out gene expression profiling for all remaining loci which, upon replication, reached genome wide significance levels ($p < 5 \times 10^{-8}$).

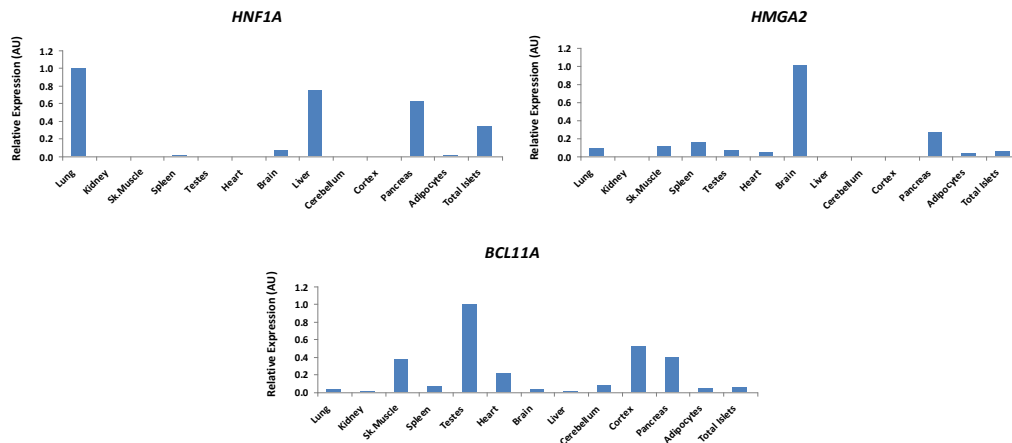


Figure 3.1 Association signals mapping to chromosomes 2p16, 12q24 and 12q14 identified *BCL11A*, *HNF1A* and *HMG2* as likely candidate genes. Expression profiles of the genes were determined in a panel of metabolically relevant tissues. Relative expression is presented in arbitrary units (AU) with highest levels of expression equalled to one and everything else presented as a fraction of this.

Signals mapping to 12q14 and 2p16 identified only *HMG2* and *BCL11A* respectively as potential susceptibility genes. Interestingly *BCL11A* had been highlighted in a previous T2D association study but failed to reach genome-wide significance (Zeggini, et al., 2008). The

same was also seen for *HNF1A* (Bonnycastle, et al., 2006; Weedon, et al., 2005b; Winckler, et al., 2005), and previous identification of rare *HNF1A* mutations as a leading cause of maturity-onset diabetes of the young (MODY) led the authors to postulate that the T2D signal mapping to 12q24 was likely working through this biologically plausible gene. Therefore at three of the novel T2D loci, only one gene was screened (Figure 3.1). Expression profiling revealed that all three of these novel susceptibility loci were expressed within the pancreas and human islets.

Chromosome 5 association signal (rs4457053)

The association signal mapping to chromosome 5q14 was situated directly upstream of *ZBED3* and downstream of *AGGF1* with an additional candidate gene *PDE8B* situated 0.1Mb away. All three genes were tested across the panel of metabolically relevant tissues (Figure 3.2). Of the three candidate genes at this locus *ZBED3* and *AGGF1* are ubiquitously expressed with maximal expression observed in liver and cortex respectively. *PDE8B* shows more selective patterns of expression with highest levels seen in cortex and testes. All three of the candidate genes were detected in both pancreas and islets at moderate levels; interestingly, *PDE8B* shows higher relative expression within islets compared to pancreas indicating this gene may be important to endocrine cells of the pancreas.

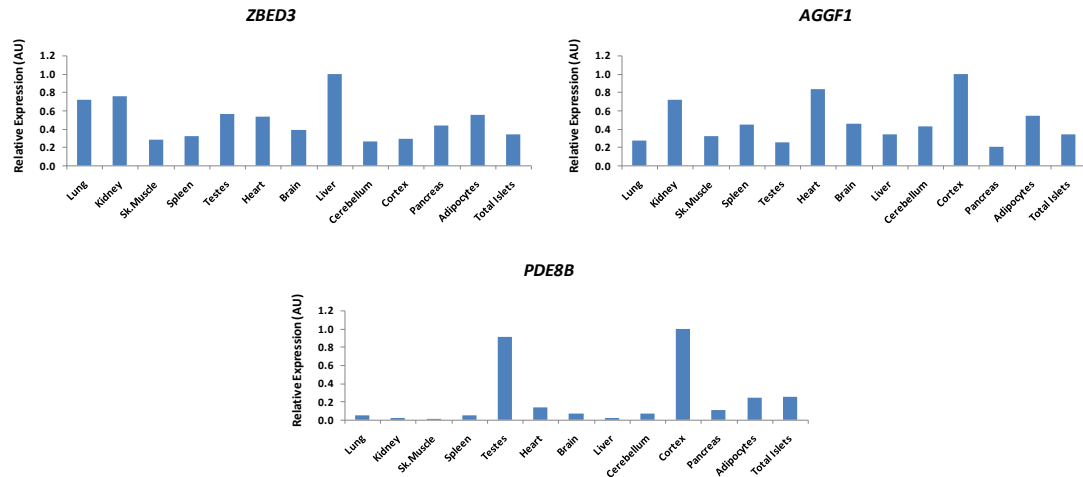


Figure 3.2 The association signal at 5q14.1 mapped close to three biologically plausible candidate genes. Expression profiling of the three candidate genes was determined across a panel of metabolically relevant tissue with maximal expression equalled to one for ease of presentation. AU = arbitrary units.

Chromosome 7 association signal (rs972283)

The association signal at chromosome 7q32 lies upstream of the single exon gene *KLF14*. A cluster of SNPs with p values $<5 \times 10^{-6}$ were also identified close to *KLF14* which were in high LD ($r^2 > 0.8$) with this index SNP. Within 0.2Mb downstream of *KLF14* lie an additional two genes *COPG2* and *TSGA13* which are transcribed in the same orientation as *KLF14* and which were included in the expression analysis to refine the causal gene (Figure 3.3). Interestingly *TSGA13* expression was only observed in brain. Of the other two candidate genes at this locus *COPG2* was seemingly ubiquitously expressed whilst *KLF14* was predominantly expressed within kidney and brain with similar levels of expression observed within skeletal muscle, adipose tissue and pancreas. Both *KLF14* and *COPG2* were expressed within human islets.

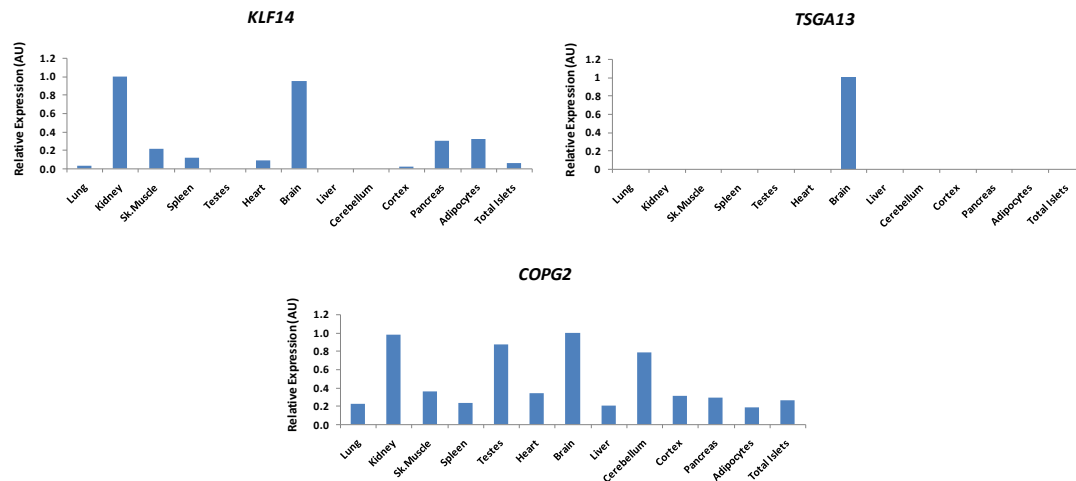


Figure 3.3 The association signal at 7q23 warranted the screening of three biologically plausible genes within 0.2Mb of the index SNP (rs972283). Expression levels were determined across metabolically relevant tissues and analysed using the $\Delta\Delta C_T$ method.

Chromosome 8 association signal (rs896854)

The association signal on chromosome 8q22 mapped to an intron of *TP53INP1*. *TP53INP1* lies within a 0.3Mb region of chromosome 8 between two recombination peaks indicating it falls within an LD block. This LD block contains a number of other genes including *CCNE2* and *INTS9* which lie downstream of *TP53INP1*. DIAGRAM+ identified a number of SNPs located across these two genes which were in LD ($r^2 > 0.6$) with the *TP53INP1* index SNP. With the presence of such a large LD block and limited biological knowledge of each of the genes it was plausible that the true causal SNP could lie within any of the highlighted genes. Of the three genes tested within this locus both *INTS8* and *TP53INP1* appear to be ubiquitously expressed. Interestingly *TP53INP1* shows maximal expression within pancreas but relatively low levels within islets. This could indicate it is playing a role within pancreatic exocrine tissue. *CCNE2* showed maximal expression within brain with comparatively lower levels in all other tissues studied.

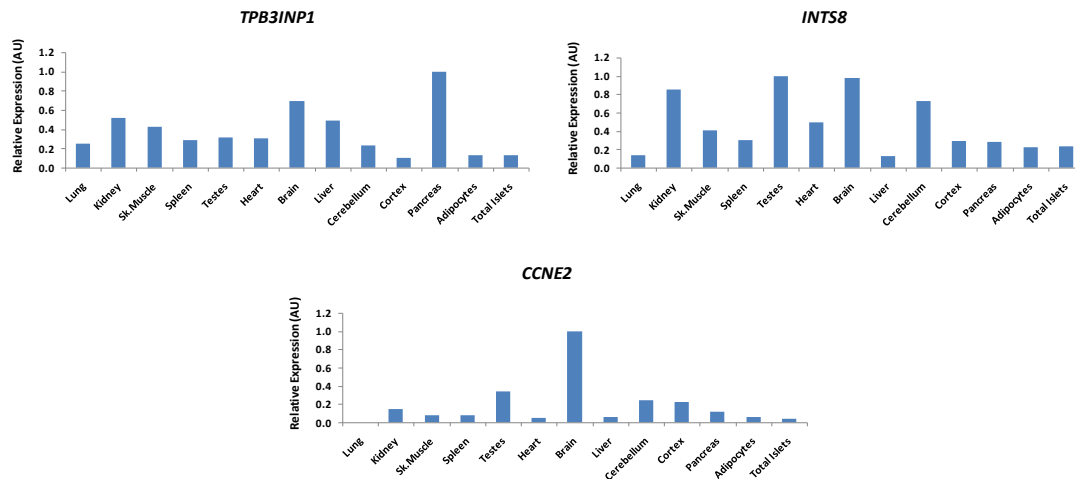


Figure 3.4 The association signal at 8q22.1 fell within a 0.3Mb LD block flanking *TP53INP1*, *INTS8* and *CCNE2*. The expression profile of each gene was ascertained within a human tissue panel through $\Delta\Delta C_T$ analysis.

Chromosome 9 association signal (rs13292136)

A peak of associated SNPs was identified on chromosome 9 around *CHCHD9* but not mapping within this gene. The only other gene in the proximity was *TLE4* and both genes were profiled across a human tissue panel. Unfortunately the *CHCHD9* assay was reproducibly shown to fail across all samples used and therefore data are not presented. *TLE4* expression was observed within all tissues tested, maximal expression was observed within brain whilst comparatively lower levels were seen in pancreas and islets. The probe used to detect *CHCHD9* is referred to as *_sH* which by definition means it was designed against a transcript with high sequence homology to *CHCHD9* but not against the gene itself. The lack of *CHCHD9* expression is likely due to probe failure however at the time of publication this was the only commercial probe available for the detection of the *CHCHD9* transcript. Therefore, using Taqman methodology, it was not possible to determine whether this gene is expressed within human islets and gene expression profiling could not be used to aid in refinement of the signal at this locus.

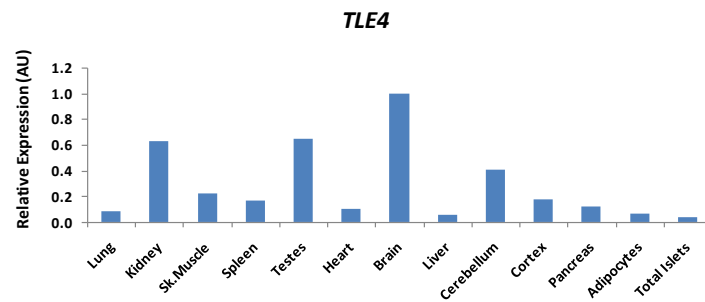


Figure 3.5 The association signal on chromosome 9 mapped to a region containing only two genes. The associated SNP did not fall within either of these genes and both were tested across a tissue panel. The expression profile of *TLE4* was analysed using $\Delta\Delta C_T$ method, *CHCHD9* assay failed across all tissues.

Chromosome 11 association signal (rs1552224)

The association signal at 11q13 mapped to the promoter of the *CENTD2* (*ARAP1*) gene. *CENTD2* however lies within a 0.6Mb region on chromosome 11 flanked by two recombination peaks. The 0.6 MB LD block contained an additional four genes (*PDE2A*, *ATG16L2*, *FCHSD2* and *STARD10*) in which additional SNPs had shown association with T2D in the DIAGRAM+ study. To elucidate which gene within this locus was likely to be driving the associated phenotype, expression analysis of all five genes was determined in human tissues. The majority of genes within this locus were ubiquitously expressed and all showed expression within both pancreas and islets, however expression of *PDE2A* was comparatively low within these depots when compared to its maximal expression within testes.

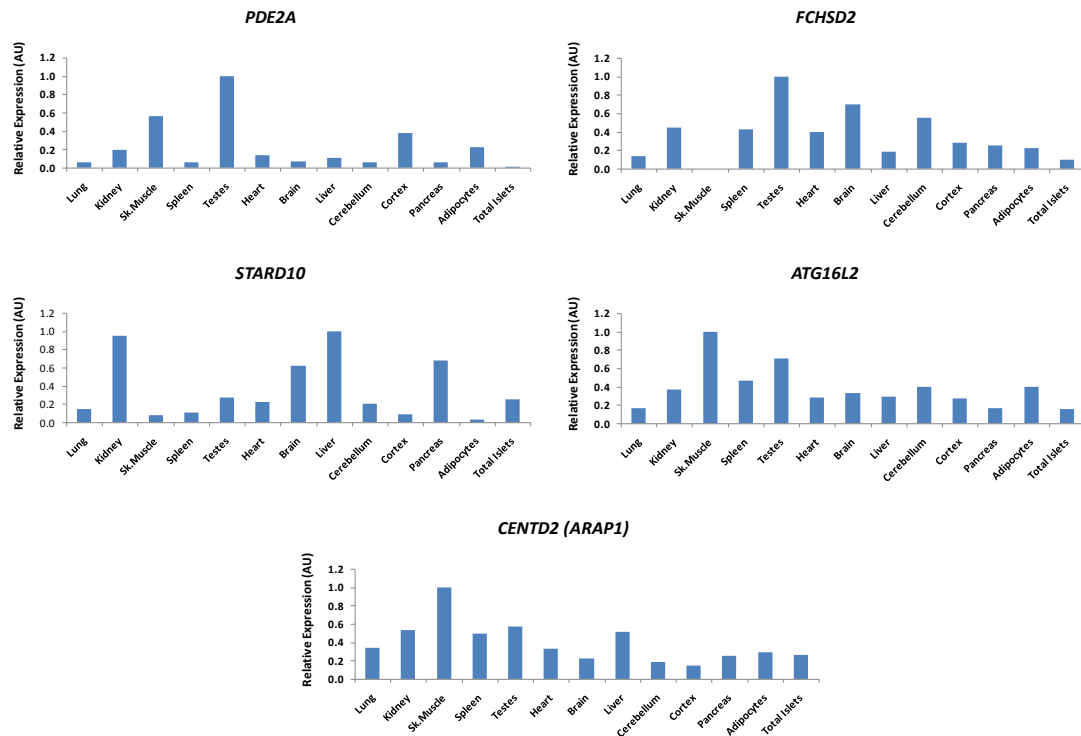


Figure 3.6 Expression analysis of the five genes within the 0.6Mb LD block on chromosome 11 to which the novel association signal (rs1552224) mapped. Analysis was performed using $\Delta\Delta C_T$ method.

Chromosome 15 association signal (rs11634397)

The association signal mapping to chromosome 15q25 lay downstream of *ZFAND6* and upstream of *FAH* between two recombination peaks. Limited knowledge of the biological role of both genes and identification within an LD block meant it necessary to determine which gene the SNP was likely to be acting through and expression profiles of both genes were determined. The expression of *ZFAND6* was relatively ubiquitous across all tissues tested with maximal expression observed within brain with comparatively lower levels within pancreas and islets. *FAH* expression was barely above background in human pancreas and islets although levels were highest within liver and adipose tissue which could suggest more of a role within insulin signalling rather than beta-cell dysfunction.

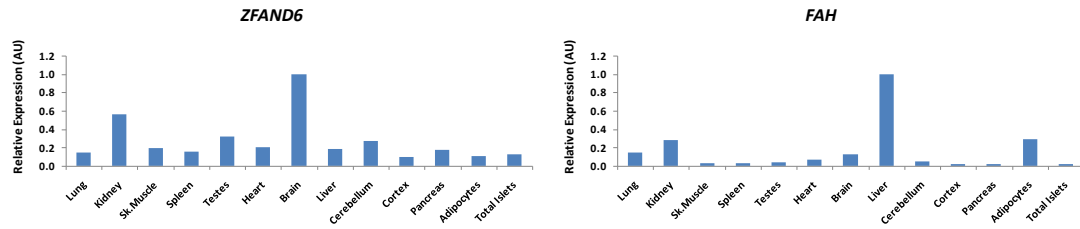


Figure 3.7 The association signal at 15q25 warranted the need to screen two potential susceptibility genes, *ZFAND6* and *FAH*. Expression profiles across a human tissue are presented for each gene with maximal tissue expression equalled to one for ease of presentation.

Chromosome 15 association signal (rs8042680)

This association signal at 15q26 mapped to an intron of *PRC1*. *PRC1* lies within a 0.25Mb region of chromosome 15 densely populated with other genes. It also represents a region of the chromosome with very low recombination rates suggesting SNPs within this region are likely to be in high LD with each other. In fact a number of other SNPs were identified in the DIAGRAM+ study across this region which were in LD ($r^2 > 0.6$) with the lead index SNP. To refine the signal, expression analysis of the eight genes within this region (*PRC1*, *FURIN*, *FES*, *UNC45A*, *RCCD1*, *MAN2A2*, *HDDC3* and *VPS33B*) was performed. *PRC1* and *FES* were expressed at comparatively low levels within human islets when compared with their maximal expression within brain and skeletal muscle respectively. *VPS33B* was not expressed at all within the pancreas or human islets. All other genes tested appear to be ubiquitously expressed with *UNC45A* and *FURIN* showing relatively high expression levels within human islets. The probe designed to detect *HDDC3* could not be validated and therefore no results were obtained for its expression across the tissue panel. In light of this we cannot rule *HDDC3* out as the causal gene.

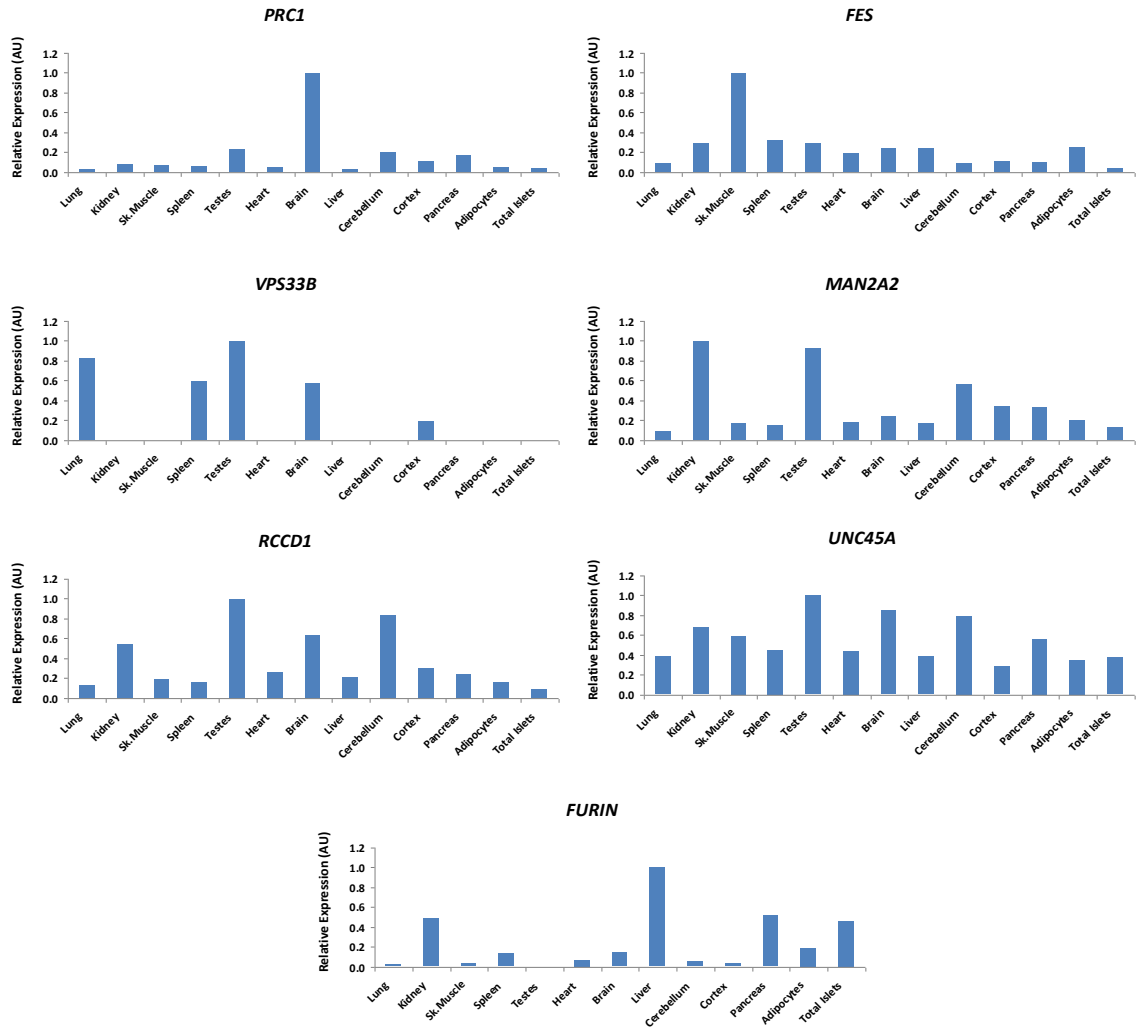


Figure 3.8 The novel association signal on chromosome 15 mapped to a 0.25Mb LD block encompassing eight genes. Expression levels of the potential susceptibility genes were determined across a human tissue panel and maximal expression equalled to one for ease of presentation. Expression of *HDDC3* is not presented due to probe failure.

3.3.2 mRNA expression profiling of genes close to novel T2D loci: Human islets

The potential susceptibility genes analysed to date have been compared within a human tissue panel, but to determine the effect and relative expression within human islets, the expression data were re-analysed within this one tissue. The $\Delta\Delta C_T$ method was used after ensuring threshold values were set to an arbitrary value for each assay (although not absolute quantification, this re-analysis should allow a trend to become evident within the data).

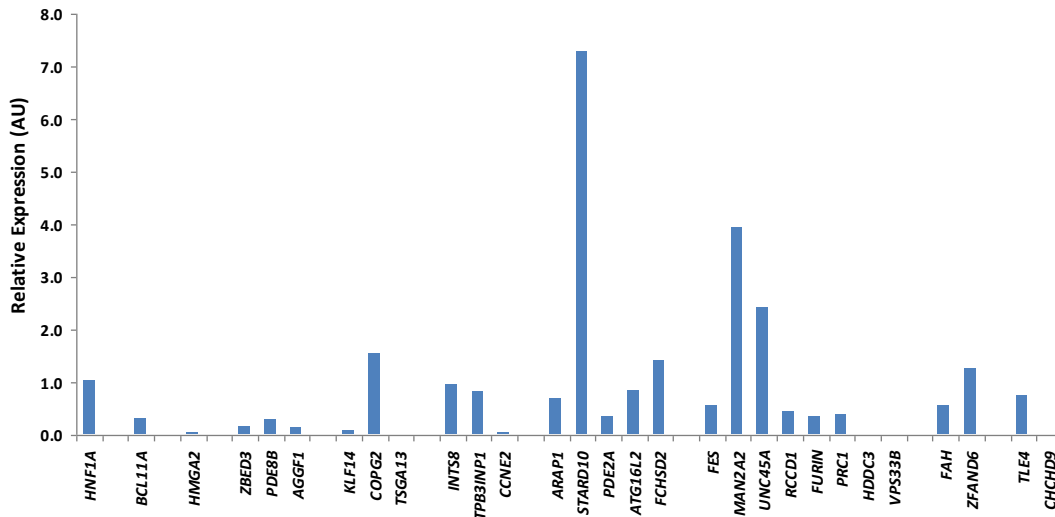


Figure 3.9 Relative expression of novel T2D loci within human islets when analysed using $\Delta\Delta C_T$ method, normalising to the mean of three housekeeping genes and making relative to the raw Ct of *HNF1A* (which we already know to be highly expressed within human islets). Genes have been grouped into novel loci for ease of presentation.

Within the 11q13 and 15q26 loci expression analysis elucidates that the association may be driven by variants within *STARD10* and *MAN2A2/UNC5A* respectively as these genes are expressed far in excess of any other genes within their respective loci. Lead candidate genes within other loci are not as evident with all three genes studied within the 5q14 loci (*ZBED3*, *PDE8B* and *AGGF1*) showing similarly low levels of expression.

3.3.3 mRNA expression profiling of genes close to novel T2D loci: Human beta-cells

The observation that the majority of genes within the associated loci were expressed within human islets was somewhat surprising. At this stage in the expression profiling it was expected that only a small subset of genes would warrant screening within human flow sorted beta-cells, instead we are able to only eliminate four genes. Our data are however supported by data from other members of the consortia (Lang & Groop, DIAGRAM+) who studied the expression of all loci within human islets using a micro-array based approach. Using this method they were unable to rule out genes based on lack of expression within

human islets, although at the time this was believed to be due to reduced sensitivity of the method used.

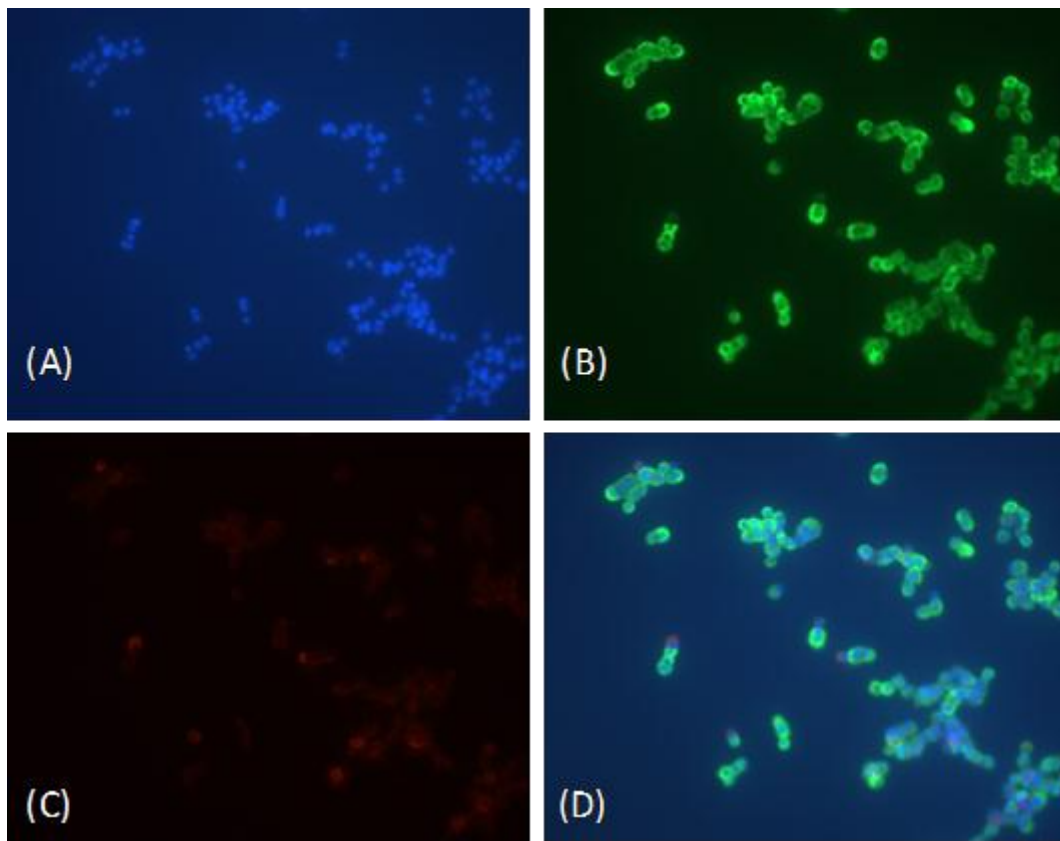


Figure 3.10 Immunohistochemistry determination of beta-cell purity. Beta-cells were fixed and permeated before a nuclear stain (A, blue, DAPI), anti-insulin (B, green, FITC) and anti-glucagon (C, red, Rhod) were added. Beta-cells were viewed using fluorescence microscopy and purity calculated as percentage of insulin-positive cells/nuclear positive cells. Overlay of the three stains demonstrates the high purity of beta-cells within the preparation (D).

Expression profiling within metabolically relevant human tissues demonstrated that *TSGA13* and *VPS33B* were not expressed within human islets whereas probe problems ruled out the detection of *CHCHD9* and *HDDC3*. All other genes were shown to be expressed within human pancreas and islets and warranted investigation within human beta-cells. Human islets preparations (n=2) were sorted using FACS and purity found to be >95% using immunohistochemistry (Figure 3.10).

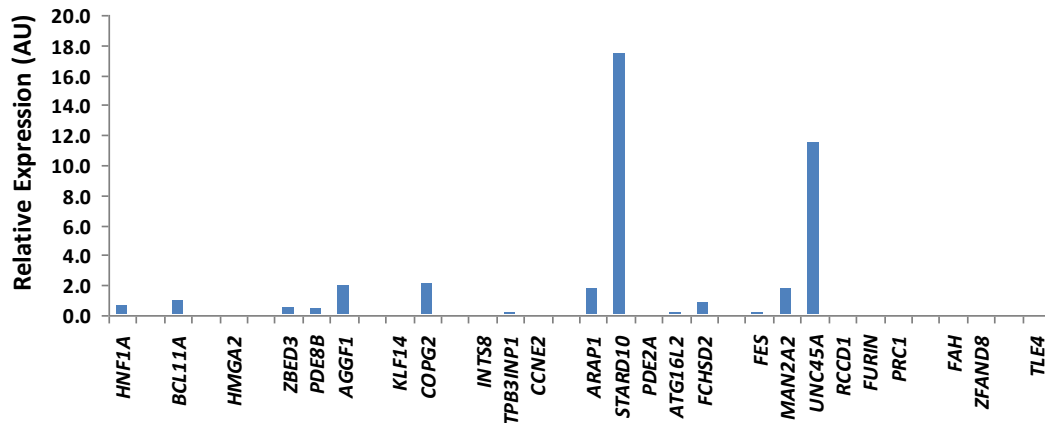


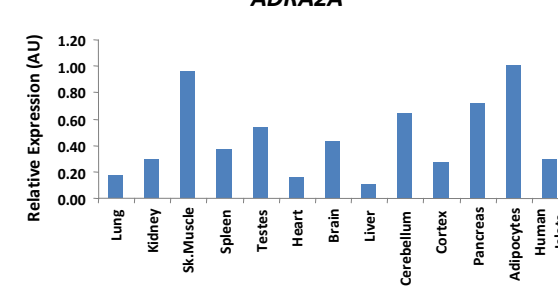
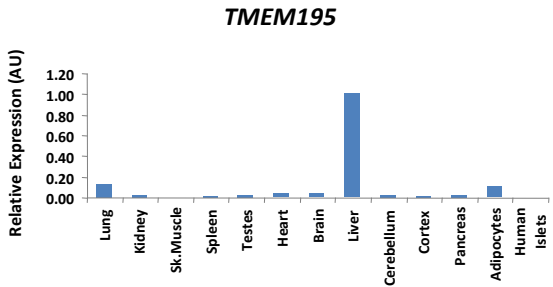
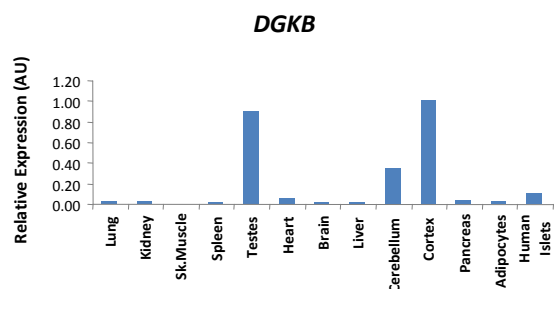
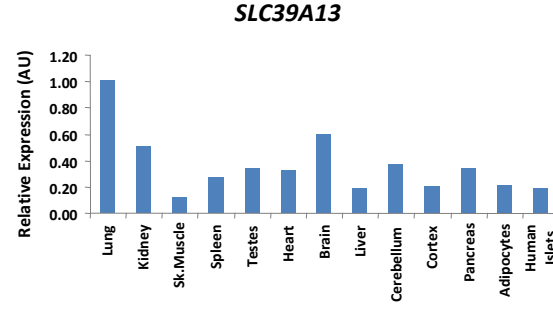
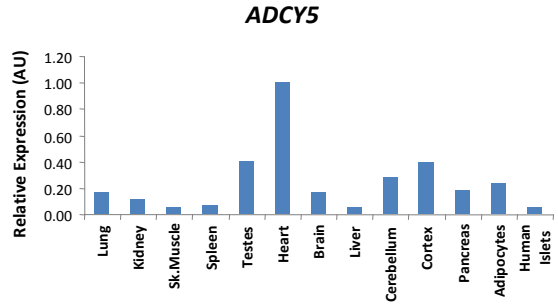
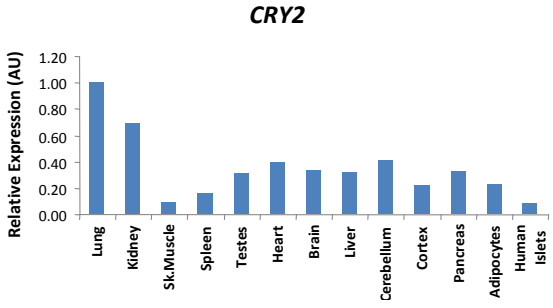
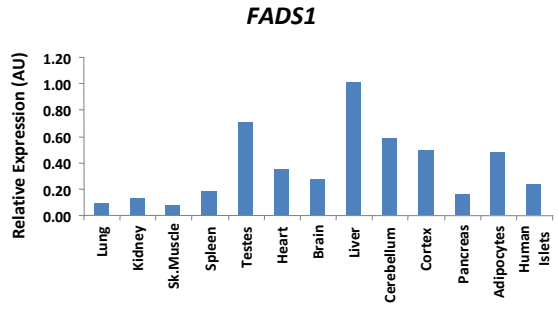
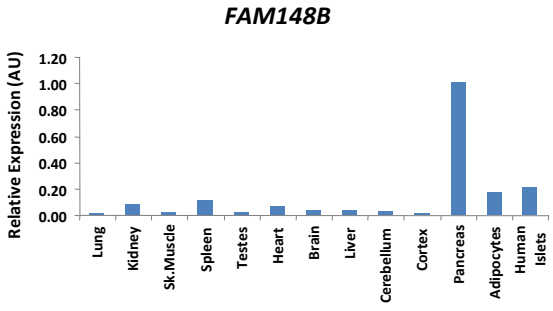
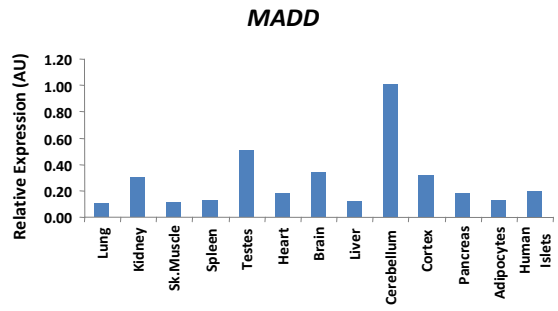
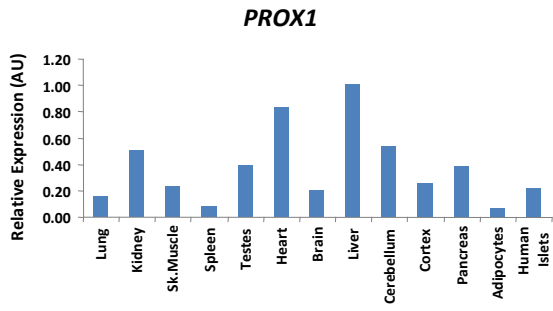
Figure 3.11 Relative expression of novel T2D loci within human beta-cells when analysed using $\Delta\Delta C_T$ method, normalising to *B2M* and making relative to the raw Ct of *HNF1A* (which we already know to be highly expressed within human islets). Genes have been grouped into novel loci for ease of presentation.

Within human beta-cells a similar pattern of expression is observed to that seen within human islets (Figure 3.11). *STARD10* remains the gene most strongly expressed at 11q13 whilst at 15q26 *UNC5A* has overtaken *MAN2A2* as the lead gene within this locus. At 5q14 *AGGF1* is expressed at higher levels than the other two candidate genes and at 7q23 *COPG2* has emerged as the most strongly expressed gene. At a number of loci, none of the highlighted genes were detected within flow sorted beta-cells. However, it should be noted that the starting material used for expression analysis within human beta-cells was considerably less than is normally used in expression studies due to limited RNA availability. Therefore, genes within these loci may still be expressed within beta-cells but at lower levels than genes which have demonstrated expression within our study. Alternatively, low expression of these genes may indicate they are exerting their effects through insulin-sensitive tissue and effects on insulin sensitivity rather than beta-cell function.

3.3.4 mRNA expression analysis of genes adjacent to novel FPG loci: Human tissue panel

Expression levels of the genes mapping closest to the lead association signals (*ADRA2A*, *ADCY5*, *CRY2*, *GLIS3*, *PROX1*, *SLC2A2*, *FADS1*, *FAM148B*, *DGKB-TMEM195*, *MADD-SLC39A13*) were determined in a panel of metabolically relevant human tissues including pancreas and islets. All genes were shown to be expressed within human islets with the sole exception of *TMEM195* (Figure 3.14). *TMEM195* lies within a region of association on chromosome 7 which also encompasses *DGKB* and had previously been highlighted as a potential FPG locus in a recent GWAS study for metabolic traits in the Northern Finnish Birth Cohort (Sabatti, et al., 2009). Both genes were included in the expression analysis to aid in refinement of this signal and although expression of *TMEM195* was not observed in islets it was shown to be expressed at highest levels within liver, another tissue through which the effects on FPG could be mediated.

Interestingly both *FAM148B* and *GLIS3* showed highest levels of expression within whole pancreas and in both cases expression within this tissue were over two fold higher than expression within islets, indicating that these genes may play critical roles within pancreas but predominantly within the exocrine tissue. Of the other genes tested *SLC2A2*, *FADS1* and *PROX1* showed high levels of expression within liver whilst *SLC39A13*, *ADRA2A* and *CRY2* were shown to be widely expressed within all tissues (Figure 3.12).



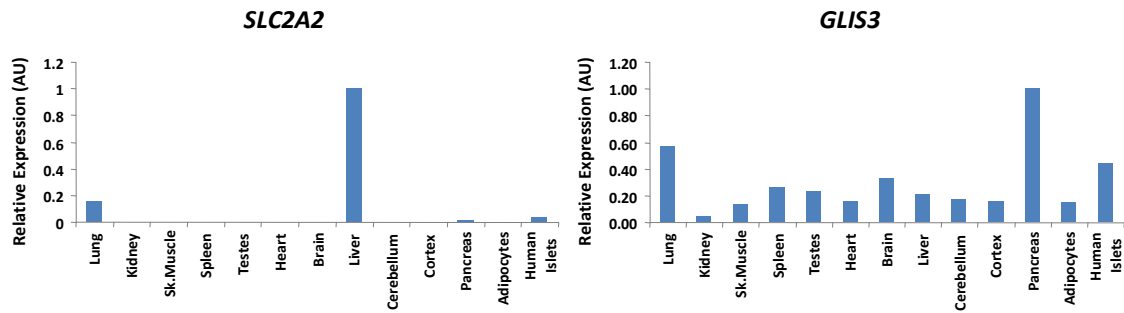


Figure 3.12 Expression of genes mapping closest to the lead association SNP and/or biological candidate genes at the association loci were determined across a human tissue panel including metabolically relevant tissues. For each gene tested the maximal tissue expression is equalled to one and expression in other tissues reported as a fraction of this for ease of presentation.

To assess the relative expression of all genes within human islets, data were reanalysed after an arbitrary threshold value was set for each assay and calibration was performed using the average expression of *GLIS3* (a known pancreatic transcription factor) within islets. When comparing expression levels within this tissue, *FADS1* and *SLC39A13* were shown to be transcribed at the highest levels. Expression of *TMEM195* was once again confirmed in its absence in this depot and interestingly expression of *DGKB*, the previously associated locus was also present at low levels within human islets (Figure 3.13).

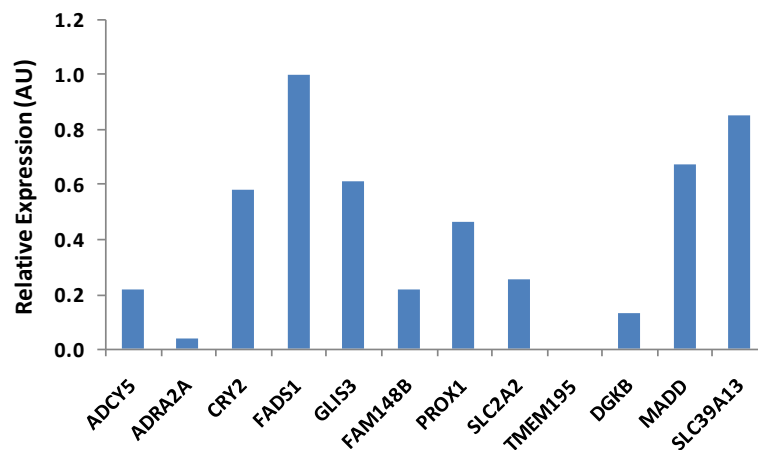


Figure 3.13 Relative expression of the twelve fpg candidate genes. Expression was calculated using the $\Delta\Delta C_T$ value, normalising to the mean of 3 HKG and calibrating to the mean expression of *GLIS3* within this tissue. Maximum expression within *FADS1* has been equalled to zero and all other presented as a percentage of this.

3.4 Discussion

Through meta-analysis of genotypic and phenotypic data from over 100,000 individuals, my statistical collaborators within the DIAGRAM+ (Voight, Scott, Steinthorsdottir, Morris and Dina) and MAGIC (Dupuis, Langenberg, Prokopenko, Saxena and Sorenzo) consortia, were able to identify 12 novel T2D and nine novel fpg loci. However, of these novel signals, many were found to map to gene-dense regions of the genome with low recombination and high LD rates or close to genes whose biological candidacy was unknown. To aid in the refinement of the association signals I performed gene expression profiling of the highlighted genes within metabolically relevant tissues including human islets and purified beta-cells to firstly determine which if any of the genes were transcribed and expressed within these depots, and secondly to postulate whether the novel variants are likely to be modulating their effects through beta-cell dysfunction or via a peripheral signalling defect.

mRNA expression profiling was only performed for genes within ten of the T2D loci as molecular mechanisms and biological candidate genes were already defined for the remaining four. The association signal mapping to 12q14 mapped 0.2Mb from *HMGA2*, high mobility group AT-hook 2, a transcriptional regulator and key component of the enhancesome which was associated with T2D for the first time in this study (Noro, et al., 2003). Other common variants within this gene have robustly been associated with height in the general population although the association signals have been shown to be independent in European populations ($r^2 < 0.01$) (Weedon, et al., 2007). Expression analysis demonstrates minimal expression of this gene within human pancreas and islets and levels within beta-cells do not exceed background. Our data would indicate this variant is unlikely to exert its functional effects through modulation of beta-cell function. Furthermore human physiological analysis, performed by DIAGRAM+ collaborators, demonstrated the risk *HMGA2* allele shows no association with HOMA-B, an index of beta-cell function, but rather shows a

more demonstrable effect on HOMA-IR, a surrogate measure of insulin sensitivity. Interestingly, data from *Hmga2* haploinsufficient mice show these animals have greatly reduced fat mass and suffer from diet-induced obesity (Zhou, et al., 1995). Our observation of high *HMGA2* expression levels within human brain alongside evidence from murine models suggest that the risk allele at *HMGA2* could be contributing to increased T2D risk via an obesity-related mechanism which requires further investigation.

Expression profiling was also of benefit for loci where the association signal mapped to regions in which a candidate gene was not always evident. The signal at 7q32 mapped upstream of the single exon gene *KLF14* but <0.1Mb from a further two genes *COPG2* and *TSGA13*. To ensure the true causal gene was not excluded and to aid in refinement of the signal the expression profile of the three transcripts were determined. *TSGA13* was originally eliminated from our beta-cell analysis after it failed to demonstrate expression within pancreas or islets when tested in the human tissue panel. *COPG2* was relatively strongly expressed in both islets and beta-cells. *COPG2* is a subunit of the Golgi coat protein or coatomer which is a complex required for Golgi budding and Golgi to endoplasmic reticulum transport (Waters, et al., 1991). Its crucial role may explain its relatively ubiquitous expression across the human tissue panel but does not lend itself to an obvious role in the pathogenesis of T2D. *KLF14* is the gene which maps closest to the lead association signal and from the expression analysis there is little if any evidence to suggest this variant may mediate its actions through beta-cell dysfunction. Conversely, this Kruppel-like transcription factor shows maximal expression within kidney, brain and adipose tissue. The T2D susceptibility variant at this locus is also associated with increased fasting insulin levels and reduced insulin sensitivity (HOMA-IR) indicating the primary effects of this variant are being driven by effects on insulin action. Further support for a role of *KLF14* in insulin action was provided by DIAGRAM+ investigators undertaking *cis*-eQTL analysis who demonstrated the index SNP

strongly associated with *KLF14* expression within adipose tissue. Since publication of these findings, the same *KLF14* cis-eQTL has also been found to act as a master trans regulator of a number of key adipose genes, the expression of which correlate with metabolic traits including body mass index (BMI), fasting insulin and HOMA-IR, therefore providing further mechanistic proof that this variant is mediating T2D susceptibility via an adipose-mediated mechanism (Small, et al., 2011).

The associations signals at 12q14 and 7q32 have therefore been somewhat aided by the use of biological analysis however there were a number of loci for which expression profiling was found to be of limited use in signal refinement. The association signal mapping to 5q14 fell between three genes, *ZBED3*, *AGGF1* and *PDE8B*. Expression profiling demonstrated that all three genes were expressed in both human islets and beta-cells and physiological and biological evidence failed to shed any further light on the true causal variant. At 11q13 the presence of a large LD block warranted the screening of eight potential causal genes. Expression analysis demonstrated that all genes with the exception of *VPS33B* were expressed in islets although *UNC45A* and *MAN2A2* were expressed at the highest levels. Pathway analysis of the same locus demonstrated that *FURIN* is an important gene required for the cleavage of *NOTCH2* and *ADAMTS9* (previously identified T2D genes) although expression of this gene within beta-cells could not be identified (Gordon, et al., 2009; Logeat, et al., 1998; Somerville, et al., 2003). Further work therefore needs to be performed at this locus to determine whether the true causal variant is working through *FURIN* in insulin-sensitive tissues or whether the true variant is potentially modulating *UNC45A* or *MAN2A2* via a beta-cells mechanism.

As with the novel T2D loci, expression profiling was performed for each of the genes within the nine novel fpg loci. The signal mapping to the *DGKB-TMEM195* loci was previously

identified but only reached genome-wide significance for the first time in this study (Sabatti, et al., 2009). *DGKB* encodes diacylglycerol kinase, a regulator of diacylglycerol, an important secondary messenger which in rodents has been shown to effect insulin secretion, whilst *TMEM195* encodes a membrane phosphoprotein believed to play an important role within hepatocytes (Peter-Riesch, et al., 1988). Expression analysis demonstrated that *TMEM195* was transcribed at highest levels within hepatocytes whilst expression in human islets was not observed. Conversely *DGKB* showed a more extensive expression profile with highest levels observed within brain and testes whilst expression was also detected within islets. The detection of the two candidate genes within metabolically relevant tissues (beta-cells [*DGKB*] and liver [*TMEM195*]) provides evidence that both genes could be driving the association at this locus. Statistical geneticists within the MAGIC consortia determined that the glucose-raising T allele has an effect size of 0.03mmol/L and a decrease in HOMA-B of 0.017 ($p=6.4 \times 10^{-8}$) however no observable differences in HOMA-IR ($p=0.61$) or fasting insulin levels ($p=0.48$) were detected. Detailed physiological characterisation of the novel variant also demonstrated that the glucose-raising allele is associated with defects in early insulin secretion as assessed by a reduced insulinogenic index (a measure of glucose-stimulated insulin secretion). No demonstrable effects on insulin sensitivity were observed as would be expected if the association was driven by the *TMEM195* gene within hepatocytes and therefore the expression and physiological data together suggest that at this locus the effects on fasting glucose and beta-cell function are driven through the *DGKB* gene (Ingelsson, et al., 2010).

The lead SNP rs7944584 mapped to an intron of *MADD* (mitogen-activated protein kinase activating death domain) an adaptor protein required for MAPK activation through interaction with the TNF α receptor (Schievella, et al., 1997). An additional gene within this association region, the zinc transporter *SLC39A13*, was also considered a likely candidate

gene and therefore included in gene expression profiling. Both genes were found to be ubiquitously expressed with equivocal levels observed within human islets. Statistical analysis by collaborators within the MAGIC consortia determined that the A allele at this locus raised blood glucose with the magnitude of 0.02mmol/L and was also associated with a reduction in beta-cell function although this failed to reach genome-wide significance (HOMA-B $p=0.07$). Detailed physiological characterisation of this variant however demonstrated that the glucose-raising A allele is also associated with abnormal insulin processing as assessed by an increase in fasting proinsulin levels ($p=2.07 \times 10^{-71}$) without a concomitant effect on insulin secretion (Ingelsson, et al., 2010).

The observation that this variant does not increase T2D risk despite such large effects on circulating proinsulin levels suggests this is an isolated processing defect (Ingelsson, et al., 2010). Of the candidate genes tested at this locus we observed the strongest expression of *SLC39A13* within human islets. Interestingly a different beta-cell specific zinc transporter *SLC30A8* (ZnT8) was robustly associated with fasting plasma glucose and T2D risk in a previous study (Sladek, et al., 2007). Determination of the molecular mechanism behind this *SLC30A8* signal was elucidated using a combination of rodent knockout and molecular modelling (Nicolson, et al., 2009). *Slc30a8*^{-/-} knockout mice demonstrated impaired glucose tolerance and insulin secretion with reduced insulin granule zinc content (Nicolson, et al., 2009). Molecular modelling of the associated non-synonymous variant revealed that the risk R allele was associated with reduced zinc transport when compared to the wildtype W allele (Nicolson, et al., 2009) demonstrating the importance of zinc transporters for the maintenance of beta-cell function and glucose homeostasis. The additional gene tested at this locus, *MADD*, works through generation of apoptotic signals via the TNF α receptor (Schievella, et al., 1997). Were variants within *MADD* driving the association, it is hypothesised that defects in beta-cell function would also be observed (Ingelsson, et al.,

2010). Taken together the expression and physiological data support a role for the zinc transporter *SLC39A13* within human islets.

Each of the remaining eight genes were detected within human islets. Statistical analysis by MAGIC consortia collaborators revealed the association signal mapping to the promoter of *PROX1* was associated with an increase in fpg of 0.013mmol/L per copy of the A allele although association with beta-cell dysfunction or insulin resistance was not observed. *PROX1* is an early marker of pancreatic and hepatic development and is known to co-repress *HNF4A*, a key nuclear transcription factor (Song, et al., 2006). The observation that *PROX1* is highly expressed within pancreas and islets provides biological evidence that the mechanism through which this novel SNP is acting is via beta-cell dysfunction. To further support this notion, physiological evidence suggests that the *PROX1* glucose-raising variant is also associated with a reduced insulinogenic index and therefore reduced insulin secretion (Ingelsson, et al., 2010). Therefore, it could be postulated that the true causal variant at this locus increases the activity of *PROX1* co-repression of *HNF4A* leading to down-regulation of a number of genes within the insulin signalling pathway and a reduction in insulin secretion.

Similarly, high levels of *FAM148B* expression were observed within pancreas and human islets contrasting with low levels of expression detected in all other tissues tested. Statistical and physiological analysis by collaborating MAGIC geneticists determined that the risk A allele associated with an increase in fpg of 0.008mmol/L (per copy), a reduction in HOMA-B ($p=8.1 \times 10^{-4}$) as well as elevated proinsulin and decreased insulin secretion (Ingelsson, et al., 2010). The expression data and the physiological data suggest this gene plays a crucial role within the insulin secretion process although the role of this nuclear localised factor on glucose homeostasis is not yet understood.

The inclusion of genetic expression profiling within human beta-cells as a tool to aid in refinement of T2D and fpg association signals was performed for the first time within the DIAGRAM+ and MAGIC meta-analysis. Despite the advantages and insight which this additional biological analysis can provide, the method is not without its limitations. Human islets are made up of a number of cells types including the glucagon-secreting alpha cells and the somatostatin-secreting delta cells. Modulation of the secretion properties of these cells may also conceivably confer susceptibility to T2D and therefore genetic expression profiling within these cells may also be of interest. This was considered outside of the remit of this project, however in the future, inclusion of an additional alpha cell sorting phase may be implemented in the FACS protocol and genetic profiling performed within these cells to provide additional and complementary information.

Although the utilisation of gene expression profiling, in combination with physiological characterisation and eQTL analysis can serve to highlight key genes within novel susceptibility loci, they are unlikely to shed any light on the molecular mechanisms through which the variants are acting. To this end, the field of T2D genetics research will now rely heavily on the work of biologists performing rigorous functional follow of each of the variants before a full picture of their mode of action is determined. This in itself is likely to take a considerable amount of time and therefore the hope that GWAS may aid in the identification of novel therapeutic discoveries is likely to be some way off becoming a reality.

In conclusion, I have demonstrated that gene expression profiling within a panel of metabolically relevant, human tissues can be used as part of a multidisciplinary approach to add biological evidence to epidemiological GWAS data. When used in combination with physiological and eQTL data the three can aid in refinement of the signal as well as providing preliminary evidence as to potential molecular mechanisms. Expression profiling of genes

within the DIAGRAM+ and MAGIC novel loci within human islets and beta-cells has now highlighted a number of key genes which must be further investigated to elucidate the roles of these genes within beta-cell physiology and pathophysiology.

Chapter 4

GLUT2 (*SLC2A2*) is not the principal glucose transporter in human pancreatic beta-cells: Implications for understanding genetic association signals at this locus

4.1 Introduction

The implementation and utilisation of genome-wide association studies (GWAS) has been of considerable benefit for researchers interested in elucidating the genetic component of complex and quantitative traits including type 2 diabetes (T2D) and fasting plasma glucose (fpg) as the DIAGRAM+ and MAGIC studies clearly demonstrate (Dupuis, et al., 2010; Voight, et al., 2010). Despite the wealth of novel susceptibility loci now robustly associated with these dichotomous and continuous traits, accompanied by biological and physiological analysis refining the loci to likely causal genes, progress in defining the molecular mechanisms underlying the signals has been slow.

One explanation for the lack of signal translation may be attributed to the high proportion of signals which map within or close to genes of unknown biological relevance. In order to correctly assess the biological relevance of these genes it is imperative to perform in depth biological analysis within the correct cellular system. As the majority of T2D and fpg association signals identified to date appear to modulate beta-cell function, and therefore insulin secretion, assessing the role of these genes within beta-cells is a necessity (Voight, et al., 2010). Unfortunately, lack of reliable human insulin-secreting cell lines, coupled with increasing evidence of the fundamental differences between rodents and humans, has hindered the translation of novel association signals and understanding of molecular mechanisms (Bosco, et al., 2010; Braun, et al., 2008; Fiaschi-Taesch, et al., 2009). One example of this struggle is seen in the work of Dos Santos *et al.* who aimed to functionally characterise a novel fpg SNP within glucose-6-phosphatase, catalytic domain 2 (*G6PC2*), the hypothesised negative regulator of islet glucokinase (Dos Santos, et al., 2009; Wang, et al., 2007). The authors identified a common promoter variant in high linkage disequilibrium ($r^2=0.96$) with the index SNP which fell within a FOXO2 transcription factor binding site. The authors were therefore able to assess the effects of the different alleles on transcription

factor binding, promoter activity and gene expression in islet-derived INS-1 and HIT-T cells (Dos Santos, et al., 2009). Despite the promise of identifying a SNP within a biologically plausible regulatory region the authors were unable to marry their in vitro data to those observed in vivo. Others have since speculated that their paradoxical observations may be due to the utilisation of islet-derived cell lines which may not truly mimic the in vivo situation (Bouatia-Naji, et al., 2010). To demonstrate the importance of using appropriate human primary cells in translating association signals we have chosen to follow-up rs11920090, an intronic *SLC2A2* SNP reproducibly associated with fpg levels in the MAGIC meta-analysis (Dupuis, et al., 2010).

SLC2A2 encodes glucose transporter-2 (GLUT2) a transmembrane protein which functions to allow the passive transport of glucose across cell membranes via facilitated diffusion. Subsequent research into this high- K_m transporter has highlighted its critical role as the principal glucose transporter within rodent islets (Guillam, et al., 1997; Thorens, et al., 1988) and it is widely accepted to play a similar role within human islets (Fajans, et al., 2001; Hussain, 2010; Kronenberg, et al., 2008; Sperling, 2006). However, detailed physiological characterisation of the *SLC2A2* glucose-raising variant in 29,000 individuals informative for proinsulin as well as fasting glucose and insulin levels, failed to show any demonstrable effects on insulin processing or secretion indicating that this variant is unlikely to be affecting beta-cell function (Ingelsson, et al., 2010).

Until recently there were only limited reports of glucose transporter expression studies in human islets due to the difficulties in obtaining this tissue. One study performed over 15 years ago, demonstrated very low levels of *SLC2A2* (GLUT2) within human islets (De Vos, et al., 1995). Using Northern Blot analysis in islets from two donors *SLC2A2* expression was shown to be minimal when directly compared to *SLC2A1* (GLUT1) and ~100-fold lower when

compared with rodents (De Vos, et al., 1995). These data suggest important differences in the regulation of glucose-sensing in humans versus rodents but despite these pertinent findings, the data are largely overlooked and GLUT2 continues to be quoted as the key glucose transporter in human beta-cells (Fajans, et al., 2001; Hussain, 2010; Kronenberg, et al., 2008; Nolan and Prentki, 2008).

In light of the recent genetic data and the controversy in the literature, we aimed to replicate the findings of De Vos *et al.* using highly sensitive methodologies in a larger number of islets, and to advance their studies by establishing for the first time the expression profile of glucose transporters within pure human beta-cells, obtained through fluorescence-activated cell sorting (FACS). Finally, we relate *SLC2A2* expression profiles to the reported genetic association with fpg levels.

4.2 Methods

4.2.1 Samples

Expression profiling of glucose transporters was performed in metabolically relevant human and mouse tissues. Human liver (n=3), subcutaneous adipose tissue (n=1) and skeletal muscle (n=2) were available through the MOLPAGE surgical biobank in collaboration with Professor Mark McCarthy. Human pancreatic islets (n=12) and FACS beta-cells (>95% purity) (n=3) were available through existing collections at Oxford University and were processed as previously described in **chapter 3**. Mouse liver (n=2), brown adipose tissue (n=2), subcutaneous adipose tissue (n=1), skeletal muscle (n=2) and pancreatic islets (n=5) were available through existing collaborations at Oxford University and were collected with full ethical consent.

4.2.2 mRNA expression analysis of *SLC2A1-4* in human tissues

Reverse transcription was performed on 300ng total RNA in a random primed first strand synthesis reaction. cDNA was diluted to a 1:10 working dilution in 0.01M Tris-HCl (pH6.8) and 4µl amplified in 10µl multiplexed reactions comprising 0.5µl *PPIA* housekeeping gene probe (VIC labelled), 0.5µl GLUT specific probe (FAM labelled) and 5µl gene expression mastermix (Applied Biosystems, Warrington, UK). Data was analysed using the ΔC_T method $([1+\text{efficiency}]^{1-C_{T[\text{gene of interest}]}})/([1+\text{efficiency}]^{1-C_{T[\text{housekeeper}]}})$ ensuring the threshold (C_T) was established at an arbitrary uniform value for each assay. Replication analysis of *SLC2A1-3* in an additional nine human islet preparations was performed on islet cDNA generated from 1000ng total RNA as RNA was not limiting. Amplification and analysis were performed as above.

4.2.3 mRNA expression analysis of *Slc2a1-4* in mouse tissues

Slc2a1, *Slc2a2*, *Slc2a3* and *Slc2a4* expression levels were determined in a panel of metabolically relevant murine tissues. 1000ng total RNA was reverse transcribed as detailed above following the removal of genomic DNA by DNase I treatment. Samples were run at a 1:50 dilution alongside three FAM labelled housekeeping genes (*Leng8*, *Pgk1*, *Hprt1*). VIC labelled housekeeping genes were not available for multiplexing in this experiment. Analysis was performed using the ΔC_T method detailed above following setting of an arbitrary threshold value.

Gene ID	Gene name	Assay ID
<i>SLC2A1</i>	Human Glucose Transporter 1	Hs00892681_m1
<i>SLC2A2</i>	Human Glucose Transporter 2	Hs01096904_m1
<i>SLC2A3</i>	Human Glucose Transporter 3	Hs00359840_m1
<i>SLC2A4</i>	Human Glucose Transporter 4	Hs00168966_m1
<i>Slc2a1</i>	Murine Glucose Transporter 1	Mm00441473_m1
<i>Slc2a2</i>	Murine Glucose Transporter 2	Mm00446229_m1
<i>Slc2a3</i>	Murine Glucose Transporter 3	Mm00441483_m1
<i>Slc2a4</i>	Murine Glucose Transporter 4	Mm00436615_m1
<i>PPIA</i>	Peptidylpolyl Isomerase A	Hs99999904_m1
<i>Hprt1</i>	Hypoxanthine guanine phosphoribosyl transferase 1	Mm00446968_m1
<i>(Leng8)</i>	Leukocyte receptor cluster (LRC) member 8	Mm00554994_m1
<i>(Pgk1)</i>	Phosphoglycerate Kinase 1	Mm00435617_m1

Table 4.1 Gene names and identification numbers of probes used to amplify human and rodent glucose transporters. Identification numbers for human and murine housekeeping genes are also provided.

4.2.4 Immunohistochemistry

Wax-embedded sections (5 μ m thick) of human pancreas and liver sections were used for immunohistochemistry. Primary antibodies used were polyclonal rabbit anti-GLUT1 1:200 (AbCam, Cambridge, UK), polyclonal rabbit anti-GLUT2 1:20 (Insight Biotechnology, Wembley, UK) or polyclonal rabbit anti-GLUT3 1:200 (AbCam). Labelling for GLUT was followed by a tyramide amplification step with Alexa Fluor 488 dye according to manufacturer's instructions (Invitrogen, Paisley, UK). Sections were also labelled for with guinea pig anti-insulin, 1:500 (in house) followed by Texas Red-conjugated goat anti-guinea pig 1:50 (Vector Laboratories, Peterborough, UK). The relative levels of labelling for the different transporters in all cell types was established by replacing their amplification step with a FITC-conjugated

goat anti-rabbit secondary antibody (Vector Laboratories). Specificity of labelling was tested by omission of the primary antibodies. Images were captured using a Zeiss LSM510 confocal laser scanning microscope (Carl Zeiss, Jena, Germany). This work was performed by another DPhil student within the Gloyn group, Martijn van de Bunt.

4.3 Results

4.3.1 GLUT mRNA expression analysis in human metabolically relevant tissues

qRT-PCR analysis of glucose transporter mRNA within human islets demonstrated that *SLC2A1* (GLUT1) and *SLC2A3* (GLUT3) were expressed at 2.8 and 2.7 fold higher levels when compared to *SLC2A2* (GLUT2) (Figure 4.1B). As expected, insulin stimulated *SLC2A4* was only detected at background levels in this tissue. As pancreatic islets consist of multiple cell types we chose to extend our expression analysis to observe the mRNA expression of the GLUT transporters specifically within purified human insulin-secreting beta-cells. Analysis in this cell type revealed a strikingly similar pattern of expression to those observed in human islets with nominal GLUT2 expression compared to GLUT1 and 3 (Figure 4.1A). Replication within an additional nine preparations of human islets demonstrated an identical pattern of GLUT mRNA expression (Figure 4.1B).

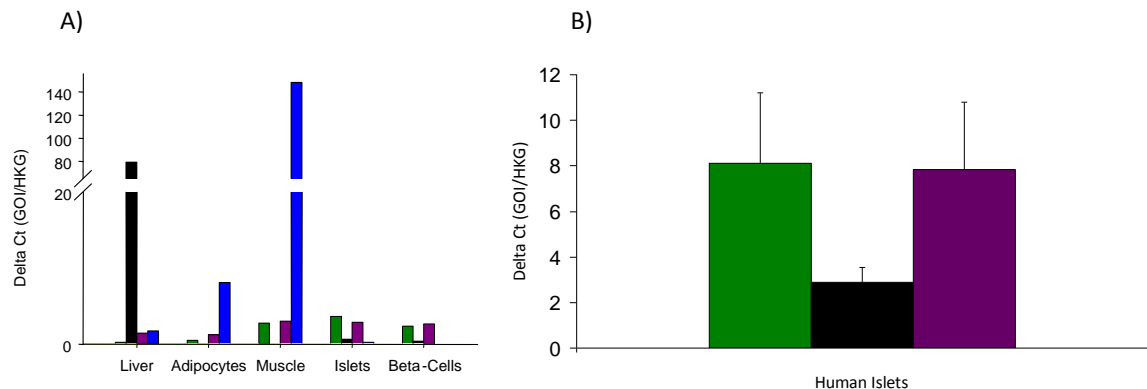


Figure 4.1 mRNA expression analysis of GLUT1-4 within metabolically relevant tissues. (A) Expression profiling of GLUT1-4 was performed across metabolically relevant tissues before replication was performed for GLUT1-3 in an additional nine preparations of human islets (B). Analysis was performed using the ΔC_T method, normalising to the multiplexed housekeeping gene, *PPIA*. GLUT1 (green bars), GLUT2 (black bars), GLUT3 (purple bars), GLUT4 (blue bars).

4.3.2 Glut mRNA expression analysis in murine metabolically relevant tissues

Glut mRNA expression analysis within metabolically relevant murine tissues revealed that *Slc2a2* is the predominant glucose transporter in mouse pancreatic islets. *Slc2a4* was not detected at all within this tissue whilst *Slc2a3* was only present at background levels. In comparison *Slc2a1* was found to be transcribed within this tissue however comparative analysis revealed *Slc2a1* expression to be around 10 fold lower than *Slc2a2* (Figure 4.2).

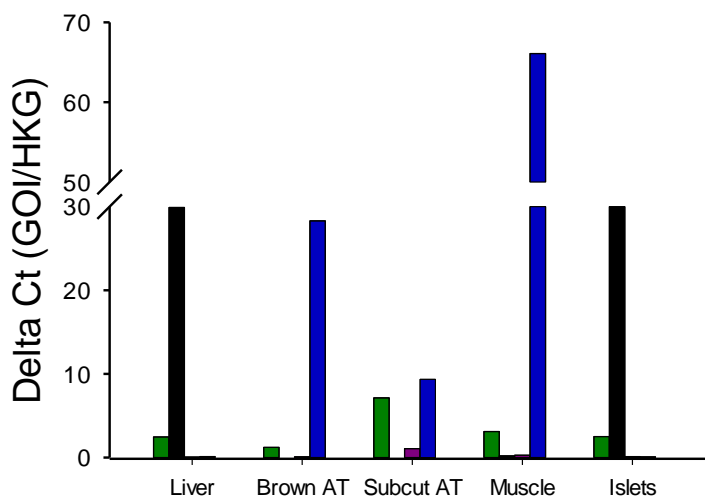


Figure 4.2. mRNA expression analysis of *Slc2a1-4* within a panel of metabolically relevant murine tissues. *Slc2a1* is represented by green bars, *Slc2a2* by black bars, *Slc2a3* by purple bars and *Slc2a4* by blue bars. Analysis was performed using the ΔC_T method normalising the geometric mean of three murine housekeeping genes (*Leng8*, *Pgk1* and *Hprt1*). AT = Adipose Tissue

Expression analysis within other metabolically relevant tissues was as expected. *Slc2a1* was found to be ubiquitously expressed within all tissues whilst *Slc2a4* was predominantly expressed within skeletal muscle and adipose tissue. *Slc2a3*, the neuronal transporter, was detected at background levels in all metabolically relevant tissues, but above background expression within mouse brain demonstrating probe efficiency (data not shown).

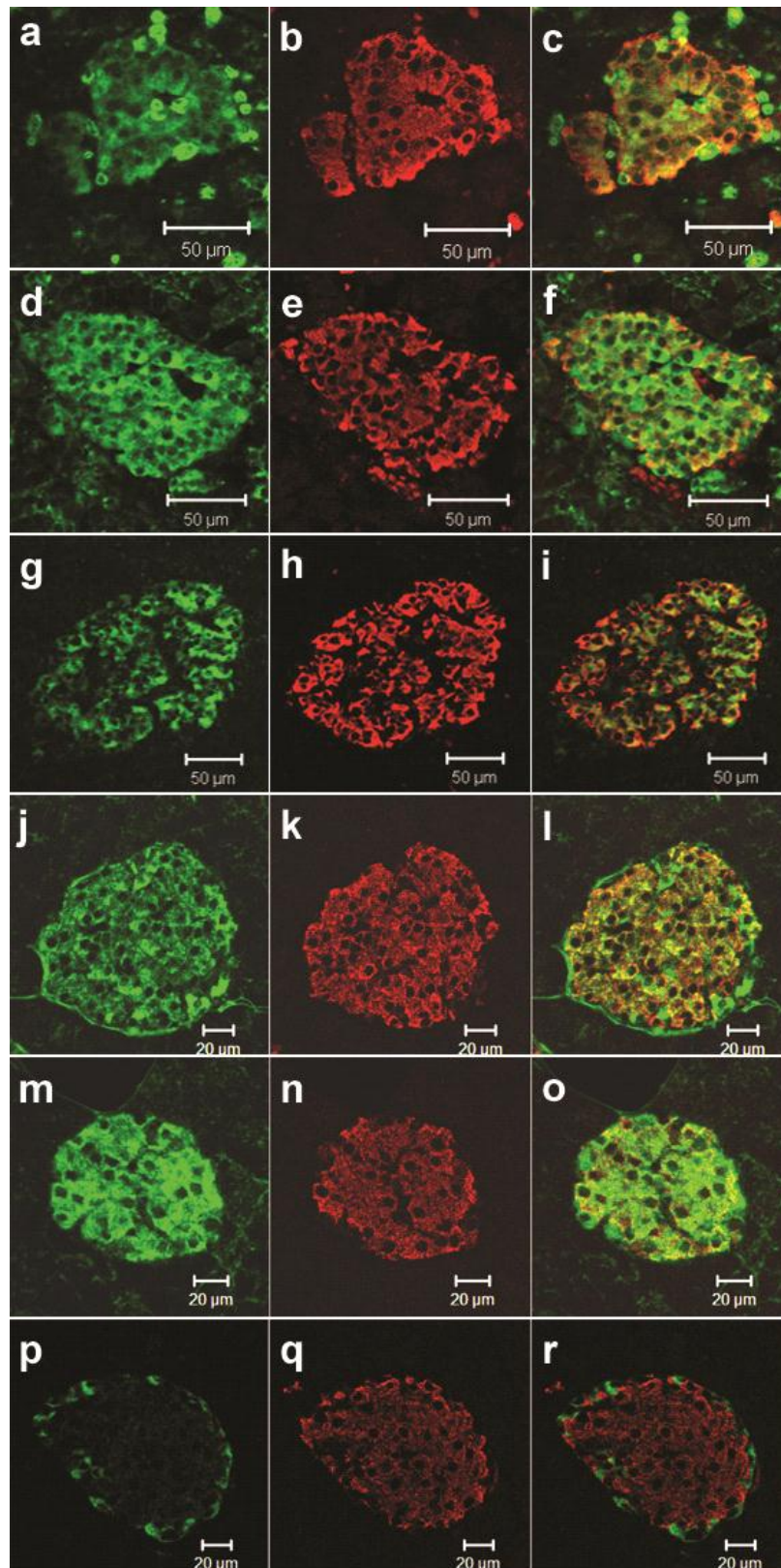


Figure 4.3 Immunohistochemistry demonstrating the presence of GLUT1, 2 and 3 in both human and mouse pancreatic islet sections. Immunolabelling for different GLUTs (green), insulin (red) and an overlay of both are represented for each glucose transporter. **a-c** GLUT1, **d-f** GLUT2, **g-i** GLUT3 in human, and **j-l** GLUT1, **m-o** GLUT2, **p-r** GLUT3 in mouse. This work was performed by Martijn van de Bunt.

4.3.3 Protein expression of GLUT1-3 within islets and FACS beta-cells

Human pancreatic islets were positive for GLUT1, 2 and 3 as demonstrated by immunohistochemistry. Co-localisation with insulin staining confirmed these were beta-cells (Figure 4.3a-i). In mouse pancreatic islets Glut1 and Glut2 labelling were similar in insulin-positive cells whilst Glut3 was not observed within this tissue (Figure 4.3j-r). The presence of GLUT1, 2 and 3 in human insulin-positive cells was confirmed in FACS human beta-cells (Figure 4.4).

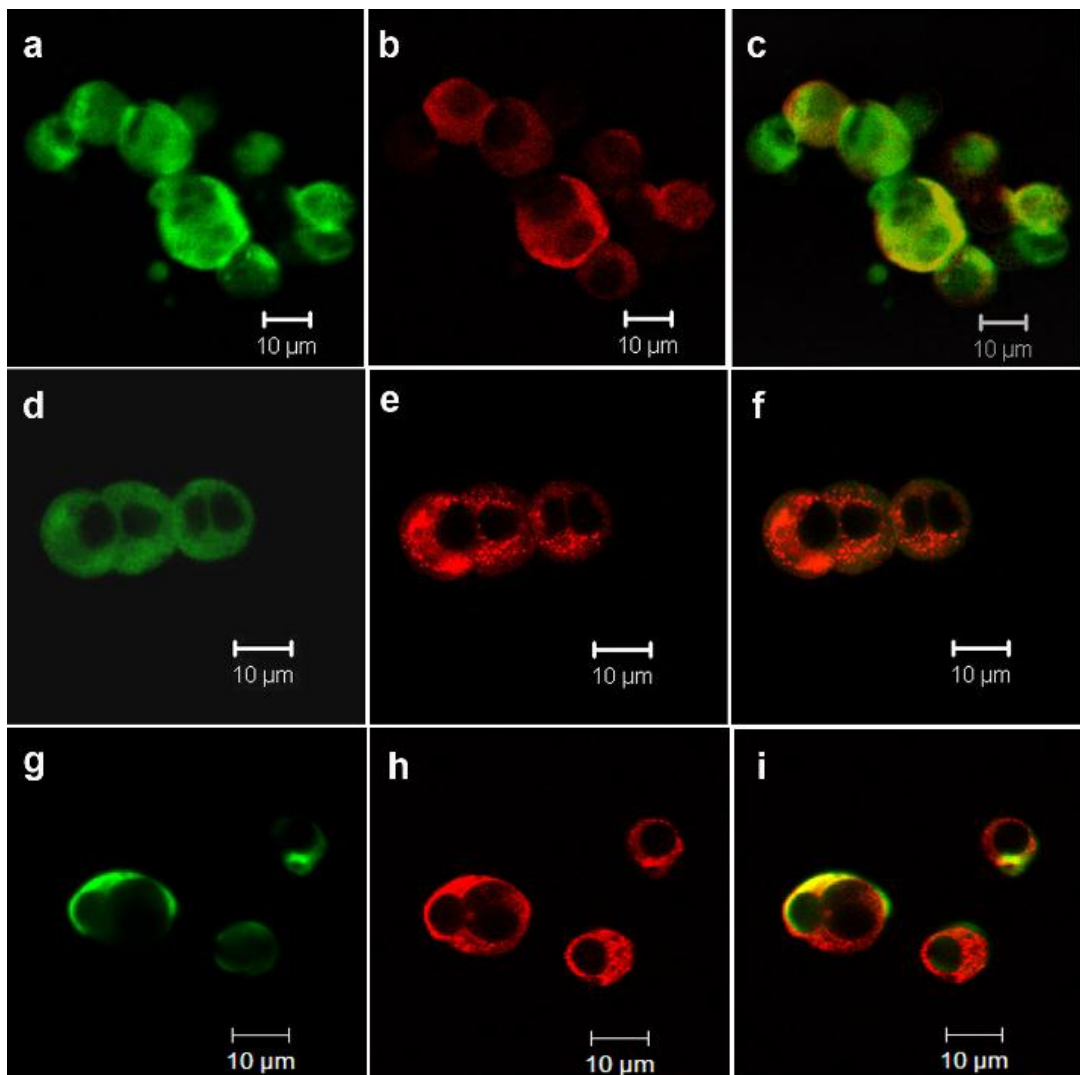


Figure 4.4 Detection of glucose transporters in human beta-cells. Immunolabelling for different GLUTs (green), insulin (red) and an overlay of both are represented for each glucose transporter. GLUT1 (a-c), GLUT2 (d-f), GLUT3 (g-i). This work was performed by Martijn van de Bunt.

4.4 Discussion

To understand why *SLC2A2* variants impacting on fpg levels do not affect pancreatic beta-cell function we investigated the relative expression profiles of glucose transporters in metabolically relevant human tissues including human pancreatic islets and FACS beta-cells. Using current sensitive methodologies we have clearly demonstrated that *SLC2A1* and *SLC2A3* are expressed at higher levels than *SLC2A2* in human islets, with immunohistochemistry demonstrating the presence of all three transporters at the protein level. Our data are in agreement with earlier work from De Vos and colleagues who also demonstrated low levels of GLUT2 expression in human islets (De Vos, et al., 1995). However, for the first time we have confirmed an identical transcript expression profile within purified beta-cells as well as demonstrating that GLUT 3 (*SLC2A3*) is as abundant as GLUT1 (*SLC2A1*), suggesting an equivocally important role for both transporters in the regulation of insulin secretion in humans.

A principle role for GLUT1 in human islets is supported by the observation that the threshold for glucose-stimulated insulin secretion (GSIS) in human beta-cells is lower than in rodents (Gould and Holman, 1993; Henquin, et al., 2006). Whilst GLUT2 has a K_m for 2-deoxyglucose of 11.2mM, the properties of GLUT1 (K_m 6.9mM) are much more in keeping with the threshold for GSIS in humans (De Vos, et al., 1995; Gould and Holman, 1993; Henquin, et al., 2006). Our data however also point to an equivocally important role for the low K_m ($K_m=1.4mM$) transporter GLUT3 which we believe is also likely to be of physiological relevance. One of the most striking differences between rodent and human GLUT expression was the distribution of GLUT3 across tested tissues, in particular pancreatic islets. In rodents, *Slc2a3* was only expressed at background levels in metabolically relevant tissues with both mRNA expression and IHC suggesting apparent lack of this transporter within murine islets. In contrast, within human tissues *SLC2A3* was relatively ubiquitously expressed with GLUT3 also

identified at the protein level in human islets and beta-cells. Taken together these data suggest that in humans GLUT3 is not limited to neuronal glucose transport, as is seen for rodents (Nagamatsu, et al., 1992), but may play more of a ubiquitous glucose transport role.

The intronic SNP identified near *SLC2A2* in the recent fpg meta-analysis study was associated with a very small but significant increase of ~ 0.02 mmol/L (Dupuis, et al., 2010). In the same meta-analysis a variant close to *FADS1* (fatty acid desaturase 1) was also associated with an increase in fasting plasma glucose with an equivalent effect on fpg levels and similar minor allele frequencies (0.64 and 0.87 respectively) (Dupuis, et al., 2010). Whilst the variant near *FADS1* was shown to reproducibly associate with abnormal insulin secretion via a reduced insulinogenic index, no demonstrable effects on insulin secretion or processing were observed for *SLC2A2* (Dupuis, et al., 2010; Ingelsson, et al., 2010). This indicates that the study was well powered to detect a change in beta-cell function even for polymorphisms with only a small effect on fpg levels. Our data may help to explain why *SLC2A2* variants do not influence beta-cell function despite their association with fpg levels.

In a study by Thorens *et al.* *Slc2a2* null mice were rescued by transgenic re-expression of either pancreatic Glut1 or Glut2. Rescued mice had lower fpg levels than their wild type litter mates demonstrating that loss of Glut2 in tissues other than the beta-cell can influence fpg levels (Thorens, et al., 2000). Furthermore, patients with Fanconi-Bickel syndrome, a rare disorder of carbohydrate metabolism caused by *SLC2A2* mutations, display marked disturbances of hepatic and renal glucose metabolism causing hepatic glycogen accumulation, fasting hypoglycaemia, postprandial hyperglycaemia and a characteristic proximal tubular nephropathy with glycosuria, rather than defective insulin secretion (Santer, et al., 1998). The latter evidence, taken alongside our observations of low beta-cell *SLC2A2* expression, indicates that GLUT2 is likely to play an important role in the control of hepatic and renal

glucose metabolism and this is the likely mechanism by which *SLC2A2* variants associate with increased fpg levels.

The expression profile of the glucose transporters in adult human islets and beta-cells has potentially important implications for characterising iPS beta-cell lineages. Expression of *SLC2A2* is used extensively as a marker for human islet-cell lineage in stem cell research (Borowiak and Melton, 2009; Jiang, et al., 2007). Whilst this may be a useful marker for rodent islet-cell development, it is likely that more than one transporter has a role in human beta-cell ontogeny; both GLUT1 and GLUT2 were detected in foetal islets both at protein and mRNA-levels throughout organogenesis (Mally, et al., 1994; Richardson, et al., 2007). Our data suggest that monitoring the development of all three transporters is likely to yield cells which have the characteristics of adult islet-cells in terms of glucose metabolism rather than focusing specifically on GLUT2.

To conclude, our data reinforce the notion that GLUT2 may not be the predominant glucose transporter in human islets and beta-cells. This work serves as an important example of how performing follow-up of novel GWAS signals within metabolically relevant human tissues can aid in understanding of molecular mechanisms and once again highlights the differences between human and rodent islets and therefore the care that should be taken when directly extrapolating between the two.

Chapter 5

Mutations within the third gene shown to affect fasting plasma glucose in the general population (*G6PC2*) are not a common cause of monogenic beta-cell dysfunction

5.1 Introduction

In healthy individuals an increase in blood glucose concentration is sensed by the pancreatic beta-cells with subsequent stimulation of glycolysis, insulin secretion and glucose clearance from the bloodstream. The pancreatic enzyme primarily responsible for glucose-sensing is glucokinase (*GCK*) which catalyses the first step of the glycolysis reaction, phosphorylating glucose on carbon 6 to form glucose-6-phosphate (G6P) (Matschinsky, 2002). Within healthy individuals *GCK* maintains the threshold for glucose-stimulated insulin secretion (GSIS) close to 5mmol/L. Mechanisms of regulation also exist for instances when blood glucose levels fall. In periods of starvation both the liver and kidney cortex increase glucose production as a compensatory mechanism (van Schaftingen and Gerin, 2002), taking the form of glycogenolysis (breakdown of glycogen to glucose-6-phosphate) within the liver and gluconeogenesis (generation of glucose from non-carbohydrate precursors) within both the liver and kidney cortex. The key terminal step in these pivotal glucose-generating pathways involves the hydrolysis of glucose-6-phosphate (G6P) to glucose and inorganic phosphate and is catalysed by the enzyme glucose-6-phosphatase (*G6PC*), itself located within the lumen of the endoplasmic reticulum (ER) (Boustead, et al., 2004).

To date three members of the glucose-6-phosphatase family have been identified. *G6PC* is primarily expressed within liver and kidneys and is responsible for the last step in gluconeogenesis and glycogenolysis. Mutations within this gene lead to glycogen storage disease type 1a which is primarily characterised by severe hypoglycaemia in the fasting state (Lei, et al., 1993; Yang Chou and Mansfield, 1999). Due to defective G6P hydrolysis patients also present with hepato- and nephromegaly (Chou and Mansfield, 2008). Glucose-6-phosphatase, catalytic subunit, 2 [*G6PC2*] (previously denoted the islet specific G6PC-related protein, *IGRP*) is an islet specific glucose-6-phosphatase. The selective expression of this gene within pancreatic islets (Arden, et al., 1999; Ebert, et al., 1999) logically led a

number of groups to hypothesise that G6PC2 functions to antagonise the actions of GCK within this tissue thus leading to modulation of the glycolytic pathway and glucose-stimulated insulin secretion (Shieh, et al., 2004; Wang, et al., 2007). This isoform however, shows only 50% homology to *G6PC* (Arden, et al., 1999; Martin, et al., 2001; Martin, et al., 2002) and research regarding its hydrolytic capabilities have been controversial and variable (Arden, et al., 1999; Martin, et al., 2001; Martin, et al., 2002; Petrolonis, et al., 2004; Shieh, et al., 2004). The differences in the published observations are believed to stem from the inherent instability of this protein or the requirement of protein-protein interaction within the cellular environment to maintain catalytic activity (Arden, et al., 1999; Hutton and O'Brien, 2009). Additional insight into the role of G6PC2 *in vivo* was demonstrated through the generation of *G6pc2* null mice. These animals were phenotyped and reproducibly found to exhibit reduced fasting plasma glucose levels compared with wildtype (~15%), indicating that loss of G6PC2 activity *in vivo* would result in loss of counter regulation of, and effective increase in, GCK activity (Wang, et al., 2007). The third family member, *G6PC3* is primarily expressed in brain, kidney and muscle but has been shown to be expressed at low levels in all tissues analysed (Martin, et al., 2002).

Individuals with fasting plasma glucose levels even at the high end (>5.6mmol/L) of the physiological range (4-6mmol/L) (WHO, 2006) are documented to be at increased risk of mortality (Bjornholt, et al., 1999; Khaw, et al., 2001). Approximately one third of inter-individual variation in fpg is believed to be heritable (Watanabe, et al., 1999) and it is therefore vital to further understand how genetics underpin fpg levels. To this end a number of genome wide association (GWA) studies have been performed with the primary aim of identifying novel loci influencing fpg in the general population. In 2008, Chen *et al* performed a meta-analysis of two independent GWA studies comprising 5,088 non-diabetic individuals of Finnish and Sardinian descent, identifying strong association between SNP rs563694 and

fasting glucose levels ($p=3.5 \times 10^{-7}$) (Chen, et al., 2008). To replicate, meta-analysis of an additional six Caucasian cohorts was performed comprising fpg data from an additional 12,114 non-diabetic individuals (Amish, METabolic Syndrome in Men [METSIM], Caerphilly, British Women's Heart and Health Study [BWHHS], Diabetes Genetics Initiative [DGI] and FUSION Stage 2). They once again demonstrated strong association of rs563694 with fpg levels ($p=1 \times 10^{-19}$) with an effect size of 0.06mmol/L increase per copy of the A allele (Chen, et al., 2008). Further analysis of the initial 5,088 Finnish/Sardinian samples following imputation (within the Sardinian samples) revealed the top 17 association signals (including rs563694) to fall within a 63.9Kb region on chromosome 2 spanning two biologically plausible candidate genes, *G6PC2* and ATP-binding cassette, subfamily B, member 11 (*ABCB11*). In this re-analysis a different SNP (rs560887) showed strongest overall association with fpg ($p=2.8 \times 10^{-10}$) with an effect size of 0.06mmol/L per copy of the G allele. rs560887 is in high linkage disequilibrium (LD) with rs563694 ($D'=0.99$, $r^2=0.84$) and lies 10.9Kb upstream within the third intron of *G6PC2* (Chen, et al., 2008). At a similar time data were also published for a fpg GWAS performed in the French population (Bouatia-Naji, et al., 2008). Analysis in 654 non-obese normoglycaemic subjects (with replication in an additional 9,353) identified their strongest association with the same *G6PC2* intronic SNP rs560887 ($p=4 \times 10^{-23}$). This G/A polymorphism was associated with an increase in fpg of 0.06mmol/L per copy of the G allele (Bouatia-Naji, et al., 2008). Both studies concluded that the likely effects on glycaemia were being driven by a variant within *G6PC2* rather than *ABCB11* due to the location of the SNP and the published literature highlighting the biological plausibility of this gene. *ABCB11* is predominantly expressed within the liver where it encodes an ABC transporter involved in the secretion of bile salts. Bile salts once in circulation are themselves involved with the formation of micelles of fatty acids. Anti-lipid medications which work through sequestration of bile salts have been shown to lower blood glucose levels and increase insulin sensitivity through a reduction in triglyceride levels (Staels and Kuipers, 2007). Chen *et al.* postulated

that were the increase in fpg being driven through effects on ABCB11 they would also have expected to observe reduced insulin sensitivity and elevated lipid levels (Chen, et al., 2008), none of which were identified in the cohorts studied.

G6PC2 was at the time only the third gene in which common genetic variation had been shown to associate with fasting glucose levels, the other genes being glucokinase regulatory protein (*GCKR*) (Orho-Melander, et al., 2008; Saxena, et al., 2007; Vaxillaire, et al., 2008) and glucokinase (*GCK*) (Weedon, et al., 2005a). Earlier studies of *GCK* had already shown this gene to harbour rare mutations causative of monogenic beta-cell dysfunction with homozygous and heterozygous inactivating mutations causing permanent neonatal diabetes mellitus (PNDM) (Njolstad, et al., 2001) and maturity-onset diabetes of the young (MODY) (Froguel, et al., 1992; Hattersley, et al., 1992) respectively, whilst heterozygous activating mutations were demonstrated to cause hyperinsulinaemic hypoglycaemia (HH) (Glaser, et al., 1998).

The association of *G6PC2* with variation in fasting glucose in the general population, the biological candidacy of this gene as a potential regulator of GSIS within the pancreatic beta-cell, and knowledge that other FPG genes harbour rare mutations causing monogenic diabetes, led to the hypothesis that *G6PC2* may also be a novel site for activating and inactivating mutations leading to monogenic beta-cell dysfunction.

5.2 Methods

5.2.1 Subjects Studied

Patients with monogenic disorders of beta-cell dysfunction were identified following consultation with expert clinicians and molecular geneticists at Peninsula Medical School or Great Ormond Street children's hospital. DNA samples from these individuals were subsequently incorporated into existing patient cohorts at these institutions to which we have access as part of an enduring collaboration. Patients were classified depending upon their clinical phenotype and providing they met the inclusion criteria detailed below. Patients were only selected for *G6PC2* screening if all known genetic aetiologies had been previously excluded. A summary of the subject characteristics are provided in Table 5.1.

Maturity onset diabetes of the young (MODY) - All patients were diagnosed before the age of 25 (median age of onset 18 years [range 3-25]) with at least 1 first degree affected relative. All patients were non-insulin dependant with a BMI < 30 kg/m².

Glucokinase (GCK) like-MODY - Patients were selected who displayed a phenotype similar to that seen in GCK-MODY but mutations within *GCK* had been previously excluded. All patients had FPG ≥ 5.5 mmol/l (mean 6.6 mmol/l [range 5.5-7.8 mmol/L]), mean BMI of 23.6 kg/m² and detectable C-peptide levels.

Permanent neonatal diabetes mellitus (PNDM) - All subjects were diagnosed before the age of 6 months (median age of onset of 5 weeks [range 0-26]) and required insulin intervention (continuing past 6 months of age). All subjects were negative for pancreatic islet autoantibodies (GAD65, ICA and IA2-Ab).

Hyperinsulinaemic hypoglycaemia (HH) - Patients selected were shown to secrete insulin at excessively high levels despite hypoglycaemia. The mean age of diagnosis for this cohort was 0.9 years [range 1 day – 5 years] with all individuals presenting with severe hypoglycaemia (mean FPG = 2.05 mmol/L [range 1.1 - 3.4 mmol/L]).

Variable	MODY	PNDM	GCK-like MODY	HH
<i>n</i>	116	72	42	79
Age at diagnosis (<i>n</i>)	116	72	42	67
Median age at diagnosis	18 years	5 weeks	18 years	1 week
Range	(3-25 years)	(0-26 weeks)	(1-30 years)	(0-35 years)
Current treatment (<i>n</i>)	116	50	40	31
Insulin	0	48	8	2
OHA/OHA+insulin/Diet/NS/ metformin/glucose	61/0/50/0/1/0	0/0/0/0/0/0	4/1/12/0/0/0	0/0/0/0/0/2
Diazoxide	0	0	0	16
None	4	2	15	11

Table 5.1 Clinical characteristics of all patients with monogenic beta-cell dysfunction of unknown genetic aetiology. *n* = total number of patients screened within each cohort. Age at diagnosis was recorded for all patients within the MODY, PNDM and GCK-like MODY however data was only available for 67/79 HH cases.

5.2.2 Patient DNA

Genomic DNA was extracted from peripheral lymphocytes using standard procedures. Quantification was performed using NanoDrop™ technology (ThermoScientific, Loughborough, UK) and all samples diluted to a working concentration of 20ng/μl in sterile water. MODY, PNDM and HH cohorts were housed at Peninsula Medical School, Exeter University and were screened by Dr Emma Edghill. Screening of the GCK-like MODY DNA was performed at the Oxford Centre for Diabetes, Endocrinology & Metabolism, Oxford University where the DNA was stored.

5.2.3 Amplification of *G6PC2* in patients with monogenic beta-cell dysfunction

G6PC2 was amplified in 7 fragments spanning the promoter, 5' and 3' UTR's, coding regions and intron-exon boundaries. Primers were designed to ensure capture of at least 100bp either each side of coding sequence. Primer sequences and amplification conditions are provided in Table 5.2. 40ng of patient DNA was amplified in 25μl reaction volumes comprising 10X PCR Buffer II (2.5μl), 25mM Magnesium Chloride (1.5μl) (Applied Biosystems, Warrington, UK), 2.5mM deoxyribonucleotide triphosphates (1μl) (Promega, Southampton, UK), 5pM forward and reverse primers (1μl) (Operon, Ebersberg, Germany), 0.1U AmpliTaq Gold (0.1μl) (Applied Biosystems, Warrington, UK) and 15.9μl distilled water. Cycling

conditions were the same for all primer sets and comprised initial denaturation at 95°C for 12 minutes followed by 35 cycles of 94°C, 1 minute, 58°C, 1 minute and 72°C, 1 minute followed by a 10 minute elongation step at 72°C.

Fragment	Region	Primer	Primer Sequence	Annealing Temperature
	Amplified	Direction		
1	Promoter	Forward	gcaaagtctttcaccaaaca	58°C
		Reverse	cattcctgtgaaggaaatcca	
2	Exon 1	Forward	catgccacaaaggcacag	58°C
		Reverse	tgaatctgggtttcaagttacc	
3	Exon 2	Forward	attaaccctgcgcttgagtc	58°C
		Reverse	gcatcctcactcatgagattttc	
4	Exon 3	Forward	tgagacagtgtttctcaggctc	58°C
		Reverse	ccaactgaaaagtggaaatagc	
5	Exon 4	Forward	aatcatgatgctatgtcacagttag	58°C
		Reverse	ttggaaagtgtattaccggg	
6	Exon 5a	Forward	cattgaaaactgtggcaaatc	58°C
		Reverse	accggaagctcagtgtgtag	
7	Exon 5b	Forward	cctgtttgcagttggctttt	58°C
		Reverse	tgcaggctctgtgttcat	

Table 5.2 Sequences of primers and reaction conditions used to amplify *G6PC2*. All primers had M13 tails added for sequencing ease (F-tgtaaacgacggccagt, R-caggaaacagctatgacc).

Samples were separated on the basis of size using agarose gel electrophoresis at 120V for 40 minutes. The fluorescent intercalating agent, ethidium bromide was added to each gel allowing visualisation of products by ultra violet light on a Gel Doc Illuminator system (BioRad, Hemel Hempstead, UK).

5.2.4 Sequencing of amplified DNA to identify novel *G6PC2* mutations

All samples were sequenced bi-directionally. 1µl of PCR product was added to 0.5µl Exonuclease I (New England Biolabs, Hitchin, UK) and 0.5µl shrimp alkaline phosphatase (Promega, Southampton, UK). Reactions were heated to 37°C for 30 minutes allowing enzymes to remove any residual PCR contaminants before a final 15 minute heat shock of 80°C to denature the enzymes. Samples were subjected to sequencing reactions using Big Dye Terminator Sequencing Mix v1.1 (0.25µl) containing fluorescently labelled dideoxy nucleoside triphosphates (ddNTPs) and Big Dye Dilution Buffer (1.875µl) (Applied Biosystems,

Warrington, UK). 5 μ M sequencing primers with M13 tails (2 μ l) (Operon, Ebersberg, Germany) and sterile water (3.875 μ l) were also added. All samples were then amplified using 25 cycles of: 96°C for 10sec, 50°C for 5sec, 60°C for 4mins. Sequencing products were centrifuged at 1000xg for 2 minutes and 5 μ l deionised water added to each well. Samples were transferred to wells of a 96 well Performa DTR V3 short clean up plate (VH Bio, Gateshead, UK) before centrifugation at 850xg for 5 minutes and eluants collected in a clean 96 well non-skirted PCR plate. Samples were then dried down at 70°C for 90 minutes.

Samples were analysed on an ABI3730xl capillary sequencer (Applied Biosystems, Warrington, UK). Sample read outs were analysed using Mutation Surveyor v3.2 (Soft Genetics, Cambridge, UK) against *G6PC2* reference sequence NM_001081686.

5.3 Results

Screening of the *G6PC2* genomic sequence in four monogenic beta-cell dysfunction cohorts was performed as a joint study between Exeter and Oxford University. I performed screening and analysis within the cohort of GCK-like MODY subjects. In total, 20 variants were identified (Table 5.3), five common (minor allele frequency [MAF]>0.05) and 15 rare (MAF≤0.05). Of these variants, eleven had previously been reported within the literature with rs numbers present on dbSNP (build 126, <http://www.ncbi.nlm.nih.gov/sites/entrez?db=snp>) whilst the remaining nine were novel. The twenty variants were located throughout *G6PC2*, five within the promoter and 3'UTR, four within intronic regions and the remaining 11 were located within coding exons.

Of the nine non-coding variants, seven had previously been described within the literature (c.-301A>G rs573225, c.-294T>C rs34746523, c.-280G>A rs2232316, IVS1-42G>A rs2232318, IVS3-26C>T rs560887, IVS3-25T>C rs2232321, c.*27>GA rs2232329) whilst the remaining two (c.*47A>G and IVS1+88C>T) were novel. The 3'UTR variant (c.*47A>G) was identified in one MODY and one GCK-like MODY proband and its location within the 3'UTR warranted further investigation of the potential disruption of micro RNA (miRNA) binding sites (www.ebi.ac.uk/enright-srv/microcosm/cgi-bin/argets/). Further analysis however revealed there to be no putative binding sites at or around this position with the closest binding site for has-miRNA-758 lying 50bp downstream of this variant. The final non-coding variant IVS1+88C>T, located within intron 1, was identified in a single proband with GCK-like MODY. Its location deep within an intron however indicates that it is unlikely to be affecting mRNA splice sites and therefore this variant was not regarded as pathogenic.

Of the eleven coding variants, four non-synonymous variants had been described previously within the literature (Y207S rs2232323, V219L rs492594, S324P rs2232326, S342C rs2232328).

The synonymous variants (c.291C>T, p.C97C and c.699G>A, p.L223L) identified in this screen were novel. c.699G>A, p.L223L was identified in a single MODY proband (MAF 0.004) however screening in 288 Europid control chromosomes confirmed its presence at a similar MAF (0.003) in the general population demonstrating this is likely to be a rare but non-pathogenic variant. c.291C>T, p.C97C was identified in a single proband with PNDM (MAF 0.006) however on this occasion screening of 140 control chromosomes failed to demonstrate its presence within the general population. To investigate the potential pathogenicity of this variant, the probands mother and father were tested for presence of the variant. We failed to demonstrate co-segregation of the variant with diabetes as the proband had inherited this variant from their normoglycaemic mother (simultaneously ruling out the possibility that this mutation had arisen *de novo*). The remaining five non-synonymous variants (Q16H, H177Y, F256L, R283X and L297_298del) were all novel *G6PC2* coding variants and warranted further investigation.

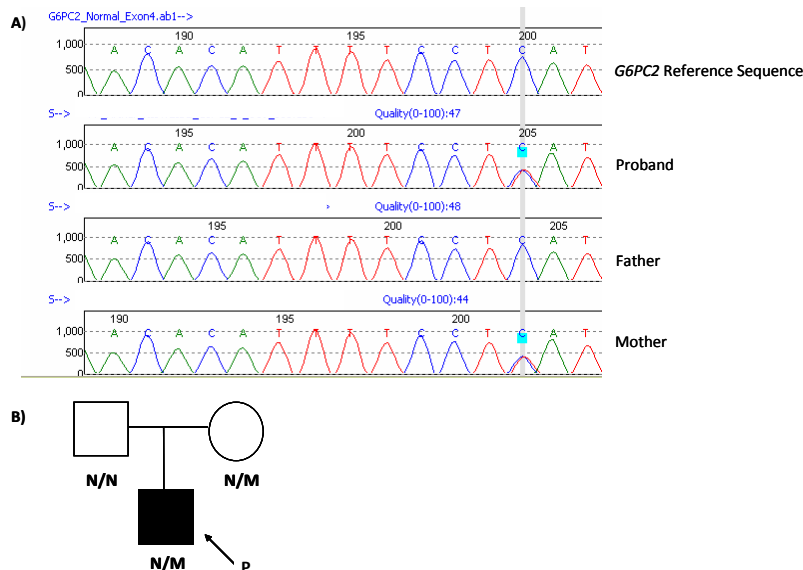


Figure 5.1 (A) Sequencing of *G6PC2* in a HH proband demonstrates presence of a heterozygous C>T base change in Exon4 (H177Y). Sequencing electropherograms illustrate inheritance of the novel variant is from the probands mother and the location of this SNP is shown by a grey bar across all individuals and reference sequence. (B) Pedigree of the same HH proband and immediate family members demonstrating the variant does not co-segregate with disease status. Filled symbols depict hypoglycaemic individuals whilst open symbols represent family members with physiological glucose levels. Males are depicted using squares, females by circles, heterozygous carriers of the variant by N/M and homozygous WT using N/N.

Variant c.529C>T, p.H177Y, located within the 4th exon of *G6PC2*, was present in the heterozygous state in two probands, one presenting with HH (MAF 0.006) and one with PNDM (MAF 0.006). Screening of 166 European chromosomes identified this variant within the control population at a similar frequency (MAF 0.006) and screening of the HH proband's immediate family demonstrated inheritance of this variant from their unaffected mother (Figure 5.1). Presence of this variant within two distinct clinical groups, healthy controls and an unaffected parent indicates it is likely to be a novel rare non-pathogenic variant.

We failed to demonstrate presence of c.48G>T, p.Q16H, c.847C>T, p.R283X and c.889_894delTGACCT, p.L297_298del within at least 172 control chromosomes. To determine likely pathogenicity of these variants we once again tested parental DNA. In each case, inheritance of the variant was shown to be from an unaffected parent therefore the failure of the variants to co-segregate with phenotype and demonstration that they are not *de novo* mutations indicates they are unlikely to be pathogenic. The final novel non-synonymous variant c.766T>C, p.F256L was identified within a single patient with HH. Screening of 288 control chromosomes did not identify the variant and parental DNA was unfortunately unavailable for genetic testing, therefore we were unable to determine co-segregation. Sequence conservation analysis revealed that phenylalanine (F) at residue 256 is highly conserved across multiple species (Figure 5.2). Bioinformatic tools were therefore used to elucidate the likely pathogenicity of this non-synonymous variant. SIFT analysis software (<http://blocks.fhcrc.org/sift/SIFT.html>) utilises the physical properties of an amino acid alongside sequence homology to assess what modifications an amino acid substitution will exert on protein function. Using this process the substitution of leucine for phenylalanine at position 256 is predicted to be tolerated by the protein. The PolyPhen prediction site which uses only physical properties of the amino acids

(<http://genetics.bwh.harvard.edu/pph/index.html>) predicted this substitution was likely to be damaging.

Homo sapiens	222	YLLLRVLNIDLLWSVPIAKKWCANPDWIHIDTT	PFA	GLVRNLGVLFGLGFAINSEMFL	SCRGGNNYTL	SFRLLCALTSL	301
Pan troglodytes	222	YLLLRVLNIDLLWSVPIAKKWCANPEWIHIDTT	PFA	GLVRNLGVLFGLGFAINSEMFL	SCRGGNNYTL	SFRLLCALTSL	301
Pongo abelii	222	YLLLRLLNIDLLWSVSIAKKWCANPDWIHIDTT	PFA	GLVRNLGVLFGLGFAINSEMFL	SCRGGNSYTL	SFRLLCAFTSL	301
Callithrix jacchus	222	YLLLRLLSIDLLWSVTIAKKWCANPDWIHIDTT	PFA	GLVRNLGVLFGLGFAINSEMIL	MSCRGGKSYTL	SFRLLCALTSL	301
Oryctolagus caniculus	222	YLLLRLLDIDLLWSVPIAKKWCANPDWIHIDTT	PFA	GLVRNLGVLFGLGFAINSEMFL	SCRGENGYKLS	SFRVLCAMTSL	301
Mus musculus	222	YLLLRVFGIDLLWSVPIAKKWCANPDWIHIDST	PFA	GLVRNLGVLFGLGFAINSEMFL	RSCQGENGKPS	SFRLLCALTSL	301
Bos taurus	222	YLLLRHLDIDLLWSVPIAKKWCANPDWIHIDTT	PFA	GLVRNLGVLFGLGFAINSEMFL	RSCGENGYGLS	SFRLLCALVSL	301
Equus ferus	222	YLLLRLLDIDLLWSVPIAKKWCANPDWIHIDTT	PFA	GLVRNLGVLFGLGFAINSEMFL	QSCRGENRYKLS	SFRLLCAAASL	301
Canis lupis	238	YLLLRLLDIDLLWSVPIAKKWCANPDWIHIDTT	PFA	GLVRNLGVLFGLGFAINSEMFL	RSCGENGYKLS	SFRLLCAGASL	317
Sus scrofa	222	YLLGLLDIDLLWSVPIAKKWCANPEWIHIDTT	PFA	GLVRNLGVLFGLGFAINSEMFL	RSCGENGYRLS	SFRLLCTMASL	301
Taeniopygia guttata	222	YLSLKLDDIDLLWSVPAKKWCANPDWINIDTT	PFA	GLVRNLGALFGLGLINSEMFIT	SCRKGNCKIS	SFRILCVAASL	301
Xenopus laevis	224	YLLKAVGVDDLWTLEKAKRWCAQPEWIHIDTT	PFA	GLLRNLGIFGLGLALNSKLYQ	ESCGGKKSQFT	SFRLLCCIVASL	303

Figure 5.2 Conservation analysis of G6PC2 protein species across multiple species reveals that phenylalanine (F) at residue 25 is a highly conserved residue.

SNP	rs number	Location	Minor Allele Frequency (MAF)					CEU HapMap (MAF)
			MODY (116)	PNDM (72)	GCK-like MODY (42)	HH (79)	Controls	
c.-301A>G	rs573225	Promoter	0.27	0.31	0.30	0.31	NA	0.36 (G)
c.-294T>C	rs34746523	Promoter	0	0.006	0.01	0	NA	NA
c.-280G>A	rs2232316	Promoter	0.02	0.006	0.1	0.08	NA	0.07 (A)
c.48G>T, p.Q16H	Novel	Exon 1	0	0	0	0.006	0	-
IVS1+88C>T	Novel	Intron 1	0	0	0.01	0	NA	-
IVS1-42G>A	rs2232318	Intron 1	0.02	0.01	0.05	0.02	NA	NA
c.291C>T, p.C97C	Novel	Exon 2	0	0.006	0	0	0	-
IVS3-26C>T	rs560887	Intron 3	0.31	0.30	0.25	0.30	NA	0.33 (T)
IVS3-25G>A	rs2232321	Intron 3	0	0	0	0.006	NA	NA
c.529C>T, p.H177Y	Novel	Exon 4	0	0.006	0	0.006	0.006	-
c.623A>C, p.Y207S	rs2232323	Exon 5	0.008	0.01	0	0.006	0.007	0.02 (C)
c.658G>C, p.V219L	rs492594	Exon 5	0.41	0.42	0.42	0.47	0.39	0.48 (C)
c.699G>A, p.L223L	Novel	Exon 5	0.004	0	0	0	0.003	-
c.766T>C, p.F256L	Novel	Exon 5	0	0	0	0.006	0	-
c.847C>T, p.R283X	Novel	Exon 5	0.002	0	0	0.01	0	-
c.889_894del TGACCT, p.L297_298del	Novel	Exon 5	0	0.006	0	0	0	-
c.967T>C, p.S324P	rs2232326	Exon 5	0	0.006	0	0	0	0.0 (C)
c.1022C>G, p.S342C	rs2232328	Exon 5	0	0.12	0.12	0.13	NA	0.08 (G)
c.*27G>A	rs2232329	3'UTR	0	0	0.01	0	0.01	NA
c.*47A>G	Novel	3'UTR	0.004	0	0.01	0	0.006	-

Table 5.3 *G6PC2* variants identified in patients with MODY, PNDM, GCK-like MODY and HH. NA = Not available. Variants shown in blue illustrate novel non-synonymous variants

5.4 Discussion

Mutational screening of the coding region, intron-exon boundaries, promoter and 3'UTR of *G6PC2* in four cohorts of patients with monogenic disorders of beta-cell dysfunction identified five novel coding variants. Through screening of ethnically matched control chromosomes and parental DNA we were able to demonstrate that four of the five novel variants were likely to be rare but non-pathogenic. Unfortunately, as parental DNA was unavailable for the proband heterozygous for the F256L variant we were unable to establish co-segregation with hypoglycaemia in this family. Similarly, bioinformatic prediction sites were inconclusive with one predicting a phenylalanine to leucine change to be damaging whilst the other predicts the variant to be tolerated. In light of this we cannot rule out the possibility that F256L is pathogenic, however we believe that mutations within *G6PC2* are unlikely to be a common cause of monogenic forms of beta-cell dysfunction. Our findings are further supported by a subsequent similar study by Bonnefond *et al* (Bonnefond, et al., 2009). They screened *G6PC2* in French cohorts of patients with monogenic beta-cell dysfunction and through testing of 16 MODY, 32 PNDM and 28 HH subjects they concluded, as we also had, that mutations within this novel fasting glucose gene were unlikely to cause monogenic forms of beta-cell dysfunction.

The original genome-wide association studies which identified common *G6PC2* variants associated with fasting glucose levels identified a region of association on chromosome 2 encompassing both *G6PC2* and *ABCB11* (Bouatia-Naji, et al., 2008; Chen, et al., 2008). rs563694 was located directly between these genes whereas rs560887 was located within the third intron of *G6PC2*. As this was the strongest associated SNP ($p=2.8 \times 10^{-8}$) in both studies, and *G6PC2* was considered the most biologically plausible due to its hypothesised function within the beta-cell, the authors believed that this was the gene through which the SNP was exerting its effects (Bouatia-Naji, et al., 2008). As no alterations in insulin sensitivity or

triglyceride levels were observed, as would be expected if *ABCB11* were driving the increase in fpg (Chen, et al., 2008; Staels and Kuipers, 2007), we too believed this to be the likely causal gene and centred our efforts on mutational screening of this candidate gene. However in light of our negative findings we cannot rule out the possibility that *ABCB11* may be the causal gene acting through an as yet unknown mechanism.

It is evident that the top hit drawn from both association studies (rs560887) is unlikely to be the true causal variant due to its location deep within the third intron of *G6PC2*, therefore it is highly plausible that a SNP in high LD with rs560887 is likely to be driving the observed phenotype. Following publication of the GWAS data numerous groups set about trying to refine the association signal and characterise potentially causal variants. Dos Santos *et al.* chose to study rs573225, a common (MAF>0.05) *G6PC2* promoter SNP which lies within a binding site for the transcription factor Foxa2 and is in high LD ($r^2=0.96$) with the original association signal (Bischof, et al., 2001; Dos Santos, et al., 2009; Ebert, et al., 1999). Their findings demonstrated that the A allele was associated with a reduction in transcription factor binding, reduced gene expression and an increase in fasting plasma glucose levels (Dos Santos, et al., 2009). The authors therefore concluded that the promoter SNP (rs573225) was likely to be the true causal variant and explain the recent GWAS signals. However, the authors failed to comment on how reduced gene expression of *G6PC2* could account for the increased fasting plasma glucose levels which were observed in carriers of the A allele in their study. Based on data from *G6pc2* knockout mice a reduction in *G6pc2* expression is associated with reduced fasting glucose levels which corresponds with the function of *G6PC2* as a regulator of GCK (Wang, et al., 2007).

A recent study carried out by Bouatia-Naji *et al.* utilised a more systematic approach to answer the same research question (Bouatia-Naji, et al., 2010). They identified two *G6PC2*

promoter SNPs which lie within transcription factor binding sites and are in high LD ($r^2 > 0.88$) with the original association signal. rs13431652 lies distal to the transcription start site (-4428) within a NF-Y binding site whereas rs573225 (the same SNP studied by Dos Santos *et al.*) is proximal and falls within a Foxa2 binding site (Bouatia-Naji, et al., 2010). Their studies demonstrated that the A allele of the Dos Santos *et al.* SNP (rs573225) is associated with decreased *G6PC2* expression and increased fasting glucose levels (Bouatia-Naji, et al., 2010; Dos Santos, et al., 2009). However, paradoxically they also demonstrated an increase in Foxa2 binding to the A allele. From their findings they conclude that their functional data do not support a mechanistic role of rs573225 as the causative SNP. However, in contrast they demonstrated that the A allele at rs13431652 was associated with an increase in NF-Y transcription factor binding, increased gene expression and an increase in fasting plasma glucose. These results are consistent with the role of *G6PC2* within islets and led the authors to postulate that rs13431652 may be the causal SNP which drives the association between *G6PC2* and fasting glucose (Bouatia-Naji, et al., 2010).

One of the most striking observations is that the *G6PC2* SNP associated with an increase in fpg is not associated with increase risk of T2D (Bouatia-Naji, et al., 2008; Chen, et al., 2008), in fact, if anything, the variant is mildly protective (OR=0.93, p=0.0017) (Dupuis, et al., 2010). This finding highlights an interesting paradox within the literature whereby not all variants associated with fpg in the general population are associated with an increase risk of T2D despite this being one of the major pathological contributors to the phenotype. In many cases there is considerable overlap between the dichotomous trait and the continual variable, as is observed for fpg raising variants within *GCK*, *GKRP* and *MTNR1B* which are all robustly associated with T2D ($p < 5 \times 10^{-8}$) (Dupuis, et al., 2010). This overlap however is not complete as a many fpg SNPs with similar effect sizes to those mentioned previously, have neutral effect on T2D risk (*SLC2A2* and *MADD*, OR=1.01) (Dupuis, et al., 2010). Taken together this

demonstrates that genetic variants which cause alterations in fpg within the physiological range may be different to those which cause pathological differences. Moreover it may be the mechanism through which the variant is acting which is the contributing factor towards disease progression (Dupuis, et al., 2010).

It was speculated that the mechanism through which the *G6PC2* G allele at rs560887 raised fpg levels was through an alteration of the glucostatic set point, but that T2D progression would require further compromise of the beta-cells (Bouatia-Naji, et al., 2008). However, physiological characterisation by two independent groups (Ingelsson, et al., 2010; Rose, et al., 2009) demonstrates a more complex interplay of factors. The G allele at rs560887 not only associates with elevated FPG levels but also with an elevated insulinogenic index, demonstrating an increased glucose-stimulated insulin release. This observation led the authors to speculate that a shift in the glucostatic set point may drive the glucose phenotype but the beta-cells may hyper respond to postprandial increases in blood glucose levels accounting for the increased insulinogenic index and potentially the protective effect against T2D (Ingelsson, et al., 2010; Rose, et al., 2009).

The functional data from these follow-up studies, although not entirely conclusive, suggest that the association signal is arising from *G6PC2* and therefore support our decision to screen monogenic patients for novel mutations within this gene rather than *ABCB11*.

Chapter 6

An investigation of the role of phosphatase and tensin homologue deleted on chromosome ten (PTEN) in patients with Type 2 diabetes

6.1 Introduction

Stimulated glucose uptake into skeletal muscle and adipose tissue coupled with the inhibition of gluconeogenesis in hepatocytes are two major mechanisms via which insulin regulates glucose homeostasis [reviewed in (Saltiel and Kahn, 2001)]. The failure of physiological insulin to increase glucose disposal and switch off gluconeogenesis can lead to the onset of insulin resistance (Dinneen, et al., 1992). Type 2 diabetes (T2D) ensues if pancreatic beta-cells are unable to increase their secretory capacity to meet the increased insulin demand (Stumvoll, et al., 2005). Therefore understanding the molecular mechanisms behind insulin resistance are of paramount importance clinically.

In healthy individuals many of the metabolic consequences of insulin are mediated via the PI3K/AKT signalling cascade (Taniguchi, et al., 2006a). The conversion of phosphatidylinositol(4,5)-bisphosphate (PIP_2) to phosphatidylinositol(3,4,5)-triphosphate (PIP_3) by PI3K triggers plasma membrane recruitment and activation of AKT (Alessi, et al., 1996; Hawkins, et al., 1992; Myers, et al., 1992). AKT is a critical node in the insulin signalling cascade as it functions as a key regulator of a number of downstream metabolic targets including glycogen synthase kinase-3 (GSK-3) and AKT substrate 160kDa (AS160), regulating glycogen storage and GLUT4 translocation respectively (Cross, et al., 1995; Sano, et al., 2003).

As the PI3K/AKT pathway plays an important role in a multitude of downstream processes its activation is closely regulated, in part by protein phosphatases including phosphatase and tensin homologue deleted on chromosome ten (PTEN), which negatively regulates the AKT pathway via dephosphorylation of PIP_3 at the 3' position (Maehama and Dixon, 1998). Its central role in antagonism of PI3K have led many groups to focus their attention on this protein and its control of insulin stimulated glucose uptake using in-vitro systems and knockout mouse models.

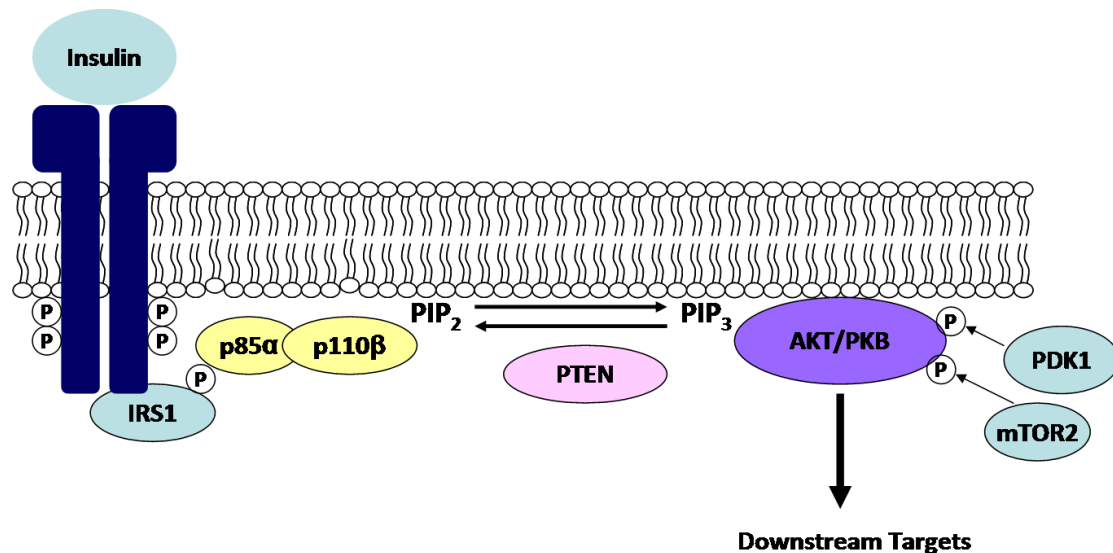


Figure 6.1 Insulin signalling via the PI3K/AKT pathway. Transduction of the signal relies on the generation of the secondary messenger PIP₃, which recruits AKT to the plasma membrane where it is phosphorylated and activated. PTEN negatively regulates this pathway via down-regulation of PIP₃ levels.

Initial studies using rodent 3T3-L1 cells demonstrated that ablation of PTEN using short interfering RNA (siRNA) knockdown was sufficient to increase insulin stimulated AKT phosphorylation resulting in increased glucose uptake. The central role of PTEN as a tumour suppressor gene and a developmental regulator in many tissues precludes the generation of global *Pten*^{-/-} as these animals cannot surpass embryonic day [E] 7.5 (Di Cristofano, et al., 1998; Podsypanina, et al., 1999). To avoid the developmental problems associated with global knockout models a number of groups have chosen to study *Pten*^{-/-} knockout within insulin target tissues of mice using the Cre-loxP system originally developed by Sauer in 1997 (Sauer, 1987; Sauer and Henderson, 1988). Using this methodology adipose tissue, skeletal muscle and liver knockouts were generated and the phenotypes of the animals studied in depth with regards to glucose homeostasis.

Adipose tissue *Pten*^{-/-} knockouts were generated using Cre under an adipose specific fatty acid binding protein promoter (Kurlawalla-Martinez, et al., 2005). When phenotyped, mutant animals were found to demonstrate increased insulin signalling in this depot as assessed by a

1.8 fold increase in p-AKT and increased phosphorylation of a number of downstream signalling molecules including GSK-3 and FOXO1. Mutant animals also demonstrated increased GLUT4 at the plasma membrane in both basal and stimulated conditions. A blunted response to a glucose challenge and inability to return to baseline after an insulin challenge were characteristics also observed within the mutant population (Kurlawalla-Martinez, et al., 2005). Taken alongside the finding that mutants presented with a 2.1 fold reduction in fasting plasma insulin, demonstrates that *Pten*^{-/-} adipose knockout animals are more insulin-sensitive when compared to their wildtype counterparts. Of interest, despite increased glucose uptake there was no alteration in fat mass within the mutants, neither did the authors report development of any tumours or neoplastic lesions within this depot (Kurlawalla-Martinez, et al., 2005).

Insulin resistance in muscle is one of the earliest signs of T2D and therefore understanding the regulation of insulin signalling in this tissue is paramount (Vaag, et al., 1992). *Pten*^{-/-} knockout within murine skeletal muscle was achieved using Cre under a muscle creatine kinase promoter (Wijesekara, et al., 2005). Animals with total ablation of *Pten* within this tissue did not display as marked phenotype as adipose tissue mutants and the majority of physiological effects were only observed upon high fat diet (HFD) feeding. At basal levels, mutant animals trended towards hypoglycaemia but this did not reach statistical significance, however, when fed a HFD, fpg remained within the normal range in mutant animals whilst a dramatic increase in fpg was observed in WT counterparts. Similarly mutant animals maintained normal insulin sensitivity after prolonged HFD feeding whilst WT animals developed insulin resistance (Wijesekara, et al., 2005). Liver tissue-specific knockouts were generated using Cre under an albumin promoter (Stiles, et al., 2004). When ablated within this tissue mutant animals exhibited hepatomegaly and increased fatty liver due to 2.5 fold increase in the rate of fatty acid synthesis. The animals also demonstrated decreased activity

of GSK-3 (50%) and glycogen accumulation within hepatocytes and were shown to be more insulin-sensitive as assessed by reduced fpg and fasting plasma insulin levels (Stiles, et al., 2004).

Each of these tissue-specific knockout models demonstrate that in tissues of action Pten plays a crucial role in the regulation of glucose homeostasis. Therefore to assess the effects of *Pten* loss on whole body physiology and insulin sensitivity, a haploinsufficient model was generated (*Pten*^{+/-}) (Wong, et al., 2007). These animals recapitulated many features observed in the tissue-specific knockout models. They were shown to exhibit hypoglycaemia in both the fasting and fed state and demonstrated increased glucose tolerance as measured by glucose and insulin challenges. Fasting plasma insulin levels were also significantly reduced in the mutant animals, suggesting that the phenotype observed is largely due to changes in insulin sensitivity as opposed to pancreatic alteration (islet function and morphology were similar between the two groups). Glucose uptake was found to be elevated in mutant mice at all time points measured, therefore demonstrating that the PKB/AKT pathway is elevated in these mutants (Wong, et al., 2007).

In light of the data generated by the multitude of *Pten*^{-/-} knockout models it was hypothesised that within human tissues of insulin action, PTEN is likely to play an equivocally important role in the regulation of insulin signalling. One phenotype which commonly associates with defective insulin signalling is T2D (Stumvoll, et al., 2005). I therefore hypothesised that in T2D patients, *PTEN* expression may be up-regulated, negatively regulating the PI3K/AKT pathway and contributing to the insulin resistance we observe in these individuals. This variation in *PTEN* expression is likely to be tissue-specific and therefore access to tissue biopsies from patients with T2D was required to assess this hypothesis. Through surgical biobanks in Oxford (MOLSURG) and Leipzig I was granted access to biopsies taken from

patients undergoing elective surgery. As liver biopsies are rarely obtained in these scenarios I chose to focus the analysis on adipose tissue (both subcutaneous and omental) and muscle biopsies and assess the expression of *PTEN* in these tissues.

6.2 Methods

6.2.1 Subjects Studied

Oxford Cohort – MOLSURG collection

Subjects with T2D were selected from the MOLPAGE surgical biobank (MOLSURG) only if subcutaneous adipose tissue, omental adipose tissue and skeletal muscle biopsies were obtained during elective surgery and multiple aliquots frozen in liquid nitrogen for long term storage. Selection based on these criteria identified 17 T2D subjects. Each case was individually matched to a normoglycaemic subject from the same biobank. Subjects were deemed 'normoglycaemic' if they were self reporting non-diabetic with FPG and/or HbA1c ≤ 7 mmol/L and 6.5% respectively. Controls were matched on the basis of age, gender and BMI and providing the same selection of tissue biopsies were available. Detailed individual level subject characteristics are provided in **Chapter 2** whilst a summary is provided in Table 6.1.

Leipzig biobank samples

For replication purposes, access was granted to an additional biobank of samples stored at the University of Leipzig in the laboratories of Professor Matthias Blüher. Forty subjects with T2D were selected from this cohort for whom both subcutaneous and omental biopsies were available (skeletal muscle expression was not determined in this cohort as a direct consequence of our observations within the Oxford cohort). As with the Oxford samples, 40 matched (age, gender, BMI) normoglycaemic individuals were also selected. A summary of the Leipzig patient characteristics is also provided in Table 6.1.

Oxford Biobank - Adipose tissue stimulated samples

To assess the effects of insulin on *PTEN* expression, access was granted to adipose tissue biopsies from patients pre and post glucose challenge. Access to patient samples was

provided by Professor Fredrik Karpe, Oxford University. Following an overnight fast, adipose biopsies were taken from both the abdomen and gluteal subcutaneous regions of 12 individuals. Subjects were then given a 75g glucose load and additional biopsies taken 90 minutes later, from the same abdominal and gluteal regions. Biopsies were stored at -20°C until RNA extractions were performed. Patient characteristics are summarised in Table 6.1.

Oxford (MOLSURG)	T2D	Normoglycaemic	p value
	n=17	n=17	
Gender	Males (9) Females (8)	Males (9) Females (8)	
Age (years)	60.4 ± 13.9	61 ± 12.4	ns
BMI (kg/m²)	28.3 ± 6.1	27.7 ± 5.5	ns
Fasting Glucose (mmol/L)	10.1 ± 4.5	6.2 ± 1.2	0.0037
HbA1C (%)	8.1 ± 2.1	5.5 ± 0.4	0.0001
Leipzig Samples	T2D	Normoglycaemic	p value
	n=40	n=40	
Gender	Male (14) Female (26)	Male (14) Female (26)	
Age (years)	48 ± 10	48 ± 10	ns
BMI (kg/m²)	36.2 ± 13.1	36.7 ± 13.4	ns
Fasting Glucose (mmol/L)	6.9 ± 1.27	5.3 ± 0.26	0.0001
HbA1C (%)	6.4 ± 0.4	5.5 ± 0.2	0.0001
Stimulated Samples	Lean	Obese	p value
	n=6	n=6	
Gender	Male (6)	Male (6)	
BMI (kg/m²)	23.2 ± 0.72	31.7 ± 4.6	0.004
Age (years)	49.5 ± 6.4	47.3 ± 3.4	0.75
Fasting Glucose (mmol/L)	5.02 ± 0.29	5.67 ± 0.47	0.03

Table 6.1 Summary information of individuals selected from the MoLSURG, Leipzig and Oxford biobanks for *PTEN* expression analysis. T2D subjects were age, gender and BMI matched to normoglycaemic controls as closely as possible. Data are presented as mean ± SD and p values calculated using the paired t-test. ns= not significant. α=0.05. Stimulated samples were taken from lean and obese patients from the Oxford Biobank, p values calculated using independent t-test.

6.2.2 RNA extraction and processing of tissue biopsies

Tissue biopsies were removed from liquid nitrogen storage tanks into a small scale dewar for intermediate handling. Samples were removed from storage cryovials and dissected on dry ice before homogenising in TRIZOL (Applied Biosystems, Warrington, UK). Care was taken to ensure the samples did not thaw before or during tissue processing. RNA was extracted using the guanidinium thiocyanate-phenol-chloroform extraction method and resuspended in sterile water (Chomczynski and Sacchi, 1987). RNA quantification was performed using spectrophotometric determination of purity and Agilent BioAnalyser determination of integrity. Samples were only subjected to cDNA synthesis and included in the experiment if RIN scores generated by the Agilent were >5.5 (Schroeder, et al., 2006). RNA was decontaminated using DNase I (Applied Biosystems, Warrington, UK) before 2µg total RNA was reverse transcribed in a first strand synthesis reaction using MultiScribe™ reverse transcriptase (Applied Biosystems, Warrington, UK).

To minimise any protocol variation, I travelled to Leipzig to perform RNA extractions, DNase I treatment and cDNA synthesis (2µg total RNA) of all adipose samples using the same methodology and equipment/reagents as previously described for the Oxford samples. cDNA samples were then shipped back to Oxford to perform all qRT-PCR analysis on the same 7900HT thermocycler, unavailable in Leipzig.

Due to the small size of stimulated adipose tissue biopsies, and subsequent low RNA yield, cDNA was generated from 300ng total RNA for all stimulated biopsies. Following amplification, all cDNA samples were stored at -20°C until required.

6.2.3 Quantitative realtime PCR (qRT-PCR) – Adipose Tissue samples

For the Oxford-MOLSURG and Leipzig biobank samples, standards were generated by serially diluting (1:50-1:800) from a stock of pooled experimental sample cDNA. Standards and adipose tissue cDNA (diluted to 1:100 working solution in 0.01M Tris-HCl [pH6.8]) were added to wells of a 96well deep storage plate (Fisher Scientific, Loughborough, UK). Due to quantity of samples to be tested, pipetting error was minimised by utilising a Hydra 96 liquid handler and dispenser (Robbins Scientific, Solihull, UK) to transfer 4 μ l of each sample and standard (in triplicate) from the 96well deep storage plate to 384well reaction plates. Multiple working stock plates were generated, dried down in a DNA oven and stored at -20°C until required.

For quantification, Taqman methodology was used whereby all samples and standards were amplified in 6 μ l reaction volumes containing 5.5 μ l gene expression mastermix and 0.5 μ l gene specific probe (Applied Biosystems, Warrington, UK). Amplification and detection were performed using an ABI7900HT thermocycler using standard amplification conditions. All genes of interest were amplified alongside two housekeeping genes *PPIA* and *UBC*, chosen due to their accuracy as adipose tissue housekeeping genes (Neville, et al., 2010). Probe identification numbers for all gene studies is provided in Table 6.2. All data were analysed using the $\Delta\Delta C_T$ method of analysis normalising to the geometric mean of the two housekeeping genes and calibrating to the 1:100 standard curve value for the specific assay.

Due to the low starting amount of RNA for the stimulated analysis (300ng), samples were run at a 1:10 dilution with samples generated serially from 1:5 – 1:80. Analysis was performed through normalisation to the same two housekeeping genes but calibration was performed to the 1:10 standard for each assay.

Gene	Probe Identification
<i>PTEN</i>	Hs01920652_m1
<i>PIK3R1 (p85α)</i>	Hs00381459_m1
<i>PIK3CB (p110β)</i>	Hs00927728_m1
<i>IRS1</i>	Hs00178563_m1
<i>AKT2</i>	Hs01086102_m1
<i>INSR</i>	Hs00961554_m1
<i>PPIA</i>	Hs99999904_m1
<i>UBC</i>	Hs00824723_m1

Table 6.2 Insulin signalling gene studies in a panel of human adipose tissue samples. Probe/primer sets were purchased from Applied Biosystems and were selected on the basis that they were designed to cross exon-exon boundaries and therefore prevent genomic amplification (_m1).

6.2.4 Quantitative realtime PCR – Muscle samples

Standards were originally generated from pooled muscle cDNA experimental samples by serially diluting from 1:50-1:800 in 0.01M Tris-HCl, the same concentrations which were reproducibly used for adipose tissue experiments. 4 μ l of 1:100 muscle sample cDNA was amplified as outlined above using identical amplification mastermix's and cycling conditions. Following poor *PTEN* expression results at this sample dilution, both the standards (1:5–1:80) and sample (1:5) dilutions were increased to try to minimise triplicate variability and amplification efficiency. *PTEN*, *PPIA* and *UBC* were used for gene expression profiling within this depot and their identification numbers are provided in Table 6.2.

6.2.5 Protein extraction and quantification – Adipose tissue samples

1ml ice cold lysis buffer and a ball bearing were added to a 2ml eppendorf tube with 10 μ l Halt Protease and Phosphatase Inhibitor cocktail. Adipose tissue samples were dissected on dry ice before adding to the lysis buffer and homogenising in a Retsch free standing homogeniser (Retsch UK, Leeds, UK). Samples were stored at 4°C for 2 hours on an orbital shaker ensuring constant agitation before centrifugation at 12,000xg for 15 minutes (4°C). Whole cell lysate was removed through the solid upper lipid layer into a clean tube. Adipose tissue lysate was

quantified using the BioRad DC assay, a colorimetric modification of the Lowry method (Lowry, et al., 1951) (BioRad Laboratories, Hemel Hempstead, UK). Protein samples were quantified against BSA standards of known concentration, and the colour change, proportional to the reduction of Folin reagent and thus protein present, was recorded on a spectrophotometer at 650nm.

6.2.6 Western Blotting – Total PTEN protein expression

Prior to western blotting, adipose tissue lysates were diluted to a starting concentration of 1mg/ml in cell lysis buffer. HEK293T lysate was diluted to the same starting concentration and used as a positive control on each western blot to act as a control for antibody efficiency. 15µg cell lysate was added to 5µl 4X NuPAGE LDS sample buffer (Invitrogen, Paisley, UK) and 5% beta-mercaptoethanol (Sigma Aldrich, Gillingham, UK). Mastermix's were heated to 70°C for 10 minutes before samples were run on a Novex 4-12% Bis-Tris mini gel (Invitrogen, Paisley, UK) in 1X 2-(N-morpholino)ethanesulfonic acid (MES) running buffer for 45 minutes (200 Volts). Proteins were transferred to polyvinylidene fluoride (PVDF) membranes, washed twice in deionised water and incubated for 1 hour in blocking solution. Gels were incubated overnight in Simply Blue Safe stain (Invitrogen, Paisley, UK) whilst membranes were incubated at 4°C in rabbit anti-PTEN primary antibody solution [1:500, SC6817] (Insight Biotechnology Ltd, Wembley, UK). The following day membranes were washed for one hour in blotting solution before incubating for one hour with goat anti-rabbit secondary antibody solution (1:5000) (BioRad, Hemel Hempstead, UK). Membranes were washed for a final hour in blotting buffer before incubating in 3ml SuperSignal West Pico Chemiluminescence detection substrate (ThermoScientific, Cramlington, UK). Membranes were exposed to Amersham hyperfilm (GE Healthcare, Chalfont St Giles, UK) for 5 minutes. Semi-quantitative analysis was performed using Image J quantification (<http://rsbweb.nih.gov/ij/>) normalising HEK293T on each membrane to one.

6.2.7 Statistical Analysis

Analysis of expression between the paired samples (T2D and normoglycaemic controls) were performed using a Wilcoxon paired test, the non-parametric equivalent of the paired t-test. This option was selected on the basis that with small numbers (<100) the data are unlikely to be normally distributed and therefore parametric tests are not suitable. Where data are represented graphically the mean \pm SEM is plotted unless otherwise stated. Where data are analysed on the basis of patient BMI, and therefore no longer paired, the non-parametric equivalent of the independent t-test (the Mann Whitney U-test) was used. All statistical analysis was performed using SPSS statistics programme v18.

6.3 Results

6.3.1 *PTEN* expression in human adipose tissue – Oxford samples

A single omental RNA sample and two subcutaneous RNA samples from the Oxford-MOLSURG collection did not meet our strict inclusion criteria (minimum of 2µg extracted RNA with RIN ≥5.5) and were excluded from the experiment. As a result statistical analysis were performed using n=16 omental pairs and n=15 subcutaneous pairs.

mRNA expression analysis revealed that *PTEN* expression is reduced in the adipose tissue of patients with T2D when directly compared with matched controls (Figure 6.2). This finding was observed in both the omental adipose tissue (0.70 ± 0.06 vs 0.93 ± 0.07 , n=16, p=0.066) and subcutaneous depot (0.62 ± 0.06 vs 0.89 ± 0.08 , n=15, p=0.004) although statistical significance (p<0.05) was only achieved within the latter.

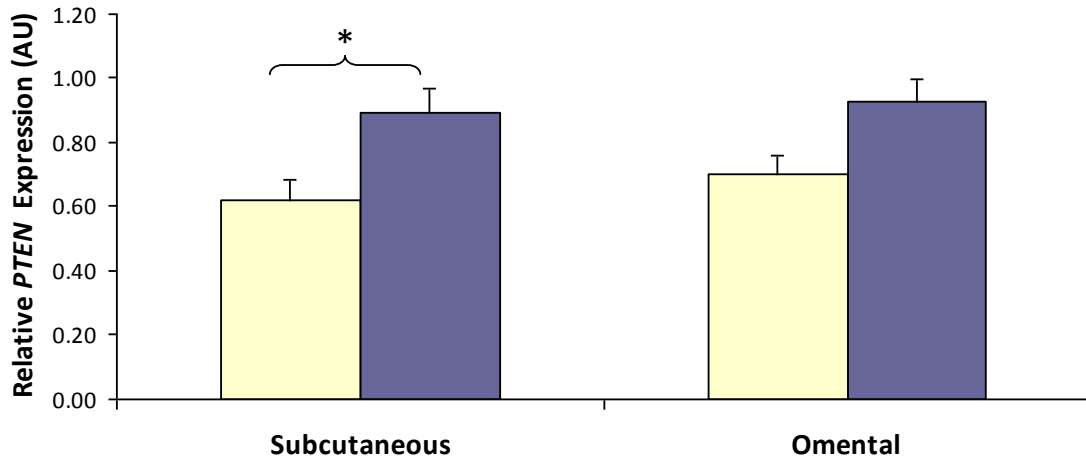


Figure 6.2 *PTEN* mRNA expression analysis within the subcutaneous and omental adipose tissue of patients with T2D (yellow bars) and controls (blue bars). Analysis was performed on 15 pairs of subcutaneous samples and 16 pairs of omental samples using Wilcoxon paired analysis. Data are presented as mean expression ± SEM. * denotes p<0.01.

Although care had been taken to match each of the pairs as closely as possible on the basis of age, gender and BMI, it was necessary to ensure that the reduction in mRNA expression was truly driven by diabetic status. To this end, correlations were determined between *PTEN*

expression versus BMI and *PTEN* expression versus age in each of the adipose depots (Figure 6.2). In subcutaneous adipose tissue neither age ($r^2=0.002$) nor BMI ($r^2=0.1457$) showed any correlation with *PTEN* expression. Lack of correlation was also observed for age ($r^2=0.0343$) and BMI ($r^2=0.0489$) in omental adipose tissue.

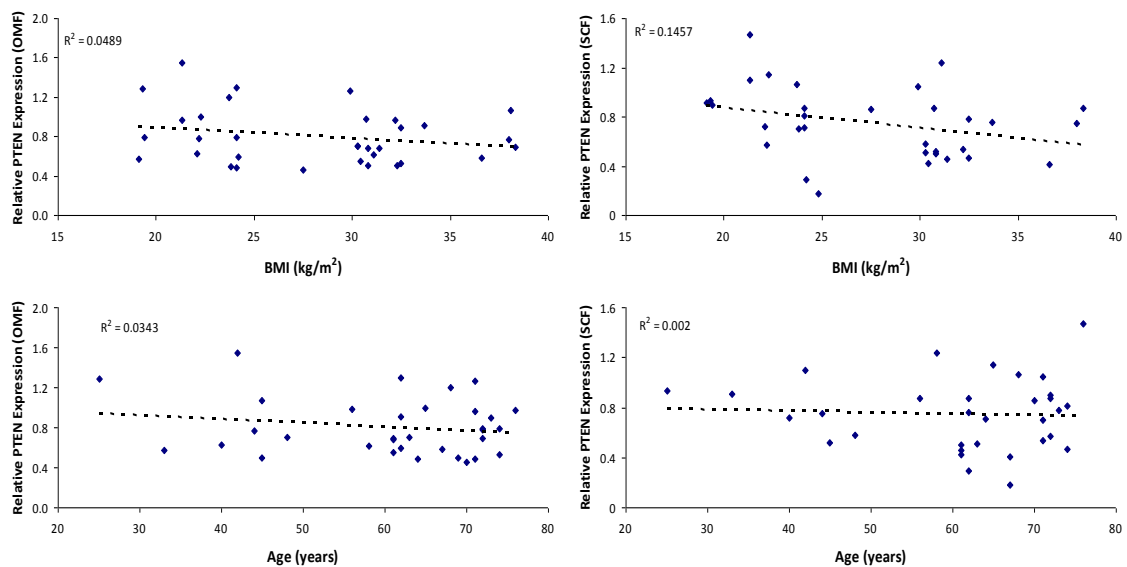


Figure 6.3 *PTEN* expression in subcutaneous adipose tissue (SCF) and omental adipose tissue (OMF) plotted against patient age and BMI. Correlations were determined using r^2 trend analysis with $r^2 < 0.3$ demonstrating no association.

To confirm that BMI was not the driving factor behind the variation in *PTEN* expression levels, data were re-analysed after stratifying all patients into one of two BMI groups, lean ($BMI \leq 25$) or obese ($BMI \geq 25.1$). Non-parametric analysis demonstrated that *PTEN* expression is not associated with BMI in either the subcutaneous or the omental adipose tissue ($p > 0.05$) therefore confirming that the variation in *PTEN* expression is truly driven by diabetic status.

One very real issue faced when studying patients with T2D is the inter-subject variability in therapeutic intervention strategy, which is exemplified in our modest cohort of T2D subjects. Of our 17 T2D subjects, one was regulating via diet alone, four via biguanide treatment only (metformin), three via sulfonylurea treatment, four were treated using a combination of oral hyperglycaemic agents whilst the remaining five were controlling their diabetes via insulin or

insulin analogue therapy. We analysed expression data to assess whether there was any association between T2D treatment and *PTEN* expression but were unable to determine any correlation (data not shown). Therefore we feel confident that therapeutics were not driving the reduction in *PTEN* expression.

6.3.2 *PTEN* expression in human muscle – Oxford Samples

Muscle cDNA at a 1:100 dilution, with standards ranging from 1:50-1:800, failed to demonstrate reproducible *PTEN* amplification (Figure 6.4B). Expression analysis utilising the same standards and samples with a probe specific for the housekeeping gene *UBC* verified this unexpected finding was not due to RNA quality or sample degradation as amplification efficiency was sound for this probe (Figure 6.4A). Further evidence suggesting lack of *PTEN* expression within human muscle is not sample dependent is seen in the integrity and purity of the extracted RNA. All 34 muscle samples extracted possessed RIN scores of >7 using Agilent technology (Figure 6.4C) whilst spectrophotometric determination of purity demonstrated 260/230 values >2 for all samples. RNA yield was also extremely high (>1000ng/ μ l). As the *PTEN*-specific probe had also previously been shown to efficiently amplify adipose tissue cDNA this was automatically ruled out as causal.

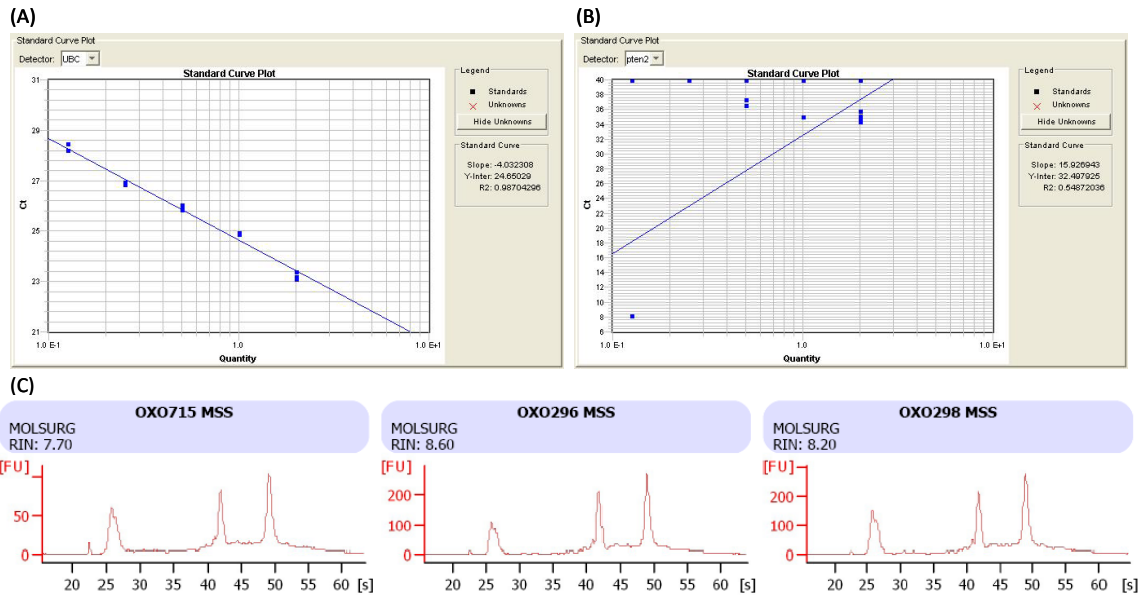


Figure 6.4 Standard curves generated through serial dilution (1:50-1:800) of pooled muscle cDNA. Amplification with a probe specific for UBC demonstrated efficient amplification and demonstrated sample integrity (A) whilst amplification of the same standards using a *PTEN*-specific probe failed to demonstrate amplification (B). Lack of amplification of this gene could not be contributed to sample quality as all samples extracted were of high integrity with RIN scores >7 (C).

Concentrations of cDNA standards were increased to 1:5-1:80 to maximise amplification efficiency whilst sample dilutions were increased to 1:5. When running at this concentration samples still only crossed the fluorescence threshold at C_T values of approximately 32 with confidence values between the three replicates often >5%. Amplification of the housekeeping genes *PPIA* and *UBC* however were crossing at C_T values close to 18 and 20 and due to the exponential nature of PCR a difference of 12 cycles (2^{12}) corresponds to a 4000 fold difference in expression of the housekeeping genes and *PTEN*. This method of quantification was therefore not sensitive enough to detect *PTEN* expression even when using concentrate samples. Amplification of *PTEN* using a number of additional *PTEN* probes targeted to different domains of the protein elucidated the same results confirming that the findings were not probe-dependent. Minimal expression of *PTEN* within human muscle was confirmed by other groups within our institute who, using microarray technology, found *PTEN* expression levels did not exceed background within this depot (M Neville, F Karpe,

personal communication). I therefore chose to focus the remainder of the investigations of *PTEN* as a negative regulator of insulin signalling solely within the adipose tissue.

6.3.3 mRNA expression – Related insulin signalling genes

The observation that *PTEN* mRNA expression is reduced within the adipose tissue of patients with T2D was unexpected and contradicted the initial hypothesis. Work performed by a number of groups interested in insulin signalling has suggested a regulatory role of the p85 α subunit of PI3K on the expression of *PTEN*, whereby down-regulation of p85 α leads to a concomitant reduction in *PTEN* (Chagpar, et al., 2009; Taniguchi, et al., 2006b; Terauchi, et al., 1999). These observations led me to investigate the mRNA expression of a number of additional key insulin signalling genes (*INSR*, *IRS1*, *p85 α* , *p110 β* and *AKT2*) to determine whether there were any parallel changes in expression of these genes within the same individuals.

Relative expression of each gene within adipose tissue biopsies was calculated via normalisation to the geometric mean of *PPIA* and *UBC*. Analysing in this manner revealed there to be no significant variation in the mRNA expression of any of the other key signalling genes between patients with T2D and controls in either adipose tissue depot (Table 6.3 and Figure 6.5). This observation suggests that the reduction in *PTEN* expression within the subcutaneous adipose tissue is an isolated effect occurring as a direct consequence of T2D and is not related to transcriptional down-regulation of, or negative regulation by, any other key genes within the insulin signalling cascade.

Gene	Subcutaneous		Omental	
	T2D vs Control	p value	T2D vs Control	p value
<i>INSR</i>	2.23 ± 0.26 vs 1.83 ± 0.15	0.42	1.79 ± 0.23 vs 1.78 ± 0.15	0.50
<i>IRS1</i>	0.81 ± 0.08 vs 0.93 ± 0.12	0.55	0.62 ± 0.08 vs 0.72 ± 0.08	0.28
<i>p85α</i>	0.99 ± 0.16 vs 0.99 ± 0.14	0.59	0.76 ± 0.14 vs 0.84 ± 0.09	0.36
<i>p110β</i>	1.15 ± 0.10 vs 1.13 ± 0.17	0.51	0.85 ± 0.10 vs 1.21 ± 0.25	0.13
<i>AKT2</i>	1.03 ± 0.10 vs 1.02 ± 0.10	0.57	0.73 ± 0.07 vs 0.87 ± 0.09	0.17

Table 6.3 Relative mRNA expression of *INSR*, *IRS1*, *p85α*, *p110β* and *AKT2*. Relative expression was calculated using the $\Delta\Delta C_T$ analysis method to the geometric mean of *PPIA* and *UBC*. Data are presented as mean ± SEM and p values calculated using the Wilcoxon paired non-parametric analysis method. As this was the second hypothesis to be tested within the sample set a Bonferonni correction was employed, whereby α of 0.05 was divided by the number of hypothesis ($p=0.05/2$) therefore the threshold for significance was $p<0.025$.

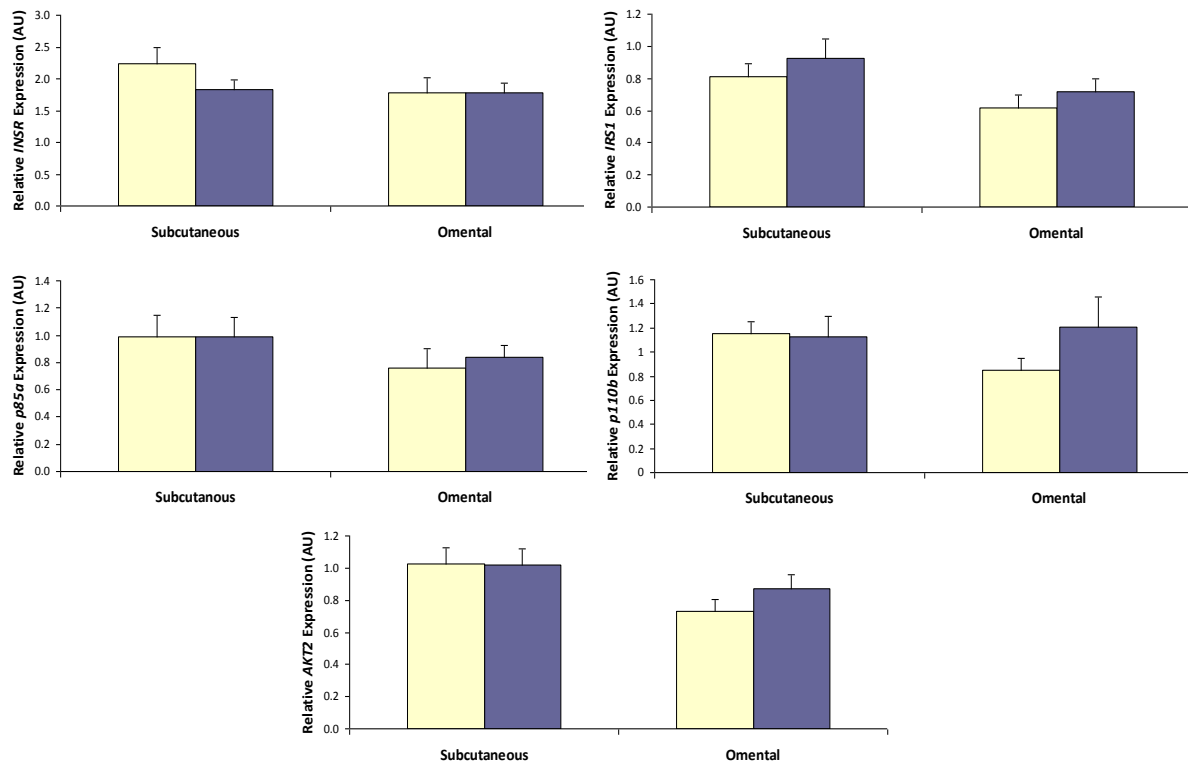


Figure 6.5 Relative mRNA expression of five key insulin signalling molecules *INSR*, *IRS1*, *p85α*, *p110β* and *AKT2* between patients with T2D (yellow bars) and matched controls (blue bars). 15 pairs were included in the omental analysis whilst 14 pairs were included in the subcutaneous analysis. Data are presented as mean relative expression ± SEM in arbitrary units (AU).

6.3.4 Replication of mRNA expression analysis – Leipzig Biobank

The observation that *PTEN* expression is significantly reduced in the subcutaneous adipose tissue of patients with T2D was identified in a relatively small sample size (n=15 pairs). As these findings were in contradiction to the initial hypothesis it was pertinent to replicate the mRNA expression study in an independent and larger cohort. Collaboration with Professors Blüher and Kovacs at Leipzig University provided us with a unique opportunity to perform our replication studies within their extensive adipose tissue biobank. Based on the strict inclusion criteria, samples were excluded from the experiment if extracted RNA was of insufficient quality or if the total amount of extracted RNA was not sufficient to generate cDNA from 2µg total RNA. Therefore although extracting from 40 pairs of samples the final analysis was based on 25 pairs of subcutaneous adipose tissue samples and 35 omental pairs.

Relative expression of *PTEN* within the subcutaneous and omental adipose tissue of paired samples was initially determined in samples from this additional biobank. As was observed within the Oxford-MOLURG samples, *PTEN* mRNA was reduced within both the subcutaneous (1.85 ± 0.17 vs 2.53 ± 0.31 , $p < 0.05$) and omental (2.49 ± 0.30 vs 3.13 ± 0.61 , $p = 0.51$) adipose depots of T2D subjects compared to age gender and BMI matched controls (Figure 6.6). This reduction in *PTEN* mRNA expression once again only reached statistical significance within the subcutaneous depot.

Secondly, as with the Oxford-MOLSURG cohort, expression of related insulin signalling genes was also determined. Unfortunately, due to limitation of RNA quantity, replication of mRNA expression studies could only be performed for four of the insulin signalling genes, *IRS1*, *p85α*, *p110β* and *AKT2* (*INSR* was not studied in this replication cohort).

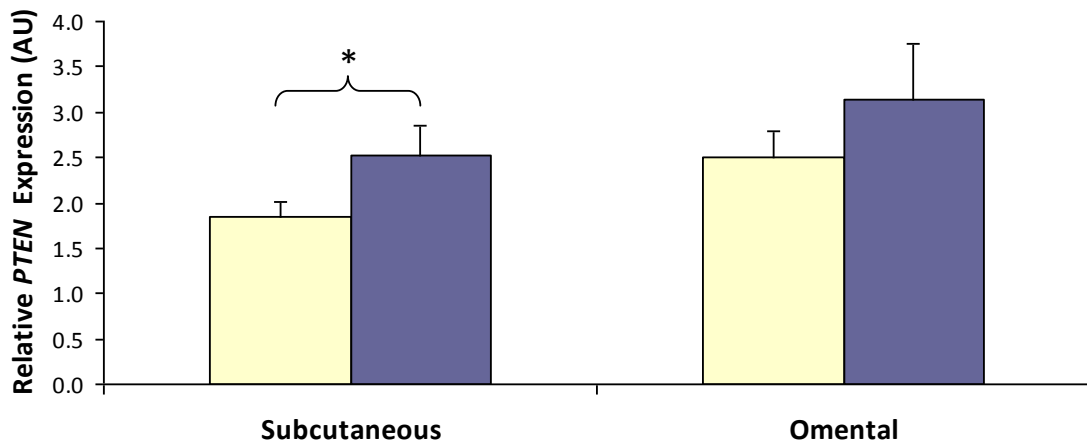


Figure 6.6 Relative mRNA expression of *PTEN* within the subcutaneous and omental adipose tissue of patients with T2D (yellow bars) and matched control subjects (blue bars) from the Leipzig cohort. Analysis was performed in 25 pairs of subcutaneous adipose tissue samples and 35 pairs of omental adipose tissue. Data are presented as mean expression in arbitrary units (AU)±SEM. * denotes $p < 0.05$.

Relative expression analysis to the geometric mean of *PPIA* and *UBC* revealed similar findings to those observed within the Oxford-MOLSURG samples. Firstly, there were no significant differences in mRNA expression of any of the key insulin signalling genes in the omental adipose tissue of our matched subjects (Table 6.4). However, our increased sample size revealed that within the subcutaneous adipose tissue *IRS1* expression is reduced in patients with T2D when compared to controls ($p < 0.05$) (Figure 6.7).

Gene	Subcutaneous		Omental	
	T2D v Controls	p value	T2D v Controls	p value
<i>IRS1</i>	1.39 ± 0.21 vs 2.27 ± 0.36	0.026	1.12 ± 0.16 vs 1.30 ± 0.17	0.22
<i>p85α</i>	1.41 ± 0.17 vs 1.58 ± 0.14	0.24	1.34 ± 0.14 vs 1.50 ± 0.18	0.45
<i>p110β</i>	2.18 ± 0.17 vs 2.82 ± 0.37	0.27	3.56 ± 0.49 vs 3.86 ± 0.62	0.78
<i>AKT2</i>	1.46 ± 0.19 vs 1.66 ± 0.13	0.16	1.11 ± 0.17 vs 1.05 ± 0.13	0.66

Table 6.4 Relative mRNA expression of *IRS1*, *p85α*, *p110β* and *AKT2*. Relative expression was calculated using the $\Delta\Delta C_T$ analysis method normalising to the geometric mean of *PPIA* and *UBC*. Data are presented as mean ± SEM and p values calculated using the Wilcoxon paired non-parametric analysis method.

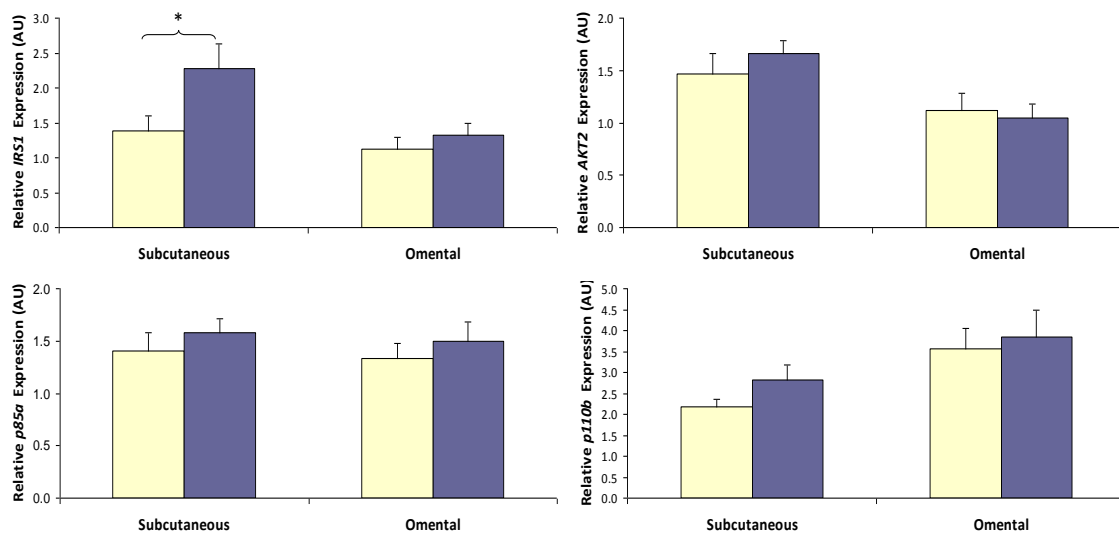


Figure 6.7 Relative mRNA expression of four key insulin signalling molecules *IRS1*, *p85α*, *p110β* and *AKT2* between patients with T2D (yellow bars) and matched controls (blue bars) taken from the Leipzig cohort. 25 pairs were included in the subcutaneous analysis whilst 35 pairs were included in the omental analysis. Data are presented as mean relative expression \pm SEM in arbitrary units (AU). * denotes $p < 0.05$. As this was the second hypothesis tested within these samples we once again set the threshold for significance at $p < 0.025$ and therefore *IRS1* verges on but does not quite reach statistical significance.

6.3.5 Combination of Oxford and Leipzig cohorts

Due to the efforts made to minimise heterogeneity wherever possible, the two independent cohorts were combined together in a meta-analysis. Data were initially log transformed to ensure normal distribution. Plotting of the data using a histogram and assessment of frequencies revealed skewness and kurtosis to fall within the designated levels for normal distribution (-0.8 to 0.8 and -3 to 3 respectively). Linear regression was then performed across the combined data sets to assess whether the dependent variable, mRNA expression, varied across diabetic status, the independent variable. Analysis of *PTEN* mRNA expression in this manner revealed that when combining the two data sets ($n=80$, 40 pairs), *PTEN* was significantly reduced within the subcutaneous adipose tissue of patients with T2D compared to controls ($p < 0.05$), confirming the initial observations in the Oxford cohort. The reduction in *PTEN* expression was not significant within the omental adipose tissue. When analysing the remainder of the insulin signalling genes we found that the only other significant

variation in gene expression was seen with *IRS1* which was significantly reduced within the subcutaneous adipose tissue of patients with T2D ($p < 0.025$) even when cautiously employing a Bonferroni correction.

6.3.6 Protein Expression of PTEN in adipose tissue biopsies

Meta-analysis of the two cohorts demonstrated that *PTEN* is significantly reduced within the subcutaneous adipose tissue of patients with T2D at the mRNA level. To assess whether this difference in transcript abundance translated to differences in protein expression, PTEN protein levels were assessed within additional biopsies (from the same individuals) from the Oxford-MOLSURG biobank. As PTEN has a molecular weight of ~55kDa we struggled to identify a loading control which was significantly higher or lower in MW to successfully allow the membrane to be subdivided for incubation with two primary antibodies (actin 42kDa, beta-tubulin 52kDa). Antibody stripping from membranes was attempted following PTEN detection and membranes subsequently re-probed with a beta-tubulin antibody, however this method was not uniform across samples or membranes and therefore was not a viable option for quantification. To overcome this problem all samples were diluted to the same starting concentration (1mg/ml) and 15 μ g loaded into wells of the protein gels. One lane on each gel was reserved for a positive control HEK293T and when quantifying we equalled this expression to one on each membrane to account for antibody efficiency.

Numbers were reduced for protein expression work due to scarcity of samples and sample degradation during extraction. Analysing in this manner demonstrated that PTEN total protein is also significantly reduced within the subcutaneous adipose tissue of patients with T2D compared to controls (0.78 ± 0.06 vs 1.27 ± 0.16 , $n=7$, $p < 0.05$) (Figure 6.8), a significant reduction in PTEN protein is not seen within the omental adipose tissue, confirming our earlier mRNA expression results.

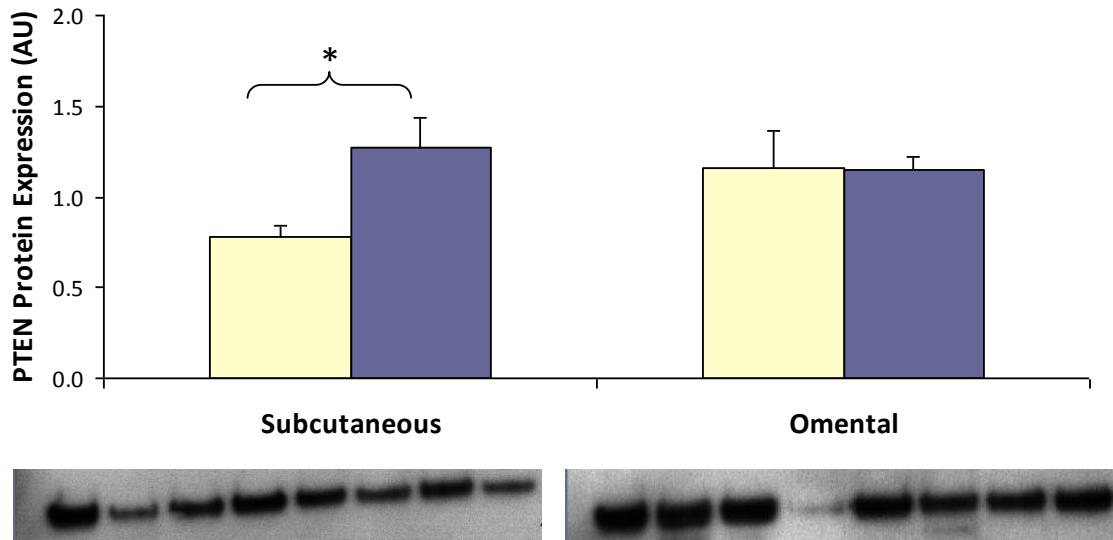


Figure 6.8 PTEN protein expression quantified using Image J analysis through normalisation to HEK293T positive controls. Expression was compared between T2D (yellow bars) and matched controls (blue bars) within both the subcutaneous and omental depots. N=7 matched subcutaneous pairs and n=4 omental pairs. Analysis was performed using the Wilcoxon nonparametric paired t-test.

6.3.7 Effects of glucose challenge on *PTEN* mRNA expression

The observation that *PTEN* is down-regulated at both the mRNA and protein level in subcutaneous adipose tissue of patients with T2D insinuates that this tissue is trying to maximise its insulin signalling capacity in times of severe insulin resistance and aberrant glycaemia. To determine whether the expression of this gene is down-regulated rapidly upon insulin stimulation, mRNA expression of *PTEN* (and the same panel of signalling genes) was assessed in adipose tissue biopsies taken from subjects before and after a glucose challenge. In the same biopsies we also assessed whether subject BMI had any effect on gene expression post glucose challenge as well as directly assessing gene expression between lean and obese subjects.

Adipose tissue mRNA expression – Pre glucose versus Post glucose stimulation

Data were initially analysed independently in separate depots (gluteal and abdominal) with an individual's mRNA expression compared pre glucose versus post glucose (n=10 pairs) for

PTEN, *INSR*, *IRS*, *p85a*, *p110b*, and *AKT2*. Analysis using the Wilcoxon paired analysis revealed there to be no significant alteration in mRNA expression of any of the genes downstream of the insulin receptor including *PTEN*, whose expression levels were maintained at similar levels in individuals pre and post glucose challenge in both the abdominal and gluteal depot (Table 6.5, Figure 6.9). Gene expression analysis of the insulin receptor gene itself however revealed there to be a significant increase in mRNA expression in both the abdominal and gluteal depot following a glucose challenge indicating that this gene can be readily up-regulated in the presence of its ligand (abdominal 5.60 ± 1.56 vs 8.84 ± 2.57 , $p < 0.01$, gluteal 4.54 ± 1.57 vs 7.25 ± 2.60 , $p < 0.05$).

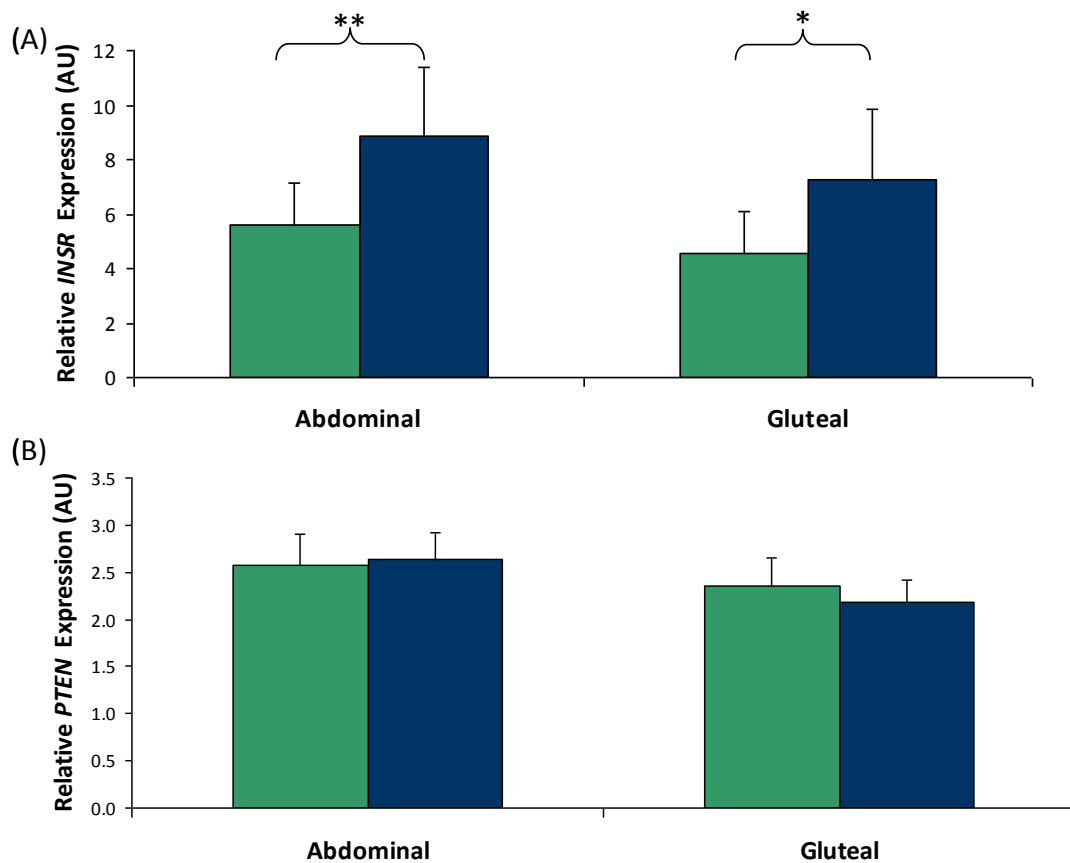


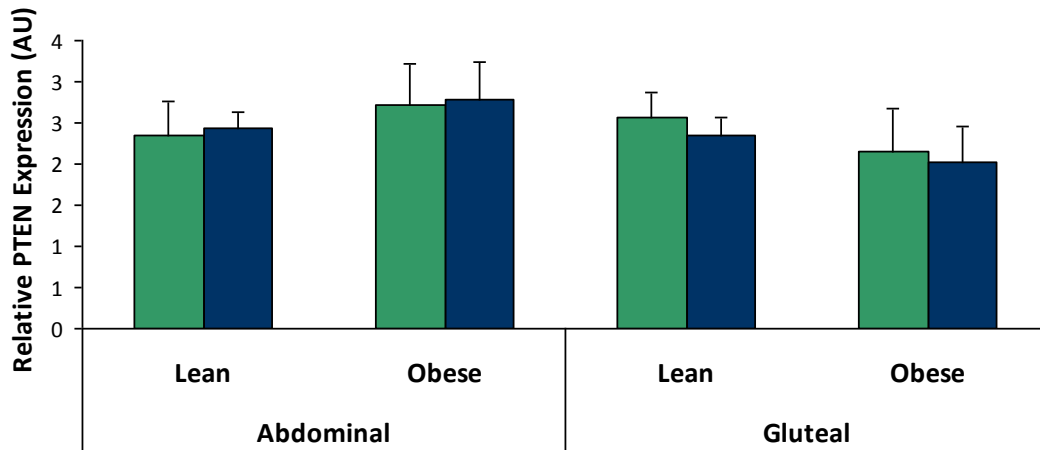
Figure 6.9 mRNA expression of *INSR*(A) and *PTEN*(B) in abdominal and gluteal adipose tissue, pre (green bars) and post (blue bars) glucose challenge. Relative expression was calculated using the $\Delta\Delta C_T$ method normalising to *PPIA* and *UBC* and is presented in arbitrary units (AU) as mean \pm SEM. * denotes $p < 0.05$, ** denotes $p < 0.01$.

Gene	Abdominal mRNA expression	p value	Gluteal mRNA expression	p value
	Pre v Post glucose		Pre v Post glucose	
<i>INSR</i>	5.60 ± 1.56 vs 8.86 ± 2.57	0.008	4.54 ± 1.57 vs 7.25 ± 2.60	0.02
<i>IRS1</i>	1.28 ± 0.1 vs 1.21 ± 0.14	0.65	1.52 ± 0.15 vs 1.36 ± 0.14	0.39
<i>p85α</i>	2.80 ± 0.53 vs 3.28 ± 0.55	0.45	2.45 ± 0.37 vs 2.80 ± 0.44	0.80
<i>p110β</i>	3.41 ± 0.62 vs 3.63 ± 0.50	0.58	3.43 ± 0.56 vs 3.38 ± 0.53	0.96
<i>PTEN</i>	2.57 ± 0.33 vs 2.64 ± 0.28	0.65	2.35 ± 0.29 vs 2.18 ± 0.24	0.31
<i>AKT2</i>	1.39 ± 0.11 vs 1.37 ± 0.10	0.96	1.41 ± 0.10 vs 1.40 ± 0.11	0.84

Table 6.5 mRNA expression levels of a number of key insulin signalling genes in abdominal and gluteal adipose tissue, pre and post-glucose challenge. Relative expression was calculated using the $\Delta\Delta C_T$ method normalising to *PPIA* and *UBC* and is presented in arbitrary units (AU) as mean \pm SEM. Statistical analysis was performed using the nonparametric Wilcoxon paired analysis method using SPSS statistical software. P value was considered significant if <0.05 with significant findings are presented in blue type.

To ensure that *PTEN* gene expression pre glucose versus post glucose was not affected by BMI, subjects were subdivided into lean ($BMI \leq 25$) or obese ($BMI > 25$) sub-groups and expression data re-analysed within these separate cohorts. When stratifying the patients based on obesity our results remained as previously described with no significant alteration in *PTEN* gene expression pre glucose versus post glucose in either the abdominal or the gluteal adipose tissue of the lean individuals (n=4) or obese subjects (n=6) (Table 6.6 and Figure 6.9).

The lack of effect of BMI was also confirmed for the remainder of the insulin signalling pathway genes downstream of *PTEN*, with no significant alteration in gene expression pre glucose versus post glucose stimulation in either the lean or obese groups (Table 6.7).



Gene	Depot	Lean (BMI \leq 25kg/m 2)		p value	Obese (BMI \geq 25.1kg/m 2)		p value
		Pre vs Post glucose			Pre vs Post glucose		
<i>PTEN</i>	abdominal	2.34 \pm 0.42 vs 2.42 \pm 0.21		0.72	2.72 \pm 0.49 vs 2.79 \pm 0.46		0.60
	gluteal	2.56 \pm 0.3 vs 2.34 \pm 0.23			2.15 \pm 0.52 vs 2.02 \pm 0.43		

Table 6.6 and Figure 6.10 mRNA expression analysis of key insulin signalling genes in individual's pre and post-glucose challenge. To assess whether obesity affects gene expression individuals have been stratified based upon BMI (lean \leq 25, obese \geq 25.1). In graphical form mean \pm SEM is presented in arbitrary units pre (green bars) and post (blue bars) glucose.

Gene	Depot	Lean (BMI \leq 25kg/m 2)		p value	Obese (BMI \geq 25.1kg/m 2)		p value
		Pre vs Post glucose			Pre vs Post glucose		
<i>INSR</i>	abdominal	8.28 \pm 1.92 vs 14.13 \pm 2.55		0.27	4.26 \pm 2.11 vs 6.72 \pm 3.49		0.028
	gluteal	4.21 \pm 0.58 vs 6.91 \pm 1.73			4.80 \pm 2.94 vs 7.53 \pm 4.74		
<i>IRS1</i>	abdominal	1.40 \pm 0.06 vs 1.66 \pm 0.13		0.07	1.20 \pm 0.15 vs 0.91 \pm 0.08		0.05
	gluteal	1.76 \pm 0.18 vs 1.55 \pm 0.16			1.29 \pm 0.22 vs 1.17 \pm 0.21		
<i>P85</i>	abdominal	1.85 \pm 0.11 vs 3.44 \pm 1.08		0.27	3.43 \pm 0.8 vs 3.18 \pm 0.67		0.92
	gluteal	2.39 \pm 0.50 vs 1.81 \pm 0.62			2.50 \pm 0.61 vs 2.73 \pm 0.71		
<i>P110b</i>	abdominal	2.99 \pm 0.60 vs 4.09 \pm 0.51		0.27	3.68 \pm 0.98 vs 3.32 \pm 0.78		0.92
	gluteal	3.51 \pm 0.56 vs 3.70 \pm 0.72			3.36 \pm 1.04 vs 3.06 \pm 0.82		
<i>PTEN</i>	abdominal	2.34 \pm 0.42 vs 2.42 \pm 0.21		0.72	2.72 \pm 0.49 vs 2.79 \pm 0.46		0.60
	gluteal	2.56 \pm 0.3 vs 2.34 \pm 0.23			2.15 \pm 0.52 vs 2.02 \pm 0.43		
<i>AKT2</i>	abdominal	1.41 \pm 0.14 vs 1.57 \pm 0.08		0.47	1.37 \pm 0.17 vs 1.24 \pm 0.13		0.46
	gluteal	1.63 \pm 0.08 vs 1.55 \pm 0.1			1.20 \pm 0.14 vs 1.26 \pm 0.18		

Table 6.7. mRNA expression analysis of key insulin signalling genes in individuals pre glucose versus post glucose stimulation. To assess whether obesity affects gene expression individuals were stratified based upon BMI into one of two groups, lean BMI \leq 25 (n=4) or obese BMI \geq 25.1 (n=6). Data are presented as mean \pm SEM and p values calculated using Wilcoxon paired analysis.

As was expected, those genes which showed no alteration in mRNA expression between pre glucose versus post glucose stimulation in either adipose tissue depot (*PTEN*, *p85*, *p110*, *AKT2* and *IRS1*) showed no significant effect when stratified based on obesity. When analysing *INSR* data in this manner we saw no significant alteration in gene expression levels between pre and post glucose challenge in either the abdominal or the gluteal adipose tissue of the lean individuals (n=4). When analysing the expression data within the obese individuals (n=6) we saw a trend towards a significant increase in expression of *INSR* following a glucose challenge in both the gluteal (p=0.08) and abdominal (p=0.028) adipose tissue however these did not however quite reach the cautious statistical threshold set at p<0.025 after employment of a Bonferonni correction.

Adipose mRNA expression – Lean subjects versus obese subjects

Finally, differences in mRNA expression between the lean and obese subjects at both the basal (pre-glucose) and stimulated (post-glucose) time points were assessed. It has been speculated that certain genes within the insulin signalling pathway are down-regulated in an insulin resistant state and therefore it was considered interesting to assess the expression of these key genes especially after stimulation within the obese individuals using the lean as a comparative measure. Again we used our same profile of expression data but this time instead of comparing paired measurements within individuals we were required to compare mRNA expression between groups of individuals.

No differences in *INSR*, *PTEN*, *p85*, *p110* or *AKT2* expression were observed between lean and obese individuals in basal or stimulated adipose tissue biopsies. These findings were true for both the abdominal and the gluteal depot (Table 6.8). When

assessing expression levels of *IRS1* mRNA we found there to be no significant difference between lean and obese individuals in the gluteal depot at either basal or stimulated levels. However, when assessing and comparing *IRS1* expression levels between lean abdominal and obese abdominal we found that at the stimulated time point there was a significant lower level of *IRS1* expression within the adipose of the obese subjects ($p < 0.05$), indicating this observation is likely to be indicative of the physiological situation within the adipose tissue of obese individuals.

Gene	Depot	Pre-Glucose		Post-Glucose	
		Lean v Obese	p value	Lean v Obese	p value
<i>INSR</i>	Abdominal	8.28 ± 1.91 vs 4.26 ± 2.11	0.088	14.13 ± 2.55 vs 6.72 ± 3.49	0.39
	Gluteal	4.21 ± 0.58 vs 4.80 ± 2.94	0.176	6.91 ± 1.73 vs 7.53 ± 4.74	0.33
<i>IRS1</i>	Abdominal	1.40 ± 0.06 vs 1.20 ± 0.15	0.59	1.66 ± 0.13 vs 0.91 ± 0.08	0.011
	Gluteal	1.76 ± 0.18 vs 1.29 ± 0.22	0.12	1.55 ± 0.16 vs 1.17 ± 0.21	0.18
<i>p85α</i>	Abdominal	1.85 ± 0.11 vs 3.43 ± 0.80	0.39	3.44 ± 1.08 vs 3.18 ± 0.67	0.83
	Gluteal	2.39 ± 0.50 vs 2.50 ± 0.61	0.92	2.86 ± 0.62 vs 2.73 ± 0.71	0.75
<i>p110β</i>	Abdominal	2.99 ± 0.60 vs 3.68 ± 0.98	1	4.09 ± 0.51 vs 3.32 ± 0.78	0.20
	Gluteal	3.51 ± 0.56 vs 3.36 ± 1.04	0.92	3.70 ± 0.12 vs 3.06 ± 0.82	0.60
<i>PTEN</i>	Abdominal	2.34 ± 0.42 vs 2.72 ± 0.49	0.67	2.42 ± 0.21 vs 2.79 ± 0.46	0.67
	Gluteal	2.56 ± 0.30 vs 2.15 ± 0.52	0.25	2.34 ± 0.23 vs 2.02 ± 0.43	0.60
<i>AKT2</i>	Abdominal	1.41 ± 0.14 vs 1.37 ± 0.17	0.83	1.57 ± 0.08 vs 1.24 ± 0.13	0.055
	Gluteal	1.63 ± 0.08 vs 1.20 ± 0.14	0.036	1.55 ± 0.10 vs 1.26 ± 0.18	0.35

Table 6.8 mRNA expression analysis of key insulin signalling genes between lean and obese individuals at both the pre and post glucose time points. Analysis was performed using the Mann Whitney non-parametric independent t-test. with significance levels adjusted to $p < 0.017$ using Bonferroni's correction.

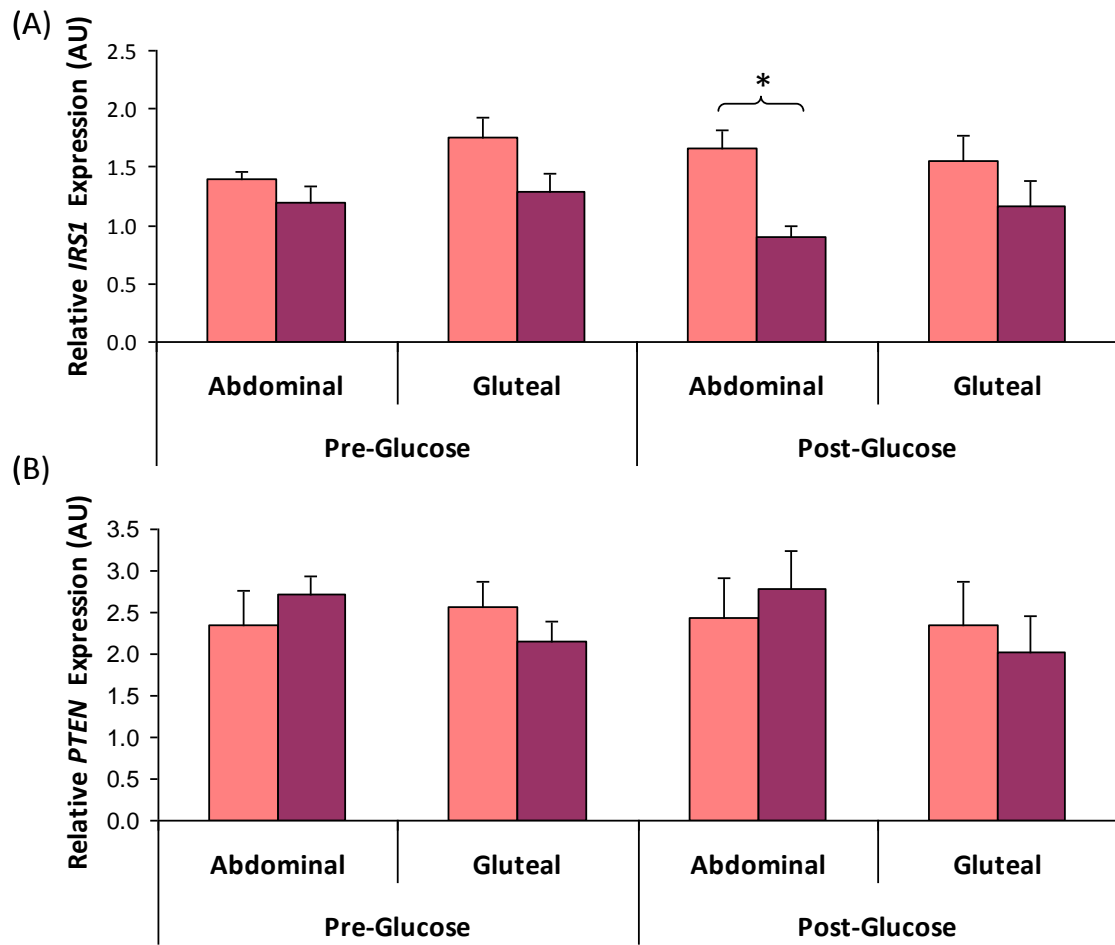


Figure 6.11 mRNA expression analysis of key insulin signalling genes between lean and obese individuals at both the pre and post glucose time points. Analysis was performed using the Mann Whitney non-parametric independent t-test, with significance levels adjusted to $p < 0.017$ using Bonferroni's correction. In graphical format, lean individuals are represented using pink bars and obese individuals using purple bars. Data are presented as mean \pm SEM.

6.4 Discussion

Insulin resistance is one of the major factors which precede the onset of T2D. Although the past decade has seen considerable progression in elucidation of the individual components of the insulin signalling pathway, our understanding of the complex molecular mechanisms behind the onset of insulin resistance are as yet relatively poorly understood (Savage, et al., 2005). Negative regulators of the insulin signalling cascade have become a hot topic of research over the past five years, not only because further understanding of regulatory mechanisms may shed light on additional pathways deregulated in T2D, but because they may act as potential novel targets for therapeutic intervention. One such negative regulator which has received considerable attention is the phosphatase and tensin homologue deleted on chromosome ten (PTEN), which dephosphorylates the key secondary messenger PIP_3 therefore reducing signalling through the AKT/PKB pathway (Maehama and Dixon, 1998). Generation of transgenic and knockout rodent models has reproducibly demonstrated that loss of PTEN within insulin target tissues results in insulin hypersensitivity and protection against the development of diabetes (Kurlawalla-Martinez, et al., 2005; Stiles, et al., 2004; Wijesekara, et al., 2005; Wong, et al., 2007). Of course, the prior discovery that PTEN functions as a tumour suppressor necessitates that caution is required when postulating this gene as a therapeutic target (Di Cristofano, et al., 1998; Podsypanina, et al., 1999), however despite this many groups have speculated that therapeutic targeting to reduce *PTEN* expression in a tissue-specific manner could be beneficial as a novel treatment for reducing insulin resistance (Kurlawalla-Martinez, et al., 2005; Sasaoka, et al., 2006; Wijesekara, et al., 2005)

Following the animal work, which clearly demonstrated a role for PTEN in regulation of insulin signalling within murine adipose tissue and muscle (Kurlawalla-Martinez, et al., 2005; Wijesekara, et al., 2005), PTEN was hypothesised to play an equivocally important role in

these same tissues in humans with increased expression of this gene potentially contributing to the insulin resistance observed in patients with T2D. As these variations in expression are likely to be tissue-specific access to a biobank of adipose and muscle biopsies was utilised to assess this hypothesis.

My findings were in many ways contradictory to this initial hypothesis. Firstly, investigation into the expression of *PTEN* in human muscle was halted following the surprising discovery that *PTEN* was lowly expressed within this depot. As expression was ~4000 fold less than standard housekeeping genes and confidence values attained between replicates extremely low, it became impossible to accurately quantify expression in this depot. As muscle is one of the primary targets of insulin action it is perhaps unexpected that *PTEN* is so lowly expressed in this depot. One explanation for this observation could be the site from which the muscle biopsy was taken. Due to the nature of the tissue collection procedure, muscle biopsies were taken from the site of surgical incision, which in the majority of cases was from the abdominal region. The difference in aerobic properties of the abdominal muscle when directly compared to voluntary, respiratory skeletal muscle such as quadriceps (a known target for insulin stimulated glucose disposal) is one potential explanation for the low *PTEN* expression. However, contrary to this hypothesis, expression analysis of *PTEN* within skeletal quadriceps biopsies using micro-array technology failed to detect *PTEN* expression levels above background (M Neville, F Karpe personal communication). Taken together these findings could indicate an interesting phenomenon whereby in myocytes, *PTEN* is transcribed at extremely low levels to maximise insulin signalling through this pathway following stimulation by its ligand. Further evidence to support this hypothesis is observed in the rodent muscle specific *Pten*^{-/-} knockout model (Wijesekara, et al., 2005). These animals were protected from the onset of insulin resistance and diabetes upon high fat feeding but they did not exhibit any of the other glycaemic alterations such as increased glucose tolerance and

insulin sensitivity as was observed within the adipose specific knockout animals therefore presenting with a far less pronounced phenotype (Wijesekara, et al., 2005).

When performing mRNA expression studies within human adipose tissue, *PTEN* was found to be relatively highly expressed within both the subcutaneous and omental depots, therefore bypassing the experimental difficulties observed with the muscle samples from the same individuals. Initial hypothesis suggested that *PTEN* would be up-regulated in the adipose tissue of patients with T2D when directly compared to matched controls. However, my investigations within the Oxford-MOLSURG samples unexpectedly revealed *PTEN* mRNA to be down-regulated in adipose tissue of T2D patients, significantly so within the subcutaneous depot. These surprising findings were supported via replication within an independent and larger sample set and confirmed by demonstrating a reduction in *PTEN* protein expression within the same individuals.

Despite the fact that paired subjects were carefully matched for age, gender and BMI it was imperative to ensure that the changes in mRNA expression were not driven by obesity. Rigorous checks at all stages of the analysis procedure revealed there to be no correlation or association between *PTEN* expression and BMI indicating that the likely effects were truly driven by an individual's diabetic status.

Numerous groups have previously published on the reduced *IRS1* expression within the adipose tissue of insulin resistant and T2D patients (Kovacs, et al., 2003; Rondinone, et al., 1997) and *IRS1* is one of only a handful of genes to be reproducibly associated with T2D, insulin resistance and hyperinsulinaemia through genome-wide association studies (Rung, et al., 2009). More recently, common *IRS1* SNPs have been shown to correlate with *IRS1* expression levels by eQTL analysis (Dupuis, et al., 2010; Rung, et al., 2009). Combination of

the Oxford and Leipzig cohorts (n=80) enabled us to observe a significant reduction in *IRS1* mRNA expression in the subcutaneous adipose tissue of our T2D subjects, a result which held true even when overcautiously introducing corrections for multiple testing ($p < 0.025$). This observation, which replicates what is previously known within the literature, highlights that our study was well powered to detect changes in gene expression serving as a positive control.

Our findings suggest that the subcutaneous adipose tissue of patients with T2D down-regulates *PTEN* expression as a compensatory mechanism to maximise glucose clearance in a physiological situation in which glucose clearance into skeletal muscle is restricted. Our investigation of *PTEN* expression within individuals pre and post glucose challenge demonstrate that *PTEN* expression is not regulated rapidly in response to high insulin levels nor is it differentially regulated between lean and obese individuals. Therefore the variation in *PTEN* expression is seemingly a phenomenon which develops over time to compensate for increasing levels of insulin resistance and circulating insulin levels and highlights the importance of adipose tissue as an active organ in the control of glucose homeostasis.

Regulation of *PTEN* is achieved via a complex interplay of multiple proteins and transcription factors including p53 and NF-kappaB and via a multitude of processes including post-transcriptional modifications, phosphorylation and oxidation, which are as yet only partially understood (Leslie and Downes, 2004). A number of groups interested in understanding the regulation of this tumour suppressor gene have postulated there may be a novel role for the regulatory subunit of PI3K (p85a) (Chagpar, et al., 2009; Taniguchi, et al., 2006b; Terauchi, et al., 1999). Although p85a is a crucial component in the PI3K complex and required for the transduction of the insulin signal, its expression is paradoxically inversely associated with insulin sensitivity whereby p85a knockout within mice corresponds with increased glucose

homeostasis (Terauchi, et al., 1999). Since this important discovery, a number of groups have further demonstrated that loss of the abundant p85a subunit leads to an increase in insulin stimulated AKT activity due to reduction in PTEN levels (Taniguchi, et al., 2006b) and further that p85a subunit is able to bind to and specifically regulate the function of PTEN (Chagpar, et al., 2009). As I observed a reduction in *PTEN* expression of unknown mechanistic action and in light of the recent association between the two genes, assessment of *p85a* mRNA expression was performed in each of the sample sets. However, no association was observed between *PTEN* and *p85a* expression, nor was there a statistical difference in *p85a* expression between the T2D and control subjects suggesting this is unlikely to be the mechanism through which reduction in *PTEN* expression is mediated.

The data suggest that the reduction in expression is present at both the mRNA and protein level and therefore it is reasonable to speculate that the mechanism of regulation could be via transcriptional regulation or increased transcript degradation. One such mechanism, via which this could take place, is an increase in micro-RNA activity. MicroRNAs are small non-coding nucleotide segments which bind to the 3'UTR of genes and target them for degradation. *PTEN* is known to be regulated by a number of miRNA but of particular interest is miR-21a. Recently, Vinciguera et al. demonstrated that unsaturated fatty acids were able to trigger the onset of steatosis within hepatocytes via down-regulation of PTEN (Vinciguerra, et al., 2009). Further investigation demonstrated that this tissue-specific down-regulation was mediated via increased microRNA-21 expression and *PTEN* degradation (Vinciguerra, et al., 2009). Furthermore, microRNA-21 has been shown to regulate the proliferation of adipose derived mesenchymal stem cells demonstrating this microRNA is likely to play an important role within human adipose tissue (Kim, et al., 2011). Interestingly, miR-21a has been shown to be significantly up-regulated within the subcutaneous adipose tissue of insulin resistant subjects (M Neville, F Karpe, personal communication). Therefore it could be

postulated that within our insulin resistant T2D patients, *PTEN* may be down-regulated via a miRNA mediated mechanism, although further work needs to be performed to elucidate the expression of miR-21a in our subjects.

Much has also been speculated on the role of adipose tissue as an endocrine organ and the role of adipokines including resistin and adiponectin and their role in the onset of insulin resistance in skeletal muscle (Flier, 2001; Mohamed-Ali, et al., 1998; Weyer, et al., 2001). The evidence reported in the literature quite clearly demonstrates that there is a unique interplay and cross-talk between these two tissues which is nicely demonstrated in the *PTEN*^{-/-} adipose specific knockout mouse model (Dietze, et al., 2002; Kurlawalla-Martinez, et al., 2005). These animals demonstrate increased insulin signalling via the AKT pathway and a six fold increase in GLUT4 at the plasma membrane of adipocytes following glucose stimulation. However, the skeletal muscle of the same animals showed three fold lower GLUT4 levels compared to control animals following glucose stimulation suggesting that there is a mechanism of cross talk between the two tissues to maintain euglycaemia (Kurlawalla-Martinez, et al., 2005). Although a wealth of published data point to the negative effects of adipokines on muscle signalling, in the future it may be interesting to investigate the effects which 'myokines' may exert reciprocally upon adipocytes. Recently, interest has been stimulated by a study in which the myokine expression profile of human myocytes was assessed pre and post TNF α -induced insulin resistance and a number of myokines were found to be expressed at greater levels in the insulin resistance state (Bouzakri, et al., 2011). These myokines were found to exert negative effects on the secretory profile of human beta-cells demonstrating that differential expression of myokines is physiologically relevant (Bouzakri, et al., 2011). It may therefore be interesting to assess, using a co-culture set up, whether culture medium obtained from insulin resistant myocytes affects the expression of key insulin signalling molecules within adipocytes.

In conclusion, I have demonstrated that PTEN expression is reduced within the subcutaneous adipose tissue of patients with T2D at the mRNA and protein level and demonstrated that this reduction in expression is not due to concomitant transcriptional down-regulation of its novel regulator p85 α . Down-regulation of *PTEN* seemingly occurs at the transcript level. It will be interesting to investigate whether transcription factor binding or microRNA targeted degradation account for reduced transcript abundance or whether myokines secreted from insulin resistant muscle potentially play a role via endocrine cross-talk between these two vital depots.

Chapter 7

Discussion

7. Discussion

Evidence from epidemiological studies clearly demonstrate there to be a substantial genetic component to Type 2 diabetes (T2D) and related quantitative traits, including fasting plasma glucose (fpg), which are as yet only modestly understood (Kobberling and Tillil, 1982; Lango, et al., 2008; Watanabe, et al., 1999). Elucidation of the genetic component of T2D and fpg is vital as it will not only shed further light on novel genes, pathways and mechanisms of regulation, but may also lend itself to assisting in the generation of novel therapeutic agents.

Therefore the aims of the work presented in this thesis were to further our understanding of the genetic component of T2D, related quantitative traits and monogenic disorders of beta-cell function using a variety of approaches and molecular genetic techniques. These included candidate gene screening in patients with monogenic beta-cell dysfunction, refinement of T2D and fpg association signals using gene expression profiling within human islets and beta-cells, follow-up of a novel fpg association signal in a physiologically relevant cellular system and finally mRNA expression profiling of insulin signalling genes in the adipose tissue of patients with T2D and matched controls.

Determining the genetic aetiology in patients with monogenic forms of beta-cell dysfunction is important as it can help dictate therapeutic intervention strategies and aid in patient management (Gloyn and Ellard, 2006). However, it has also long been recognised that studying monogenic disorders may facilitate our understanding of related complex diseases. Monogenic disorders of beta-cell dysfunction account for 1-2% of all non-insulin dependent forms of diabetes mellitus (Ledermann, 1995) and to date pathogenic variants have been identified in a number of key beta-cell genes (Babenko, et al., 2006; Edghill, et al., 2006a; Flanagan, et al., 2007; Garin, et al., 2010; Gloyn, et al., 2004; Kristinsson, et al., 2001; Njolstad, et al., 2001; Stanley, et al., 1998; Stoffers, et al., 1997a; Yamagata, et al., 1996).

Identification of mutations within the pancreatic beta-cell glucose sensor glucokinase (*GCK*) (Glaser, et al., 1998; Hattersley, et al., 1992; Njolstad, et al., 2001) have important implications not only for affected individuals, many of whom have seen their treatment strategy improved as a result of their genetic aetiology elucidation (Gill-Carey, et al., 2007; Murphy, et al., 2008), but has also led to the identification of common fpg and T2D susceptibility variants within the same gene (Dupuis, et al., 2010; Weedon, et al., 2005a). Pharmaceutical companies have also utilised the invaluable information gleaned from the study of these pathogenic variants to aid in the development of novel therapeutic strategies for the treatment of complex T2D (Grimsby, et al., 2003).

The observation that common variants within the islet specific glucose-6-phosphatase enzyme, *G6PC2*, also associate with elevated fpg (Bouatia-Naji, et al., 2008; Chen, et al., 2008; Dupuis, et al., 2010), coupled with the hypothesised function of *G6PC2* as a regulator of *GCK* and glycolysis (Wang, et al., 2007), led me to hypothesise that mutations within *G6PC2* may be a novel cause of beta-cell dysfunction. Patients with monogenic beta-cell dysfunction (permanent neonatal diabetes mellitus [PNDM], maturity onset diabetes of the young [MODY], glucokinase-like MODY [GCK-like MODY] and hyperinsulinaemic hypoglycaemia [HH]) of unknown genetic aetiology were screened for *G6PC2* mutations. Novel intronic, synonymous and non-synonymous variants were identified in our screen, however pathogenicity was considered unlikely for the majority of variants following familial co-segregation analysis and the assessment of variants in an ethnically matched control population. However for the F256L variant, identified in single proband with HH, parental DNA was unavailable for co-segregation analysis and screening within 288 Eurpoid control chromosomes was found to be negative. To further assess the likely pathogenicity of this amino acid substitution, analysis was performed using the bioinformatics tools, SIFT and POLYPHEN. Although providing contradictory results, SIFT, which combines both the physical

properties of the amino acids and sequence homology, predicts that the amino acid substitution would be tolerated by the protein. Taken alongside the observation that this variant was only present within a single proband, and absent in all other hypoglycaemic probands and families, led me to conclude that mutations within *G6PC2* are unlikely to be a common cause of monogenic disorders of beta-cell dysfunction.

Candidate gene screening of biologically plausible genes has historically been a useful technique for identifying novel monogenic mutations. However, exhaustion of the list of plausible candidate genes, coupled with our limited understanding of beta-cell biology, dictates that additional approaches will be required for mutation detection. It could be postulated that as the number of T2D and fpg associated loci increase through implementation of genome-wide association studies (GWAS), so do the number of candidate genes for mutational screening within monogenic patient cohorts. This would seem a plausible option as the overlap between monogenic and complex genetic aetiology becomes ever the more apparent (Agostini, et al., 2006; Altshuler, et al., 2000; Gloyn, et al., 2004; Gloyn, et al., 2003; Hattersley, et al., 1992; Voight, et al., 2010; Yamagata, et al., 1996).

Although this approach bypasses the requirement for prior hypothesis generation, screening each of these genes in affected individuals would be highly expensive and equally time consuming and laborious. As the majority of monogenic mutations are located within exonic regions, the future of monogenic mutation discovery is likely to rely heavily on the utilisation of next generation sequencing techniques including exome resequencing. Although of irrefutable benefit, it is worth noting that researchers may be faced with difficulties when trying to decipher true pathogenic variants from non-synonymous variants which will inevitably be identified using this methodology. Lack of large-scale families in which to perform linkage analysis and co-segregation studies is also likely to generate difficulties

however, despite this, the methodology has already been successfully implemented by groups interested in understanding the genetic aetiology of PNDM (Bonnetfond, et al., 2010a).

The field of T2D genetics was revolutionised following the implementation of GWAS in 2007. Utilisation of this methodology increased the number of T2D susceptibility loci from three (Altshuler, et al., 2000; Gloyn, et al., 2003; Grant, et al., 2006) to over 25 (Saxena, et al., 2007; Scott, et al., 2007; Steinthorsdottir, et al., 2007; WTCCC, 2007; Zeggini, et al., 2008; Zeggini, et al., 2007). Despite this, empirical studies concluded that collectively these loci were still only able to account for <10% of the heritability of T2D (Bonnetfond, et al., 2010b; Lango, et al., 2008) whilst definitive causal genes and molecular mechanisms underlying the signals remained largely unknown.

The missing heritability gap was hypothesised to reside in the inability of poorly powered GWAS to capture common variants of a more modest effect size, therefore necessitating multiple centre data sharing and meta-analysis for the detection of additional susceptibility variants. As such, the MAGIC and DIAGRAM+ consortia were established as an international collaborative incentive to determine variants associated with fasting glycaemic traits and T2D susceptibility respectively. As a result of my knowledge of fluorescence-activated cell sorting (FACS) of human islets and therefore ability to purify human beta-cells, I was asked to join both consortia. My specific role within the consortia was to provide transcript profiling of genes within novel susceptibility loci, in human islets and beta-cells, to aid in signal refinement and elucidation of potential molecular mechanisms (**chapter 3**). This was the first time transcript profiling within human beta-cells had been used to aid in T2D and fpg GWAS signal refinement and was of benefit to both consortia.

The association between fpg and the *DGKB-TMEM195* locus had previously been identified in a Northern Finnish Birth Cohort study, although the authors failed to determine which of these genes was likely to be driving the elevation in fasting glucose levels (Sabatti, et al., 2009). Statistical collaborators within the MAGIC consortia replicated this association, additionally demonstrating association with reduced beta-cell function and reduced insulinogenic index (Ingelsson, et al., 2010), dictating the likely variant is mediating its effects through the beta-cell via beta-cell dysfunction. For the first time, expression profiling within metabolically relevant tissues was performed to aid in refinement of the association signal, and I was able to demonstrate that *TMEM195* was not transcribed and expressed within human islets or beta-cells. Conversely, *DGKB* was present in both depots therefore establishing that the signal was likely conferring increased fpg levels and T2D risk via the biologically plausible *DGKB*, thus providing a starting point for functional follow-up. FACS of human islets has now been implemented at the Oxford Centre for Diabetes, Endocrinology & Metabolism, one of only a few centres in the UK to utilise this technique, and I have established a pipeline through which transcript profiling can be utilised to complement prospective GWAS for glycaemic traits.

My work of transcript profiling within human beta-cells, although of benefit when performed in parallel with physiological and eQTL analysis, provides only a starting point for fine mapping of association signals. Additional analysis is required to identify the 'true' susceptibility variant which, in homogeneous North European populations, is often made difficult by the strong LD structures dispersed throughout the genome (Helgason, et al., 2007). Replication in ethnically diverse populations, in whom genetic background and therefore LD structures are distinct, is an increasingly common tool for susceptibility loci refinement (Helgason, et al., 2007). The future of understanding common variant-T2D susceptibility risk

is likely to rely heavily on this refinement process and is now a main focus of an international collaborative project, T2Dgenes (Horikoshi, et al., 2011).

One obvious caveat of the GWAS approach to T2D susceptibility variant identification is their preponderance to detect common variants. The observation that these variants account for only a small proportion of T2D heritability has now led many to speculate that the heritability gap is likely to lie in low frequency variants (MAF 0.05-5%) which have until recently evaded capture. The recent advances in technology and implementation of next generation sequencing approaches (including whole genome, exome and targeted gene deep resequencing), now provide researchers with an additional approach to variant identification. The hope is that the search for these low frequency variants will identify SNPs within coding regions and regulatory elements, providing more tractable variants for functional follow-up and subsequently account for a significant proportion of T2D heritability.

The observation that the majority of T2D-associated susceptibility loci associate with defective beta-cell function (HOMA-B) (Dupuis, et al., 2010) dictates that the success of molecular mechanism elucidation and functional follow-up will lie in performing the correct biological investigation in islets and beta-cells. When one considers that there is an overwhelming lack of biologically appropriate human insulin-secreting cell lines, alongside accumulating evidence of the differences between rodent and human islets (Bosco, et al., 2010; Braun, et al., 2008; Fiaschi-Taesch, et al., 2009), downstream functional work in human primary islets and beta-cells is likely to be of paramount importance. My investigation of *SLC2A2* demonstrated the difficulties faced when following up GWAS signals especially when trying to directly extrapolate from rodents to humans (**chapter 4**).

A variant within *SLC2A2* was robustly associated with FPG levels in the MAGIC meta-analysis. However my transcript profiling demonstrated little expression within human islets, whilst a complementary physiological analysis paper observed no demonstrable effects on insulin secretion or processing (Ingelsson, et al., 2010). *SLC2A2* is known to function as the predominant transporter in rodent islets and beta-cells and is widely accepted to play a similar role in humans (Fajans, et al., 2001; Hussain, 2010; Kronenberg, et al., 2008; Sperling, 2006). However, combining data from both physiological and in vivo analysis of *SLC2A2* mutation carriers cast doubt on the legitimacy of this hypothesis (Ingelsson, et al., 2010; Santer, et al., 1998). Through transcript profiling in human and rodent beta-cells I was able to demonstrate that the GLUT transcript profile differed between the two species, with GLUT1 and GLUT3 predominating in humans whilst GLUT2 was predominant in rodents. These observations may go some way to explaining the lack of beta-cell effect despite common *SLC2A2* SNPs increasing fpg levels. The data once again serves to highlight the differences between rodents and humans, the care that needs to be taken when using one as a model of the other and the necessity of following up T2D GWAS signals in human islets and beta-cells where possible.

These findings are likely to be of interest not only to those interested in translating T2D association signals but also to scientists working on the generation of adult insulin-secreting beta-cells from stem cells. GLUT2 is commonly used as a marker of islet cell lineage (Borowiak and Melton, 2009; Jiang, et al., 2007), however our observations would indicate this may be inappropriate. Our data suggest that in the future monitoring the expression of the three glucose transporters is likely to yield cells with properties of adult islet cells.

As previously mentioned, one of the most interesting aspects of T2D genetic investigation to date has been the disproportional number of variants associated with beta-cell dysfunction

when compared to those associated with insulin resistance (Dupuis, et al., 2010). Explanations for this observation may be that 1) variants affecting insulin action are confounded by environmental factors including obesity or 2) variants associated with insulin action are present in lower numbers compared to those associated with beta-cell function and are low frequency variants of a larger effect size. These variants may have evaded capture using GWAS common SNP methodology. Until data is available from next generation sequencing platforms, our understanding of this concept is unlikely to be explained.

Therefore, additional biological approaches are likely to be required to further understand the genetic component of insulin resistance. The generation of tissue-specific knockout models for crucial genes within the insulin signalling pathway has been of importance to date. Of particular interest to our research group were the data generated from the *Pten* knockout models, which in both adipose tissue and muscle clearly demonstrated the importance of this tumour suppressor gene in the maintenance of glucose homeostasis (Kurlawalla-Martinez, et al., 2005; Wijesekara, et al., 2005). Work performed by our own group has since demonstrated that patients with Cowden's Syndrome (*PTEN* haploinsufficient) are insulin-sensitive (Aparna Pal, personal communication). Taken alongside the rodent data, led me to hypothesise that upregulation of *PTEN* gene expression in patients with T2D may contribute to the reduced insulin sensitivity observed in these patients. Although I was unable to detect *PTEN* expression within myocytes from either T2D or normoglycaemic subjects my data paradoxically demonstrated that, within the adipose tissue of T2D subjects, *PTEN* was downregulated at both the mRNA and protein level. My data also demonstrated that this phenomenon is not a temporal response to insulin stimulation but rather that it is likely to be a response to prolonged hyperglycaemia.

Unfortunately my investigation of the role of PTEN in adipose tissue remains incomplete. I hypothesise that, in the adipose tissue of T2D subjects, a reduction in PTEN expression may lead to an alteration in the ratio of cellular phosphatidylinositol 4,5-bisphosphate: phosphatidylinositol 3,4,5 triphosphate (PIP₂:PIP₃) thus increasing signalling via the AKT pathway. Future work is required to elucidate the effects of reduced PTEN expression on these key secondary messengers and downstream targets. Of particular interest will be the assessment of PIP₃ levels in adipose tissue biopsies from our T2D subjects, as well as direct investigation of AKT phosphorylation levels between our subjects and controls. Determining the mechanism of PTEN downregulation will also be of importance. Investigating whether PTEN downregulation is mediated via a miRNA feedback mechanism, myokine cross talk between insulin resistant muscle and subcutaneous adipose tissue, or by an additional regulatory mechanism which is as yet not understood, will hopefully provide further insight and explanation for my novel findings.

These observations are likely to be of importance as there is substantial interest in lipid phosphatases (including PTEN) as T2D therapeutic targets (Beguilot, 2007; Sasaoka, et al., 2006). Although systemic targeting of PTEN is not feasible due to adverse oncogenic side effects (Di Cristofano, et al., 1998; Podsypanina, et al., 1999), studies on adipose and muscle specific Pten knockouts provided evidence that tissue-specific targeting not only improves insulin sensitivity but also bypasses these oncogenic adverse effects (Kurlawalla-Martinez, et al., 2005; Wijesekara, et al., 2005). These observations led many to speculate that specifically targeting PTEN knockdown in the adipose tissue and muscle of humans would be a viable target for novel T2D therapeutic agents (Beguilot, 2007; Sasaoka, et al., 2006). However my data, accumulated from human studies, casts doubt on the benefit of therapeutic intervention at this level. Although further work is necessary, my initial studies suggest that *PTEN* is only expressed at background levels within human muscle and therefore therapeutic

targeting and knockdown in this tissue is unlikely to produce the desired insulin sensitising effects. In addition, my data also suggests that the subcutaneous adipose tissue of humans can adapt to prolonged hyperglycaemia and intrinsically downregulates PTEN expression to a physiologically 'safe' level. Enhancing this downregulation further, using novel therapeutic agents in T2D patients, may be detrimental as PTEN plays a key role in many other cellular processes, the effects of which would require close monitoring. My data therefore casts doubt on whether targeting this specific lipid phosphatase is likely to be beneficially as a novel T2D sensitising agent.

In summary, the data presented in this thesis demonstrate the power of utilising a broad, multidisciplinary approach to investigate the genetic component of diabetes mellitus. Continued investigation of this field is likely to be of paramount importance if we are to see breakthroughs in the generation of novel pharmacological therapies to combat the ever increasing diabetes epidemic.

References

- Executive summary: Standards of medical care in diabetes--2010. *Diabetes Care* 33 Suppl 1:S4-10.
- Abbasakoor NO, Healy ML, O'Shea D, Maguire D, Muldoon C, Sheahan K, O'Toole D. 2011. Metastatic insulinoma in a patient with type 2 diabetes mellitus: case report and review of the literature. *Int J Endocrinol* 2011:124078.
- Agostini M, Schoenmakers E, Mitchell C, Szatmari I, Savage D, Smith A, Rajanayagam O, Semple R, Luan J, Bath L and others. 2006. Non-DNA binding, dominant-negative, human PPARgamma mutations cause lipodystrophic insulin resistance. *Cell Metab* 4(4):303-11.
- Aguilar-Bryan L, Bryan J. 2008. Neonatal diabetes mellitus. *Endocr Rev* 29(3):265-91.
- Alessi DR, Andjelkovic M, Caudwell B, Cron P, Morrice N, Cohen P, Hemmings BA. 1996. Mechanism of activation of protein kinase B by insulin and IGF-1. *EMBO J* 15(23):6541-51.
- Alessi DR, Deak M, Casamayor A, Caudwell FB, Morrice N, Norman DG, Gaffney P, Reese CB, MacDougall CN, Harbison D and others. 1997a. 3-Phosphoinositide-dependent protein kinase-1 (PDK1): structural and functional homology with the Drosophila DSTPK61 kinase. *Curr Biol* 7(10):776-89.
- Alessi DR, James SR, Downes CP, Holmes AB, Gaffney PR, Reese CB, Cohen P. 1997b. Characterization of a 3-phosphoinositide-dependent protein kinase which phosphorylates and activates protein kinase Balpha. *Curr Biol* 7(4):261-9.
- Altshuler D, Hirschhorn JN, Klannemark M, Lindgren CM, Vohl MC, Nemesh J, Lane CR, Schaffner SF, Bolk S, Brewer C and others. 2000. The common PPARgamma Pro12Ala polymorphism is associated with decreased risk of type 2 diabetes. *Nat Genet* 26(1):76-80.
- Arden SD, Zahn T, Steegers S, Webb S, Bergman B, O'Brien RM, Hutton JC. 1999. Molecular cloning of a pancreatic islet-specific glucose-6-phosphatase catalytic subunit-related protein. *Diabetes* 48(3):531-42.
- Ashcroft SJ, Bassett JM, Randle PJ. 1972. Insulin secretion mechanisms and glucose metabolism in isolated islets. *Diabetes* 21(2 Suppl):538-45.
- Asuncion M, Calvo RM, San Millan JL, Sancho J, Avila S, Escobar-Morreale HF. 2000. A prospective study of the prevalence of the polycystic ovary syndrome in unselected Caucasian women from Spain. *J Clin Endocrinol Metab* 85(7):2434-8.
- Azziz R. 2006. Controversy in clinical endocrinology: diagnosis of polycystic ovarian syndrome: the Rotterdam criteria are premature. *J Clin Endocrinol Metab* 91(3):781-5.
- Azziz R, Woods KS, Reyna R, Key TJ, Knochenhauer ES, Yildiz BO. 2004. The prevalence and features of the polycystic ovary syndrome in an unselected population. *J Clin Endocrinol Metab* 89(6):2745-9.
- Babenko AP. 2008. A novel ABCC8 (SUR1)-dependent mechanism of metabolism-excitation uncoupling. *J Biol Chem* 283(14):8778-82.
- Babenko AP, Polak M, Cave H, Busiah K, Czernichow P, Scharfmann R, Bryan J, Aguilar-Bryan L, Vaxillaire M, Froguel P. 2006. Activating mutations in the ABCC8 gene in neonatal diabetes mellitus. *N Engl J Med* 355(5):456-66.
- Bajaj M, Suraamornkul S, Pratipanawatr T, Hardies LJ, Pratipanawatr W, Glass L, Cersosimo E, Miyazaki Y, DeFronzo RA. 2003. Pioglitazone reduces hepatic fat content and augments splanchnic glucose uptake in patients with type 2 diabetes. *Diabetes* 52(6):1364-70.
- Banerjee M, Otonkoski T. 2009. A simple two-step protocol for the purification of human pancreatic beta cells. *Diabetologia* 52(4):621-5.
- Banting FG, Best CH, Collip JB, Campbell WR, Fletcher AA. 1922. Pancreatic Extracts in the Treatment of Diabetes Mellitus. *Can Med Assoc J* 12(3):141-6.

- Baptiste CG, Battista MC, Trottier A, Baillargeon JP. 2010. Insulin and hyperandrogenism in women with polycystic ovary syndrome. *J Steroid Biochem Mol Biol* 122(1-3):42-52.
- Barbosa RM, Silva AM, Tome AR, Stamford JA, Santos RM, Rosario LM. 1998. Control of pulsatile 5-HT/insulin secretion from single mouse pancreatic islets by intracellular calcium dynamics. *J Physiol* 510 (Pt 1):135-43.
- Barnett AH, Eff C, Leslie RD, Pyke DA. 1981. Diabetes in identical twins. A study of 200 pairs. *Diabetologia* 20(2):87-93.
- Beguino F. 2007. PTEN targeting: the search for novel insulin sensitizers provides new insight into obesity research. *Diabetologia* 50(2):247-9.
- Bell GI, Pictet RL, Rutter WJ, Cordell B, Tischler E, Goodman HM. 1980. Sequence of the human insulin gene. *Nature* 284(5751):26-32.
- Bell GI, Swain WF, Pictet R, Cordell B, Goodman HM, Rutter WJ. 1979. Nucleotide sequence of a cDNA clone encoding human preproinsulin. *Nature* 282(5738):525-7.
- Below JE, Gamazon ER, Morrison JV, Konkashbaev A, Pluzhnikov A, McKeigue PM, Parra EJ, Elbein SC, Hallman DM, Nicolae DL and others. 2011. Genome-wide association and meta-analysis in populations from Starr County, Texas, and Mexico City identify type 2 diabetes susceptibility loci and enrichment for expression quantitative trait loci in top signals. *Diabetologia*.
- Benedict C, Hallschmid M, Hatke A, Schultes B, Fehm HL, Born J, Kern W. 2004. Intranasal insulin improves memory in humans. *Psychoneuroendocrinology* 29(10):1326-34.
- Bergsten P, Grapengiesser E, Gylfe E, Tengholm A, Hellman B. 1994. Synchronous oscillations of cytoplasmic Ca²⁺ and insulin release in glucose-stimulated pancreatic islets. *J Biol Chem* 269(12):8749-53.
- Bernard-Kargar C, Kassis N, Berthault MF, Pralong W, Ktorza A. 2001. Sialylated form of the neural cell adhesion molecule (NCAM): a new tool for the identification and sorting of beta-cell subpopulations with different functional activity. *Diabetes* 50 Suppl 1:S125-30.
- Bischof LJ, Martin CC, Svitek CA, Stadelmaier BT, Hornbuckle LA, Goldman JK, Oeser JK, Hutton JC, O'Brien RM. 2001. Characterization of the mouse islet-specific glucose-6-phosphatase catalytic subunit-related protein gene promoter by in situ footprinting: correlation with fusion gene expression in the islet-derived betaTC-3 and hamster insulinoma tumor cell lines. *Diabetes* 50(3):502-14.
- Bjornholt JV, Erikssen G, Aaser E, Sandvik L, Nitter-Hauge S, Jervell J, Erikssen J, Thaulow E. 1999. Fasting blood glucose: an underestimated risk factor for cardiovascular death. Results from a 22-year follow-up of healthy nondiabetic men. *Diabetes Care* 22(1):45-9.
- Boden G. 1997. Role of fatty acids in the pathogenesis of insulin resistance and NIDDM. *Diabetes* 46(1):3-10.
- Boden G, Shulman GI. 2002. Free fatty acids in obesity and type 2 diabetes: defining their role in the development of insulin resistance and beta-cell dysfunction. *Eur J Clin Invest* 32 Suppl 3:14-23.
- Boni-Schnetzler M, Boller S, Debray S, Bouzakri K, Meier DT, Prazak R, Kerr-Conte J, Pattou F, Ehses JA, Schuit FC and others. 2009. Free fatty acids induce a proinflammatory response in islets via the abundantly expressed interleukin-1 receptor 1. *Endocrinology* 150(12):5218-29.
- Bonfond A, Bouatia-Naji N, Simon A, Saint-Martin C, Dechaume A, de Lonlay P, Polak M, Bellanne-Chantelot C, Froguel P, Vaxillaire M. 2009. Mutations in G6PC2 do not contribute to monogenic forms of early infancy diabetes and beta cell dysfunction. *Diabetologia* 52(5):982-5.
- Bonfond A, Durand E, Sand O, De Graeve F, Gallina S, Busiah K, Lobbens S, Simon A, Bellanne-Chantelot C, Letourneau L and others. 2010a. Molecular diagnosis of

- neonatal diabetes mellitus using next-generation sequencing of the whole exome. *PLoS One* 5(10):e13630.
- Bonnefond A, Froguel P, Vaxillaire M. 2010b. The emerging genetics of type 2 diabetes. *Trends Mol Med* 16(9):407-16.
- Bonnycastle LL, Willer CJ, Conneely KN, Jackson AU, Burrill CP, Watanabe RM, Chines PS, Narisu N, Scott LJ, Enloe ST and others. 2006. Common variants in maturity-onset diabetes of the young genes contribute to risk of type 2 diabetes in Finns. *Diabetes* 55(9):2534-40.
- Borowiak M, Melton DA. 2009. How to make beta cells? *Curr Opin Cell Biol* 21(6):727-32.
- Bosco D, Armanet M, Morel P, Niclauss N, Sgroi A, Muller YD, Giovannoni L, Parnaud G, Berney T. 2010. Unique arrangement of alpha- and beta-cells in human islets of Langerhans. *Diabetes* 59(5):1202-10.
- Bouatia-Naji N, Bonnefond A, Baerenwald DA, Marchand M, Bugliani M, Marchetti P, Pattou F, Printz RL, Flemming BP, Umunakwe OC and others. 2010. Genetic and functional assessment of the role of the rs13431652-A and rs573225-A alleles in the G6PC2 promoter that are strongly associated with elevated fasting glucose levels. *Diabetes* 59(10):2662-71.
- Bouatia-Naji N, Bonnefond A, Cavalcanti-Proenca C, Sparso T, Holmkvist J, Marchand M, Delplanque J, Lobbens S, Rocheleau G, Durand E and others. 2009. A variant near MTNR1B is associated with increased fasting plasma glucose levels and type 2 diabetes risk. *Nat Genet* 41(1):89-94.
- Bouatia-Naji N, Rocheleau G, Van Lommel L, Lemaire K, Schuit F, Cavalcanti-Proenca C, Marchand M, Hartikainen AL, Sovio U, De Graeve F and others. 2008. A polymorphism within the G6PC2 gene is associated with fasting plasma glucose levels. *Science* 320(5879):1085-8.
- Boustead JN, Martin CC, Oeser JK, Svitek CA, Hunter SI, Hutton JC, O'Brien RM. 2004. Identification and characterization of a cDNA and the gene encoding the mouse ubiquitously expressed glucose-6-phosphatase catalytic subunit-related protein. *J Mol Endocrinol* 32(1):33-53.
- Bouzakri K, Plomgaard P, Berney T, Donath MY, Pedersen BK, Halban PA. 2011. Bimodal Effect on Pancreatic {beta}-Cells of Secretory Products From Normal or Insulin-Resistant Human Skeletal Muscle. *Diabetes* 60(4):1111-21.
- Bouzakri K, Ribaux P, Halban PA. 2009. Silencing mitogen-activated protein 4 kinase 4 (MAP4K4) protects beta cells from tumor necrosis factor-alpha-induced decrease of IRS-2 and inhibition of glucose-stimulated insulin secretion. *J Biol Chem* 284(41):27892-8.
- Braun M, Ramracheya R, Bengtsson M, Zhang Q, Karanauskaite J, Partridge C, Johnson PR, Rorsman P. 2008. Voltage-gated ion channels in human pancreatic beta-cells: electrophysiological characterization and role in insulin secretion. *Diabetes* 57(6):1618-28.
- Burghen GA, Givens JR, Kitabchi AE. 1980. Correlation of hyperandrogenism with hyperinsulinism in polycystic ovarian disease. *J Clin Endocrinol Metab* 50(1):113-6.
- Byrne MM, Sturis J, Clement K, Vionnet N, Pueyo ME, Stoffel M, Takeda J, Passa P, Cohen D, Bell GI and others. 1994. Insulin secretory abnormalities in subjects with hyperglycemia due to glucokinase mutations. *J Clin Invest* 93(3):1120-30.
- Byrne MM, Sturis J, Menzel S, Yamagata K, Fajans SS, Dronsfield MJ, Bain SC, Hattersley AT, Velho G, Froguel P and others. 1996. Altered insulin secretory responses to glucose in diabetic and nondiabetic subjects with mutations in the diabetes susceptibility gene MODY3 on chromosome 12. *Diabetes* 45(11):1503-10.

- Campfield LA, Smith FJ, Guisez Y, Devos R, Burn P. 1995. Recombinant mouse OB protein: evidence for a peripheral signal linking adiposity and central neural networks. *Science* 269(5223):546-9.
- Chagpar RB, Links PH, Pastor MC, Furber LA, Hawrysh AD, Chamberlain MD, Anderson DH. 2009. Direct positive regulation of PTEN by the p85 subunit of phosphatidylinositol 3-kinase. *Proc Natl Acad Sci U S A* 107(12):5471-6.
- Chan SJ, Keim P, Steiner DF. 1976. Cell-free synthesis of rat preproinsulins: characterization and partial amino acid sequence determination. *Proc Natl Acad Sci U S A* 73(6):1964-8.
- Chance RE, Ellis RM, Bromer WW. 1968. Porcine proinsulin: characterization and amino acid sequence. *Science* 161(837):165-7.
- Chawla A, Lazar MA. 1994. Peroxisome proliferator and retinoid signaling pathways co-regulate preadipocyte phenotype and survival. *Proc Natl Acad Sci U S A* 91(5):1786-90.
- Chen WM, Erdos MR, Jackson AU, Saxena R, Sanna S, Silver KD, Timpson NJ, Hansen T, Orru M, Grazia Piras M and others. 2008. Variations in the G6PC2/ABCB11 genomic region are associated with fasting glucose levels. *J Clin Invest* 118(7):2620-8.
- Chomczynski P, Sacchi N. 1987. Single-step method of RNA isolation by acid guanidinium thiocyanate-phenol-chloroform extraction. *Anal Biochem* 162(1):156-9.
- Chou JY, Mansfield BC. 2008. Mutations in the glucose-6-phosphatase-alpha (G6PC) gene that cause type Ia glycogen storage disease. *Hum Mutat* 29(7):921-30.
- Christesen HB, Tribble ND, Molven A, Siddiqui J, Sandal T, Brusgaard K, Ellard S, Njolstad PR, Alm J, Brock Jacobsen B and others. 2008. Activating glucokinase (GCK) mutations as a cause of medically responsive congenital hyperinsulinism: prevalence in children and characterisation of a novel GCK mutation. *Eur J Endocrinol* 159(1):27-34.
- Clayton PT, Eaton S, Aynsley-Green A, Edginton M, Hussain K, Krywawych S, Datta V, Malingre HE, Berger R, van den Berg IE. 2001. Hyperinsulinism in short-chain L-3-hydroxyacyl-CoA dehydrogenase deficiency reveals the importance of beta-oxidation in insulin secretion. *J Clin Invest* 108(3):457-65.
- Cnop M, Hughes SJ, Igoillo-Estevé M, Hoppa MB, Sayyed F, van de Laar L, Gunter JH, de Koning EJ, Walls GV, Gray DW and others. 2010. The long lifespan and low turnover of human islet beta cells estimated by mathematical modelling of lipofuscin accumulation. *Diabetologia* 53(2):321-30.
- Coutinho M, Gerstein HC, Wang Y, Yusuf S. 1999. The relationship between glucose and incident cardiovascular events. A metaregression analysis of published data from 20 studies of 95,783 individuals followed for 12.4 years. *Diabetes Care* 22(2):233-40.
- Cross DA, Alessi DR, Cohen P, Andjelkovich M, Hemmings BA. 1995. Inhibition of glycogen synthase kinase-3 by insulin mediated by protein kinase B. *Nature* 378(6559):785-9.
- Dash S, Sano H, Rochford JJ, Semple RK, Yeo G, Hyden CS, Soos MA, Clark J, Rodin A, Langenberg C and others. 2009. A truncation mutation in TBC1D4 in a family with acanthosis nigricans and postprandial hyperinsulinemia. *Proc Natl Acad Sci U S A* 106(23):9350-5.
- Dawn Teare M, Barrett JH. 2005. Genetic linkage studies. *Lancet* 366(9490):1036-44.
- De Leon DD, Stanley CA. 2007. Mechanisms of Disease: advances in diagnosis and treatment of hyperinsulinism in neonates. *Nat Clin Pract Endocrinol Metab* 3(1):57-68.
- De Vos A, Heimberg H, Quartier E, Huypens P, Bouwens L, Pipeleers D, Schuit F. 1995. Human and rat beta cells differ in glucose transporter but not in glucokinase gene expression. *J Clin Invest* 96(5):2489-95.
- Di Cristofano A, Pesce B, Cordon-Cardo C, Pandolfi PP. 1998. Pten is essential for embryonic development and tumour suppression. *Nat Genet* 19(4):348-55.
- Diamanti-Kandaraki E, Papavassiliou AG. 2006. Molecular mechanisms of insulin resistance in polycystic ovary syndrome. *Trends Mol Med* 12(7):324-32.

- Diatloff-Zito C, Nicole A, Marcelin G, Labit H, Marquis E, Bellanne-Chantelot C, Robert JJ. 2007. Genetic and epigenetic defects at the 6q24 imprinted locus in a cohort of 13 patients with transient neonatal diabetes: new hypothesis raised by the finding of a unique case with hemizygotic deletion in the critical region. *J Med Genet* 44(1):31-7.
- Dietze D, Koenen M, Rohrig K, Horikoshi H, Hauner H, Eckel J. 2002. Impairment of insulin signaling in human skeletal muscle cells by co-culture with human adipocytes. *Diabetes* 51(8):2369-76.
- Dinneen S, Gerich J, Rizza R. 1992. Carbohydrate metabolism in non-insulin-dependent diabetes mellitus. *N Engl J Med* 327(10):707-13.
- Donohue WL, Uchida I. 1954. Leprechaunism: a euphemism for a rare familial disorder. *J Pediatr* 45(5):505-19.
- Dos Santos C, Bougneres P, Fradin D. 2009. A single-nucleotide polymorphism in a methylatable Foxa2 binding site of the G6PC2 promoter is associated with insulin secretion in vivo and increased promoter activity in vitro. *Diabetes* 58(2):489-92.
- Duggirala R, Blangero J, Almasy L, Dyer TD, Williams KL, Leach RJ, O'Connell P, Stern MP. 1999. Linkage of type 2 diabetes mellitus and of age at onset to a genetic location on chromosome 10q in Mexican Americans. *Am J Hum Genet* 64(4):1127-40.
- Dunaif A, Thomas A. 2001. Current concepts in the polycystic ovary syndrome. *Annu Rev Med* 52:401-19.
- Dunaif A, Xia J, Book CB, Schenker E, Tang Z. 1995. Excessive insulin receptor serine phosphorylation in cultured fibroblasts and in skeletal muscle. A potential mechanism for insulin resistance in the polycystic ovary syndrome. *J Clin Invest* 96(2):801-10.
- Dupuis J, Langenberg C, Prokopenko I, Saxena R, Soranzo N, Jackson AU, Wheeler E, Glazer NL, Bouatia-Naji N, Gloyn AL and others. 2010. New genetic loci implicated in fasting glucose homeostasis and their impact on type 2 diabetes risk. *Nat Genet* 42(2):105-16.
- Ebert DH, Bischof LJ, Streeper RS, Chapman SC, Svitek CA, Goldman JK, Mathews CE, Leiter EH, Hutton JC, O'Brien RM. 1999. Structure and promoter activity of an islet-specific glucose-6-phosphatase catalytic subunit-related gene. *Diabetes* 48(3):543-51.
- Edghill EL, Bingham C, Ellard S, Hattersley AT. 2006a. Mutations in hepatocyte nuclear factor-1beta and their related phenotypes. *J Med Genet* 43(1):84-90.
- Edghill EL, Dix RJ, Flanagan SE, Bingley PJ, Hattersley AT, Ellard S, Gillespie KM. 2006b. HLA genotyping supports a nonautoimmune etiology in patients diagnosed with diabetes under the age of 6 months. *Diabetes* 55(6):1895-8.
- Edghill EL, Flanagan SE, Patch AM, Boustred C, Parrish A, Shields B, Shepherd MH, Hussain K, Kapoor RR, Malecki M and others. 2008. Insulin mutation screening in 1,044 patients with diabetes: mutations in the INS gene are a common cause of neonatal diabetes but a rare cause of diabetes diagnosed in childhood or adulthood. *Diabetes* 57(4):1034-42.
- Edghill EL, Gloyn AL, Goriely A, Harries LW, Flanagan SE, Rankin J, Hattersley AT, Ellard S. 2007. Origin of de novo KCNJ11 mutations and risk of neonatal diabetes for subsequent siblings. *J Clin Endocrinol Metab* 92(5):1773-7.
- Ehm MG, Karnoub MC, Sakul H, Gottschalk K, Holt DC, Weber JL, Vaske D, Briley D, Briley L, Kopf J and others. 2000. Genomewide search for type 2 diabetes susceptibility genes in four American populations. *Am J Hum Genet* 66(6):1871-81.
- Elbein SC, Hoffman MD, Teng K, Leppert MF, Hasstedt SJ. 1999. A genome-wide search for type 2 diabetes susceptibility genes in Utah Caucasians. *Diabetes* 48(5):1175-82.
- Ellard S, Bellanne-Chantelot C, Hattersley AT. 2008. Best practice guidelines for the molecular genetic diagnosis of maturity-onset diabetes of the young. *Diabetologia* 51(4):546-53.
- Elsas LJ, Endo F, Strumlauf E, Elders J, Priest JH. 1985. Leprechaunism: an inherited defect in a high-affinity insulin receptor. *Am J Hum Genet* 37(1):73-88.

- Emanuelli B, Eberle D, Suzuki R, Kahn CR. 2008. Overexpression of the dual-specificity phosphatase MKP-4/DUSP-9 protects against stress-induced insulin resistance. *Proc Natl Acad Sci U S A* 105(9):3545-50.
- Fagerholm V, Gronroos T, Marjamaki P, Viljanen T, Scheinin M, Haaparanta M. 2004. Altered glucose homeostasis in alpha2A-adrenoceptor knockout mice. *Eur J Pharmacol* 505(1-3):243-52.
- Fahien LA, MacDonald MJ, Kmietek EH, Mertz RJ, Fahien CM. 1988. Regulation of insulin release by factors that also modify glutamate dehydrogenase. *J Biol Chem* 263(27):13610-4.
- Fajans SS, Bell GI, Polonsky KS. 2001. Molecular mechanisms and clinical pathophysiology of maturity-onset diabetes of the young. *N Engl J Med* 345(13):971-80.
- Farooqi IS, Jebb SA, Langmack G, Lawrence E, Cheetham CH, Prentice AM, Hughes IA, McCamish MA, O'Rahilly S. 1999. Effects of recombinant leptin therapy in a child with congenital leptin deficiency. *N Engl J Med* 341(12):879-84.
- Farooqi IS, Matarese G, Lord GM, Keogh JM, Lawrence E, Agwu C, Sanna V, Jebb SA, Perna F, Fontana S and others. 2002. Beneficial effects of leptin on obesity, T cell hyporesponsiveness, and neuroendocrine/metabolic dysfunction of human congenital leptin deficiency. *J Clin Invest* 110(8):1093-103.
- Fiaschi-Taesch N, Bigatel TA, Sicari B, Takane KK, Salim F, Velazquez-Garcia S, Harb G, Selk K, Cozar-Castellano I, Stewart AF. 2009. Survey of the human pancreatic beta-cell G1/S proteome reveals a potential therapeutic role for cdk-6 and cyclin D1 in enhancing human beta-cell replication and function in vivo. *Diabetes* 58(4):882-93.
- Flanagan SE, Edghill EL, Gloyn AL, Ellard S, Hattersley AT. 2006. Mutations in KCNJ11, which encodes Kir6.2, are a common cause of diabetes diagnosed in the first 6 months of life, with the phenotype determined by genotype. *Diabetologia* 49(6):1190-7.
- Flanagan SE, Kapoor RR, Banerjee I, Hall C, Smith VV, Hussain K, Ellard S. 2011. Dominantly acting ABCC8 mutations in patients with medically unresponsive hyperinsulinaemic hypoglycaemia. *Clin Genet* 79(6):582-7.
- Flanagan SE, Patch AM, Mackay DJ, Edghill EL, Gloyn AL, Robinson D, Shield JP, Temple K, Ellard S, Hattersley AT. 2007. Mutations in ATP-sensitive K⁺ channel genes cause transient neonatal diabetes and permanent diabetes in childhood or adulthood. *Diabetes* 56(7):1930-7.
- Flier JS. 2001. Diabetes. The missing link with obesity? *Nature* 409(6818):292-3.
- Fonseca V. 2003. Effect of thiazolidinediones on body weight in patients with diabetes mellitus. *Am J Med* 115 Suppl 8A:42S-48S.
- Fosel S. 1995. Transient and permanent neonatal diabetes. *Eur J Pediatr* 154(12):944-8.
- Fowler MJ. 2008. Microvascular and Macrovascular complications of diabetes. *Clin Diabetes* 26(2):77-82.
- Frayling TM, Bulamn MP, Ellard S, Appleton M, Dronsfield MJ, Mackie AD, Baird JD, Kaisaki PJ, Yamagata K, Bell GI and others. 1997. Mutations in the hepatocyte nuclear factor-1alpha gene are a common cause of maturity-onset diabetes of the young in the U.K. *Diabetes* 46(4):720-5.
- Frayling TM, Evans JC, Bulman MP, Pearson E, Allen L, Owen K, Bingham C, Hannemann M, Shepherd M, Ellard S and others. 2001. beta-cell genes and diabetes: molecular and clinical characterization of mutations in transcription factors. *Diabetes* 50 Suppl 1:S94-100.
- Frayling TM, Lindgren CM, Chevre JC, Menzel S, Wishart M, Benmezroua Y, Brown A, Evans JC, Rao PS, Dina C and others. 2003. A genome-wide scan in families with maturity-onset diabetes of the young: evidence for further genetic heterogeneity. *Diabetes* 52(3):872-81.

- Frazer KA, Ballinger DG, Cox DR, Hinds DA, Stuve LL, Gibbs RA, Belmont JW, Boudreau A, Hardenbol P, Leal SM and others. 2007. A second generation human haplotype map of over 3.1 million SNPs. *Nature* 449(7164):851-61.
- Froguel P, Vaxillaire M, Sun F, Velho G, Zouali H, Butel MO, Lesage S, Vionnet N, Clement K, Fougerousse F and others. 1992. Close linkage of glucokinase locus on chromosome 7p to early-onset non-insulin-dependent diabetes mellitus. *Nature* 356(6365):162-4.
- Froguel P, Zouali H, Vionnet N, Velho G, Vaxillaire M, Sun F, Lesage S, Stoffel M, Takeda J, Passa P and others. 1993. Familial hyperglycemia due to mutations in glucokinase. Definition of a subtype of diabetes mellitus. *N Engl J Med* 328(10):697-702.
- Gabriel SB, Schaffner SF, Nguyen H, Moore JM, Roy J, Blumenstiel B, Higgins J, DeFelice M, Lochner A, Faggart M and others. 2002. The structure of haplotype blocks in the human genome. *Science* 296(5576):2225-9.
- Galli J, Fakhrai-Rad H, Kamel A, Marcus C, Norgren S, Luthman H. 1999. Pathophysiological and genetic characterization of the major diabetes locus in GK rats. *Diabetes* 48(12):2463-70.
- Garg A. 2004. Acquired and inherited lipodystrophies. *N Engl J Med* 350(12):1220-34.
- Garin I, Edghill EL, Akerman I, Rubio-Cabezas O, Rica I, Locke JM, Maestro MA, Alshaikh A, Bundak R, del Castillo G and others. 2010. Recessive mutations in the INS gene result in neonatal diabetes through reduced insulin biosynthesis. *Proc Natl Acad Sci U S A* 107(7):3105-10.
- Genuth S, Alberti KG, Bennett P, Buse J, Defronzo R, Kahn R, Kitzmiller J, Knowler WC, Lebovitz H, Lernmark A and others. 2003. Follow-up report on the diagnosis of diabetes mellitus. *Diabetes Care* 26(11):3160-7.
- George S, Rochford JJ, Wolfrum C, Gray SL, Schinner S, Wilson JC, Soos MA, Murgatroyd PR, Williams RM, Acerini CL and others. 2004. A family with severe insulin resistance and diabetes due to a mutation in AKT2. *Science* 304(5675):1325-8.
- Gibbs RA. 2003. The International HapMap Project. *Nature* 426(6968):789-96.
- Gibson WT, Farooqi IS, Moreau M, DePaoli AM, Lawrence E, O'Rahilly S, Trussell RA. 2004. Congenital leptin deficiency due to homozygosity for the Delta133G mutation: report of another case and evaluation of response to four years of leptin therapy. *J Clin Endocrinol Metab* 89(10):4821-6.
- Gilad Y, Rifkin SA, Pritchard JK. 2008. Revealing the architecture of gene regulation: the promise of eQTL studies. *Trends Genet* 24(8):408-15.
- Gill-Carey O, Shields B, Colclough K, Ellard S, Hattersley AT. 2007. Finding a glucokinase mutation alters patient treatment. *Diabet Med* 24 (Suppl 1)(6 (Abstract)).
- Gill GV, Rauf O, MacFarlane IA. 1997. Diazoxide treatment for insulinoma: a national UK survey. *Postgrad Med J* 73(864):640-1.
- Glaser B, Kesavan P, Heyman M, Davis E, Cuesta A, Buchs A, Stanley CA, Thornton PS, Permutt MA, Matschinsky FM and others. 1998. Familial hyperinsulinism caused by an activating glucokinase mutation. *N Engl J Med* 338(4):226-30.
- Glaser B, Ryan F, Donath M, Landau H, Stanley CA, Baker L, Barton DE, Thornton PS. 1999. Hyperinsulinism caused by paternal-specific inheritance of a recessive mutation in the sulfonylurea-receptor gene. *Diabetes* 48(8):1652-7.
- Glaser B, Thornton P, Otonkoski T, Junien C. 2000. Genetics of neonatal hyperinsulinism. *Arch Dis Child Fetal Neonatal Ed* 82(2):F79-86.
- Gloyn AL, Ellard S. 2006. Defining the genetic aetiology of monogenic diabetes can improve treatment. *Expert Opin Pharmacother* 7(13):1759-67.
- Gloyn AL, Pearson ER, Antcliff JF, Proks P, Bruining GJ, Slingerland AS, Howard N, Srinivasan S, Silva JM, Molnes J and others. 2004. Activating mutations in the gene encoding the ATP-sensitive potassium-channel subunit Kir6.2 and permanent neonatal diabetes. *N Engl J Med* 350(18):1838-49.

- Gloyn AL, Reimann F, Girard C, Edghill EL, Proks P, Pearson ER, Temple IK, Mackay DJ, Shield JP, Freedenberg D and others. 2005. Relapsing diabetes can result from moderately activating mutations in KCNJ11. *Hum Mol Genet* 14(7):925-34.
- Gloyn AL, Weedon MN, Owen KR, Turner MJ, Knight BA, Hitman G, Walker M, Levy JC, Sampson M, Halford S and others. 2003. Large-scale association studies of variants in genes encoding the pancreatic beta-cell KATP channel subunits Kir6.2 (KCNJ11) and SUR1 (ABCC8) confirm that the KCNJ11 E23K variant is associated with type 2 diabetes. *Diabetes* 52(2):568-72.
- Gmyr V, Belaich S, Muharram G, Lukowiak B, Vandewalle B, Pattou F, Kerr-Conte J. 2004. Rapid purification of human ductal cells from human pancreatic fractions with surface antibody CA19-9. *Biochem Biophys Res Commun* 320(1):27-33.
- Goldstein BJ, Scalia R. 2004. Adiponectin: A novel adipokine linking adipocytes and vascular function. *J Clin Endocrinol Metab* 89(6):2563-8.
- Gordon WR, Vardar-Ulu D, L'Heureux S, Ashworth T, Malecki MJ, Sanchez-Irizarry C, McArthur DG, Histén G, Mitchell JL, Aster JC and others. 2009. Effects of S1 cleavage on the structure, surface export, and signaling activity of human Notch1 and Notch2. *PLoS One* 4(8):e6613.
- Goto Y, Kakizaki M, Masaki N. 1976. Production of spontaneous diabetic rats by repetition of selective breeding. *Tohoku J Exp Med* 119(1):85-90.
- Gould GW, Holman GD. 1993. The glucose transporter family: structure, function and tissue-specific expression. *Biochem J* 295 (Pt 2):329-41.
- Granhall C, Rosengren AH, Renstrom E, Luthman H. 2006. Separately inherited defects in insulin exocytosis and beta-cell glucose metabolism contribute to type 2 diabetes. *Diabetes* 55(12):3494-500.
- Grant SF, Thorleifsson G, Reynisdottir I, Benediktsson R, Manolescu A, Sainz J, Helgason A, Stefansson H, Emilsson V, Helgadóttir A and others. 2006. Variant of transcription factor 7-like 2 (TCF7L2) gene confers risk of type 2 diabetes. *Nat Genet* 38(3):320-3.
- Grimsby J, Sarabu R, Corbett WL, Haynes NE, Bizzarro FT, Coffey JW, Guertin KR, Hilliard DW, Kester RF, Mahaney PE and others. 2003. Allosteric activators of glucokinase: potential role in diabetes therapy. *Science* 301(5631):370-3.
- Grodsky GM, Curry DL, Bennett LL, Rodrigo JJ. 1968. [Factors influencing different rates of insulin release in vitro]. *Acta Diabetol Lat* 5 Suppl 1:140-61.
- Guillam MT, Hummler E, Schaerer E, Yeh JI, Birnbaum MJ, Beermann F, Schmidt A, Deriaz N, Thorens B. 1997. Early diabetes and abnormal postnatal pancreatic islet development in mice lacking Glut-2. *Nat Genet* 17(3):327-30.
- Halaas JL, Gajiwala KS, Maffei M, Cohen SL, Chait BT, Rabinowitz D, Lallone RL, Burley SK, Friedman JM. 1995. Weight-reducing effects of the plasma protein encoded by the obese gene. *Science* 269(5223):543-6.
- Hanis CL, Boerwinkle E, Chakraborty R, Ellsworth DL, Concannon P, Stirling B, Morrison VA, Wapelhorst B, Spielman RS, Gogolin-Ewens KJ and others. 1996. A genome-wide search for human non-insulin-dependent (type 2) diabetes genes reveals a major susceptibility locus on chromosome 2. *Nat Genet* 13(2):161-6.
- Hanson RL, Ehm MG, Pettitt DJ, Prochazka M, Thompson DB, Timberlake D, Foroud T, Kobes S, Baier L, Burns DK and others. 1998. An autosomal genomic scan for loci linked to type II diabetes mellitus and body-mass index in Pima Indians. *Am J Hum Genet* 63(4):1130-8.
- Harris TE, Lawrence JC, Jr. 2003. TOR signaling. *Sci STKE* 2003(212):re15.
- Hattersley AT, Beards F, Ballantyne E, Appleton M, Harvey R, Ellard S. 1998. Mutations in the glucokinase gene of the fetus result in reduced birth weight. *Nat Genet* 19(3):268-70.

- Hattersley AT, Turner RC, Permutt MA, Patel P, Tanizawa Y, Chiu KC, O'Rahilly S, Watkins PJ, Wainscoat JS. 1992. Linkage of type 2 diabetes to the glucokinase gene. *Lancet* 339(8805):1307-10.
- Hawkins PT, Jackson TR, Stephens LR. 1992. Platelet-derived growth factor stimulates synthesis of PtdIns(3,4,5)P₃ by activating a PtdIns(4,5)P₂ 3-OH kinase. *Nature* 358(6382):157-9.
- Hedekov CJ. 1980. Mechanism of glucose-induced insulin secretion. *Physiol Rev* 60(2):442-509.
- Helgason A, Palsson S, Thorleifsson G, Grant SF, Emilsson V, Gunnarsdottir S, Adeyemo A, Chen Y, Chen G, Reynisdottir I and others. 2007. Refining the impact of TCF7L2 gene variants on type 2 diabetes and adaptive evolution. *Nat Genet* 39(2):218-25.
- Hellman B, Sehlin J, Taljedal IB. 1971. Evidence for mediated transport of glucose in mammalian pancreatic β -cells. *Biochim Biophys Acta* 241(1):147-54.
- Henquin JC. 1978a. D-glucose inhibits potassium efflux from pancreatic islet cells. *Nature* 271(5642):271-3.
- Henquin JC. 1978b. Relative importance of extracellular and intracellular calcium for the two phases of glucose-stimulated insulin release: studies with theophylline. *Endocrinology* 102(3):723-30.
- Henquin JC, Dufrane D, Nenquin M. 2006. Nutrient control of insulin secretion in isolated normal human islets. *Diabetes* 55(12):3470-7.
- Hirschhorn JN, Daly MJ. 2005. Genome-wide association studies for common diseases and complex traits. *Nat Rev Genet* 6(2):95-108.
- Holland PM, Abramson RD, Watson R, Gelfand DH. 1991. Detection of specific polymerase chain reaction product by utilizing the 5' to 3' exonuclease activity of *Thermus aquaticus* DNA polymerase. *Proc Natl Acad Sci U S A* 88(16):7276-80.
- Horikawa Y, Iwasaki N, Hara M, Furuta H, Hinokio Y, Cockburn BN, Lindner T, Yamagata K, Ogata M, Tomonaga O and others. 1997. Mutation in hepatocyte nuclear factor-1 beta gene (TCF2) associated with MODY. *Nat Genet* 17(4):384-5.
- Horikoshi M, Kato N, Wiltshire S, Asimit J, Rayner NW, Robertson N, Takeuchi F, Ying TY, Zeggini E, McCarthy MI and others. 2011. Trans-ethnic fine-mapping of T2D susceptibility loci. *Diabetes* 60(supplement 1):A352-A397.
- Hotamisligil GS, Arner P, Caro JF, Atkinson RL, Spiegelman BM. 1995. Increased adipose tissue expression of tumor necrosis factor- α in human obesity and insulin resistance. *J Clin Invest* 95(5):2409-15.
- Humbel RE, Bosshard HR, Zahn H. 1972. Chemistry of insulin. In: Steiner DF, Freinkel N, editors. *Handbook of Physiology: Endocrinology*. Baltimore: Williams and Wilkins. p 111-132.
- Huopio H, Reimann F, Ashfield R, Komulainen J, Lenko HL, Rahier J, Vauhkonen I, Kere J, Laakso M, Ashcroft F and others. 2000. Dominantly inherited hyperinsulinism caused by a mutation in the sulfonylurea receptor type 1. *J Clin Invest* 106(7):897-906.
- Hussain K. 2008. Diagnosis and management of hyperinsulinaemic hypoglycaemia of infancy. *Horm Res* 69(1):2-13.
- Hussain K. 2010. Mutations in pancreatic β -cell Glucokinase as a cause of hyperinsulinaemic hypoglycaemia and neonatal diabetes mellitus. *Rev Endocr Metab Disord*.
- Hutton JC, O'Brien RM. 2009. Glucose-6-phosphatase catalytic subunit gene family. *J Biol Chem* 284(43):29241-5.
- Iafusco D, Stazi MA, Cotichini R, Cotellessa M, Martinucci ME, Mazzella M, Cherubini V, Barbetti F, Martinetti M, Cerutti F and others. 2002. Permanent diabetes mellitus in the first year of life. *Diabetologia* 45(6):798-804.
- Ichii H, Inverardi L, Pileggi A, Molano RD, Cabrera O, Caicedo A, Messinger S, Kuroda Y, Berggren PO, Ricordi C. 2005. A novel method for the assessment of cellular

- composition and beta-cell viability in human islet preparations. *Am J Transplant* 5(7):1635-45.
- Ingalls AM, Dickie MM, Snell GD. 1950. Obese, a new mutation in the house mouse. *J Hered* 41(12):317-8.
- Ingelsson E, Langenberg C, Hivert MF, Prokopenko I, Lyssenko V, Dupuis J, Magi R, Sharp S, Jackson AU, Assimes TL and others. 2010. Detailed physiologic characterization reveals diverse mechanisms for novel genetic Loci regulating glucose and insulin metabolism in humans. *Diabetes* 59(5):1266-75.
- Jackson SN, Howlett TA, McNally PG, O'Rahilly S, Trembath RC. 1997. Dunnigan-Kobberling syndrome: an autosomal dominant form of partial lipodystrophy. *QJM* 90(1):27-36.
- James C, Kapoor RR, Ismail D, Hussain K. 2009. The genetic basis of congenital hyperinsulinism. *J Med Genet* 46(5):289-99.
- Jiang W, Shi Y, Zhao D, Chen S, Yong J, Zhang J, Qing T, Sun X, Zhang P, Ding M and others. 2007. In vitro derivation of functional insulin-producing cells from human embryonic stem cells. *Cell Res* 17(4):333-44.
- Johnson GC, Esposito L, Barratt BJ, Smith AN, Heward J, Di Genova G, Ueda H, Cordell HJ, Eaves IA, Dudbridge F and others. 2001. Haplotype tagging for the identification of common disease genes. *Nat Genet* 29(2):233-7.
- Jolles S. 2002. Paul Langerhans. *J Clin Pathol* 55(4):243.
- Kapoor RR, Flanagan SE, James CT, McKiernan J, Thomas AM, Harmer SC, Shield JP, Tinker A, Ellard S, Hussain K. 2011. Hyperinsulinaemic hypoglycaemia and diabetes mellitus due to dominant ABCC8/KCNJ11 mutations. *Diabetologia*.
- Kaprio J, Tuomilehto J, Koskenvuo M, Romanov K, Reunanen A, Eriksson J, Stengard J, Kesaniemi YA. 1992. Concordance for type 1 (insulin-dependent) and type 2 (non-insulin-dependent) diabetes mellitus in a population-based cohort of twins in Finland. *Diabetologia* 35(11):1060-7.
- Kasuga M, Karlsson FA, Kahn CR. 1982. Insulin stimulates the phosphorylation of the 95,000-dalton subunit of its own receptor. *Science* 215(4529):185-7.
- Kent WJ, Sugnet CW, Furey TS, Roskin KM, Pringle TH, Zahler AM, Haussler D. 2002. The human genome browser at UCSC. *Genome Res* 12(6):996-1006.
- Khaw KT, Wareham N, Luben R, Bingham S, Oakes S, Welch A, Day N. 2001. Glycated haemoglobin, diabetes, and mortality in men in Norfolk cohort of european prospective investigation of cancer and nutrition (EPIC-Norfolk). *BMJ* 322(7277):15-8.
- Kim YD, Park KG, Lee YS, Park YY, Kim DK, Nedumaran B, Jang WG, Cho WJ, Ha J, Lee IK and others. 2008. Metformin inhibits hepatic gluconeogenesis through AMP-activated protein kinase-dependent regulation of the orphan nuclear receptor SHP. *Diabetes* 57(2):306-14.
- Kim YJ, Hwang SH, Cho HH, Shin KK, Bae YC, Jung JS. 2011. MicroRNA 21 regulates the proliferation of human adipose tissue-derived mesenchymal stem cells and high-fat diet-induced obesity alters microRNA 21. *J Cell Physiol*.
- Kirkpatrick CL, Marchetti P, Purrello F, Piro S, Bugliani M, Bosco D, de Koning EJ, Engelse MA, Kerr-Conte J, Pattou F and others. 2010. Type 2 diabetes susceptibility gene expression in normal or diabetic sorted human alpha and beta cells: correlations with age or BMI of islet donors. *PLoS One* 5(6):e11053.
- Knip M, Veijola R, Virtanen SM, Hyoty H, Vaarala O, Akerblom HK. 2005. Environmental triggers and determinants of type 1 diabetes. *Diabetes* 54 Suppl 2:S125-36.
- Kobberling J, Tillil H. 1982. Empirical risk figures for first degree relatives of non-insulin-dependent diabetics. In: Kobberling J, Tattersall R, editors. *The Genetics of Diabetes Mellitus*. London: Academic Press. p 201-209.
- Koster JC, Marshall BA, Ensor N, Corbett JA, Nichols CG. 2000. Targeted overactivity of beta cell K(ATP) channels induces profound neonatal diabetes. *Cell* 100(6):645-54.

- Kovacs P, Hanson RL, Lee YH, Yang X, Kobes S, Permana PA, Bogardus C, Baier LJ. 2003. The role of insulin receptor substrate-1 gene (IRS1) in type 2 diabetes in Pima Indians. *Diabetes* 52(12):3005-9.
- Kristinsson SY, Thorolfsson ET, Talseth B, Steingrimsson E, Thorsson AV, Helgason T, Hreidarsson AB, Arngrimsson R. 2001. MODY in Iceland is associated with mutations in HNF-1alpha and a novel mutation in NeuroD1. *Diabetologia* 44(11):2098-103.
- Kronenberg HM, Melmed S, Polonsky KS, Reed Larsen PR. 2008. *Willimas textbook of Endocrinology*. Philadelphia: Saunders/Elsevier.
- Kurlawalla-Martinez C, Stiles B, Wang Y, Devaskar SU, Kahn BB, Wu H. 2005. Insulin hypersensitivity and resistance to streptozotocin-induced diabetes in mice lacking PTEN in adipose tissue. *Mol Cell Biol* 25(6):2498-510.
- Lander ES, Linton LM, Birren B, Nusbaum C, Zody MC, Baldwin J, Devon K, Dewar K, Doyle M, FitzHugh W and others. 2001. Initial sequencing and analysis of the human genome. *Nature* 409(6822):860-921.
- Lango H, Palmer CN, Morris AD, Zeggini E, Hattersley AT, McCarthy MI, Frayling TM, Weedon MN. 2008. Assessing the combined impact of 18 common genetic variants of modest effect sizes on type 2 diabetes risk. *Diabetes* 57(11):3129-35.
- Le Good JA, Ziegler WH, Parekh DB, Alessi DR, Cohen P, Parker PJ. 1998. Protein kinase C isotypes controlled by phosphoinositide 3-kinase through the protein kinase PDK1. *Science* 281(5385):2042-5.
- Ledermann HM. 1995. Is maturity onset diabetes at young age (MODY) more common in Europe than previously assumed? *Lancet* 345(8950):648.
- Lee TC, Barshes NR, Brunnicardi FC, Alejandro R, Ricordi C, Nguyen L, Goss JA. 2004. Procurement of the human pancreas for pancreatic islet transplantation. *Transplantation* 78(3):481-3.
- Lei KJ, Shelly LL, Pan CJ, Sidbury JB, Chou JY. 1993. Mutations in the glucose-6-phosphatase gene that cause glycogen storage disease type 1a. *Science* 262(5133):580-3.
- Leslie NR, Downes CP. 2004. PTEN function: how normal cells control it and tumour cells lose it. *Biochem J* 382(Pt 1):1-11.
- Lin JM, Ortsater H, Fakhrai-Rad H, Galli J, Luthman H, Bergsten P. 2001. Phenotyping of individual pancreatic islets locates genetic defects in stimulus secretion coupling to Niddm1i within the major diabetes locus in GK rats. *Diabetes* 50(12):2737-43.
- Logeat F, Bessia C, Brou C, LeBail O, Jarriault S, Seidah NG, Israel A. 1998. The Notch1 receptor is cleaved constitutively by a furin-like convertase. *Proc Natl Acad Sci U S A* 95(14):8108-12.
- Longo N, Singh R, Griffin LD, Langley SD, Parks JS, Elsas LJ. 1994. Impaired growth in Rabson-Mendenhall syndrome: lack of effect of growth hormone and insulin-like growth factor-I. *J Clin Endocrinol Metab* 79(3):799-805.
- Longo N, Wang Y, Pasquali M. 1999. Progressive decline in insulin levels in Rabson-Mendenhall syndrome. *J Clin Endocrinol Metab* 84(8):2623-9.
- Longo N, Wang Y, Smith SA, Langley SD, DiMeglio LA, Giannella-Neto D. 2002. Genotype-phenotype correlation in inherited severe insulin resistance. *Hum Mol Genet* 11(12):1465-75.
- Lowry OH, Rosebrough NJ, Farr AL, Randall RJ. 1951. Protein measurement with the Folin phenol reagent. *J Biol Chem* 193(1):265-75.
- Luft R. 1989. Oskar Minkowski: discovery of the pancreatic origin of diabetes, 1889. *Diabetologia* 32(7):399-401.
- Lukowiak B, Vandewalle B, Riachy R, Kerr-Conte J, Gmyr V, Belaich S, Lefebvre J, Pattou F. 2001. Identification and purification of functional human beta-cells by a new specific zinc-fluorescent probe. *J Histochem Cytochem* 49(4):519-28.

- Lyssenko V, Nagorny CL, Erdos MR, Wierup N, Jonsson A, Spegel P, Bugliani M, Saxena R, Fex M, Pulizzi N and others. 2009. Common variant in MTNR1B associated with increased risk of type 2 diabetes and impaired early insulin secretion. *Nat Genet* 41(1):82-8.
- Machann J, Haring H, Schick F, Stumvoll M. 2004. Intramyocellular lipids and insulin resistance. *Diabetes Obes Metab* 6(4):239-48.
- Mackay DJ, Temple IK. 2010. Transient neonatal diabetes mellitus type 1. *Am J Med Genet C Semin Med Genet* 154C(3):335-42.
- Maehama T, Dixon JE. 1998. The tumor suppressor, PTEN/MMAC1, dephosphorylates the lipid second messenger, phosphatidylinositol 3,4,5-trisphosphate. *J Biol Chem* 273(22):13375-8.
- Maffei M, Fei H, Lee GH, Dani C, Leroy P, Zhang Y, Proenca R, Negrel R, Ailhaud G, Friedman JM. 1995. Increased expression in adipocytes of ob RNA in mice with lesions of the hypothalamus and with mutations at the db locus. *Proc Natl Acad Sci U S A* 92(15):6957-60.
- Mahtani MM, Widen E, Lehto M, Thomas J, McCarthy M, Brayer J, Bryant B, Chan G, Daly M, Forsblom C and others. 1996. Mapping of a gene for type 2 diabetes associated with an insulin secretion defect by a genome scan in Finnish families. *Nat Genet* 14(1):90-4.
- Malecki MT, Jhala US, Antonellis A, Fields L, Doria A, Orban T, Saad M, Warram JH, Montminy M, Krolewski AS. 1999. Mutations in NEUROD1 are associated with the development of type 2 diabetes mellitus. *Nat Genet* 23(3):323-8.
- Mally MI, Otonkoski T, Lopez AD, Hayek A. 1994. Developmental gene expression in the human fetal pancreas. *Pediatr Res* 36(4):537-44.
- Marselli L, Thorne J, Ahn YB, Omer A, Sgroi DC, Libermann T, Otu HH, Sharma A, Bonner-Weir S, Weir GC. 2008. Gene expression of purified beta-cell tissue obtained from human pancreas with laser capture microdissection. *J Clin Endocrinol Metab* 93(3):1046-53.
- Martin CC, Bischof LJ, Bergman B, Hornbuckle LA, Hilliker C, Frigeri C, Wahl D, Svitek CA, Wong R, Goldman JK and others. 2001. Cloning and characterization of the human and rat islet-specific glucose-6-phosphatase catalytic subunit-related protein (IGRP) genes. *J Biol Chem* 276(27):25197-207.
- Martin CC, Oeser JK, Svitek CA, Hunter SI, Hutton JC, O'Brien RM. 2002. Identification and characterization of a human cDNA and gene encoding a ubiquitously expressed glucose-6-phosphatase catalytic subunit-related protein. *J Mol Endocrinol* 29(2):205-22.
- Mason CC, Hanson RL, Knowler WC. 2007. Progression to type 2 diabetes characterized by moderate then rapid glucose increases. *Diabetes* 56(8):2054-61.
- Massa O, Iafusco D, D'Amato E, Gloyn AL, Hattersley AT, Pasquino B, Tonini G, Dammacco F, Zanette G, Meschi F and others. 2005. KCNJ11 activating mutations in Italian patients with permanent neonatal diabetes. *Hum Mutat* 25(1):22-7.
- Matschinsky FM. 2002. Regulation of pancreatic beta-cell glucokinase: from basics to therapeutics. *Diabetes* 51 Suppl 3:S394-404.
- Menni F, de Lonlay P, Sevin C, Touati G, Peigne C, Barbier V, Nihoul-Fekete C, Saudubray JM, Robert JJ. 2001. Neurologic outcomes of 90 neonates and infants with persistent hyperinsulinemic hypoglycemia. *Pediatrics* 107(3):476-9.
- Metz C, Cave H, Bertrand AM, Deffert C, Gueguen-Giroux B, Czernichow P, Polak M. 2002. Neonatal diabetes mellitus: chromosomal analysis in transient and permanent cases. *J Pediatr* 141(4):483-9.
- Mohamed-Ali V, Pinkney JH, Coppack SW. 1998. Adipose tissue as an endocrine and paracrine organ. *Int J Obes Relat Metab Disord* 22(12):1145-58.
- Molven A, Ringdal M, Nordbo AM, Raeder H, Stoy J, Lipkind GM, Steiner DF, Philipson LH, Bergmann I, Aarskog D and others. 2008. Mutations in the insulin gene can cause MODY and autoantibody-negative type 1 diabetes. *Diabetes* 57(4):1131-5.

- Montague CT, Farooqi IS, Whitehead JP, Soos MA, Rau H, Wareham NJ, Sewter CP, Digby JE, Mohammed SN, Hurst JA and others. 1997. Congenital leptin deficiency is associated with severe early-onset obesity in humans. *Nature* 387(6636):903-8.
- Morton NE. 1955. Sequential tests for the detection of linkage. *Am J Hum Genet* 7(3):277-318.
- Murphy R, Ellard S, Hattersley AT. 2008. Clinical implications of a molecular genetic classification of monogenic beta-cell diabetes. *Nat Clin Pract Endocrinol Metab* 4(4):200-13.
- Musso C, Cochran E, Moran SA, Skarulis MC, Oral EA, Taylor S, Gorden P. 2004. Clinical course of genetic diseases of the insulin receptor (type A and Rabson-Mendenhall syndromes): a 30-year prospective. *Medicine (Baltimore)* 83(4):209-22.
- Myers MG, Jr., Backer JM, Sun XJ, Shoelson S, Hu P, Schlessinger J, Yoakim M, Schaffhausen B, White MF. 1992. IRS-1 activates phosphatidylinositol 3'-kinase by associating with src homology 2 domains of p85. *Proc Natl Acad Sci U S A* 89(21):10350-4.
- Nagamatsu S, Kornhauser JM, Burant CF, Seino S, Mayo KE, Bell GI. 1992. Glucose transporter expression in brain. cDNA sequence of mouse GLUT3, the brain facilitative glucose transporter isoform, and identification of sites of expression by in situ hybridization. *J Biol Chem* 267(1):467-72.
- Nelson-Degrave VL, Wickenheisser JK, Hendricks KL, Asano T, Fujishiro M, Legro RS, Kimball SR, Strauss JF, 3rd, McAllister JM. 2005. Alterations in mitogen-activated protein kinase kinase and extracellular regulated kinase signaling in theca cells contribute to excessive androgen production in polycystic ovary syndrome. *Mol Endocrinol* 19(2):379-90.
- Nestorowicz A, Inagaki N, Gono T, Schoor KP, Wilson BA, Glaser B, Landau H, Stanley CA, Thornton PS, Seino S and others. 1997. A nonsense mutation in the inward rectifier potassium channel gene, Kir6.2, is associated with familial hyperinsulinism. *Diabetes* 46(11):1743-8.
- Neville MJ, Collins JM, Gloyn AL, McCarthy MI, Karpe F. 2010. *Comprehensive Human Adipose Tissue mRNA and MicroRNA Endogenous Control Selection for Quantitative Real-Time-PCR Normalization*. Obesity (Silver Spring).
- Nicolson TJ, Bellomo EA, Wijesekara N, Loder MK, Baldwin JM, Gyulkhandanyan AV, Koshkin V, Tarasov AI, Carzaniga R, Kronenberger K and others. 2009. Insulin storage and glucose homeostasis in mice null for the granule zinc transporter ZnT8 and studies of the type 2 diabetes-associated variants. *Diabetes* 58(9):2070-83.
- Njolstad PR, Sagen JV, Bjorkhaug L, Odili S, Shehadeh N, Bakry D, Sarici SU, Alpay F, Molnes J, Molven A and others. 2003. Permanent neonatal diabetes caused by glucokinase deficiency: inborn error of the glucose-insulin signaling pathway. *Diabetes* 52(11):2854-60.
- Njolstad PR, Sovik O, Cuesta-Munoz A, Bjorkhaug L, Massa O, Barbetti F, Undlien DE, Shiota C, Magnuson MA, Molven A and others. 2001. Neonatal diabetes mellitus due to complete glucokinase deficiency. *N Engl J Med* 344(21):1588-92.
- Noble JA, Valdes AM, Cook M, Klitz W, Thomson G, Erlich HA. 1996. The role of HLA class II genes in insulin-dependent diabetes mellitus: molecular analysis of 180 Caucasian, multiplex families. *Am J Hum Genet* 59(5):1134-48.
- Nolan C, Margoliash E, Peterson JD, Steiner DF. 1971. The structure of bovine proinsulin. *J Biol Chem* 246(9):2780-95.
- Nolan CJ, Prentki M. 2008. The islet beta-cell: fuel responsive and vulnerable. *Trends Endocrinol Metab* 19(8):285-91.
- Noro B, Licheri B, Sgarra R, Rustighi A, Tessari MA, Chau KY, Ono SJ, Giancotti V, Manfioletti G. 2003. Molecular dissection of the architectural transcription factor HMG2A. *Biochemistry* 42(15):4569-77.

- O'Moore-Sullivan TM, Prins JB. 2002. Thiazolidinediones and type 2 diabetes: new drugs for an old disease. *Med J Aust* 176(8):381-6.
- Orho-Melander M, Melander O, Guiducci C, Perez-Martinez P, Corella D, Roos C, Tewhey R, Rieder MJ, Hall J, Abecasis G and others. 2008. Common missense variant in the glucokinase regulatory protein gene is associated with increased plasma triglyceride and C-reactive protein but lower fasting glucose concentrations. *Diabetes* 57(11):3112-21.
- Otonkoski T, Jiao H, Kaminen-Ahola N, Tapia-Paez I, Ullah MS, Parton LE, Schuit F, Quintens R, Sipila I, Mayatepek E and others. 2007. Physical exercise-induced hypoglycemia caused by failed silencing of monocarboxylate transporter 1 in pancreatic beta cells. *Am J Hum Genet* 81(3):467-74.
- Owerbach D, Bell GI, Rutter WJ, Shows TB. 1980. The insulin gene is located on chromosome 11 in humans. *Nature* 286(5768):82-4.
- Parker A, Meyer J, Lewitzky S, Rennich JS, Chan G, Thomas JD, Orho-Melander M, Lehtovirta M, Forsblom C, Hyrko A and others. 2001. A gene conferring susceptibility to type 2 diabetes in conjunction with obesity is located on chromosome 18p11. *Diabetes* 50(3):675-80.
- Parnaud G, Bosco D, Berney T, Pattou F, Kerr-Conte J, Donath MY, Bruun C, Mandrup-Poulsen T, Billestrup N, Halban PA. 2008. Proliferation of sorted human and rat beta cells. *Diabetologia* 51(1):91-100.
- Parsons TD, Coorsen JR, Horstmann H, Almers W. 1995. Docked granules, the exocytic burst, and the need for ATP hydrolysis in endocrine cells. *Neuron* 15(5):1085-96.
- Patton JS, Shepard HM, Wilking H, Lewis G, Aggarwal BB, Eessalu TE, Gavin LA, Grunfeld C. 1986. Interferons and tumor necrosis factors have similar catabolic effects on 3T3 L1 cells. *Proc Natl Acad Sci U S A* 83(21):8313-7.
- Pearson ER, Boj SF, Steele AM, Barrett T, Stals K, Shield JP, Ellard S, Ferrer J, Hattersley AT. 2007. Macrosomia and hyperinsulinaemic hypoglycaemia in patients with heterozygous mutations in the HNF4A gene. *PLoS Med* 4(4):e118.
- Pearson ER, Flechtner I, Njolstad PR, Malecki MT, Flanagan SE, Larkin B, Ashcroft FM, Klimes I, Codner E, Iotova V and others. 2006. Switching from insulin to oral sulfonylureas in patients with diabetes due to Kir6.2 mutations. *N Engl J Med* 355(5):467-77.
- Pearson ER, Starkey BJ, Powell RJ, Gribble FM, Clark PM, Hattersley AT. 2003. Genetic cause of hyperglycaemia and response to treatment in diabetes. *Lancet* 362(9392):1275-81.
- Peter-Riesch B, Fathi M, Schlegel W, Wollheim CB. 1988. Glucose and carbachol generate 1,2-diacylglycerols by different mechanisms in pancreatic islets. *J Clin Invest* 81(4):1154-61.
- Petrolonis AJ, Yang Q, Tummino PJ, Fish SM, Prack AE, Jain S, Parsons TF, Li P, Dales NA, Ge L and others. 2004. Enzymatic characterization of the pancreatic islet-specific glucose-6-phosphatase-related protein (IGRP). *J Biol Chem* 279(14):13976-83.
- Pfaffl MW. 2001. A new mathematical model for relative quantification in real-time RT-PCR. *Nucleic Acids Res* 29(9):e45.
- Pinney SE, MacMullen C, Becker S, Lin YW, Hanna C, Thornton P, Ganguly A, Shyng SL, Stanley CA. 2008. Clinical characteristics and biochemical mechanisms of congenital hyperinsulinism associated with dominant KATP channel mutations. *J Clin Invest* 118(8):2877-86.
- Plomgaard P, Bouzakri K, Krogh-Madsen R, Mittendorfer B, Zierath JR, Pedersen BK. 2005. Tumor necrosis factor-alpha induces skeletal muscle insulin resistance in healthy human subjects via inhibition of Akt substrate 160 phosphorylation. *Diabetes* 54(10):2939-45.

- Podsypanina K, Ellenson LH, Nemes A, Gu J, Tamura M, Yamada KM, Cordon-Cardo C, Catoretti G, Fisher PE, Parsons R. 1999. Mutation of Pten/Mmac1 in mice causes neoplasia in multiple organ systems. *Proc Natl Acad Sci U S A* 96(4):1563-8.
- Prentki M, Matschinsky FM. 1987. Ca²⁺, cAMP, and phospholipid-derived messengers in coupling mechanisms of insulin secretion. *Physiol Rev* 67(4):1185-248.
- Prokopenko I, Langenberg C, Florez JC, Saxena R, Soranzo N, Thorleifsson G, Loos RJ, Manning AK, Jackson AU, Aulchenko Y and others. 2009a. Variants in MTNR1B influence fasting glucose levels. *Nat Genet* 41(1):77-81.
- Prokopenko I, Zeggini E, Hanson RL, Mitchell BD, Rayner NW, Akan P, Baier L, Das SK, Elliott KS, Fu M and others. 2009b. Linkage disequilibrium mapping of the replicated type 2 diabetes linkage signal on chromosome 1q. *Diabetes* 58(7):1704-9.
- Psiachou H, Mitton S, Alagband-Zadeh J, Hone J, Taylor SI, Sinclair L. 1993. Leprechaunism and homozygous nonsense mutation in the insulin receptor gene. *Lancet* 342(8876):924.
- Rabson SM, Mendenhall EN. 1956. Familial hypertrophy of pineal body, hyperplasia of adrenal cortex and diabetes mellitus; report of 3 cases. *Am J Clin Pathol* 26(3):283-90.
- Raeder H, Johansson S, Holm PI, Haldorsen IS, Mas E, Sbarra V, Neramo I, Eide SA, Grevle L, Bjorkhaug L and others. 2006. Mutations in the CEL VNTR cause a syndrome of diabetes and pancreatic exocrine dysfunction. *Nat Genet* 38(1):54-62.
- Rafiq M, Flanagan SE, Patch AM, Shields BM, Ellard S, Hattersley AT. 2008. Effective treatment with oral sulfonylureas in patients with diabetes due to sulfonylurea receptor 1 (SUR1) mutations. *Diabetes Care* 31(2):204-9.
- Richardson CC, Hussain K, Jones PM, Persaud S, Lobner K, Boehm A, Clark A, Christie MR. 2007. Low levels of glucose transporters and K⁺ATP channels in human pancreatic beta cells early in development. *Diabetologia* 50(5):1000-5.
- Risch N. 1987. Assessing the role of HLA-linked and unlinked determinants of disease. *Am J Hum Genet* 40(1):1-14.
- Rondinone CM, Wang LM, Lonroth P, Wesslau C, Pierce JH, Smith U. 1997. Insulin receptor substrate (IRS) 1 is reduced and IRS-2 is the main docking protein for phosphatidylinositol 3-kinase in adipocytes from subjects with non-insulin-dependent diabetes mellitus. *Proc Natl Acad Sci U S A* 94(8):4171-5.
- Rose CS, Grarup N, Krarup NT, Poulsen P, Wegner L, Nielsen T, Banasik K, Faerch K, Andersen G, Albrechtsen A and others. 2009. A variant in the G6PC2/ABCB11 locus is associated with increased fasting plasma glucose, increased basal hepatic glucose production and increased insulin release after oral and intravenous glucose loads. *Diabetologia* 52(10):2122-9.
- Rosengren AH, Jokubka R, Tojjar D, Granhall C, Hansson O, Li DQ, Nagaraj V, Reinbothe TM, Tuncel J, Eliasson L and others. 2010. Overexpression of alpha2A-adrenergic receptors contributes to type 2 diabetes. *Science* 327(5962):217-20.
- Rozen S, Skaletsky HJ. 2000. Primer 3 on the WWW for general users and for biologist programmers. In: Krawetz S, Misener S, editors. *Bioinformatics Methods and Protocols: Methods in Molecular Biology*. New Jersey: Humana Press. p 365-386.
- Rung J, Cauchi S, Albrechtsen A, Shen L, Rocheleau G, Cavalcanti-Proenca C, Bacot F, Balkau B, Belisle A, Borch-Johnsen K and others. 2009. Genetic variant near IRS1 is associated with type 2 diabetes, insulin resistance and hyperinsulinemia. *Nat Genet* 41(10):1110-5.
- Sabatti C, Service SK, Hartikainen AL, Pouta A, Ripatti S, Brodsky J, Jones CG, Zaitlen NA, Varilo T, Kaakinen M and others. 2009. Genome-wide association analysis of metabolic traits in a birth cohort from a founder population. *Nat Genet* 41(1):35-46.
- Sachidanandam R, Weissman D, Schmidt SC, Kakol JM, Stein LD, Marth G, Sherry S, Mullikin JC, Mortimore BJ, Willey DL and others. 2001. A map of human genome sequence

- variation containing 1.42 million single nucleotide polymorphisms. *Nature* 409(6822):928-33.
- Sagen JV, Raeder H, Hathout E, Shehadeh N, Gudmundsson K, Baevre H, Abuelo D, Phornphutkul C, Molnes J, Bell GI and others. 2004. Permanent neonatal diabetes due to mutations in *KCNJ11* encoding Kir6.2: patient characteristics and initial response to sulfonylurea therapy. *Diabetes* 53(10):2713-8.
- Saltiel AR, Kahn CR. 2001. Insulin signalling and the regulation of glucose and lipid metabolism. *Nature* 414(6865):799-806.
- Sanger F, Tuppy H. 1951a. The amino-acid sequence in the phenylalanyl chain of insulin. 2. The investigation of peptides from enzymic hydrolysates. *Biochem J* 49(4):481-90.
- Sanger F, Tuppy H. 1951b. The amino-acid sequence in the phenylalanyl chain of insulin. 1. The identification of lower peptides from partial hydrolysates. *Biochem J* 49(4):463-81.
- Sano H, Kane S, Sano E, Miinea CP, Asara JM, Lane WS, Garner CW, Lienhard GE. 2003. Insulin-stimulated phosphorylation of a Rab GTPase-activating protein regulates GLUT4 translocation. *J Biol Chem* 278(17):14599-602.
- Santer R, Schneppenheim R, Suter D, Schaub J, Steinmann B. 1998. Fanconi-Bickel syndrome--the original patient and his natural history, historical steps leading to the primary defect, and a review of the literature. *Eur J Pediatr* 157(10):783-97.
- Sarbassov DD, Guertin DA, Ali SM, Sabatini DM. 2005. Phosphorylation and regulation of Akt/PKB by the rictor-mTOR complex. *Science* 307(5712):1098-101.
- Sasaoka T, Wada T, Tsuneki H. 2006. Lipid phosphatases as a possible therapeutic target in cases of type 2 diabetes and obesity. *Pharmacol Ther* 112(3):799-809.
- Sauer B. 1987. Functional expression of the cre-lox site-specific recombination system in the yeast *Saccharomyces cerevisiae*. *Mol Cell Biol* 7(6):2087-96.
- Sauer B, Henderson N. 1988. Site-specific DNA recombination in mammalian cells by the Cre recombinase of bacteriophage P1. *Proc Natl Acad Sci U S A* 85(14):5166-70.
- Savage DB. 2009. Mouse models of inherited lipodystrophy. *Dis Model Mech* 2(11-12):554-62.
- Savage DB, Agostini M, Barroso I, Gurnell M, Luan J, Meirhaeghe A, Harding AH, Ihrke G, Rajanayagam O, Soos MA and others. 2002. Digenic inheritance of severe insulin resistance in a human pedigree. *Nat Genet* 31(4):379-84.
- Savage DB, Petersen KF, Shulman GI. 2005. Mechanisms of insulin resistance in humans and possible links with inflammation. *Hypertension* 45(5):828-33.
- Savage DB, Tan GD, Acerini CL, Jebb SA, Agostini M, Gurnell M, Williams RL, Umpleby AM, Thomas EL, Bell JD and others. 2003. Human metabolic syndrome resulting from dominant-negative mutations in the nuclear receptor peroxisome proliferator-activated receptor-gamma. *Diabetes* 52(4):910-7.
- Savage DB, Zhai L, Ravikumar B, Choi CS, Snaar JE, McGuire AC, Wou SE, Medina-Gomez G, Kim S, Bock CB and others. 2008. A prevalent variant in *PPP1R3A* impairs glycogen synthesis and reduces muscle glycogen content in humans and mice. *PLoS Med* 5(1):e27.
- Saxena R, Hivert MF, Langenberg C, Tanaka T, Pankow JS, Vollenweider P, Lyssenko V, Bouatia-Naji N, Dupuis J, Jackson AU and others. 2010. Genetic variation in *GIPR* influences the glucose and insulin responses to an oral glucose challenge. *Nat Genet* 42(2):142-8.
- Saxena R, Voight BF, Lyssenko V, Burt NP, de Bakker PI, Chen H, Roix JJ, Kathiresan S, Hirschhorn JN, Daly MJ and others. 2007. Genome-wide association analysis identifies loci for type 2 diabetes and triglyceride levels. *Science* 316(5829):1331-6.
- Schievella AR, Chen JH, Graham JR, Lin LL. 1997. MADD, a novel death domain protein that interacts with the type 1 tumor necrosis factor receptor and activates mitogen-activated protein kinase. *J Biol Chem* 272(18):12069-75.

- Schroeder A, Mueller O, Stocker S, Salowsky R, Leiber M, Gassmann M, Lightfoot S, Menzel W, Granzow M, Ragg T. 2006. The RIN: an RNA integrity number for assigning integrity values to RNA measurements. *BMC Mol Biol* 7:3.
- Scott LJ, Mohlke KL, Bonnycastle LL, Willer CJ, Li Y, Duren WL, Erdos MR, Stringham HM, Chines PS, Jackson AU and others. 2007. A genome-wide association study of type 2 diabetes in Finns detects multiple susceptibility variants. *Science* 316(5829):1341-5.
- Semple R, Savage D, O'Rahilly S. 2010. Genetics of severe insulin resistance. In: Wass JA, Shalet S, editors. *Oxford textbook of Endocrinology and Diabetes*. Oxford: Oxford University Press.
- Semple RK, Chatterjee VK, O'Rahilly S. 2006. PPAR gamma and human metabolic disease. *J Clin Invest* 116(3):581-9.
- Semple RK, Savage DB, Cochran EK, Gorden P, O'Rahilly S. 2011. Genetic Syndromes of Severe Insulin Resistance. *Endocr Rev*.
- Senee V, Vatter KM, Delepine M, Rainbow LA, Haton C, Lecoq A, Shaw NJ, Robert JJ, Rومان R, Diatloff-Zito C and others. 2004. Wolcott-Rallison Syndrome: clinical, genetic, and functional study of EIF2AK3 mutations and suggestion of genetic heterogeneity. *Diabetes* 53(7):1876-83.
- Service FJ, McMahon MM, O'Brien PC, Ballard DJ. 1991. Functioning insulinoma--incidence, recurrence, and long-term survival of patients: a 60-year study. *Mayo Clin Proc* 66(7):711-9.
- Sheehan MT. 2004. Polycystic ovarian syndrome: diagnosis and management. *Clin Med Res* 2(1):13-27.
- Shepherd M, Hattersley AT. 2004. 'I don't feel like a diabetic any more': the impact of stopping insulin in patients with maturity onset diabetes of the young following genetic testing. *Clin Med* 4(2):144-7.
- Shepherd M, Pearson ER, Houghton J, Salt G, Ellard S, Hattersley AT. 2003. No deterioration in glycemic control in HNF-1alpha maturity-onset diabetes of the young following transfer from long-term insulin to sulphonylureas. *Diabetes Care* 26(11):3191-2.
- Shieh JJ, Pan CJ, Mansfield BC, Chou JY. 2004. The islet-specific glucose-6-phosphatase-related protein, implicated in diabetes, is a glycoprotein embedded in the endoplasmic reticulum membrane. *FEBS Lett* 562(1-3):160-4.
- Shield JP, Gardner RJ, Wadsworth EJ, Whiteford ML, James RS, Robinson DO, Baum JD, Temple IK. 1997. Aetiopathology and genetic basis of neonatal diabetes. *Arch Dis Child Fetal Neonatal Ed* 76(1):F39-42.
- Shulman GI. 2000. Cellular mechanisms of insulin resistance. *J Clin Invest* 106(2):171-6.
- Shyng S, Nichols CG. 1997. Octameric stoichiometry of the KATP channel complex. *J Gen Physiol* 110(6):655-64.
- Sladek R, Rocheleau G, Rung J, Dina C, Shen L, Serre D, Boutin P, Vincent D, Belisle A, Hadjadj S and others. 2007. A genome-wide association study identifies novel risk loci for type 2 diabetes. *Nature* 445(7130):881-5.
- Slingerland AS, Hattersley AT. 2005. Mutations in the Kir6.2 subunit of the KATP channel and permanent neonatal diabetes: new insights and new treatment. *Ann Med* 37(3):186-95.
- Slingerland AS, Shields BM, Flanagan SE, Bruining GJ, Noordam K, Gach A, Mlynarski W, Malecki MT, Hattersley AT, Ellard S. 2009. Referral rates for diagnostic testing support an incidence of permanent neonatal diabetes in three European countries of at least 1 in 260,000 live births. *Diabetologia* 52(8):1683-5.
- Small KS, Hedman AK, Grundberg E, Nica AC, Thorleifsson G, Kong A, Thorsteindottir U, Shin SY, Richards HB, Soranzo N and others. 2011. Identification of an imprinted master trans regulator at the KLF14 locus related to multiple metabolic phenotypes. *Nat Genet* 43(6):561-564.

- Smith LM, Sanders JZ, Kaiser RJ, Hughes P, Dodd C, Connell CR, Heiner C, Kent SB, Hood LE. 1986. Fluorescence detection in automated DNA sequence analysis. *Nature* 321(6071):674-9.
- Somerville RP, Longpre JM, Jungers KA, Engle JM, Ross M, Evanko S, Wight TN, Leduc R, Apte SS. 2003. Characterization of ADAMTS-9 and ADAMTS-20 as a distinct ADAMTS subfamily related to *Caenorhabditis elegans* GON-1. *J Biol Chem* 278(11):9503-13.
- Song KH, Li T, Chiang JY. 2006. A Prospero-related homeodomain protein is a novel co-regulator of hepatocyte nuclear factor 4 α that regulates the cholesterol 7 α -hydroxylase gene. *J Biol Chem* 281(15):10081-8.
- Sperling MA. 2006. ATP-sensitive potassium channels--neonatal diabetes mellitus and beyond. *N Engl J Med* 355(5):507-10.
- Spiegelman BM. 1998. PPAR- γ : adipogenic regulator and thiazolidinedione receptor. *Diabetes* 47(4):507-14.
- Spyer G, Hattersley AT, Sykes JE, Sturley RH, MacLeod KM. 2001. Influence of maternal and fetal glucokinase mutations in gestational diabetes. *Am J Obstet Gynecol* 185(1):240-1.
- Staels B, Kuipers F. 2007. Bile acid sequestrants and the treatment of type 2 diabetes mellitus. *Drugs* 67(10):1383-92.
- Stanley CA, Fang J, Kutyna K, Hsu BY, Ming JE, Glaser B, Poncz M. 2000. Molecular basis and characterization of the hyperinsulinism/hyperammonemia syndrome: predominance of mutations in exons 11 and 12 of the glutamate dehydrogenase gene. *HI/HA Contributing Investigators. Diabetes* 49(4):667-73.
- Stanley CA, Lieu YK, Hsu BY, Burlina AB, Greenberg CR, Hopwood NJ, Perlman K, Rich BH, Zammarchi E, Poncz M. 1998. Hyperinsulinism and hyperammonemia in infants with regulatory mutations of the glutamate dehydrogenase gene. *N Engl J Med* 338(19):1352-7.
- Steiner DF. 1976. Insulin Sequences. In: Fasman GD, editor. *Handbook of Biochemistry and Molecular Biology*. Cleveland: CRC. p 378-81.
- Steiner DF, Chan SJ, Welsh JM, Kwok SC. 1985. Structure and evolution of the insulin gene. *Annu Rev Genet* 19:463-84.
- Steiner DF, Cho S, Oyer PE, Terris S, Peterson JD, Rubenstein AH. 1971. Isolation and characterization of proinsulin C-peptide from bovine pancreas. *J Biol Chem* 246(5):1365-74.
- Steiner DF, Docherty K, Carroll R. 1984. Golgi/granule processing of peptide hormone and neuropeptide precursors: a minireview. *J Cell Biochem* 24(2):121-30.
- Steiner DF, Oyer PE. 1967. The biosynthesis of insulin and a probable precursor of insulin by a human islet cell adenoma. *Proc Natl Acad Sci U S A* 57(2):473-80.
- Steinthorsdottir V, Thorleifsson G, Reynisdottir I, Benediktsson R, Jonsdottir T, Walters GB, Styrkarsdottir U, Gretarsdottir S, Emilsson V, Ghosh S and others. 2007. A variant in CDKAL1 influences insulin response and risk of type 2 diabetes. *Nat Genet* 39(6):770-5.
- Stiles B, Wang Y, Stahl A, Bassilian S, Lee WP, Kim YJ, Sherwin R, Devaskar S, Lesche R, Magnuson MA and others. 2004. Liver-specific deletion of negative regulator Pten results in fatty liver and insulin hypersensitivity [corrected]. *Proc Natl Acad Sci U S A* 101(7):2082-7.
- Stoffers DA, Ferrer J, Clarke WL, Habener JF. 1997a. Early-onset type-II diabetes mellitus (MODY4) linked to IPF1. *Nat Genet* 17(2):138-9.
- Stoffers DA, Zinkin NT, Stanojevic V, Clarke WL, Habener JF. 1997b. Pancreatic agenesis attributable to a single nucleotide deletion in the human IPF1 gene coding sequence. *Nat Genet* 15(1):106-10.

- Stoy J, Edghill EL, Flanagan SE, Ye H, Paz VP, Pluzhnikov A, Below JE, Hayes MG, Cox NJ, Lipkind GM and others. 2007. Insulin gene mutations as a cause of permanent neonatal diabetes. *Proc Natl Acad Sci U S A* 104(38):15040-4.
- Stranger BE, Nica AC, Forrest MS, Dimas A, Bird CP, Beazley C, Ingle CE, Dunning M, Flicek P, Koller D and others. 2007. Population genomics of human gene expression. *Nat Genet* 39(10):1217-24.
- Street CN, Lakey JR, Shapiro AM, Imes S, Rajotte RV, Ryan EA, Lyon JG, Kin T, Avila J, Tsujimura T and others. 2004. Islet graft assessment in the Edmonton Protocol: implications for predicting long-term clinical outcome. *Diabetes* 53(12):3107-14.
- Stride A, Vaxillaire M, Tuomi T, Barbetti F, Njolstad PR, Hansen T, Costa A, Conget I, Pedersen O, Sovik O and others. 2002. The genetic abnormality in the beta cell determines the response to an oral glucose load. *Diabetologia* 45(3):427-35.
- Strobel A, Issad T, Camoin L, Ozata M, Strosberg AD. 1998. A leptin missense mutation associated with hypogonadism and morbid obesity. *Nat Genet* 18(3):213-5.
- Stumvoll M, Goldstein BJ, van Haeften TW. 2005. Type 2 diabetes: principles of pathogenesis and therapy. *Lancet* 365(9467):1333-46.
- Stumvoll M, Tataranni PA, Stefan N, Vozarova B, Bogardus C. 2003. Glucose allostasis. *Diabetes* 52(4):903-9.
- Suliman SG, Stanik J, McCulloch LJ, Wilson N, Edghill EL, Misovicova N, Gasperikova D, Sandrikova V, Elliott KS, Barak L and others. 2009. Severe insulin resistance and intrauterine growth deficiency associated with haploinsufficiency for INSR and CHN2: new insights into synergistic pathways involved in growth and metabolism. *Diabetes* 58(12):2954-61.
- Sun XJ, Rothenberg P, Kahn CR, Backer JM, Araki E, Wilden PA, Cahill DA, Goldstein BJ, White MF. 1991. Structure of the insulin receptor substrate IRS-1 defines a unique signal transduction protein. *Nature* 352(6330):73-7.
- Sun XJ, Wang LM, Zhang Y, Yenush L, Myers MG, Jr., Glasheen E, Lane WS, Pierce JH, White MF. 1995. Role of IRS-2 in insulin and cytokine signalling. *Nature* 377(6545):173-7.
- Tan GD, Savage DB, Fielding BA, Collins J, Hodson L, Humphreys SM, O'Rahilly S, Chatterjee K, Frayn KN, Karpe F. 2008. Fatty acid metabolism in patients with PPARGgamma mutations. *J Clin Endocrinol Metab* 93(11):4462-70.
- Taniguchi CM, Emanuelli B, Kahn CR. 2006a. Critical nodes in signalling pathways: insights into insulin action. *Nat Rev Mol Cell Biol* 7(2):85-96.
- Taniguchi CM, Tran TT, Kondo T, Luo J, Ueki K, Cantley LC, Kahn CR. 2006b. Phosphoinositide 3-kinase regulatory subunit p85alpha suppresses insulin action via positive regulation of PTEN. *Proc Natl Acad Sci U S A* 103(32):12093-7.
- Tattersall RB. 1974. Mild familial diabetes with dominant inheritance. *Q J Med* 43(170):339-57.
- Temple IK, Gardner RJ, Mackay DJ, Barber JC, Robinson DO, Shield JP. 2000. Transient neonatal diabetes: widening the understanding of the etiopathogenesis of diabetes. *Diabetes* 49(8):1359-66.
- Temple IK, Gardner RJ, Robinson DO, Kibirige MS, Ferguson AW, Baum JD, Barber JC, James RS, Shield JP. 1996. Further evidence for an imprinted gene for neonatal diabetes localised to chromosome 6q22-q23. *Hum Mol Genet* 5(8):1117-21.
- Terauchi Y, Tsuji Y, Satoh S, Minoura H, Murakami K, Okuno A, Inukai K, Asano T, Kaburagi Y, Ueki K and others. 1999. Increased insulin sensitivity and hypoglycaemia in mice lacking the p85 alpha subunit of phosphoinositide 3-kinase. *Nat Genet* 21(2):230-5.
- Thomas P, Ye Y, Lightner E. 1996. Mutation of the pancreatic islet inward rectifier Kir6.2 also leads to familial persistent hyperinsulinemic hypoglycemia of infancy. *Hum Mol Genet* 5(11):1809-12.

- Thomas PM, Cote GJ, Hallman DM, Mathew PM. 1995a. Homozygosity mapping, to chromosome 11p, of the gene for familial persistent hyperinsulinemic hypoglycemia of infancy. *Am J Hum Genet* 56(2):416-21.
- Thomas PM, Cote GJ, Wohlk N, Haddad B, Mathew PM, Rabl W, Aguilar-Bryan L, Gagel RF, Bryan J. 1995b. Mutations in the sulfonylurea receptor gene in familial persistent hyperinsulinemic hypoglycemia of infancy. *Science* 268(5209):426-9.
- Thorens B, Guillam MT, Beermann F, Burcelin R, Jaquet M. 2000. Transgenic reexpression of GLUT1 or GLUT2 in pancreatic beta cells rescues GLUT2-null mice from early death and restores normal glucose-stimulated insulin secretion. *J Biol Chem* 275(31):23751-8.
- Thorens B, Sarkar HK, Kaback HR, Lodish HF. 1988. Cloning and functional expression in bacteria of a novel glucose transporter present in liver, intestine, kidney, and beta-pancreatic islet cells. *Cell* 55(2):281-90.
- Todd JA, Walker NM, Cooper JD, Smyth DJ, Downes K, Plagnol V, Bailey R, Nejentsev S, Field SF, Payne F and others. 2007. Robust associations of four new chromosome regions from genome-wide analyses of type 1 diabetes. *Nat Genet* 39(7):857-64.
- Tontonoz P, Nagy L, Alvarez JG, Thomazy VA, Evans RM. 1998. PPARgamma promotes monocyte/macrophage differentiation and uptake of oxidized LDL. *Cell* 93(2):241-52.
- Tran H, Brunet A, Griffith EC, Greenberg ME. 2003. The many forks in FOXO's road. *Sci STKE* 2003(172):RE5.
- Tucker SJ, Gribble FM, Zhao C, Trapp S, Ashcroft FM. 1997. Truncation of Kir6.2 produces ATP-sensitive K⁺ channels in the absence of the sulphonylurea receptor. *Nature* 387(6629):179-83.
- Unoki H, Takahashi A, Kawaguchi T, Hara K, Horikoshi M, Andersen G, Ng DP, Holmkvist J, Borch-Johnsen K, Jorgensen T and others. 2008. SNPs in KCNQ1 are associated with susceptibility to type 2 diabetes in East Asian and European populations. *Nat Genet* 40(9):1098-102.
- Vaag A, Henriksen JE, Beck-Nielsen H. 1992. Decreased insulin activation of glycogen synthase in skeletal muscles in young nonobese Caucasian first-degree relatives of patients with non-insulin-dependent diabetes mellitus. *J Clin Invest* 89(3):782-8.
- Vaisse C, Halaas JL, Horvath CM, Darnell JE, Jr., Stoffel M, Friedman JM. 1996. Leptin activation of Stat3 in the hypothalamus of wild-type and ob/ob mice but not db/db mice. *Nat Genet* 14(1):95-7.
- van Schaftingen E, Gerin I. 2002. The glucose-6-phosphatase system. *Biochem J* 362(Pt 3):513-32.
- Vandesompele J, De Preter K, Pattyn F, Poppe B, Van Roy N, De Paepe A, Speleman F. 2002. Accurate normalization of real-time quantitative RT-PCR data by geometric averaging of multiple internal control genes. *Genome Biol* 3(7):RESEARCH0034.
- Vaxillaire M, Cavalcanti-Proenca C, Dechaume A, Tichet J, Marre M, Balkau B, Froguel P. 2008. The common P446L polymorphism in GCKR inversely modulates fasting glucose and triglyceride levels and reduces type 2 diabetes risk in the DESIR prospective general French population. *Diabetes* 57(8):2253-7.
- Vaxillaire M, Populaire C, Busiah K, Cave H, Gloyn AL, Hattersley AT, Czernichow P, Froguel P, Polak M. 2004. Kir6.2 mutations are a common cause of permanent neonatal diabetes in a large cohort of French patients. *Diabetes* 53(10):2719-22.
- Velho G, Hattersley AT, Froguel P. 2000. Maternal diabetes alters birth weight in glucokinase-deficient (MODY2) kindred but has no influence on adult weight, height, insulin secretion or insulin sensitivity. *Diabetologia* 43(8):1060-3.
- Venter JC, Adams MD, Myers EW, Li PW, Mural RJ, Sutton GG, Smith HO, Yandell M, Evans CA, Holt RA and others. 2001. The sequence of the human genome. *Science* 291(5507):1304-51.

- Verkarre V, Fournet JC, de Lonlay P, Gross-Morand MS, Devillers M, Rahier J, Brunelle F, Robert JJ, Nihoul-Fekete C, Saudubray JM and others. 1998. Paternal mutation of the sulfonylurea receptor (SUR1) gene and maternal loss of 11p15 imprinted genes lead to persistent hyperinsulinism in focal adenomatous hyperplasia. *J Clin Invest* 102(7):1286-91.
- Vinciguerra M, Sgroi A, Veyrat-Durebex C, Rubbia-Brandt L, Buhler LH, Foti M. 2009. Unsaturated fatty acids inhibit the expression of tumor suppressor phosphatase and tensin homolog (PTEN) via microRNA-21 up-regulation in hepatocytes. *Hepatology* 49(4):1176-84.
- Vionnet N, Hani EH, Dupont S, Gallina S, Francke S, Dotte S, De Matos F, Durand E, Lepretre F, Lecoeur C and others. 2000. Genomewide search for type 2 diabetes-susceptibility genes in French whites: evidence for a novel susceptibility locus for early-onset diabetes on chromosome 3q27-qter and independent replication of a type 2-diabetes locus on chromosome 1q21-q24. *Am J Hum Genet* 67(6):1470-80.
- Voight BF, Scott LJ, Steinthorsdottir V, Morris AP, Dina C, Welch RP, Zeggini E, Huth C, Aulchenko YS, Thorleifsson G and others. 2010. Twelve type 2 diabetes susceptibility loci identified through large-scale association analysis. *Nat Genet* 42(7):579-89.
- Vollenweider F, Kaufmann J, Irminger JC, Halban PA. 1995. Processing of proinsulin by furin, PC2, and PC3 in (co) transfected COS (monkey kidney) cells. *Diabetes* 44(9):1075-80.
- Wang H, Hays NP, Das SK, Craig RL, Chu WS, Sharma N, Elbein SC. 2009. Phenotypic and molecular evaluation of a chromosome 1q region with linkage and association to type 2 diabetes in humans. *J Clin Endocrinol Metab* 94(4):1401-8.
- Wang Y, Martin CC, Oeser JK, Sarkar S, McGuinness OP, Hutton JC, O'Brien RM. 2007. Deletion of the gene encoding the islet-specific glucose-6-phosphatase catalytic subunit-related protein autoantigen results in a mild metabolic phenotype. *Diabetologia* 50(4):774-8.
- Watanabe RM, Valle T, Hauser ER, Ghosh S, Eriksson J, Kohtamaki K, Ehnholm C, Tuomilehto J, Collins FS, Bergman RN and others. 1999. Familiality of quantitative metabolic traits in Finnish families with non-insulin-dependent diabetes mellitus. Finland-United States Investigation of NIDDM Genetics (FUSION) Study investigators. *Hum Hered* 49(3):159-68.
- Waters MG, Serafini T, Rothman JE. 1991. 'Coatomer': a cytosolic protein complex containing subunits of non-clathrin-coated Golgi transport vesicles. *Nature* 349(6306):248-51.
- Weedon MN, Frayling TM, Shields B, Knight B, Turner T, Metcalf BS, Voss L, Wilkin TJ, McCarthy A, Ben-Shlomo Y and others. 2005a. Genetic regulation of birth weight and fasting glucose by a common polymorphism in the islet cell promoter of the glucokinase gene. *Diabetes* 54(2):576-81.
- Weedon MN, Lettre G, Freathy RM, Lindgren CM, Voight BF, Perry JR, Elliott KS, Hackett R, Guiducci C, Shields B and others. 2007. A common variant of HMG2 is associated with adult and childhood height in the general population. *Nat Genet* 39(10):1245-50.
- Weedon MN, Owen KR, Shields B, Hitman G, Walker M, McCarthy MI, Hattersley AT, Frayling TM. 2005b. A large-scale association analysis of common variation of the HNF1alpha gene with type 2 diabetes in the U.K. Caucasian population. *Diabetes* 54(8):2487-91.
- Weir GC, Marselli L, Marchetti P, Katsuta H, Jung MH, Bonner-Weir S. 2009. Towards better understanding of the contributions of overwork and glucotoxicity to the beta-cell inadequacy of type 2 diabetes. *Diabetes Obes Metab* 11 Suppl 4:82-90.
- Weyer C, Funahashi T, Tanaka S, Hotta K, Matsuzawa Y, Pratley RE, Tataranni PA. 2001. Hypoadiponectinemia in obesity and type 2 diabetes: close association with insulin resistance and hyperinsulinemia. *J Clin Endocrinol Metab* 86(5):1930-5.
- White ML, Doherty GM. 2008. Multiple endocrine neoplasia. *Surg Oncol Clin N Am* 17(2):439-59, x.

- WHO. 2006. Definition and Diagnosis of diabetes mellitus and intermediate hyperglycaemia:report of a WHO/IDF consultation.
- WHO. 2011. WHO Diabetes Programme
- Wijesekara N, Konrad D, Eweida M, Jefferies C, Liadis N, Giacca A, Crackower M, Suzuki A, Mak TW, Kahn CR and others. 2005. Muscle-specific Pten deletion protects against insulin resistance and diabetes. *Mol Cell Biol* 25(3):1135-45.
- Wiltshire S, Hattersley AT, Hitman GA, Walker M, Levy JC, Sampson M, O'Rahilly S, Frayling TM, Bell JI, Lathrop GM and others. 2001. A genomewide scan for loci predisposing to type 2 diabetes in a U.K. population (the Diabetes UK Warren 2 Repository): analysis of 573 pedigrees provides independent replication of a susceptibility locus on chromosome 1q. *Am J Hum Genet* 69(3):553-69.
- Winckler W, Burt NP, Holmkvist J, Cervin C, de Bakker PI, Sun M, Almgren P, Tuomi T, Gaudet D, Hudson TJ and others. 2005. Association of common variation in the HNF1alpha gene region with risk of type 2 diabetes. *Diabetes* 54(8):2336-42.
- Wong JT, Kim PT, Peacock JW, Yau TY, Mui AL, Chung SW, Sossi V, Doudet D, Green D, Ruth TJ and others. 2007. Pten (phosphatase and tensin homologue gene) haploinsufficiency promotes insulin hypersensitivity. *Diabetologia* 50(2):395-403.
- WTCCC. 2007. Genome-wide association study of 14,000 cases of seven common diseases and 3,000 shared controls. *Nature* 447(7145):661-78.
- Xiang AH, Wang C, Peters RK, Trigo E, Kjos SL, Buchanan TA. 2006. Coordinate changes in plasma glucose and pancreatic beta-cell function in Latino women at high risk for type 2 diabetes. *Diabetes* 55(4):1074-9.
- Yamagata K, Oda N, Kaisaki PJ, Menzel S, Furuta H, Vaxillaire M, Southam L, Cox RD, Lathrop GM, Boriraj VV and others. 1996. Mutations in the hepatocyte nuclear factor-1alpha gene in maturity-onset diabetes of the young (MODY3). *Nature* 384(6608):455-8.
- Yang BT, Dayeh TA, Kirkpatrick CL, Taneera J, Kumar R, Groop L, Wollheim CB, Nitert MD, Ling C. Insulin promoter DNA methylation correlates negatively with insulin gene expression and positively with HbA(1c) levels in human pancreatic islets. *Diabetologia* 54(2):360-7.
- Yang Chou J, Mansfield BC. 1999. Molecular Genetics of Type 1 Glycogen Storage Diseases. *Trends Endocrinol Metab* 10(3):104-113.
- Yasuda K, Miyake K, Horikawa Y, Hara K, Osawa H, Furuta H, Hirota Y, Mori H, Jonsson A, Sato Y and others. 2008. Variants in KCNQ1 are associated with susceptibility to type 2 diabetes mellitus. *Nat Genet* 40(9):1092-7.
- Yorifuji T, Kurokawa K, Mamada M, Imai T, Kawai M, Nishi Y, Shishido S, Hasegawa Y, Nakahata T. 2004. Neonatal diabetes mellitus and neonatal polycystic, dysplastic kidneys: Phenotypically discordant recurrence of a mutation in the hepatocyte nuclear factor-1beta gene due to germline mosaicism. *J Clin Endocrinol Metab* 89(6):2905-8.
- Zahn H. 2002. *Insulin and Related Proteins - Structure to Function and Pharmacology*. Dordrecht: Kluwer Academic Publishers.
- Zeggini E, Scott LJ, Saxena R, Voight BF, Marchini JL, Hu T, de Bakker PI, Abecasis GR, Almgren P, Andersen G and others. 2008. Meta-analysis of genome-wide association data and large-scale replication identifies additional susceptibility loci for type 2 diabetes. *Nat Genet* 40(5):638-45.
- Zeggini E, Weedon MN, Lindgren CM, Frayling TM, Elliott KS, Lango H, Timpson NJ, Perry JR, Rayner NW, Freathy RM and others. 2007. Replication of genome-wide association signals in UK samples reveals risk loci for type 2 diabetes. *Science* 316(5829):1336-41.
- Zeng G, Quon MJ. 1996. Insulin-stimulated production of nitric oxide is inhibited by wortmannin. Direct measurement in vascular endothelial cells. *J Clin Invest* 98(4):894-8.

- Zhang Y, Proenca R, Maffei M, Barone M, Leopold L, Friedman JM. 1994. Positional cloning of the mouse obese gene and its human homologue. *Nature* 372(6505):425-32.
- Zhou G, Myers R, Li Y, Chen Y, Shen X, Fenyk-Melody J, Wu M, Ventre J, Doebber T, Fujii N and others. 2001. Role of AMP-activated protein kinase in mechanism of metformin action. *J Clin Invest* 108(8):1167-74.
- Zhou X, Benson KF, Ashar HR, Chada K. 1995. Mutation responsible for the mouse pygmy phenotype in the developmentally regulated factor HMGI-C. *Nature* 376(6543):771-4.
- Zimmet P, Alberti KG, Shaw J. 2001. Global and societal implications of the diabetes epidemic. *Nature* 414(6865):782-7.

Published Manuscripts